

The role of phytochemicals in modulating breast cancer resistance protein at the blood- brain barrier and the blood- tumour barrier

**Basma Ahmed Elbakary
Doctor of Philosophy**

Aston University

March 2021

©Basma Ahmed Elbakary, 2021

Basma Ahmed Elbakary asserts her moral right to be identified as the author of
this thesis

This copy of the thesis has been supplied on condition that anyone who
consults it is understood to recognise that its copyright belongs to its author and
that no quotation from the thesis and no information derived from it may be
published without appropriate permission or acknowledgement.

Aston University

The role of phytochemicals in modulating breast cancer resistance protein function at the blood-brain barrier and the blood-tumour barrier

Basma Elbakary

Doctor of philosophy

2021

Thesis summary

The blood-brain barrier (BBB) and the blood-tumour barrier (BTB) represent insidious obstacles for the delivery of anti-cancer agents to solid brain tumours, not only because of their morphological features, but also due to the presence of the drug efflux transporter breast cancer resistant protein (BCRP), localised at both the BBB and BTB. This efflux transporter restricts the permeation of anti-cancer agents across both barriers leading to suboptimal concentrations of drugs at the intended site of action.

This work examined 13 naturally occurring phytochemicals, which were screened for their dual ability to modulate the efflux function of BCRP in addition to their anti-cancer properties in human LN229 glioblastoma cells, namely: (i) inhibition of cellular migration; (ii) activation of apoptosis; (iii) reactive oxygen species (ROS) production and (iv) activation of caspase pathways. Phytochemicals displayed minimal cytotoxicity, were able to modulate BCRP which led to enhancing the permeability of the fluorescent probe substrate H33342, in addition to inhibiting cellular migration. Hesperetin and baicalin displayed the optimal modulatory potential and demonstrated a similar ability to generate ROS and activate Caspase-3/7 when compared to the anti-cancer agents methotrexate and temozolomide. Subsequently, hesperetin was progressed as the optimal candidate, and its ability to permeate across the BBB was confirmed after conducting a permeability study using an *in-vitro* primary porcine brain microvascular endothelial cell (PBMEC) BBB model. We demonstrated that hesperetin was highly permeable across the BBB, can modulate the efflux function of BCRP and overall enhance the apparent permeability (P_{app}) of mitoxantrone and methotrexate. Thereafter, we assessed the impact of shear stress fashioned by laminal flow on the morphology of PBMEC using a Quasi Vivo 600[®] perfusion system. The results displayed a significant increase in Transepithelial Electrical Resistance (TEER) values, improved formation of zonula occludens-1 (ZO-1), and higher expression of efflux transporter proteins, suggesting the formation of a better *in-vitro* BBB model with hesperetin still being highly permeable across the barrier further confirming its ability to bypass the BBB and reach the BTB. This work highlights the anti-cancer and BCRP modulatory capabilities of phytochemicals as well as the ability of hesperetin to bypass the BBB.

Acknowledgements

I would like to extend my deepest appreciation to my supervisor Dr Raj Badhan for his kindness, patience, guidance, support, and encouragement throughout the last few years. You are, without a doubt, the best, most generous teacher I have ever had. A true example of how supervisors and teachers should be. I am forever in your debt.

Thank you to the Aston technicians' team: Racheal, Danni, Hailey and Jit for their timely help, support and understanding.

I would like to thank my peers in labs MB328 and MB330 for their help and support, I wish you all the best of luck.

I would like to thank Aston University for funding my research and Aston Medical School for allowing me to use their facility.

I would like to thank all my friends and every kind soul I have had the pleasure of knowing. Thank you. You have helped me more than you know.

Finally, my grandest expression of gratitude to my father, Dr. Ahmed Elbakary, my mother, Dr. Sohir Hatem, and my sister Dr. Basant Elbakary. I wouldn't have been able to do this without your unconditional love and support. I hope I made you proud. This is for you.

I hope my work and the path I am on will make a difference in people's lives one day.

List of Publications

List of published peer reviewed articles

Elbakary, B. and R. K. S. Badhan (2020). "A dynamic perfusion based blood-brain barrier model for cytotoxicity testing and drug permeation." Scientific Reports **10**(1): 1-12.

List of articles submitted for publication

Elbakary, B. and R. K. S. Badhan (March 2021). " Phytochemical mediated modulation of breast cancer resistance protein in human glioblastoma cells." Brain research

List of Abstracts

Basma Elbakary and Raj Badhan., 2018. Flavonoids modulate the action of BCRP at the blood brain barrier. Advanced cell and tissue culture (ACTC) the school of biosciences, Cardiff University, Cardiff.

Basma Elbakary and Raj Badhan., 2018. Flavonoids modulate the action of BCRP at the blood brain barrier. LHS PG research day, Aston University, Birmingham, UK

Basma Elbakary and Raj Badhan., 2019. Flavonoids modulate the action of BCRP at the blood brain barrier and enhance the permeability of anti-cancer agents. Advanced cell and tissue culture (ACTC) the School of Biosciences, Cardiff University, Cardiff.

Basma Elbakary and Raj Bandhan., 2019. Establishing a better in-vitro BBB model for testing brain drug delivery. The Academy of Pharmaceutical Sciences (APS), university of Greenwich, London.

List of Oral Presentations

A dynamic perfusion-based blood brain barrier model for cytotoxicity testing and drug permeation. The BBB symposium, The Open University, Milton Keynes (2019).

A dynamic perfusion-based blood brain barrier model for cytotoxicity testing and drug permeation. Advanced Cell and Tissue Culture (ACTC), virtual (2020).

A dynamic perfusion-based blood brain barrier model for cytotoxicity testing and drug permeation. Kirkstall monthly webinar, virtual (2020).

List of Contents

Acknowledgements	3
List of Publications	4
List of Abstracts	4
List of Oral Presentations	4
List of Contents	5
List of figures	12
List of tables	15
Chapter 1	16
Introduction	16
1.1 Cancer biology and pharmacology	17
1.1.1 Formation of reactive oxygen species (ROS) in cancer	20
1.1.2 Apoptosis in cancer	22
1.1.2.1 Caspases: the executioners of apoptosis	23
1.1.3 Migration, invasion, and metastasis	24
1.1.4 Histological classification of cancers	24
1.2 Cancers of the central nervous system	25
1.3 Drug delivery to brain tumours	28
1.3.1 The blood brain barrier (BBB)	29
1.3.2 The blood tumour barrier (BTB)	32
1.3.3 Drug transport across the BBB.....	33
1.3.4 Drug transport across the BTB.....	36
1.4 The ABC family of efflux transporters	37
1.4.1 The role of ABC transporters in influencing tumour phenotype and progression.....	41
1.4.2 Breast Cancer Resistance Protein: A key transporter at the BBB.....	42
1.4.3 Modulation of ABC efflux transporter activity	44
1.5 Natural product phytochemicals	46
1.5.1 Flavonoids as ABC transporter modulators at the BBB and the BTB	48
1.5.2 Anti-cancer properties of phytochemicals	50
1.6 Cellular models of the glioblastoma	52
1.6.1 Human U251 glioma models	52
1.6.2 Human U87 glioma models	53
1.6.3 Rat C6 glioma models	53
1.6.4 Human LN229 glioma model.....	54
1.7 <i>In-vitro</i> models of the blood-brain barrier	54
1.7.1 Immortalised cellular models.....	54
1.7.1.1 Human origin models	54
1.7.1.2 Rodent origin models	55
1.7.1.3 Bovine based models.....	56
1.7.1.4 Porcine based models	56
1.7.2 Primary porcine based model.....	57
1.8 Limitations of current BBB cell culture models	58
1.8.1 The impact of shear stress on BBB phenotype	59

1.8.2 Dynamic <i>in-vitro</i> blood brain barrier models	61
1.8.2.1 Hollow fibre models	61
1.8.2.2 Microfluidic platforms	62
1.8.2.3 Perfusion based interconnected chamber	63
1.9 Thesis aims and objectives	65
Chapter 2	68
Phytochemical mediated modulation of breast cancer resistance protein in human glioblastoma cells	68
2.1 Background	69
2.2 Aims and objectives	77
2.3 Materials	78
2.4 Methods	78
2.4.1 Culture of LN229 human glioblastoma cells	78
2.4.2 Methylthiazol diphenyl tetrazolium bromide (MTT) assay	79
2.4.3 Intracellular accumulation of the fluorescent BCRP probe substrate, Hoescht-33342	79
2.4.4 Cellular migration assay	80
2.4.5 The impact of phytochemicals on the expression of BCRP using Western blotting ..	80
2.4.6 Radical oxygen species (ROS) detection assay	82
2.4.7 The activation of Caspase-3/7 pathways	82
2.5 Statistical Analysis	83
2.6 Results	84
2.6.1 Assessing the cellular toxicity of the phytochemicals in LN229 cells	84
2.6.2 Cellular toxicity of methotrexate and temozolomide towards LN229 cells	84
2.6.3 Modulator mediated inhibition of BCRP efflux function in a Hoechst H33342 intracellular accumulation assay	87
2.6.4 Cellular migration of LN229 in the presence of flavonoids	91
2.6.5 The effect of the modulators on the expression of BCRP	94
2.6.6 The impact of flavonoids in modulating ROS pathways	97
2.6.7 The impact of flavonoids to modulate Caspase-3/7 activity	98
2.7 Discussion	100
2.7.1 Cellular toxicity of modulators towards LN229 cells	100
2.7.2 Hoechst-33342 intracellular accumulation assay	101
2.7.3 Cellular migration assay	101
2.7.4 Effect of the modulators on the expression of BCRP	102
2.7.5 Ability of hesperetin and baicalin to induce ROS production	103
2.7.5.1 Ability of hesperetin and baicalin to activate caspase pathways	104
2.8 Conclusion	106
Chapter 3	107
Enhancing the permeability of anti-cancer agents across an in-vitro BBB model by modulation of BCRP using hesperetin	107
3.1 Background	108
3.2 Aims and objectives	110
3.3 Materials	111

3.4 Methods	111
3.4.1 Development of an <i>in-vitro</i> permeable insert BBB model.....	111
3.4.1.1 Culture of C6 rat astrocytes	111
3.4.1.2 Culture of immortalised PBMEC/C1-2	112
3.4.1.3 The impact of species-specific collagen on the formation of a robust BBB model	113
3.4.2 Isolation of porcine brain capillaries	113
3.4.3 Growth of PBMEC cells.....	114
3.4.4 Development of a PBMEC <i>in-vitro</i> BBB model.....	115
3.4.4.1 Immunostaining detection of ZO-1 and F-actin in PBMECs <i>in-vitro</i> BBB model	116
3.4.5 Cellular toxicity in PBMECs.....	117
3.4.6 Transport of methotrexate, mitoxantrone and hesperetin across PBMECs <i>in-vitro</i> BBB model	117
3.4.6.1 Lucifer yellow permeability assay	118
3.4.7 High pressure liquid chromatography detection of compounds	119
3.4.7.1 HPLC-UV detection of hesperetin	119
3.4.7.2 HPLC-UV detection for methotrexate	119
3.4.8 Fluorescence detection of mitoxantrone	120
3.5 Statistical analysis	120
3.6 Results	120
3.6.1 The impact of species-specific collagen on the formation of a robust BBB model..	120
3.6.2 Cellular morphology and culturing of primary brain microvascular endothelial cells (PBMEC)	121
3.6.3 Development of a PBMEC <i>in-vitro</i> BBB model.....	122
3.6.3.1 Lucifer yellow permeability assay	123
3.6.3.2 Immunocytochemistry of tight junction protein ZO-1 and F-actin.....	124
3.6.4 Cytotoxicity assays.....	127
3.6.4.1 Cellular toxicity of methotrexate towards PBMEC	127
3.6.4.2 Cellular cytotoxicity of mitoxantrone	127
3.6.4.3 Cellular cytotoxicity of hesperetin	128
3.6.4.4 Cellular toxicity of methotrexate in the presence of hesperetin	129
3.6.4.5 Cytotoxicity of mitoxantrone in combination with hesperetin	130
3.6.5 HPLC-UV detection for hesperetin	131
3.6.6 HPLC-UV detection for methotrexate.....	133
3.6.7 Fluorescence detection of mitoxantrone	135
3.6.8 Modulating the efflux action of BCRP to enhance the permeability of methotrexate and mitoxantrone across an <i>in-vitro</i> BBB model	136
3.6.8.1 Methotrexate permeability across an <i>in-vitro</i> BBB model	137
3.6.8.2 Hesperetin permeability across an <i>in-vitro</i> BBB model.....	138
3.6.8.3 Assessing the impact of hesperetin on the modulating the permeability of methotrexate across an <i>in-vitro</i> BBB model.....	139
3.6.8.4 Mitoxantrone permeability across an <i>in-vitro</i> BBB model	140
3.6.8.5 Assessing the impact of hesperetin on the modulating the permeability of mitoxantrone across an <i>in-vitro</i> BBB model.....	141
3.6.8.6 Changes in the basolateral to apical flux of anti-cancer agents in the presence of hesperetin	142
3.7 Discussion	143
3.7.1 The impact of species-specific collagen on immortalised PBMEC/C1-2 growth.....	144
3.7.2 Developing an <i>in-vitro</i> BBB permeable insert model.....	145
3.7.3 Assessing the cytotoxicity of methotrexate, mitoxantrone and hesperetin in PBMECs	147
3.7.4 Assessing the permeability of methotrexate and mitoxantrone in the presence and absence of hesperetin.....	148
3.8 Conclusion:	151

Chapter 4	152
A dynamic perfusion- based in-vitro model to enhance BBB characteristics	152
4.1 Background:	153
4.2 Aims and objectives	157
4.3 Materials:	158
4.4 Methods	158
4.4.1 Isolation of porcine brain capillaries	158
4.4.2 Development of PBMEC <i>in-vitro</i> BBB model under static conditions	158
4.4.3 Preparation of the QV600 perfusion system	158
4.4.4 Determination of optimal flow rate.....	160
4.4.5 Cellular viability in the presence of shear stress	161
4.4.6 The impact of shear stress on the BBB <i>in-vitro</i> model	161
4.4.7 Mitoxantrone transport assay	Error! Bookmark not defined.
4.4.8 Permeability of hesperetin across the <i>in-vitro</i> BBB model, developed under shear stress.....	162
4.5 Statistical analysis	162
4.6 Results	163
4.6.1 Identification of optimal sheer stress	163
4.6.2 Cellular viability under shear stress.....	167
4.6.3 Assessment of the impact of shear stress on the trans epithelial electrical resistance of PBMECs <i>in-vitro</i> BBB model	167
4.6.4 Tight junction formation and cellular reorganisation under shear stress	170
4.6.5 Mitoxantrone permeability across PBEMCs BBB <i>in-vitro</i> model under static and dynamic conditions	174
4.6.6 Hesperetin permeability across a PBEMC <i>in-vitro</i> BBB model, under static and dynamic conditions.....	177
4.7 Discussion	179
4.7.1 The effect of shear stress on the morphology and viability of PBMEC grown on coverslips	179
4.7.2 The impact of shear stress on the development PBMECs <i>in-vitro</i> BBB characteristics	181
4.7.3 The impact of shear stress on small molecule transport.....	183
4.8 Conclusion	184
Chapter 5	187
Conclusions and future work	187
5.1 Conclusion	188
5.2 Future works	190
References	192
Appendix A: Chemical structures	240

List of abbreviations

Abs	Absorbance
AhR	Aryl hydrocarbon receptor
ALI	Air liquid interface
AMT	Adsorptive mediated transcytosis
ATP	Adenosine triphosphate
Bax	Bcl-2-associated X protein
BBB	Blood brain barrier
Bcl-2	B-cell lymphoma-2
Bcl-xl	B-cell lymphoma- extra large
BCRP	Breast cancer resistant protein
BSA	Bovine serum albumin
BTB	Blood tumour barrier
C	Celsius
cAMP	Cyclic adenosine monophosphate
CAR	Constitute androstane receptor
cm	Centimetre
CO₂	Carbon dioxide
Da	Dalton
EGCG	Epigallocatechin gallate
GBM	Glioblastoma multiforme
GFAP	Glial fibrillary acidic protein
GLUT-1	Glucose Transporter-1
GLUT-3	Glucose Transporter-3
GPX	Glutathione peroxidase

h	Hour
HGF	Hepatocyte growth factor
HIFS	Hypoxia inducing factors
HPLC	High pressure liquid chromatography
ICAM-1	Intracellular adhesion molecule -1
JAMs	Junctional adhesion molecules
LAT-1	Large neutral amino acid transporter-1
LOD	Limit of detection
LOQ	Limit of quantification
MDR	Multi drug resistance
mg	Milligram
μM	Micro molar
MMP-3	Matrix metalloproteinases-3
MMP-9	Matrix metalloproteinases-9
MRP-1	Multidrug resistance-associated protein-1
MTT	Dimethylthiazol diphenyltetrazolium bromide
NADP	Nicotinamide adenine dinucleotide phosphate
NBD	Nucleotide binding domain
Ω	Ohm
P-gp	Permeability glycoprotein
PBMECs	Porcine brain microvasculites endothelial cells
PBS	Phosphate buffered saline
PDSM	Polydimethylsiloxane
PECAM-1	Platelet endothelial cell adhesion molecule-1
PG	Prostaglandins

PI3K	Phosphoinositide 3-kinase
PS	Phosphatidyl serine
PTEN	Phosphatase and tensin homolog
PVDF	Polyvinylidene difluoride
PXR	Pregnane-X-receptor
ROS	Reactive oxygen species
s	Seconds
SDS	Sodium dodecyl sulphate
SFM	Serum free media
SOD	Superoxide dismutase
TBST	Tris-buffered saline
TIGAR	Tp53-induced glycolysis and apoptosis regulator
TJ	Tight junction
TMD	Transmembrane domain
TP53INP1	Tumour protein p53-inducible nuclear protein 1
TRAIL	Tumour necrosis factor related apoptosis inducing legend
VCAM-1	Vascular cell adhesion molecule-1
VEGF	Vascular endothelial growth factor
ZO-1	Zonula occludens-1

List of Figures

Figure 1.1 Six hallmarks of cancer	19
Figure 1.2 Emerging cancer hallmarks	20
Figure 1.3 Location of different types of brain tumour.....	27
Figure 1.4 The neurovascular unit.....	31
Figure 1.5 Endothelial tight junction and adhesion junction structure	32
Figure 1.6 Transport pathways in the blood-brain barrier	35
Figure 1.7 A typical structure of an ABC transporter	41
Figure 1.8 The structure of breast cancer resistance protein (BCRP)	43
Figure 1.9 Basic structure of flavonoids	47
Figure 1.10 Normal stress compared to shear stress.....	60
Figure 1.11 Hollow fibre BBB model using PBMEC1/2.....	62
Figure 1.12 Schematic representation of a microfluidic based model.....	63
Figure 1.13 The Quasi vivo® 500 system.....	64
Figure 1.14 The Quasi vivo® 600 system.....	65
Figure 2.1 Cellular cytotoxicity of modulators of BCRP in LN229 cells.....	85
Figure 2.2 Cellular cytotoxicity of methotrexate and temozolomide in LN229	87
Figure 2.3 H33342 accumulation assay for BCRP function in LN229 cells.	88
Figure 2.4 Cellular migration assay	92
Figure 2.5 Changes on BCRP expression after 24-hour incubation with the modulators.....	95
Figure 2.6 Fold change in BCRP expression.....	96
Figure 2.7 Radical oxygen species detection assay.....	97

Figure 2.8 Caspase-3/7 assay	99
Figure 3.1 TEER measurements following growth of PBMEC1/2 on permeable cell culture inserts	121
Figure 3.2 Morphology of PBMEC cultured on bovine collagen coated plasticware.....	122
Figure 3.3 TEER measurement of PBMECs on 12 well permeable insert	123
Figure 3.4 Lucifer yellow permeability assay	124
Figure 3.5 ZO1 Immunocytochemistry images for PBMEC.....	125
Figure 3.6 F-Actin Immunocytochemistry images for PBMEC	126
Figure 3.7 Cellular toxicity of methotrexate.....	127
Figure 3.8 Cellular toxicity of mitoxantrone	128
Figure 3.9 Cellular toxicity of hesperetin	129
Figure 3.10 Cellular cytotoxicity of methotrexate in combination with hesperetin	130
Figure 3.11 Cellular cytotoxicity mitoxantrone in combination with hesperetin	131
Figure 3.12 HPLC chromatogram for hesperetin	132
Figure 3.13 HPLC linearity calibration plot for hesperetin.....	133
Figure 3.14 HPLC chromatogram for methotrexate	134
Figure 3.15 HPLC linearity calibration plot for methotrexate.....	135
Figure 3.16 Fluorescence detection linearity calibration plot for mitoxantrone	136
Figure 3.17 The permeability of methotrexate across an <i>in-vitro</i> BBB model established with PBMEC grown on permeable inserts.....	137
Figure 3.18 The permeability of hesperetin across an <i>in-vitro</i> BBB model established with PBMEC grown on permeable inserts	138
Figure 3.19 The permeability of methotrexate across an <i>in-vitro</i> BBB model established with PBMEC grown on permeable inserts.....	139
Figure 3.20 The permeability of mitoxantrone across an <i>in-vitro</i> BBB model established with PBMEC grown on permeable inserts.....	140

Figure 3.21 The permeability of mitoxantrone across an <i>in-vitro</i> BBB model established with PBMEC grown on permeable insert, in the presence of hesperetin	141
Figure 3.22 The apparent permeability (A) and efflux ratio (B) of methotrexate and me mitoxantrone in the absence and presence of hesperetin	142
Figure 4.1 Diagrammatical representation of the QuasiVivo® 600.....	159
Figure 4.2 Immunocytochemistry images obtained following ZO-1 staining under static conditions on coverslips	164
Figure 4.3 Immunocytochemistry images obtained following ZO-1 staining following exposure to low flow rate on coverslips	165
Figure 4.4 Immunocytochemistry images obtained following ZO-1 staining following exposure to high flow rate on coverslips	166
Figure 4.5 Cellular viability of PBMECs grown in static and dynamic conditions	167
Figure 4.6 TEER measurements under static and dynamic conditions ...	169
Figure 4.7 Immunocytochemistry images obtained following ZO-1 staining under static conditions in inserts.....	171
Figure 4.8 Immunocytochemistry images obtained following ZO-1 staining following exposure to high flow in inserts for 24 hours	172
Figure 4.9 Immunocytochemistry images obtained following ZO-1 staining following exposure to high flow in inserts for 48 hours	173
Figure 4.10 ZO-1 junctional fluorescence intensity	174
Figure 4.11 Mitoxantrone flux across PBMEC grown on permeable insets	176
Figure 4.12 Hesperetin flux across PBMEC grown on permeable inserts	178

List of Tables

Table 1.1 Examples of gene mutations in cancer	18
Table 1.2 Subfamily members of the caspase family	23
Table 1.3 Classification of CNS tumours grades I,II,III and IV based on the molecular phenotype (Louis et al., 2016).....	27
Table 1.4 Examples of influx transporters and substrates	37
Table 1.5 Examples of flavonoids and food source	47
Table 2.1 phytochemicals reported anti-cancer proprieties, blood brain barrier permeability and interaction with members of the ABC efflux transporter family NR: Not Reported	73
Table 3.1 System precision and method precision for UV-HPLC detection of hesperetin.....	132
Table 3.2 System precision and method precision for UV-HPLC detection of methotrexate	134

Chapter 1

Introduction

1.1 Cancer biology and pharmacology

The term 'cancer' can be defined as a group of cells that grow at an uncontrollable rate disregarding tenets of cell division. In healthy mammals, cells are subjected to many signals that direct them to either divide, differentiate or die. Cancer cells, however, are immune to these signals and consequently grow and proliferate uncontrollably. If cancer cells are allowed to grow and spread uncontrolled, the consequences can be deadly. Approximately 90% of cancer related mortalities are due to the dispersion of cancerous cells across the body, a process termed metastasis (Emuss, 2006). Tumours can be benign or malignant with malignant tumours being larger in size (> 3 cm) and capable of spreading at a greater rate than benign tumours (Shields et al., 2017).

The cell cycle is normally stringently controlled by various regulatory pathways therefore, it is not surprising that genes responsible for cell cycle regulation are often found mis-regulated and mutated in cancers (Table 1.1) (Collins et al., 1997, Malumbres and Barbacid, 2009, Kastan and Bartek, 2004). Genes where a mutation leads to a gain or an increased level in function which results in malignancies, are called protooncogenes and typically encode for growth promoting proteins. Genes that lead to a reduced or loss in function, typically result in malignancies and are termed tumour suppressor genes, encoding negative regulation of growth (De Vita and Lawrence, 2011).

Table 1.1 Examples of gene mutations in cancer

Gene	Protein	Function	Alteration in cancer
CCND1,2,3	D cyclins	Positive regulator of CDK4/6	Overexpressed
CCNE1	Cyclin E1	Positive regulator for CDK2	Overexpressed, deregulated
RB1	pRb	Repress E2f transcription	Mutated, deleted
TP53	p53	Check points, apoptosis	Mutated, deleted
MTBP	MDM-2	Inhibitor of p53	Overexpressed
CDKN2A	p14 <i>Arf,a</i>	Activator of p53	Mutated, deleted
ATM	ATM	Checkpoints, repair	Mutated, deleted

Table adapted from (De Vita and Lawrence, 2011)

Hanahan and Weinberg (2000) suggested that there are six hallmarks of cancer that, when combined together, result in a malignant growth (Figure 1.1). These were updated a decade later to include 4 additional emerging hallmarks (Figure 1.2). Each of these physiological deviations obtained during tumour development signifies a complication in the anti-cancer defence mechanism. While cancers arising from different tissues have some differences, it is assumed that most, if not all human cancers share these ten hallmarks (Hanahan and Weinberg, 2000, Hanahan and Weinberg, 2011).

Cancer cells have a high rate of proliferation and cell growth, consequently, they require a high level of amino acids, lipids, nucleotides, and energy. To fulfil that high demand of energy levels, oxidative phosphorylation and glycolysis are promoted which leads to an increase in the production of ATP. This insures the survival of cancer cells (Tennant et al., 2009).

Cancer cells not only need glucose to produce energy, but also utilise it under hypoxic conditions to regulate various pathways that affect cancer progression.

One of these pathways include metabolic adaptation. Cancer cells undergo metabolic adaptation when the tumour microenvironment is derived of any oxygen supply (hypoxic conditions), and therefore glucose transport genes such as GLUT1 and GLUT3 are promoted. As a result of metabolic adaptation, an increase in reactive oxygen species (ROS) production occurs which can activate hypoxia inducible factors (HIFs), which play an essential role in cancer initiation, proliferation and growth (Dang et al., 2008, Bertout et al., 2008). This metabolic imbalance and the pro-oxidative state of cancer cells is supported and maintained by many changes in the cellular metabolic activity, oncogenic alteration and as a result, the loss of the functions of tumour suppressor genes such as p53 (Pelicano et al., 2004).

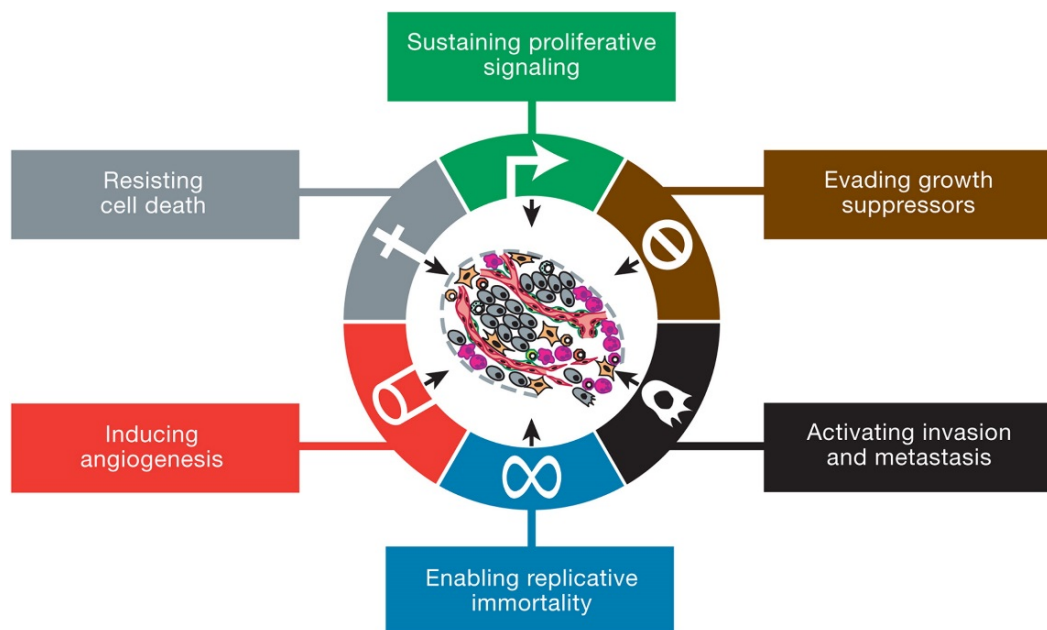


Figure 1.1 Six hallmarks of cancer

The six hallmarks are: (i) evading cell death (apoptosis); (ii) self-sufficiency in growth signals; (iii) insensitivity to anti-growth signals; (iv) tissue invasion and metastasis; (v) sustained angiogenesis and (vi) unlimited replicative power (Hanahan and Weinberg, 2000)

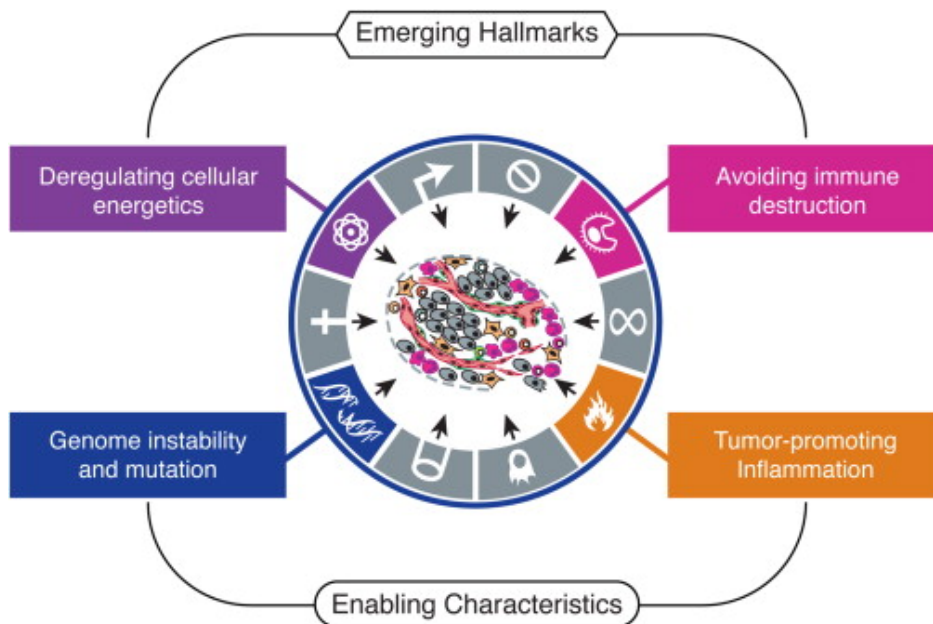


Figure 1.2 Emerging cancer hallmarks

The 4 additional hallmarks that were later updated are, (i) avoiding immune destruction, (ii) tumour promoting inflammation, (iii) genome instability and mutation and (iv) deregulation of cellular energetics (Hanahan and Weinberg, 2011).

1.1.1 Formation of reactive oxygen species (ROS) in cancer

Persistent intrinsic oxidative stress is one of the main features of cancer cells. Excessive ROS generation was reported in *in-vitro* cancer models such as breast and ovarian cancer, melanoma, pancreatic carcinoma, and neuroblastoma, where an increase in hydrogen peroxide has been reported when compared to healthy tissue (Szatrowski and Nathan, 1991, Liou and Storz, 2010).

Cellular ROS can be generally divided into two main categories: (i) ROS generation as a byproduct of biological processes such as mitochondrial oxidative metabolism (Finkel, 2011, Grivennikova and Vinogradov, 2013); (ii) intentional ROS generation as a cellular response or cell defence mechanism to xenobiotics, bacterial invasion and cytokines (Starkov, 2008, Zakki et al., 2018).

ROS at appropriate levels has been shown to play an integral role in the modulation of numerous physiologic responses as part of regulating cells signalling (Schieber and Chandel, 2014, Liu et al., 2008). Within the normal threshold of ROS in healthy cells, ROS acts as a signal for peroxide mediated oxidation of protein cysteine residues which can trigger cell proliferation (Schieber and Chandel, 2014). In addition, it mediates DNA repair by inducing p53 (Liu et al., 2008). However, if production of ROS exceeds that threshold and is no longer controlled by the redox homeostasis, oxidative DNA damage can occur which leads to cells death.

An increase in intracellular ROS levels, in addition to a flawed antioxidant system, can lead to the rise of pathological conditions (Rhee, 2006) such as cancer (Dhillon et al., 2014), inflammation (Nijland et al., 2014) heart disease (Dhar and Prasad, 2014) and diabetes (Rehman et al., 2014). Increased ROS production within the cell leads to the depolarisation of the mitochondria which releases cytochrome C. Normally, cytochrome C contributes to the synthesis of ATP, however when the cell receives an apoptotic signal, cytochrome C is released into the cytosol which triggers cell death. This process involves the induction of caspase-9 which stimulates nucleotide binding to APAF-1 (apoptotic protein activation factor 1), that results in the activation of caspase (NavaneethaKrishnan et al., 2018). Increased ROS levels have also been associated with the mediated cleavage of caspase-3 via triggering caspase-8 (Redza-Dutordoir and Averill-Bates, 2016). In cancer cells, ROS generation elevates the rate of mutagenicity and leads to chromosomal instability, DNA base pairs damage and hence promotes cancer progression (Radisky et al., 2005, Samper et al., 2003). Oxidative stress also plays a role in inactivation of apoptotic proteins by upregulating anti-apoptotic genes such as Bcl-2 (McCubrey et al., 2007). Additionally, ROS generation in cancer cells can participate in the metastatic process by stimulating the cells to invade surrounding healthy tissue, form new blood vessels (angiogenesis) and eventually migrate to new locations (Mori et al., 2004, Coussens and Werb, 1996).

1.1.2 Apoptosis in cancer

Apoptosis is an orchestrated and well organised process that occurs in pathological and physiological conditions (Wong, 2011). In cancer, there is an imbalance between cell proliferation and cell death, with cells that otherwise are due to undergo apoptosis, fail to receive an appropriate cascade signal and develop the ability to evade the apoptosis regulatory process (Wong, 2011).

TP53, which codes for p53, is one of the most studied tumour suppressor genes due to its ability to regulate cellular metabolism, transcriptional processes, genomic stability, proliferation, autophagy, and apoptosis (McCubrey et al., 2007, Budanov, 2014). In normal cells, p53 can increase the expression of various antioxidant genes such as the tumour protein p53-inducible nuclear protein 1 (TP53INP1), TP53-induced glycolysis and apoptosis regulator (TIGAR) (Cano et al., 2009, Sablina et al., 2005). In p53 depleted cancer cells, there is an absence of p53 dependant antioxidant regulators which leads to a surge in oxidative stress within the cells permitting ROS build-up.

p53 mutation is one of the most common genetic abnormalities in cancer patients and is regarded as a hallmark of cancer (Kumar and Pandey, 2013), with a mutated p53 protein leading to triggering of apoptosis in addition to lack of cell proliferation control.

Three key biochemical changes occur during apoptosis, namely: (i) DNA and protein break down, (ii) activation of caspases and (iii) membrane changes and recognition by phagocytic cells (Wong, 2011). Early in the apoptotic process, phosphatidylserine (PS), present in the inner layer of the cell membrane, undergoes reorientation to the outer layers of the cell membrane allowing for its recognition by macrophages which lead to phagocytosis. Thereafter, DNA break down takes places where 50-300 kilobase pieces are formed (Vaux and Silke, 2003). Afterwards, endonucleases cleave the inter-nucleosomal DNA into multiple 180 to 200 base pair fragments (Vaux and Silke, 2003, McCarthy and Evan, 1998).

Morphologically, the presence of chromatin condensation and nuclear fragmentation are considered hallmarks of apoptosis. This is usually accompanied by rounding up of the cell, retraction of pseudopods and pyknosis (Kroemer et al., 2009). The cell membrane remains intact throughout the apoptotic process, however, in the later stages of apoptosis, loss of cell membrane integrity and membrane blebbing takes place; a process ending with phagocytes consuming the cell before apoptotic bodies emerge (Ziegler and Groscurth, 2004, Kroemer et al., 2009, Wong, 2011).

1.1.2.1 Caspases: the executioners of apoptosis

Caspases are cysteine proteases that are synthesised as inactive proenzymes known as procaspases, with a pro-domain N-terminal and two subunits, one large and one small (Cohen, 1997). There are 14 members of the caspases family, 11 of which are found in humans and are divided into 3 subfamilies (Table 1.2) (Friedlander, 2003). A process that is characteristic to apoptosis is the activation of caspases. Caspases are a group of cysteine protease enzymes when activated, the N-terminal is cleaved and a heterodimer is formed from the small and the large subunits (Fan et al., 2005). Active caspases cleave vital proteins and nuclear cytoskeleton as well as activating DNase which further breaks down nuclear DNA (Lavrik, 2005, Shalini et al., 2015).

Table 1.2 Subfamily members of the caspase family

Subfamily	Role	Caspase members
I	Apoptosis activator	2, 8, 9, 10
II	Apoptosis executioner	3, 6, 7
III	Inflammatory mediator	1, 4, 5, 11, 12, 13, 14

Table adapted from (Fan et al., 2005)

1.1.3 Migration, invasion, and metastasis

A feature of malignant tumours is their ability to initiate a unique, multi-stage biological phenomenon known as the “metastatic cascade” where cell invasion is a major trigger and a critical factor for additional cancer progression and metastasis in the surrounding and/or distant tissue and organs (Krakhmal et al., 2015, van Zijl et al., 2011).

Cellular migration requires the formation of cytoplasmic lamellipodia and filopodia extensions which are controlled by actin filaments. These are used to promote polarized morphology. At the ends of the lamellipodia, cells are connected to the extracellular matrix through the actin cytoskeleton network and this allowed anchorage of the cytoplasmic extensions. A consequence of this is the ability to drag the cell body (Le Clairche and Carlier, 2008).

Metastasis is a term used to describe the spread of cancer cells from the originating or primary tumour site to neighbouring tissue and distant organs (Tarin, 2011, Chambers et al., 2002). Cancer metastases is considered the main cause of cancer related mortalities which is estimated to be at 90% (Chaffer and Weinberg, 2011). For metastasis to occur, cancer cells must first detach from the originating tumour site, enter the circulatory and lymphatic systems, avoid immune attack, extravasate at a distant capillary network and then invade and divide in new organs (Welch and Hurst, 2019, Bacac and Stamenkovic, 2008). Metastatic cancer cells have the ability to create a microenvironment that enables proliferation and angiogenesis, which results in the formation of malignant secondary tumours (Lazebnik, 2010, Seyfried et al., 2014).

1.1.4 Histological classification of cancers

The National Cancer Institute (NCI) classifies cancers based on the type of tissue from which the cancer originates (histological) or by the site (organ) which the cancer first appears (NCI, 2021).

There are six major histological origins:

- i) **Carcinomas** are cancers that arise from epithelial tissue and can appear in the breast, prostate, lung, and colon. They account for more than 80% of reported cancer cases.
- ii) **Sarcomas** arise from connective tissue such as bones, cartilages, fat and muscles. Sarcomas usually occur in younger individuals, examples include, fibrosarcoma, chondrosarcoma and osteogenic sarcoma.
- iii) **Myeloma** is a cancer that originates in plasma cells of bone marrow.
- iv) **Leukaemia** refers to liquid cancers and usually begins in the bone marrow.
- v) **Lymphoma** is the type of cancer that develops in the glands or nodules of the lymph system, lymphomas are known as solid cancers and can occur in specific organs such as the stomach or the brain.
- vi) **Mixed origin** cancers are those that arise from more than one tissue such as carcinosarcoma, teratocarcinoma and mixed mesodermal tumour.

1.2 Cancers of the central nervous system

Worldwide, 250,000 cases of brain and CNS tumours are diagnosed every year, this makes up 3% of all cancer cases (Miranda-Filho et al., 2016). CNS cancers are ranked as the 8th overall cause of death in the UK (Parrish et al., 2015), and have had an increased incidence of 39% since the 1990s. They are the leading cause of cancer death in men under 40 years old and women under 20 years old (Siegel et al., 2020). In the UK, 30 cases of brain and other CNS tumours are diagnosed every day with a reported mortality rate of approximately 52% for malignant brain tumours.

Gliomas are divided into 4 grades: (i) **Grade 1** are slow growing, unlikely to spread and can be cured with surgical removal; (ii) **Grade 2** are less likely to metastasis but more likely to re-occur after treatment; (iii) **Grade 3** have a rapid rate of proliferating cells and can rapidly grow; (iv) **Grade 4** cells have a high proliferation rate as well as the presence of blood vessel growth and areas of necrotic cells, in addition to being highly likely to metastasise.

The most aggressive and most common is grade 4, which is also known as glioblastoma multiforme (GBM). These tumours have garnered significant attention given that most patients with GBM die within 12 month of diagnosis (Holland, 2000).

The main mode of treatment for GBM has remained unchanged for decades, commencing with surgical removal of the tumour mass, followed by radiotherapy and chemotherapy (Holland, 2000, Abbruzzese et al., 2017). Assuming all of the tumour tissue was surgically removed and followed up with radiation and chemotherapy, the survival rate of the patient can extends by up to 15 month and a 5-year survival rate from diagnosis of less than 5% (Abbruzzese et al., 2017).

Variations exist in the types of gliomas, and this is dictated by the molecular phenotype (Table 1.3). CNS tumours exist and are location specific, for example, meningiomas (tumour of the meninges), schwannomas (benign tumours similar to meningiomas), medulloblastomas (found near the midline of the cerebellum) and craniopharyngiomas (benign tumours at the base of the brain) (Behin et al., 2003, Cohen and Weller, 2007, Louis et al., 2016) (Figure 1.3).

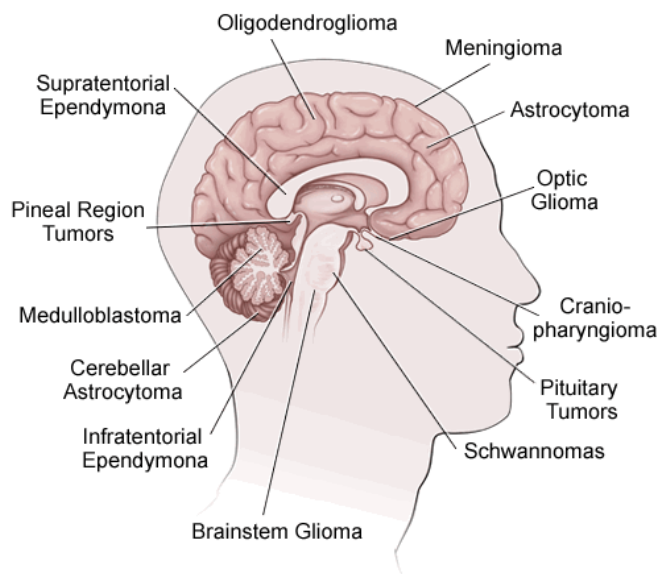


Figure 1.3 Location of different types of brain tumour

Location and types of CNS tumours include (UH, 2018).

Table 1.3 Classification of CNS tumours grades I,II,III and IV based on the molecular phenotype (Louis et al., 2016)

Grade	WHO grades of select CNS tumours
I	Pilocytic astrocytoma, subependymoma giant cell astrocytoma, subependymoma, myxopapillary ependymoma, angiocentric glioma, choroid plexus papilloma, gangliocytoma, ganglioglioma, schwannoma, neurofibroma, perineurioma, meningioma, spindle cell oncocytoma, pituicytoma, granular cell tumour, craniopharyngioma, pineocytoma and haemangioblastoma.
II	Ependymoma, pleomorphic xanthoastrocytoma, choroid glioma of third ventricle, atypical choroid plexus papilloma, central neurocytoma, extra ventricular neurocytoma, cerebellar liponeurocytoma, atypical meningioma and papillary tumour of the pineal region.
III	Anaplastic pleomorphic xanthoastrocytoma, anaplastic ependymoma, choroid plexus carcinoma, anaplastic ganglioglioma, pineal parenchymal

	tumour of the intermediate deafferentation, papillary tumour of the pineal region, anaplastic meningioma and haemangiopericytoma
IV	Glioblastoma IDH-wildtype, glioblastoma IDH-mutant, diffuse midline glioma H3K27M-mutant, pineoblastoma, medulloblastoma, medulloepithelioma, CNS embryonal tumour, atypical teratoid tumour and malignant peripheral nerve sheath tumour MPNST.

The most common type of primary brain cancer originates from glial cells and are termed glioblastoma multiform (GBM). Glial cells include microglia, astrocytes and oligodendrocyte lineage cells and they make up a large portion of the human brain (Jäkel and Dimou, 2017). Similar to other cancers, GBM is thought to arise from stem cells, more precisely from precursor cells that otherwise create glia and neurons (Zong et al., 2012). The standard treatment for GBM is typically surgical resection, followed by radiotherapy and finally a treatment with an alkylating agent such as temozolomide.

Furthermore, the highly malignant nature of glioblastomas is mainly a result of the excessive cell proliferation and invasion of surrounding brain tissue, in addition to suppression of any immune anti-tumour response. Tumour invasion to surrounding tissues occurs where neoplastic cells initiate migration while adhering to the extracellular matrix (ECM) starting at the primary tumour site. These cells then degrade the ECM through the secretion of proteolytic enzymes such as matrix metalloproteinases (MMPs) and then invade normal tissue (Demuth, T. and Berens, M.E. 2004; Singh, R.D. et al., 2010).

1.3 Drug delivery to brain tumours

Generally, the number of hydrogen bond donors and the ability of a compound to form hydrogen bonds can significantly impact their ability to penetrate into the CNS. Moderately lipophilic molecules are thought to cross the BBB through passive diffusion (Pajouhesh and Lenz, 2005). Molecules with high polarity are poor CNS agents unless they undergo active transport to penetrate the CNS. The

size of molecules, ionisation and molecular flexibility are other factors that affect transport of compounds across the BBB (Mouritsen and Jørgensen, 1998).

In 1997, Christopher Lipinski assessed the physicochemical characteristics of clinical drug candidates and proposed the 'rule of 5' that could predict the possibility of compounds to permeate through the BBB (Lipinski et al., 1997). The rule of five noted that in order for molecules to permeate across the BBB, they should possess the following key properties: (i) a molecular mass less than 500 Da; (ii) high lipophilicity with octanol-water partition coefficient (log P) less than 5; (iii) 5 or less hydrogen donating bonds; (iv) 10 or less hydrogen accepting bonds (Mikitsh and Chacko, 2014). Unfortunately, some chemotherapeutic agents, do not fall within this category and so drug delivery of chemotherapeutic agents requires a strategy to overcome this problem and be able to achieve clinically relevant drug concentration levels at the tumour site.

Since brain tumours are essentially located within the brain parenchyma, any systemically administered chemotherapeutic agents will have to permeate across the BBB and BTB in order to reach their target tumour site, hence limiting xenobiotic entry. The scarcity of effective CNS cancer therapeutics is often a result of poor delivery into CNS tissue as a result of the BBB and the BTB (Ganipineni et al., 2018, Arvanitis et al., 2020a).

1.3.1 The blood brain barrier (BBB)

The BBB was first described in the late 19th century by Paul Ehrlich, a German scientist who injected mice with a trypan blue dye and identified that the dye had stained all tissues except for the spinal cord and the brain. Later Edwin Codman conducted an experiment where trypan blue was injected into the cerebrospinal fluid and observed brain tissue staining only (Goldmann, 1912, Haseloff et al., 2005). These two experiments lead to the concept that the brain and other body organs were in distinct compartments separated by a barrier (Friedemann, 1942).

The BBB consists of cerebral endothelial cells, astrocyte end feet, pericytes, neurons and extracellular matrix. These together make up the neurovascular unit

(NVU) (Bagchi et al., 2019). Each component of the NVU is mutually connected to each other forming a highly efficient system that regulates cerebral blood flow. Each element of the NVU plays a distinct active role to maintain brain homeostasis (Bagchi et al., 2019) (Figure 1.4).

Neurons are known as the pacemaker of the neurovascular unit (Banerjee and Bhat, 2007), because of their highly sophisticated function where they are capable of detecting the smallest changes in nutrients and oxygen supply and in response send electrical and chemical messages to the vessels in order to return to normal physiological conditions, thus influencing the vasculature and blood supply to the adjoining areas (Figley and Stroman, 2011).

At first, the role of astrocytes was unknown, however, it was later demonstrated that astrocytes are incredibly versatile within the NVU, and possess the ability to communicate with both the neurons and blood vessels simultaneously (López-Bayghen and Ortega, 2011, Santello et al., 2012). It has been also reported that astrocytes have an effect on the formation of tight and adhesion junctions in the BBB and hence regulate the tightness of the barrier itself in addition to upregulating the expression of a range of transporters and enzymes within endothelial cells (Haseloff et al., 2005).

Pericytes are embedded within the basement membrane that covers 30% of the endothelium, and given their close contact to endothelial cells, they play a significant role in their development and maturation (Sá-Pereira et al., 2012). Much like astrocytes, the role of pericytes was unknown as they were considered as simple support cells (Armulik et al., 2010). However, it was displayed that they secrete adhesion molecules and growth factors as a response to ATP increase (Kawamura et al., 2003). Pericytes are also essential in controlling blood vessel proliferation, formation and are able to control the diameter of blood vessels to help modulate cerebral blood flow (Di Pietro et al., 2002, Peppiatt et al., 2006).

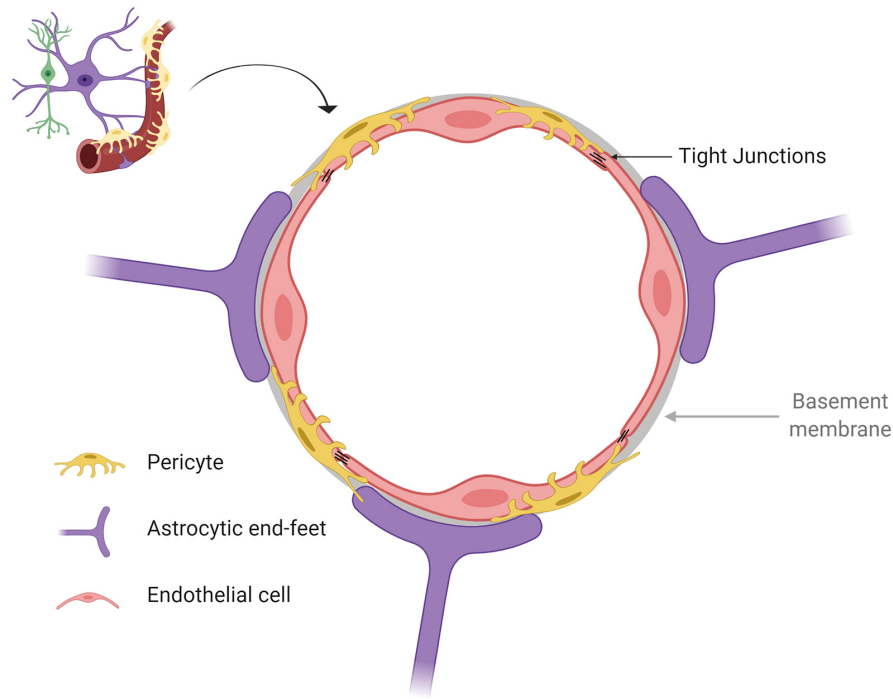


Figure 1.4 The neurovascular unit

The basement membrane surrounds the endothelial cells and embeds the pericytes. Endothelial cells are connected through tight junctions. Astrocyte end feet are connected with the endothelial cells (Delsing et al., 2020)

The BBB is formed primarily of microvascular endothelial cells that are tightly fused together and form a tight continuous lipid layer that heavily restricts free diffusion of drugs into the brain (Emanuelli et al., 2003, Duchemin et al., 2012). Key to the barrier function of the BBB is the presence of proteins termed ‘tight-junction’ proteins, which primarily serve to restrict paracellular diffusion of drugs between adjacent endothelial cells. Tight junctions (TJ) are formed by link zones between cells, in which the intercellular cleft is sealed. TJ are controlled and maintained by the expression of a range of proteins such as occludins, claudins and junctional adhesion molecules (JAM) (Figure 1.5).

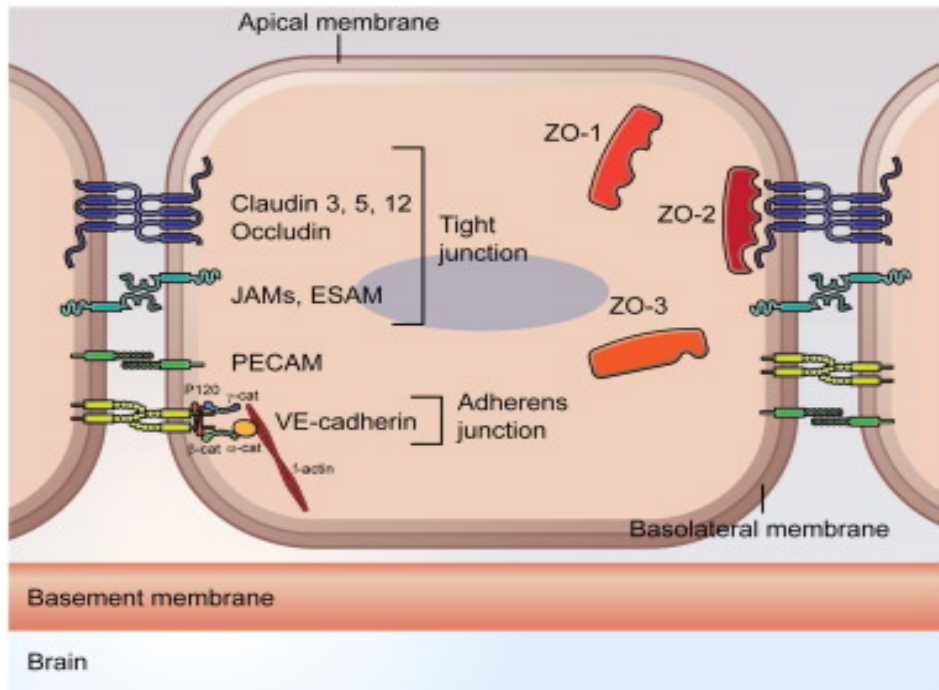


Figure 1.5 Endothelial tight junction and adhesion junction structure

Occludins and claudin proteins are the main components of TJs, ZO-1, -2, and -3 provide structural basis for the assembly of TJs. AJs and JAMS take part in the formation and maintenance of TJs (Derada Troletti et al., 2016)

1.3.2 The blood tumour barrier (BTB)

Under pathological conditions such as epilepsy, multiple sclerosis, AIDS, dementia and stroke, the performance and organisation of the BBB can be disturbed (de Vries et al., 2012, van Tellingen et al., 2015). This is also the case with brain cancers (Abbott et al., 2006). Changes in the barrier triggered by the presence of the tumour is not linked to tumour size, type or location and is different within every single neoplasm (van Tellingen et al., 2015). In low grade gliomas, the morphology and function of the BTB remains mostly intact and resemble that of the BBB. However, in high grade gliomas, as confirmed by MRI (Dhermain et al., 2010), there are major alterations of the normal vasculature of the BTB.

The BTB is a visibly distinctive barrier from the BBB and is formed by tumour capillaries. It is composed of three separate microvessel populations: (i) non-fenestrated and continuous much like normal brain capillaries; (ii) capillaries enclosing inter-endothelial gaps (iii) fenestrated and continuous capillaries (Groothuis, 2000, Schlageter et al., 1999, van Tellingen et al., 2015). Much like the BBB, endothelial cells of the BTB express drug efflux transporters from the ABC family such as *ABCG2/BCRP* (Aronica et al., 2005, Iorio et al., 2016) and *ABCB1/P-gp* (Lin et al., 2014), as well as other ABC efflux transporters (Arvanitis et al., 2020a, Bronger et al., 2005).

The BTB is considered a leaky barrier and is characterised by pericyte disruption, loss of neuronal connection and loss of astrocyte end feet (Dubois et al., 2014). In addition, tight junction proteins and stem cell derived pericytes are downregulated and pericyte cell coverage is disrupted (Dubois et al., 2014, Achrol et al., 2019, Cheng et al., 2013). This is indicated by the detection of peripheral monocytes and T-cell subpopulation in brain tumours suggesting the permeability of the neurovascular unit to circulating cells (Achrol et al., 2019). Moreover, the disruption in BBB permeability is evident by the detection of circulating brain tumour markers and the higher drug accumulation within brain tumours in comparison with unaltered brains (Arvanitis et al., 2020a). Despite these observations, the BTB maintains critical features of the BBB including the expression of active efflux transporters in endothelial and tumour cells (van Tellingen et al., 2015). It is worth noting that an intact BBB can be present in advanced glioblastoma cases displaying a variety of efflux transporters that restrict permeation of anti-cancer agents (Arvanitis et al., 2020a, van Tellingen et al., 2015, Sarkaria et al., 2018). Consequently, in both low-grade and high-grade glioblastomas, the BBB and the BTB form an arduous obstacle in brain tumour treatment by preventing the delivery of appropriate quantities of possibly effective chemotherapeutic agents (Juillerat-Jeanneret, 2008, Korfel and Thiel, 2007).

1.3.3 Drug transport across the BBB

In order for adequate amounts of chemotherapeutic agents to reach the sight of the tumour, bypassing the BBB is a prerequisite (Kim et al., 2018). The

primary function of the BBB is maintaining the homeostasis of the CNS by restricting the permeation of ions, molecules, fluids and cells between the blood and the brain, in addition to providing the brain with nutrients. The BBB also acts as a xenobiotic barrier through the presence of a significant network of membrane localised uptake/efflux transporter proteins responsible for the carrier-mediated transport of molecules (Abbott, 2005).

Two key pathways exist through which molecules are able to permeate across the BBB, namely transcellular pathways and paracellular pathways (Figure 1.5), both of which are primarily passive diffusion pathways. The paracellular route refers to movement of molecular across the endothelium by passing through intercellular spaces located between adjacent cells. In the BBB, this route is considered an essential and unique phenotype for the BBB as molecular diffusion is strictly controlled by TJs, which play a key role in regulating permeability across the BBB, whilst also maintaining the polarity of receptors and enzymes on the luminal and abluminal membrane domains (Banik et al., 2010).

In contrast, transcellular pathways allow passage of small lipophilic molecules across the lipid bilayer of the endothelial cells and is primarily a pathway for lipophilic, non-polar molecules (Pardridge, 2002).

Transcytosis refers to the transport of macromolecules from the apical to the basolateral side of the cell. This process takes place in different cells including endothelial cells and neurons (Pulgar, 2019). There are two types of transcytosis in the brain, receptor mediated transcytosis and adsorptive mediated transcytosis (Figure 1.6). Receptor mediated transcytosis (RMT) are specific receptors in the lumen of endothelial cells and are responsible for the transport of specific ligands. This is the main mechanism through which molecules such as insulin and transferrin are transported across the BBB (Abbott, 2013).

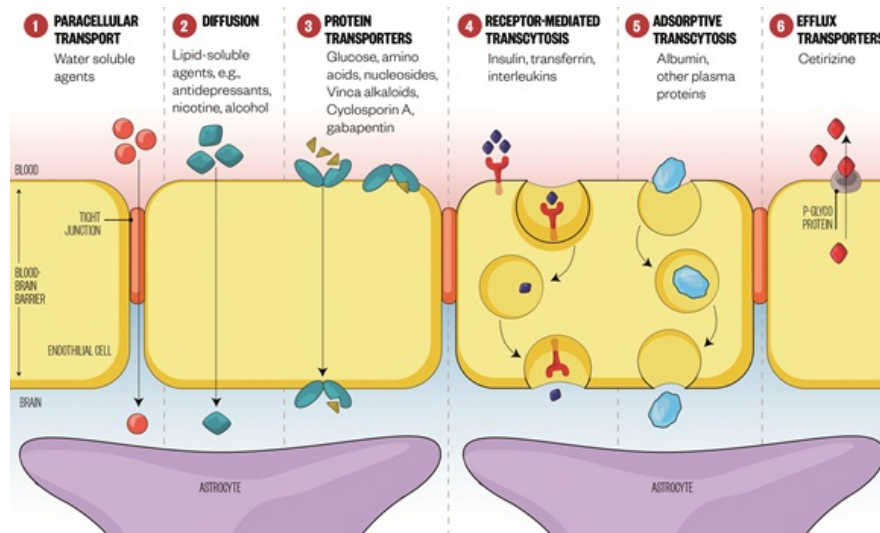


Figure 1.6 Transport pathways in the blood-brain barrier

(1) Paracellular aqueous pathway through which limited amount of water-soluble molecule can diffuse. (2) transcellular lipophilic pathway through which lipid soluble molecules diffuse across the BBB. (3) protein transporters pathway is responsible for diffusion of glucose, purine bases, amino acids, chlorine and other substances. (4) receptor mediated transcytosis that transport insulin, transferrin and certain proteins. (5) adsorptive transcytosis transports poorly absorbed proteins such as albumin. (6) Efflux transporters (Brazil, 2017)

Adsorptive mediated transcytosis (AMT) is responsible for transport of molecules that are polycationic in nature such as neuropeptides, proteins, and large therapeutic molecules. For these molecules, binding to anionic molecules at the surface of the cell is critical for their resultant transportation and passage across the endothelia through vesicular systems (Patel and Patel, 2017).

The BBB also contains an insidious network of membrane bound transporter proteins which are responsible for the active efflux or active uptake of molecules across the BBB through an energy-mediated (hydrolysis of ATP) process. Typical examples of these can be found in the membrane bound transporter proteins P-glycoprotein (P-gp/ABCB1), breast cancer resistant protein (BCRP/ABCG2), multi-drug resistant proteins (MRP-1, -4, -5 and -6) and organic anion transporting poly peptides (OATP2). For the transport of larger molecular, a carrier mediated transport pathway also exists for transport of nutrients into the brain such as amino acid large transporter LAT-1, glucose transporter GLUT-1,

monocarboxylic acid transporter MCT-1 and sodium coupled nucleoside transporter (CNT2) (Pardridge, 2002).

1.3.4 Drug transport across the BTB

Despite the BTB being a leakier barrier, studies have shown that it displays heterogenous drug permeability where, the centre of the tumour demonstrates higher leakiness in comparison with the adjoining brain microenvironment and the peritumoral area (Arvanitis et al., 2020b). This was shown in a malignant murine glioma model where dasatinib distribution was heterogeneous in the tumour lesion and was higher than that of the surround brain tissue (Agarwal et al., 2012). Further, low molecular weight compounds administered systemically in brain metastasis mouse models have shown irregular distribution within the tumour tissue (Lyle et al., 2016). Moreover, the permeability of ¹⁴C-paclitaxel and ¹⁴C-doxorubicin was assessed across the BTB in brain tumour metastasis mice models and demonstrated that 89% of the lesions displayed a heterogeneous BTB permeability, with drug uptake generally greater than that in normal brain tissue yet, drug concentrations reached cytotoxic levels in less than 10% of the metastatic models examined (Lockman et al., 2010).

Circulating drugs are exposed to multiple barriers imposed by the NVU, namely reduced transcytosis, reduced paracellular transport of hydrophilic compounds and efflux transporters that inhibit the passage of lipophilic molecules across the BTB (Banks, 2016). Many of these circulating drugs have an affinity to ABC transporters which are often responsible for reducing the uptake of drugs across the BBB (Seelig, 2007, Nałęcz, 2016, Carmeliet and Jain, 2011). Evolving insights into the BBB/BTB structure and function, have granted novel approaches to overcome the limitations they impose and enhance drug delivery to brain tumours. Some invasive approaches include, intrathecal and intraventricular injections (Groothuis, 2000, Beauchesne, 2010), implantation of wafer and microchips (Bregy et al., 2013, Chowdhary et al., 2015) and convection enhanced delivery by direct injection (Zhou et al., 2017b, Lonser et al., 2015).

Another popular approach to overcome multi drug resistance MDR at the BBB/BTB is through overcoming efflux pumps. Studies conducted pre-clinically have focused on the co-administration of the chemotherapeutic agent with a transporter inhibitor. This approach has shown a significant enhancement in chemotherapeutic agent concentration within the brain. This was evident by a 1.5-fold increase of temozolomide when co-administered with elacridar, a BCRP and P-gp inhibitor, in mice (de Gooijer et al., 2018). The increased recognition of the role ABC transporters play in BBB and brain tumour drug permeability suggests the need for more potent, more specific inhibitors that can target specific transporters and improve cancer cell drug uptake (Robey et al., 2018, Kim et al., 2018, Lin et al., 2014).

1.4 The ABC family of efflux transporters

Active transport of molecules across barriers refers to the movement of molecules against a concentration gradient and often requires the energy released from ATP hydrolysis in order to shuttle molecules across the cell membrane. Many therapeutic agents are transported into the brain and extruded out of the brain through active transport. Multiple efflux transporters such as ATP-binding cassette (ABC) transporters and influx transporters such as peptide transports, nucleoside transporters, organic cation transporters and (Sanchez-Covarrubias et al., 2014) have been identified in the BBB and the BTB (Table 1.4).

Table 1.4 Examples of influx transporters and substrates

Transporter	Substrate
Energy transport system	
GLUT-1	D-Glucose
MCT-1	L-Lactose
CRT	Creatine
Amino acid transport system	
LAT-1	Large neutral amino acids
CAT-1	Cationic amino acids

xCT	L-Cystine/L-Glutamine
Organic anion transport system	
Oatp14	Thyroid hormones
OCTN2	Carnitine
Nucleoside transport system	
CNT2	Nucleosides

Adapted from (Ohrsuki et al., 2003).

The ABC superfamily of drug transporters are amongst the largest and the most abundantly expressed transporter proteins found in prokaryotes (Sanchez-Covarrubias et al., 2014). The ABC family is subdivided into 7 subfamilies (*ABCA-ABCG*) and consists of 49 genes in total (Dréan et al., 2018). The ABC family has many functions which include, peptide transport and maintenance of the lipid bilayer. However, the most notable and widely studied role is their contribution in the development of the MDR phenotypes (Dean et al., 2001).

ABC transporters are either expressed as 'full' (Figure 1.7) or 'half' (Figure 1.8) transporters with full transporters having two transmembrane domains (TMD) and two nucleotide binding domains (NBD) and half transporters having only one of each. The ABC transporters are thought to undergo homodimerization in order to become functional (Dréan et al., 2018, Hyde et al., 1990, Dean et al., 2001).

All members of the ABC family exhibit two primary structural motifs, namely 'Walker A', a phosphate binding loop and 'Walker B' magnesium binding loop. Besides these two motifs, three other motifs are found in the ABC cassette, the 'LSGGQ' motif is specific to ABC transporters, 'the switch region' which attach to water molecules for hydrolysis and the Q-motif found between walker A and walker B and interacts with gamma phosphates through water bond formation. Walker A, walker B and the Q-motif make up the nucleotide binding site (Zhou, 2008, Higgins, 2001). In order to transport molecules across a cell membrane,

ABC transporters utilise energy from ATP hydrolysis in order to function (You and Morris, 2006).

The reasoning behind the ability of the ABC transporters to bind to a variety of structurally unrelated compounds and molecules is still unclear. However, two theories have come to light as possible explanations. The first theory claims that, when the transporter is facing inwards, the binding pocket of the transporter has a higher affinity to substrates. The binding of the transporter to the substrate leads to a conformational change leading the transporter to face outwards resulting in a reduced affinity to the substrate and hence the efflux of the substrate into the extracellular matrix. This theory is termed the “altering access model” (Clay, 2013). The second theory describes how the dimerization of the NBD after ATP hydrolysis causes a switch in the binding pocket from facing inward to facing outward. This inversion leads to a conformational change in the transporter leading to a reduced affinity to the substrate and its efflux. This theory is known as the “ATP-switch model” (Higgins and Linton, 2004).

Examples of members of the ABC family of transporters include:

ABCA: plays an essential role in cholesterol transport across the plasma membrane. Mutations in *ABCA1* leads to individuals developing dyslipidaemia (M. et al., 2001).

ABCB: consists of 11 members and are known to transport many molecules such as drugs, peptides and intracellular heme/iron (Sanchez-Covarrubias et al., 2014). *ABCB11* also known as bile salt export pump (BSEP) is responsible for the production and transport of hydrophobic bile salts such as taurine which is located in the liver. Consequently, it plays a major role in homeostasis of hepatic bile acids and regulation of biliary lipid secretion (Hayashi and Sugiyama, 2013) mutations in *ABCB11* are associated hepatomegaly and pruritus (Chiang, 2013). The most widely researched and reported on member of this family is *ABCB1* or P-glycoprotein (P-gp) and is known to be a major contributor in MDR which responsible for efflux of drugs (Sanchez-Covarrubias et al., 2014). P-glycoprotein (P-gp) was the first member of the ABC transporter family to be identified in

Chinese hamster ovaries (Juliano and Ling, 1976), and since then many studies identified a wide range of other efflux transporters that play a critical role in drug delivery across the BBB (Löscher and Potschka, 2005, Amin, 2013, Chung et al., 2016).

ABCC: consists of 13 members. They play role in signal transduction, toxin secretion and ion transport (M. et al., 2001). Mutations in the members of the *ABCC* subfamily can result in a range of pathophysiological consists such as hypoglycaemia (Fournet et al., 2001), cystic fibrosis (Cohen and Prince, 2012) and Dubin-Johnson syndrome (Wada et al., 1998). A major contributor towards the MDR phenotype from the *ABCC* family is MRP-1 (Sanchez-Covarrubias et al., 2014).

ABCD: has 4 members which are all half transporters. They function in the transport of very long chain fatty acids (Wanders et al., 2007). Mutations in this subfamily are linked with impairment in vision, cognition and hearing (Cappa et al., 2011).

ABCE and ABCF: are the least characterised of all the subfamilies with one known member of the *ABCE* family known as OABP protein and is known to play a role in identifying oligodendylate synthesis that takes place due to viral infections (Tian et al., 2012).

ABCG: subfamily has 6 members, *ABCG1*, *ABCG5* and *ABCG8* play a role in sterol transport (Tama and A., 2000). *ABCG2* also known as BCRP plays a key role in the MDR phenotype and takes part in the efflux of wide range of diverse therapeutic agents.

The most pharmacologically relevant ABC transporters are P-gp, BCRP and MRP-1. These are expressed in the apical side of cells in the brain, liver and intestine (Alvarez et al., 2010). The action of the transporters is initiated by interaction of the binding site with a certain substrate, which induces a conformational change that is transmitted to the binding domain where ATP binding activates. ATP binding leads to changes in the positioning and affinity of

the substrate binding site and thereby the substrate is discharged at the extracellular side of the cell (Higgins, 2001).

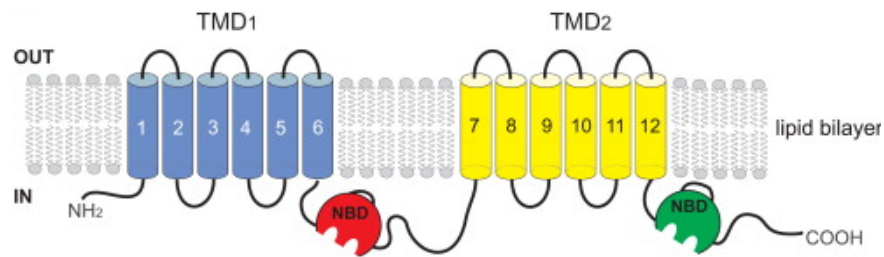


Figure 1.7 A typical structure of an ABC transporter

Structure of a typical ABC transporter includes transmembrane binding domains (TMD) and nucleotide binding domains (NBD). The functioning transporter consists of repeated units of TMD-NBD (Dermauw and Van Leeuwen, 2014)

1.4.1 The role of ABC transporters in influencing tumour phenotype and progression

ABC transporters are often associated with the aggressive nature of cancer progression, in part due to their ability to efflux chemotherapeutic agents and hence imparting a MDR phenotype, however irregularities in ABC transporter expression and function can also play a role in cancer progression beyond MDR (Muriithi, 2020).

Studies have reported that the dysregulated ABC protein expression is often linked to an aggressive tumour prototype as measured by tumour stage, size and the possibility of metastasis (Scotto, 2003). Even though the irregularities in ABC protein expression can merely be a consequence of genetic alterations that accompany tumour formation, the possibility that these proteins play a pro-tumour role cannot be ignored (Muriithi, 2020).

More commonly, ABC transporters have been implicated in MDR phenotypes, hindering intracellular accumulation of anti-cancer agents, and leading to tumour progression and growth. The overexpression of P-gp, BCRP and MRP-1 has been directly associated with poor prognosis in glioblastoma patients (Balça-Silva

et al., 2017, Balça-Silva et al., 2019, Matias et al., 2018). In breast cancer, overexpression of *ABCC11* was associated with an aggressive tumour subtype (Yamada et al., 2013). It was also reported that overexpression of *ABCC4* was associated with MYCN gene amplification which lead to the spread of the tumour, more importantly it was noted that its expression in primary untreated neuroblastomas was linked to reduced overall survival (Huynh et al., 2012).

Cancer cells are known to propagate outside the original tumour site in a process termed “invasion”, with ABC transporters being partly implicated. A study reported that *ABCB5* aided in the invasion of colorectal cancer *in-vivo* and *in-vitro* (Guo et al., 2018). It was also reported that in melanomas, MRP-1 was linked to the invasion and metastasis of the cancer when compared to tumours that didn't express MRP-1 (Landreville et al., 2011). In the U251 glioblastoma cell line, it was shown that downregulation of BCRP was correlated with reduced invasion and metastasis (Gong et al., 2014). Likewise, when comparing the effect of P-gp on the progression of breast cancer, it was reported that expression of P-gp in breast cancer cells in axillary nodes resulted in an increase in metastasis when compared to cells that lacked P-gp (Schneider et al., 2001).

The ability of cancer cells to evade apoptosis is essential to their persistent proliferation and survival (Hanahan and Weinberg, 2000), combined with the fact that majority of chemotherapeutic agents are cytostatic, cancer cells that evade apoptosis are resistant to treatment hence contributing to MDR (Muriithi, 2020).

1.4.2 Breast Cancer Resistance Protein: A key transporter at the BBB

Breast Cancer Resistance Protein was first identified in the breast cancer cell line MCF-7/AdrVp. Despite the absence of MRP and P-gp in these cells, the limited permeability of rhodamine 123 and adriamycin suggested the presence of a new transporter protein (Chen et al., 1990, Lee et al., 1997). This transporter was later termed as ‘breast cancer resistant protein’ (BCRP) (Doyle et al., 1998). BCRP has a molecular weight of 72 KDa, 655 amino acids, and is a half transporter (Figure 1.7) with the C-terminal and N-terminal located on the intracellular side of plasma membrane (Doyle et al., 1998).

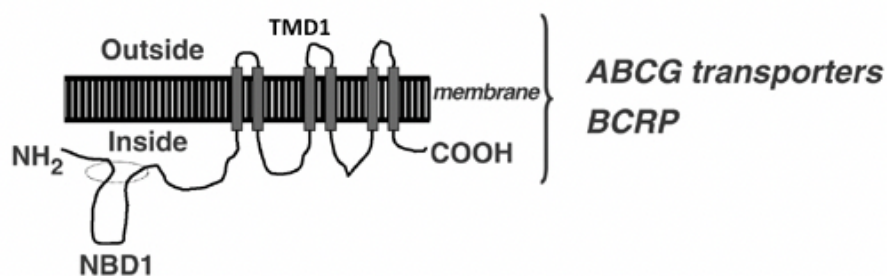


Figure 1.8 The structure of breast cancer resistance protein (BCRP)

BCRP a half transporter comprising of one transmembrane binding (TMD) and one nucleotide binding domain (NMD), comprised of 6 trans-membrane spanning regions (Austin Doyle and Ross, 2003).

In order for BCRP to act as an efflux transporter, it is believed that it undergoes homodimerization or heterodimerization (Graf et al., 2003, Austin Doyle and Ross, 2003, Shigeta et al., 2010). BCRP has been reported to be expressed in various tissue sanctuary sites, such as the placenta, gastrointestinal tract, testicles, heart, liver and brain (Sanchez-Covarrubias et al., 2014, Meissner et al., 2006, Cooray et al., 2004a).

Within the brain, BCRP is expressed in the luminal region of the endothelial cells of the BBB in addition to astrocytes and microglia (Gloria et al., 2007). Based on mRNA analysis, BCRP was found to be expressed in higher quantities in the BBB than P-gp and MRP-1 (Eisenblätter et al., 2003). Later studies employing quantitative proteomics have reported an absolute protein abundance of transporter proteins at the BBB and have stated that BCRP (8.14 fmol/μg protein) and P-gp (6.06 fmol/μg protein) are the most abundant transporter proteins at the human BBB (Uchida et al., 2011).

BCRP has a primary protective function in human physiology by restricting access of therapeutic agents as well as some endogenous substrate molecules (Oostendorp et al., 2009, Chen et al., 2003). The overexpression of certain ABC transporters was found to increase MDR, which significantly influences failure of

chemotherapy (Sun et al., 2012), with BCRP being prominent in accounting for the multidrug resistance phenotype in humans (Dean et al., 2001, Roundhill et al., 2015).

BCRP has a wide range of chemotherapeutic substrates such as mitoxantrone, irinotecan, imatinib, doxorubicin, methotrexate and SN-38 (Cooray et al., 2004b). Mitoxantrone resistant colon cancer cell line was found to overexpress BCRP and hence its resistant to mitoxantrone (Miyata et al., 1999). Many other cell lines that overexpress BCRP, such as glioblastoma, fibrosarcoma, non-small cell lung cancer and gastric carcinoma were found to also be drug resistant (Ross et al., 1999). *In-vitro*, it was reported that the resistance of human ovarian cancer cell line IGROV1 to type-1 topoisomerase inhibitor topotecan was a direct correlation to the over expression of BCRP in the cell line (Maliepaard et al., 1999), in addition, its overexpression in gastric carcinoma cell line (EPG85-257RNOV) and glioblastoma cell line (SF295/MX) rendered them refractory to mitoxantrone therapy (Robey et al., 2001a). Furthermore, in MCF7 cell line, over expression of BCRP lead to resistance to both methotrexate and mitoxantrone (Volk et al., 2002).

Within animal studies, a direct correlation has been demonstrated between methotrexate resistance and the expression of BCRP at the BBB (Li et al., 2013). In addition, the distribution of methotrexate when used in the treatment of CNS lymphoma was very limited, with only 5% of the drug crossing the BBB (Zhu et al., 2009). Also, in patients with high grade gliomas, cerebral penetration of methotrexate was shown to be very low (Blakeley et al., 2009). Furthermore, brain uptake for mitoxantrone was shown to increase by 3-fold when co-administered with a BCRP and a P-gp inhibitor in mice, demonstrating that BCRP plays a critical role in limiting the permeability of mitoxantrone across the BBB (Cisternino et al., 2004).

1.4.3 Modulation of ABC efflux transporter activity

Developing strategies to modulate efflux transporter activity have been promoted by the increasing awareness of the influence these transporters have on CNS drug delivery (Arvanitis et al., 2020a, Löscher and Potschka, 2005). Mechanisms to inhibit efflux transporters at the BBB/BTB include approaches such as the use

of direct inhibitors and transcriptional modulation (Banik et al., 2010). Over the last two decades, developing agents that modulate the action of P-gp have been the primary focus of many studies attempting to reverse the MDR phenotype. First generation inhibitors of P-gp include verapamil, cyclosporine A, quinidine, yohimbine and tamoxifen. These agents failed to clinically translate to successful modulators due to their poor specificity and binding properties which required administering these agents in high doses which lead to non-specific binding and major systemic toxicities (Ferry et al., 1996)

Second generation inhibitors include dexverapamil, valsopodar and dexniguldipine (Fardel et al., 1993, Kolitz et al., 2010, Summers et al., 2004). These agents displayed a greater inhibitory effect on transporter proteins with reduced toxicity. However, these agents still demonstrated limitations, such as inhibition of the metabolism of chemotherapeutic agents when administered concurrently leading to accumulation of the chemotherapy in the blood and systemic toxicity. For instance, valsopodar reduces the hepatic metabolism of vinblastine and paclitaxel through inhibition of CYP 3A4, leading to increased concentration of the cytotoxic agents in the blood (Bates et al., 2004). In a similar fashion, a study in patients with solid tumours demonstrated that combined administration of paclitaxel and biricodar resulted in a significant decrease in paclitaxel clearance, as a result of biricodar interfering with paclitaxel's metabolism (Rowinsky et al., 1998).

More recently third generation inhibitors such as tariquidar, mitotane, elacridar and zosuquidar were found to be clinically effective with less toxicity when compared to previous generations (Leitner et al., 2011). However, later clinical trials showed that these inhibitors possessed major toxicities and had low survival benefits (Dash et al., 2017).

More recently, attention has turned towards modulation of BCRP. An extract from the fermentation broth of *Aspergillus fumigatus*, fumitremorgin C (FTC), was the first discovered BCRP inhibitor, but failed to translate clinically due to its severe neurotoxicity profile (Hirsch et al., 2009). Thereafter, 42 derivatives from FTC were later developed with only two of those (Ko143 and Ko132) showing promising results. These were however discontinued clinically due to their

cytotoxicity (Pick et al., 2011). Many tyrosine kinase inhibitors (TKI) such as gefitinib has been reported as inhibitors of the efflux function of BCRP (Leggas et al., 2006, Stewart et al., 2004). However, exposing cells to gefitinib lead to an increase in the expression of BCRP, and an increased resistance to anti-cancer agent SN-38 when administered concurrently, proposing that gefitinib is a BCRP substrate (Azzariti et al., 2010). Another TKI, sunitinib, was found to modulate BCRP mediated efflux function (Shukla et al., 2009a).

Despite research highlighting some current inhibitors of BCRP, their poor specificity and cytotoxicity remain a major limiting factor in their clinical translation (Tang et al., 2012, Pick et al., 2011, Hirsch et al., 2009). There is still a need for effective BCRP inhibitors that are safe, effective and are able to modulate the efflux action of BCRP.

More recently, a group of naturally occurring phytochemicals have come to light as BCRP modulators. These have garnered great attention due to their effectivity and safety as ABC transporter modulators in addition to their other health benefits.

1.5 Natural product phytochemicals

Phytochemicals are naturally occurring chemicals in foods that are widely consumed within the diet of mammals. A major category of phytochemicals are flavonoids, which are found naturally in fruits, vegetables, and herbs (Table 1.5). flavonoids fall into the food category and are deemed tolerable with reported daily exposure through dietary intake exceeding 1 gram (Pick et al., 2011, Perez-Vizcaino and Fraga, 2018). Over 6500 chemicals have been identified as belonging to the general category of flavonoids (Panche et al., 2016, Rashid et al., 2019).

Flavonoids structurally consist of aromatic rings A and C and a heterocyclic benzene ring B (Figure 1.9). They are categorised into subgroups based on the position of the attached substitution (R_x).

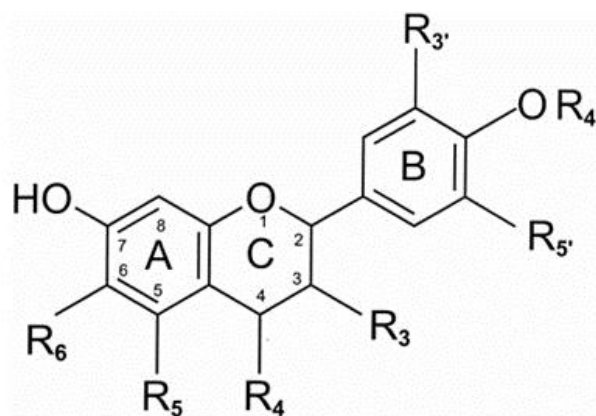


Figure 1.9 Basic structure of flavonoids

Flavonoids consist of ring A and B which are aromatic rings and ring C which links rings A and B together. Based on the positions of substitutions (Rx) and hydroxylation, flavonoids are divided into 7 subgroups (Dwivedi et al., 2017).

Table 1.5 Examples of flavonoids and food source

Group	Example	Food source
Flavonols	Quercetin, Kaempferol, Myricetin, Quercetin	Blueberry, black tea, leek, yellow onion, cherry, apple, tomato, curly kale.
Flavones	Chrysin, luteolin, tangeretin, tricetin, sinensetin, apigenin, nobiletin	Celery, parsley, capsicum.
Flavanones	Hesperetin, naringenin, eridodicytol, dihydrofisetin	Orange juice, lemon juice, grapefruit juice.
Flavanols	Taxifolin, silibinin, silymarin, pinobaxin	Cocoa, chocolates, cocoa drinks.
Catechins	(-) Epicatechin, (+) catechin gallic acid, epigallocatechin, epigallocatechin 3-gallate	Beans, apricot, peach, red wine, grapes, cherry, chocolate
Isoflavones	Daidzein, Genistein, glycitein	Soybean, tofu, legumes
Anthocyanins	Pelargonidin, malvidin, peonidin, cyanidin, delphinidin.	Red berries, purple grapes, rhubarb plum, red cabbage, strawberries

Some examples of flavonoids and their presence in food. Table adapted and modified from (Lakhanpal and Ral, 2007)

1.5.1 Flavonoids as ABC transporter modulators at the BBB and the BTB

Studying the structure and function of BCRP and its substrates have revealed insights into the mechanisms underlining BCRP-mediated multidrug resistance in cancer and healthy tissue. The interaction of flavonoids with BCRP appear to resemble those shown in the interaction of flavonoids with P-gp (Conseil et al., 1998, Boumendjel et al., 2001) where flavonoids interact with the C-terminal region of the NBD. That said, two mechanisms of action have been proposed for the ability of flavonoids to inhibit BCRP, binding to either the nucleotide binding domain or the transmembrane domain substrate binding sites (Figure 1.8) (Alvarez et al., 2010, Pulido et al., 2006, Bock et al., 2000).

Flavonoids such as quercetin, genistein, naringenin and kaempferol were shown to competitively inhibit the action of BCRP and bind with stronger affinity to the transporter (Katayama et al., 2007, Di Pietro et al., 2002, Zhang and Morris, 2003, Walgren et al., 2000). On the other hand, other studies have demonstrated that quercetin, benzo-a-pyrene and kaempferol are known to inhibit BCRP by binding to the ATP binding site and hence lead to the inactivation of the transporter (Yarla and Ganapaty, 2013b, Guohua et al., 2011, Wang, 2007).

The known BCRP inhibitors Ko143 (Ozvegy-Laczka et al., 2005) and FTC (Özvegy et al., 2001, Robey et al., 2001b) were shown to modulate BCRP by inhibiting its ATPase activity, however, flavone derivatives were shown to increase the activity of ATPase much like mitoxantrone, suggesting the presence of a large poly-specific drug binding site in BCRP much akin to those demonstrated in P-gp and MRP-1 (Ozvegy-Laczka et al., 2005).

Additionally, variation in the substitutions in flavonoids (Figure 1.8) play a key role in their ability to modulate BCRP. A study reported that the presence of hydroxyl and hydrophobic substitutions rendered flavones such as luteolin and apigenin more effective in the inhibition of drug efflux function of BCRP compared to other

classes of flavonoids, with a hydroxyl substitution at position 5 in ring-A resulting in the best inhibitory effect. In addition, the presence of hydrophobic substitutions at positions 6' and 7' correlated with a higher binding affinity with BCRP (Ahmed-Belkacem et al., 2005a).

Furthermore, pharmacophore calculations suggested hydrophobic groups in position 4' in aromatic ring B and the presence of hydrogen bond acceptors in positions 5' and 7' play a critical role in the ability of flavonoids to modulate the action of BCRP (Fang et al., 2016). In addition, the occurrence of a 2,3-double bond in ring C, ring B branched at position 2, hydroxylation at position 5 and absence of hydroxylation at position 3 all seem to be critical for potent BCRP inhibition (Morris and Zhang, 2006).

Genetic polymorphisms of BCRP play a major role in the ability for flavonoids and substrates to bind. Phenylalanine at position 439 (Phe 439), found in the internal cavity of BCRP in the NBD is a critical factor in the binding affinity of flavonoids to BCRP. Biochanin-a, chrysin, naringenin and diosimin modulate BCRP through the formation of a non-covalent bond between the aromatic ring in these flavonoids and Phe 439 which is present in the substrates binding pocket (Fan et al., 2019). Furthermore, arginine at position 482 (Arg 482) in BCRP has been shown to have a major role in the substrate selection process for BCRP (Noguchi et al., 2009). Arg 482 with a positive charge has an effect on the interaction between BCRP and its drug substrates and consequently the carboxyl group at the transmembrane binding site that is in close juxtaposition to Arg 482 seems to take part in the substrate binding pocket interface of BCRP (Ejendal et al., 2006, Hazai and Bikádi, 2008, Li et al., 2007).

The most well studied mutations in BCRP occur when arginine 482 (R482), is replaced with threonine (R482T) or glycine (R482G) (Breedveld et al., 2006, Honjo et al., 2001, Robey et al., 2001b). The MCF7 and S1-M1-80 cell lines were identified to have mutation of the 482 amino acid, these mutations were associated with overexpression of BCRP. Furthermore, they were reported to be highly resistant to mitoxantrone and doxorubicin in addition to the efflux of rhodamine and anthracycline resistance (Volk et al., 2002, Honjo et al., 2001).

Additionally, variants of the amino acid 482 lead to lack of affinity to methotrexate in MCF cells and at the same time increased mitoxantrone resistance (Li et al., 2007, Ozvegy et al., 2002, Volk et al., 2002).

The inhibitory effect of BCRP by flavonoids was also suggested to be result of the parent compound rather than their metabolites. For example, genistein was shown to be transported unchanged by BCRP (Imai et al., 2004a) whilst naringin and phoridzin had no effect on the efflux action of BCRP. However, their aglycon counterparts were found to be strong inhibitors in MCF cells suggesting that the presence of the sugar moiety significantly affects the BCRP inhibitory activity of flavonoids (Zhang et al., 2004b).

1.5.2 Anti-cancer properties of phytochemicals

Naturally occurring phytochemicals have been reported on as having numerous anti-cancer properties such as inhibiting cell migration and invasion, inducing apoptosis, and participating in cancer cell cycle arrest (Yahfoufi et al., 2018, Gorlach et al., 2015, Perez-Vizcaino and Fraga, 2018, Kopustinskiene et al., 2020). In addition, studies have shown that conjugated metabolites of flavonoids possess anti-inflammatory activates (Zhang et al., 2004b, Perez-Vizcaino and Fraga, 2018), angiogenic properties and anti-oxidative action (Harada et al., 1999, Xiao et al., 2011).

Overproduction of reactive oxygen species (ROS) occurs when the homeostatic balance between anti-oxidant defence and pro-oxidant activities is compromised, thus leading to free radical accumulation (Rodríguez-García et al., 2019). Flavonoids have dual abilities as anti-oxidants and pro-oxidants (Link et al., 2010, Hadi et al., 2000), both of which are involved in their anti-cancer properties (Oliveira-Marques et al., 2009, Valko et al., 2007). In addition, they increase expression of tumour suppressor TP53 and cell death regulator protein Bax and downregulate apoptosis suppressor gene Bcl-2 (Zhang et al., 2015b, Abotaleb et al., 2018). Subsequently, this suppresses cancer cell proliferation, migration and activates apoptosis (Shen et al., 2010, Liskova et al., 2020).

Flavonoids are also able to exhibit their anti-oxidant ability by scavenging of free radicals through hydrogen atom donation which results in inactivation of the free radical (Nijveldt et al., 2001). The arrangement of the functional groups in the flavonoids' structure can also influence their antioxidant ability (Heim et al., 2002). The presence of a hydroxyl substitution in ring B is crucial for ROS scavenging, however, A- and C- ring substitutions have small impact on the ROS scavenging rate (Procházková et al., 2011). Flavonoids' ability as anti-oxidants has also been proposed to be due to the redox activity of phenolic hydroxyl groups such as those found in catechol moieties which are easily oxidized (Chobot and Hadacek, 2011).

Furthermore, flavonoids can exhibit their antioxidant abilities by suppressing pro-oxidative enzymes and stimulating phase II detoxification enzymes (Youn et al., 2006). *In-vitro* studies have also demonstrated that the glycosylation of the 3-OH group strongly inhibits the flavonoids ability to scavenge ROS (Burda and Oleszek, 2001, Taubert et al., 2003) where the aglycon hesperetin was a better anti-oxidant than its glycoside counterpart hesperidin and baicalin was better than baicalein (Rice-Evans et al., 1996, Procházková et al., 2011).

Additionally, flavonoids can exhibit their anti-oxidant abilities by activating anti-oxidant enzymes (Ferrali et al., 1997), chelating metals such as copper and iron and thereby removing spontaneous factors available for the formation of free radicals (Ferrali et al., 1997). They also inhibit oxidases (Cos et al., 1998) such as xanthine oxidase and protein kinase C (Hanasaki et al., 1994, Procházková et al., 2011) and enhance anti-oxidant properties of low molecular weight antioxidants (Yeh et al., 2005)

Numerous reports have also demonstrated the pro-oxidants properties of flavonoids, under certain conditions, where the number of hydroxyl group substitution is directly proportional to their pro-oxidant abilities (Haenen et al., 1997). More specifically, hydroxyl groups present in ring B were shown to significantly increase their ability to produce ROS (Heim et al., 2002, Hanasaki et al., 1994). Flavonoids are also able to reduce Cu^{2+} to Cu^{+} and induce free radicals formation as a result (Cao et al., 1997). This is particularly important in

cancer cells, where Cu^{2+} has been reported to increase cancer cell proliferation and tumour growth (Wang et al., 2010a). In addition, the reduction of oxygen to a superoxide anion as well as reduction of Fe^{3+} to Fe^{2+} contributes to this phenomena (Procházková et al., 2011).

Within cancer cells, reports have also demonstrated how flavonoids can act as pro-oxidants by inhibiting enzymes involved in cell growth, proliferation and mobility, such as phosphatidylinositol 3-kinase PI3K (Abotaleb et al., 2018), protein kinase B (Neagu et al., 2019) as well as inhibiting epidermal growth factor receptor proteins (Rodríguez-García et al., 2019). The pro-oxidant ability of flavonoids can be associated with their anti-oxidant feature where, the formed compound after flavonoids ROS scavenging is a highly reactive flavonoid phenoxyl (Bayrakçeken et al., 2003) which is subjected to additional oxidation yielding more stable compounds such as quinones (Hernández et al., 2009, Awad et al., 2002). The pro-oxidant properties of naringenin, naringin and apigenin were attributed to the formation of phenoxyl radicals which oxidize NADPH that leads to increase in oxygen uptake and formation of a highly reactive superoxide (Chan et al., 1999, Galati et al., 2002, Galati et al., 1999).

1.6 Cellular models of the glioblastoma

As researchers begin to better understand the complex interaction between gliomas and their surrounding micro-environment, a transition away from xenograft tumour models towards nonimmunogenic *in-vitro* models is now at the forefront of preliminary GBM research. This is a result of their ability to mimic many *in-vivo* GBM characteristics as well as the high throughput nature of *in-vitro* models. A variety of *in-vitro* cellular models exist that replicate GBM *in-vitro*. The subsequent sections will briefly highlight some common examples.

1.6.1 Human U251 glioma models

This malignant glioma cell line was established by Ponten and collages in 1975 (Ponten, 1975) from a 75 year old patient. This cell line has been extensively used over the last 40 years in *in-vitro* and xenograft models (Radaelli et al., 2009,

Husain et al., 1998). It is capable of mimicking many immunohistochemical and histological features of human GBM as well as mimicking changes in tumour suppressor genes and oncogenic pathways (Wen and Kesari, 2008, Candolfi et al., 2007). Moreover, the tumour cells showed high level of cellular proliferation and expression, with 19 of the known ABC transporters reported to be expressed. It is also suggested that high passages after the establishment of the cell line leads to loss of ABC transporter protein expression (Dréan et al., 2018).

1.6.2 Human U87 glioma models

This model was established from a 44 year old female by Ponten in 1975 (Ponten, 1975). Despite major differences that exist between human GBM and the U87 cell model such as having more homogenous, leaky vessels and less invasive non-diffusive growth pattern (de Vries et al., 2009), the U87 model has been utilised in assessing GBM angiogenesis and tumour angiogenic therapy (Radaelli et al., 2009). U87 cell line was reported to express P-gp and BCRP (Wijaya et al., 2017, Gil-Martins et al., 2020).

1.6.3 Rat C6 glioma models

The C6 rat glioma model is the one most commonly used in neuro-oncology in the study of low grade and high grade gliomas (Giakoumettis et al., 2018).

This model was established by injecting adult Wistar-Furth rats with a carcinogenic chemical known as methylnitrosourea (Benda et al., 1968). C6 display a similar diffusive infiltrating invasion pattern to human GBM such as nuclear polymorphism, foci of tumour necrosis and high mitotic index (Chicoine and Silbergeld, 1995, Doblaz et al., 2010, Gieryng et al., 2017). As well as having the ability to invade and migrate in a similar fashion to that of human xenografts (Giakoumettis et al., 2018).

However, a key histological difference when compared to human GBM is the lack of expression of glial fibrillary acidic protein GFAP which is a main component of astrocytes within the CNS (Chou et al., 2003). The expression of the tumour suppressor genes p53 and PTEN are also reported to be minimal compared to

human GBM (Asai et al., 1994). In addition, the cells were reported to lose their invasive nature and grow in an encapsulated mode when transplanted in Wistar rats (San-Galli et al., 1989).

1.6.4 Human LN229 glioma model

The LN229 model was established from a 60 year old female in 1979 (Diserens et al., 1981). The cells are reported to express mutated p53 and PTEN in a similar fashion to human GBM (Ishii et al., 1999). LN229 cells were reported to have the highest migration speed when compared to U251 and U87 models (Diao et al., 2019). Immunoblot studies confirmed a 2-fold higher expression of BCRP in the nucleus of the cells compared to cytoplasmic extract, which suggested a possible secondary efflux site (Bhatia, 2013). P-gp, MRP-1 and MRP-2 were reportedly expressed in LN229 although in a lesser amount than BCRP (Bhatia, 2013, Bhatia et al., 2012). The LN229 model has been used to study apoptosis in addition to cellular migration and invasion (Zhang et al., 2009, Liu et al., 2014, Wang et al., 2018).

1.7 *In-vitro* models of the blood-brain barrier

Many models for *in-vitro* BBB research have been developed and characterised over the last four decades to study BBB biology and drug transport. However, none of the models used behave exactly the same and hence irregularities in the outcome and the lack of a consensus on a gold standard model (Helms et al., 2016). Small variabilities such as different laboratory conditions and different providers impose a challenge in obtaining a well-defined view of the benefits and drawbacks of BBB *in-vitro* models. The following sections highlight some commonly used *in-vitro* BBB models.

1.7.1 Immortalised cellular models

1.7.1.1 Human origin models

Human BBB models have been used in *in-vitro* research for over 15 years. The most widely used immortalised human BBB model is the hCMEC/D3 cell line

(Poller et al., 2008, Ohtsuki et al., 2013). This cell line has been extensively characterised compared to other models. hCMEC/D3 possess essential endothelial markers such as CD34, CD31, CD40 and von Willenbrand factor. In addition, this cell line expresses TJ proteins and efflux transporters such as P-gp and BCRP (Weksler et al., 2013, Poller et al., 2008, Vu et al., 2009).

However, the expression of claudin-5, an important member of tight junction protein, has been reported to be low when compared to microvessels *in-vivo* (Urich et al., 2012). In addition, hCMEC/D3 monolayers demonstrated low transepithelial electrical resistance (TEER) values of 30-50 $\Omega\cdot\text{cm}^2$, which is significantly below the *in-vivo* TEER of approximately 1000 $\Omega\cdot\text{cm}^2$ and making them less suited for drug transporter studies (Weksler et al., 2005, Weksler et al., 2013, Biemans et al., 2017).

Another human cell line used in BBB research is the endothelial progenitor cells (EPC) which is derived from bone marrow or the umbilical cord. These cells were shown to express tight junction proteins ZO-1 and claudin-5. In addition, they expressed transporters such as GLUT-1, P-gp and BCRP. Much like hCMEC/D3 cells, the limitation of the model is their low TEER values < 60 $\Omega\cdot\text{cm}^2$. However, an elevation in TEER values was reported when cocultured with Bovine pericytes (Helms et al., 2016, Ponio et al., 2014).

1.7.1.2 Rodent origin models

Rat brain endothelial cell lines were first isolated and established in 1994 (Roux et al., 1994). Rat endothelial cells express many drug efflux transporters such as P-gp and BCRP (Qosa et al., 2015) and proteins that are specific to BBB characteristics, such as tight junction proteins ZO-1 and occludin (Watanabe et al., 2013). Extensively used rat cell lines in BBB drug permeability studies include bEND.3, bEND.5, GP8 and GPNT (Olesen and Leonardi, 2003). A further widely used rat model is the TR-CSFB model, which was optimised for permeability and transport studies. However, these cells are known to form leaky barriers (TEER: $\sim 90 \Omega\cdot\text{cm}^2$) and require growth at lower temperatures (Kitazawa et al., 2001, Hosoya et al., 2004).

1.7.1.3 Bovine based models

Bovine endothelial models such as the BBEC-117 (Sobue et al., 1999) and SV-BEC (Durieu-Trautmann et al., 1991) have been widely used as *in-vitro* BBB models. Bovine monolayers have a reported TEER value of 120-130 $\Omega\cdot\text{cm}^2$ (Gaillard and de Boer, 2000) and have been used in drug transport and permeability studies (Ahmed-Belkacem et al., 2005a, Valdameri et al., 2011). Bovine models have been reported to being subpar in regards to transport activity and barrier tightness as well as lack of functional activity of ABC transporters (Hakkarainen et al., 2014, Anfuso et al., 2014). Bovine models are not frequently used in BBB models due to labour intensive extraction of primary cells and irregularities in reproducibility (Helms et al., 2016) as well as risk of infection of the cells with Creutzfeldt-Jakob or obtaining cells from a cow infected with mad cow disease.

1.7.1.4 Porcine based models

The immortalised porcine brain endothelial cell line PBMEC/C12 was developed in 1996 (Teifel and Friedl, 1996) and has been successfully used in numerous studies to assess small molecular transport, gene/protein expression and endothelial cell surface receptor studies (Kaur and Badhan, 2017, Helms et al., 2016, Torok et al., 2003, Franke, 2000, Lauer et al., 2004).

PBMEC/C12 cells demonstrated key BBB characteristics such as restrictive paracellular pathways, expression of tight junctions such as ZO-1, and expression of efflux transporters such as BCRP and P-gp. The reported TEER values were in the region of 80-100 $\Omega\cdot\text{cm}^2$ and are enhanced by supplementing the cells with fibronectin (Patabendige et al., 2013, Neuhaus et al., 2006).

Immortalised cell lines have been an integral part of *in-vitro* research since the 20th century, providing a powerful tool for applications such as studying cytotoxicity, drug metabolism, drug permeability, gene functions and producing vaccines and antibodies (Kaur and Dufour, 2012). However, there are limitations associated with using immortalised cell lines such as genetic and phenotypic

alterations from the originating tissue with an increase passage number (Pan et al., 2009). Furthermore, following prolonged periods of time, immortalised cell lines are prone to contamination (Lorsch et al., 2014). In contrast to primary porcine cells, the PBMEC/C12 cell line lose their morphological and phenotypical features as well as important biological *in-vivo* markers compared to the originating primary cells (Pan et al., 2009).

Although immortalised BBB models are broadly used for *in-vitro* studies, they lack many BBB features and demonstrated comparatively low TEER values to human BBB cellular monolayer resistance. However, a novel BBB *in-vitro* model has gained traction from the isolation of brain microvascular endothelial cells directly from recently slaughtered pigs, resulting in high yield of endothelial cells with excellent monolayer formation and high resistance to drug permeation (Patabendige et al., 2013, Pardridge, 2005).

1.7.2 Primary porcine based model

The first complete reported method for the isolation of primary porcine brain microvascular endothelial cells (PBMEC) was based on an isolation and extraction method used for extracting primary rat endothelial cells (Bowman et al., 1981, Franke, 2000). This method was later modified to provide a detailed method for isolation (Patabendige et al., 2013). The primary PBMEC model was developed due to the ease and convenience of obtaining pigs brains, higher yield of cells when compared to rat brain hemispheres and the ability of endothelial cells to retain their BBB phenotype characteristics when compared to primary bovine and rat cells. It has been reported that PBMEC grown in non-contact co-cultures with astrocytes was critical for the development of BBB characteristics (Rubin et al., 1991). However it was later demonstrated that growing the cells in an astrocyte conditioned media (ACM) in addition to adding BBB forming additives such as hydrocortisone and cAMP would yield a robust BBB *in-vitro* model suitable for drug permeability studies (Skinner et al., 2009, Gaillard et al., 2001, Patabendige et al., 2013, Hoheisel et al., 1998, Thomsen et al., 2015). The high TEER values reported for PBMEC, in excess of $800 \Omega \cdot \text{cm}^2$, correspond to a restrictive model and reported low permeability of small molecules with sucrose

permeability ranging between $0.2-8 \times 10^{-6}$ cm/s (Patabendige et al., 2013, Lohmann et al., 2002, Franke et al., 1999)

PBMEC were confirmed by western blot and PCR to express tight junction such as ZO-1 and ZO-2 (Huwyler et al., 1996, Matthes et al., 2011, Schulze et al., 1997), Claudin-5 (Rempe et al., 2014, Kröll et al., 2009) and occludin (Rempe et al., 2014, Malina et al., 2009). Furthermore, a range of ABC efflux transporters have been identified within the model, which includes P-gp, BCRP, MRP-1 and MRP-4 (Lemmen et al., 2013, Parlow et al., 2009, Matthes et al., 2011).

The well-defined expression of tight junctions and efflux transporters makes this an excellent model for drug permeation studies across the BBB (Helms et al., 2016) as well as the model of choice to introduce continuous impedance TEER analysis due to the consistency of reported TEER values (Benson et al., 2013).

1.8 Limitations of current BBB cell culture models

The endothelial microenvironment is coordinated through a variety of complicated chemical and mechanical signalling which makes the accomplishment of physiological endothelial phenotype in the laboratory a challenging task (Abaci et al., 2015, James and Allen, 2018). Systematic explorations of complex biological operations entail *in-vitro* models that mimic *in-vivo* interactions such as interstitial blood flow and intracellular communication, A feature that is missing in many *in-vitro* BBB models. Many of the main elements of the *in-vivo* vasculature are relevant for tissue engineering, regenerative medicine, and vascular biology, these include hemodynamic shear stress, the extracellular matrix and interactions between multiple cell types (Srigunapalan et al., 2011).

Modern *in-vitro* BBB models do not account for the role of shear stress, as a result of it being considered to have a negligible effect to the extracellular microenvironment, cellular morphology, and characteristics. An argument was made by Di and Kerns (Di and Kerns, 2015) which suggested that shear stress is insignificant since blood flow in the brain capillaries is very low, additionally, Difficulties in determining optimal cell culture conditions, conceptualising,

developing and scaling up flow-based cell models, has made them an unattractive option of *in-vitro* BBB research. These claims were later contested by studies that illustrated the importance of shear stress in replicating the *in-vivo* microenvironment as well as providing easy to set up flow models that replicate the homeostatic state of the brain and other organs (Elbakary and Badhan, 2020, Mazzei et al., 2010, Chien, 2006, Abaci et al., 2015, Wang et al., 2017)

1.8.1 The impact of shear stress on BBB phenotype

Shear stress is a mechanical force that cells experience due to blood flow and interstitial fluid flow which produces frictional potencies. It plays essential roles in maintaining homeostasis and cellular remodelling (Chiu and Chien, 2011). Moreover, shear stress caused by laminal flow, is one of the key regulators of the endothelial phenotype and barrier integrity exhibited to have a fundamental role in the formation of distinctive phenotypes (Abaci et al., 2015).

Endothelial cells act in response to shear stress by altering intracellular signalling, gene and protein expression (Chien, 2007). Mechanical forces acting on the vessel wall incorporate those of normal and circumferential stresses, both of which are caused by the activity of pressure and shear stress that acts parallel to the luminal surface of the vessels due to flow (Figure 1.10) (Nerem, 1993). Circumference pressure acts along the vessel wall boundary to cause stretching, while shear stress acts parallel to the cell surface and is a consequence of fluid viscosity and the velocity gradient amid adjacent layers of flowing fluid (Nerem, 1993, Chien, 2007).

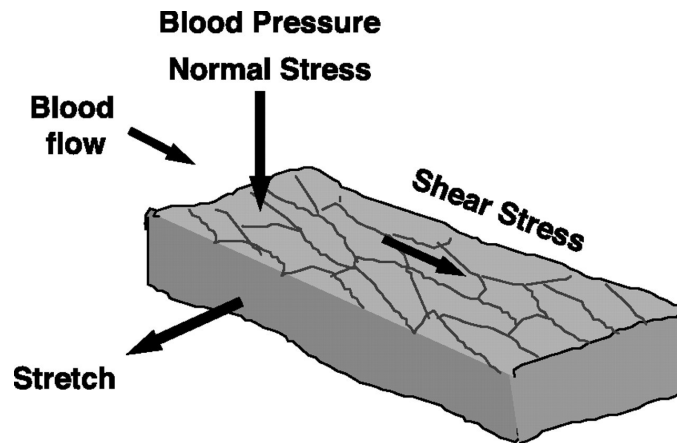


Figure 1.10 Normal stress compared to shear stress

Schematic illustration showing the generation of shear stress by blood flow (parallel) and the generation of normal stress (perpendicular) (Chien, 2006).

In the brain, microvascular capillaries typically are 10 μm in diameter and experience a flow rate of 6-12 nL/min which equates to 10-20 dynes/cm² (Wong et al., 2013). In the local endothelium, normal and abnormal (disturbed) blood flow patterns induce different responses (Kaisar et al., 2017). Shear stress is determined using (Equation 1) which illustrates that shear stress is directly proportional to flow and indirectly proportion to the radius of capillaries i.e. narrower capillaries produce higher shear stress (Redmond, 1995).

$$SS=4\mu Q/\pi r^3 \quad (1)$$

where SS is shear stress, μ is viscosity (mPa.s), Q is flow rate (mL/s), R is capillary radius (cm).

Areas where flow has been disturbed become pathological, in that the balance between pro- and anti-angiogenic/pro- and anti-inflammatory states is no longer present leading to the occurrences of pathophysiological states such as ischemic stroke (Balaguru et al., 2016). Studies have demonstrated that intraluminal flow has a vital part in the development and maintenance of BBB *in-vitro* and *in-vivo* phenotypes (Desai et al., 2002, Stanness et al., 2020).

1.8.2 Dynamic *in-vitro* blood brain barrier models

1.8.2.1 Hollow fibre models

Tissue culture on hollow fibres were first developed by Kanazek et al (Knazek et al., 1972). The model was later modified by *Janirgo et al.* and there after by *Cucullo et al* (Janigro et al., 1999, Cucullo et al., 2002). The hollow fibre system consists of a polycarbonate hollow fibre chamber which is sealed by a glass bottom and a removable acrylic top (Figure 1.11). The hollow fibre is connected to a media reservoir through gas permeable tubing which allows the exchange of O₂ and CO₂. This is connected to a pumping system that can generate a media flow rate of up to 50 mL/min (Cucullo et al., 2002).

An advantage of this system is the negligible extravasation of proteins, expression of ion channels and efflux transporters. However, drawbacks of this model include the requirement for a high seeding density during the initial set up of the system and the lack of visual observation of the intraluminal compartments to evaluate morphological and phenotypical changes in the endothelium. In addition, the system is not designed for high throughput screening and is technically challenging (Naik and Cucullo. L, 2012, Sivandzade and Cucullo, 2018)

The only BBB cell model to have been studied using this system is the PBMEC1/2 system. Cells grown in this system demonstrated higher viability compared to models grown under static conditions and was less permeable to FITC-dextran compared to that in a non-flow model. The highest flow rate the cells were subjected to was reported to be 14 mL/min. No TEER values were reported in this study (Neuhaus et al., 2006), however, another study reported TEER values of < 250 Ω.cm² (Cucullo et al., 2013).

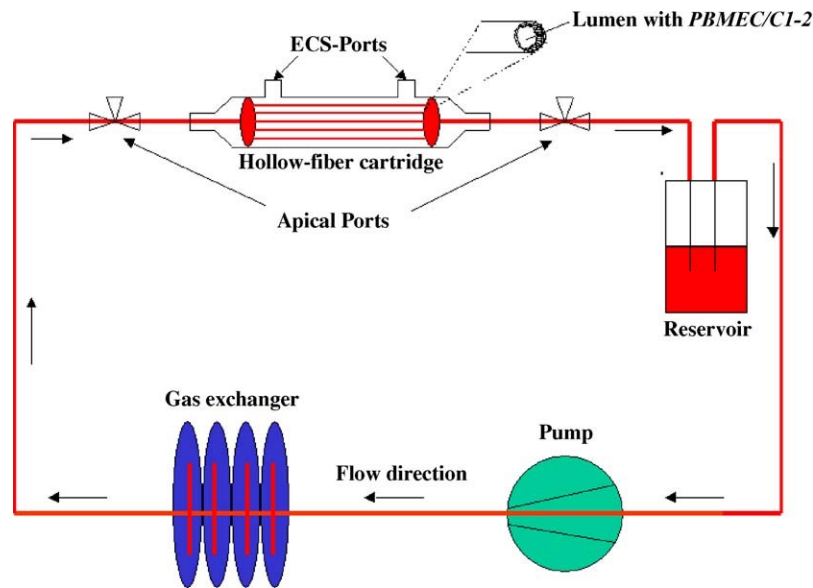


Figure 1.11 Hollow fibre BBB model using PBMEC1/2

The hollow fibre cartridge where PBMEC1/2 cells are seeded is connected by gas permeable tubing to a reservoir media bottle. Media is circulated by a pumping system with a maximum flow rate of 50 mL/min. Rat C6 cells were seeded in the extra capsular space (ECS) (Neuhaus et al., 2006).

1.8.2.2 Microfluidic platforms

Microfluidic systems are a type of three dimensional *in-vitro* models consisting of an 'organ-on-a chip' device constructed from polydimethylsiloxane (PDMS) channels moulded using a photo-defined master mould and a porous tissue culture substrate which is then sealed between two channel networks (Figure 1.12) (Esch et al., 2012). The benefits of this system in BBB modelling is having realistic dimensions and allows for the observing the cells in a 3D engineered physiological microenvironment by exposing the endothelium to physiological flow (Griep et al., 2013, Booth and Kim. H, 2012). Drawbacks of this model involve limited scalability, requiring high technical skills and equipment to achieve the model, in addition to the lack of quantification of critical BBB parameters such as TEER and selective permeability (Gastfriend et al., 2018).

A study using bEND.3 mouse brain cells showed a significant improvement in TEER values when cells were exposed to 0.0223 dynes/cm² with a reported TEER value of 140 Ω.cm² in comparison to 15 Ω.cm² when cells were grown under static conditions (Booth and Kim. H, 2012). Another study using human

hCMEC/D3 cells were exposed for 3 days to flow rate of 5.8 dynes/cm² and demonstrated 3 fold increase in TEER values from 37 Ω.cm² to 120 Ω.cm² (Griep et al., 2013).

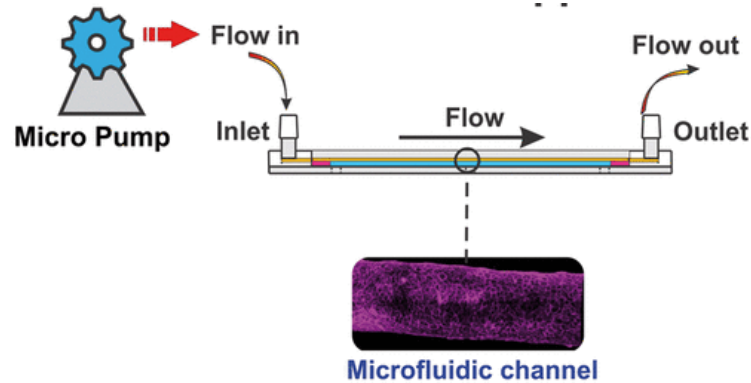


Figure 1.12 Schematic representation of a microfluidic based model

A microfluidic model made up of, a pump connected to the inlet of the channel to allow for the passage of media beneath the cells. The cells are seeded on a porous cell culture substrate and is sandwiched between two PDMS channels (Sivandzade and Cucullo, 2018).

1.8.2.3 Perfusion based interconnected chamber

Recently, a novel cell culture flow-based chamber technology was developed and commercialised (Vozz, 2008, Iori et al., 2012), the QuasiVivo[®] system (Kirstall, Sheffield, UK). The QuasiVivo[®] system utilises a flow model that is able to simulate blood flow between different cell culture chambers which represent tissues (Elbakary and Badhan, 2020, Haycock, 2014). There are 3 QuasiVivo[®] models, the QV 500, 600 and 900.

The QV500 system consists of 10 mm deep, 15 mm in width and can hold up to 2 mL in volume (Figure 1.13). The chambers are suitable for surface culture models such as cells grown on coverslips but cannot house cell culture insert systems. The QV500 system was used by other groups to assess the benefit of dynamic media flow within an interconnected systems of chambers with differing cell lines such as pericytes, astrocytes and endothelial cells (Miranda-Azpiazu et al., 2018).



Figure 1.13 The Quasi vivo® 500 system

An experimental set up of the QV500 system inside an incubator displaying a peristaltic pump, media reservoir, chambers were coverslips are places (Azimi et al., 2020)

The QV600 system has chambers that are 22 mm deep, 15 mm in width and can hold up to 4 mL in volume (Figure 1.14). This system can be utilised using coverslips and 24-well inserts and can be used to establish a liquid/liquid interface (LLI) and air/liquid interface (ALI) (Sbrana and Ahluwalia, 2012). The system has a reservoir bottle where media exchange takes place and a peristaltic pump that can be housed in an incubator. The QV600 has been utilised with permeable insert systems. For example an increase in barrier tightness (measured by TEER) was noted when using the QV600 ALI to develop an *in-vitro* pulmonary model cultured using NHBE on semi-permeable inserts (Chandorkar et al., 2017).



Figure 1.14 The Quasi vivo® 600 system

The QV600 model showing a peristaltic pump, a reservoir bottle, an outlet for O₂/CO₂ exchange with a filter attached, a 2 mL chamber and connectors.

Recently, a number of groups have utilised the QV600 system with cellular barrier models such as the intestinal epithelial cells (Caco-2) and pulmonary cells (NHBE, SAE) to assess the impact of shear stress produced by laminal flow on cellular viability, barrier proprieties and increased barrier tightness to better enhance *in-vitro* models and their suitability for drug permeability and toxicity testing by optimizing the microenvironment (Elbakary and Badhan, 2020, Giusti et al., 2014, Chandorkar et al., 2017).

1.9 Thesis aims and objectives

The overall aim of this thesis is to enhance drug delivery to brain tumours by overcoming MDR resulting due to the presence of BCRP in the BBB and the BTB as well as assess the duality of phytochemicals as BCRP modulators and anti-cancer agents. For this we commenced with the tumour site rather than the BBB, where we aimed to assess the dual ability of phytochemicals to modulate the

efflux action of BCRP and the anti-cancer properties they might exhibit in LN229 human glioblastoma cells. Upon completing the first stage we then assessed the ability of optimal flavonoids to modulate the action of BCRP at the BBB. Once this stage was accomplished, we then utilised shear stress in the form of laminal flow to enhance BBB characteristics and increase barrier tightness that is to assess the permeability of optimal flavonoids across a more restrictive barrier. To realise those aims, the overall objectives were:

Chapter 2:

- To assess the cytotoxicity of phytochemicals and anti-cancer agents
- To assess the ability of phytochemicals to modulate the efflux action of BCRP
- To assess the effect of phytochemicals to modulate the expression of BCRP
- To assess the effect of phytochemicals on cellular migration
- To assess the effect of flavonoids and anti-cancer agents on reactive oxygen species generation
- To assess the effect of flavonoids and anti-cancer agents on the activation of caspases

Chapter 3:

- To optimise collagen culture surface coating using PBMEC/C12 cells
- To develop and characterise an *in-vitro* BBB model using primary porcine brain cells
- To assess the cytotoxicity of hesperetin, methotrexate and mitoxantrone within primary porcine brain cells
- To demonstrate the efflux function of BCRP using the substrates methotrexate and mitoxantrone
- To assess the permeability of hesperetin across the BBB model
- To demonstrate the ability of hesperetin to modulate the efflux action of BCRP and enhance drug permeation across the BBB

Chapter 4:

- To create a blood brain barrier model using PBMEC grown in 24-well inserts for use in the QV600 chamber
- To determine the optimal flow rate suitable for PBMEC growth
- To examine the effect of shear stress on cell proliferation
- To examine the effect of shear stress on TEER values
- To examine the effect of shear stress on ZO-1 tight junction protein expression
- To assess the permeability of mitoxantrone and hesperetin across the BBB model, following exposure to shear stress

Chapter 2

Phytochemical mediated modulation of breast cancer resistance protein in human glioblastoma cells

Elements of this chapter have been submitted for publication as follows:

Elbakary, B. and R. K. S. Badhan (2021). " Phytochemical mediated modulation of breast cancer resistance protein in human glioblastoma cells." [Brain research](#)

Manuscript under review: submitted 11/02/21

2.1 Background

Gliomas are a common type of tumour occurring in the brain and spinal column and can be classified by their originating cell location. Gliomas contribute to about 78% of all malignant tumours (Louis et al., 2007), with glioblastoma multiforme being the most frequent and malignant type. According to the World Health Organisation (Gaillard, 2021), 80% of these tumours are grade 4 and 5 which is considered high grade tumours. Glioblastomas are a form of aggressive brain tumour which often presents with poor prognosis and a median survival time of less than 1.5 years (Rock et al., 2012, Ohka et al., 2012, Thakkar et al., 2014, Santos et al., 2011).

Brain tumours among other CNS illnesses remain difficult to treat due to the inability of many therapeutic agents to obtain efficacious concentrations in the brain. Partly that's because of active efflux transporters that limit blood to brain drug uptake. The impact of the limitations imposed by BBB and BTB on CNS indicated drug discovery/development pathways is clearly illustrated by the fact that it takes longer to develop CNS-indicated drugs (15 years) compared to non-CNS indicated drugs (7-9 years) with a higher failure rate in clinical sitting (Alvarez et al., 2010).

Glioblastoma, much like other malignancies, occur due to the uncontrollable cell proliferation, cell migration, invasion and infiltration to neighbouring tissue (Achrol et al., 2019, Demuth and Berens, 2004, Singh et al., 2010).

Furthermore, the presence of active efflux transporters on the apical and basolateral membrane of the BBB and the BTB can significantly hinder drug transport into the brain (Stieger and Gao, 2015, On and Miller, 2014).

The overexpression of ABC transporters, primarily BCRP and P-gp, has been reported in solid tumours and in drug-naïve tumours, where the originating tissue showed little to no expression of the transporters, with irregularities in the expression of ABC transporters related to more aggressive tumour phenotype (Scotto, 2003, Muriithi, 2020). This suggests that ABC transporters play a vital role in cancer progression beyond MDR and is contributor towards poor

prognosis (Wijaya et al., 2017, Ginguené et al., 2010). In some cases, the tumour compromises the integrity of the BBB and forms a heterogenous vasculature known as the blood tumour barrier (BTB). The BTB has numerous distinct characteristics such as non-fenestrated capillaries, ununiform permeability and expression of efflux transporters (Arvanitis et al., 2020a) These impose major obstacles for drug delivery targeting GBM (Groothuis, 2000, Schlageter et al., 1999).

Current chemotherapeutics routinely used for treatment of GBM alone or in combination with radiotherapy (Stupp et al., 2007) have low efficacy because most tumours are resistant to multimodality approaches and multiple anti-cancer agents, none of which are considered curative (Weller et al., 2015, van Tellingen et al., 2015, Gomez-Zepeda et al., 2019). Despite agents such as temozolomide being widely used clinically, it has been reported that at least 50% of patients are refractory to it as a solo agent, with the remaining requiring additional modes of therapy such as temozolomide with radiotherapy, resulting in an improved overall mean survival rates (Johnson and O'Neill, 2012). There is an urgent need to improve the efficacy of anti-cancer agents rather than devising new ones. One recent approach to overcome the limited permeability of anti-cancer agents at the BBB and the BTB is to modulate the efflux functions of members of the ABC family of transporters that take part in the MDR phenotype such as BCRP (Mao and Unadkat, 2015, Ni et al., 2010, M. F. Gonçalves et al., 2020)

A common concern with more recent transporter inhibitors has been their toxicity profile and poor specificity which have resulted in clinical failure (Gimenez-Bonafe et al., 2008). Therefore, there is a need to identify and develop newer inhibitors or modulators of both drug transporters and their regulatory elements, to enable a broad approach to the modulation of the transport function at CNS barriers.

One potential group of candidate compounds which are often perceived as being 'safe' are natural product derived phytochemicals, commonly from the flavonoids group, which have demonstrated an ability to modulate the expression and

function of xenobiotic clearance pathways (Cooray et al., 2004b, Imai et al., 2004a, Ahmed-Belkacem et al., 2007, Pick et al., 2011, Valdameri et al., 2012).

Several flavones, flavonols and flavanones were reported to possess potent anti-tumour activity (Edenharder et al., 1993), with these properties being associated with their ability to induce ROS production (Hadi et al., 2000), induce apoptosis (Abotaleb et al., 2018), participate in cell cycle arrest and suppress cancer invasion (Rodríguez-García et al., 2019). Similar activities have been demonstrated with all flavonoid groups (Braganhol et al., 2006, Nguyen et al., 2004, Santos et al., 2011, Lin et al., 2008, Shen et al., 2010, Wang et al., 2010c). Furthermore, a variety of flavonoids demonstrate pro-oxidative properties, in contrast to their activity as antioxidants, inducing cancer cell death often by increasing ROS production (Gibellini et al., 2010, Sharma et al., 2007b, Kachadourian and Day, 2006, Jeong et al., 2009, Lee et al., 2010, Hattori et al., 2009, Matsuzawa and Ichijo, 2008).

Combining phytochemicals with well-known anticancer agents *in-vitro* and *in-vivo* has been shown to exhibit promising results. For example, combining genistein with cisplatin was able to significantly reduce cancer cell proliferation and induce apoptosis in BxPC-3 pancreatic tumour xenografts (Mohammad et al., 2006). In laryngeal cancer cells HeP-2 using a combination of cisplatin and quercetin lead to an increased induction of apoptosis within the cells via ROS production and activation of caspases-8 and 9 (Sharma et al., 2005). Similarly, in MCF-7 breast cancer cells, combining doxorubicin with quercetin distinctly reduced cancer cell migration, and reduced cancer cell proliferation. In addition, quercetin was able to reduce unwanted cytotoxic effects to healthy normal cells (Staedler et al., 2011).

Moreover, current clinical trials have displayed the safety and efficacy of phytochemicals either solely as anti-cancer agents (Fantini et al., 2015) or in combination with a chemotherapeutic agent (Saldanha and Tollefsbol, 2011, Gupta et al., 2013, Kanwar et al., 2012). Breast cancer patients undergoing radiotherapy were administered ECGC 400 mg orally three times a day. Compared to patients undergoing radiotherapy alone, the results showed

reduced serum level of VEGF and HGF, in addition to suppressed activation of MMP-9 and MMP-3 (Zhang et al., 2012). Indeed, within the *in-vitro* glioblastoma cell models such as LN229, flavonoids have been shown to modulate BCRP functional transporter activity and trigger apoptosis pathways (Sharma et al., 2007a, Siegelin et al., 2009, Gibellini et al., 2010, Kachadourian and Day, 2006, Jeong et al., 2009, Lee et al., 2010, Hattori et al., 2009, Matsuzawa and Ichijo, 2008).

The phytochemicals were selected for this experimental study based on reports that demonstrated the compounds' anti-cancer properties and/or modulatory action of ABC efflux transporters and/or ability to permeate across *in-vitro* BBB models since chemotherapeutic agents must first bypass the BBB in order to reach the tumour site (Table 2.1). In addition, previous work by our group have demonstrated the potential for flavonoids to modulate BCRP functional transporter activity at the BBB and blood-CSF-barrier (Kaur and Badhan, 2017). These compounds were not reported to have been screened in the LN229 human glioblastoma cell line previous nor did their effect on the expression of ABC efflux transports in that cell line. Further, availability and affordability of the phytochemicals was also considered.

Table 2.1 phytochemicals reported anti-cancer proprieties, blood brain barrier permeability and interaction with members of the ABC efflux transporter family

phytocompound	Anti-cancer proprieties	Cancer cell line	Reported BBB permeability (AB flux)	Interaction with ABC transporters
Hesperetin	Induce cell cycle arrest, Apoptosis (Sambantham et al., 2013), inhibit proliferation (Ersoz et al., 2019)	MCF-7(Choi, 2007) C6 (Ersoz et al., 2019) PC-3 (Sambantham et al., 2013) SiHa (Alshatwi, 2012)	J 5.75 ± 0.4 nmol/min/mg protein in Caco-2 monolayer using 500 µM of the compound (Kobayashi et al., 2008)	BCRP substrate (Brand et al., 2011) BCRP inhibitor (Morris and Zhang, 2006) P-gp inhibitor (Morris and Zhang, 2006)
Rutin	Reduce tumour growth, Induce apoptosis and cell cycle arrest (Chen et al., 2013, Ganeshpurkar and Saluja, 2017, Caparica et al., 2020)	LAN-5 (Chen et al., 2013) C6 (da Silva et al., 2020) 786-O (Caparica et al., 2020)	P_{app} 0.05 x 10 ⁻⁶ ± 0.03 cm/s in Caco-2 monolayer using 100 µM of the compound (Yang et al., 2014)	P-gp inhibitor (Mohana et al., 2016)

Quercetin	Reduces cell proliferation and Induces of Cell death (Lu et al., 2006, Chen et al., 2004)	HL-60 (Kang and Liang, 1997) HT-29, HepG2, PC-3 (Pan et al., 2018)	65.54% permeable across BMVEC monolayer model (Ren et al., 2010) P_{app} 147.7 \pm 20.8 nm/s across ECV304 monolayer (Youdim et al., 2004a) P_{app} 2.02 \times 10 ⁻⁶ \pm 0.38 cm/s in Caco-2 monolayer using 100 μ M of the compound (Yang et al., 2014)	P-gp Substrate (Wang et al., 2005b) BCRP substrate (Sesink et al., 2005) BCRP inhibitor (Yoshikawa et al., 2004, Cooray et al., 2004a) BCRP inducer (Ebert et al., 2006)
Estrone	NR	NR	NR	BCRP inhibitor (Kaur and Badhan, 2017)
Baicalin	Induces Apoptosis (Chen et al., 2001, Yu et al., 2015, Shieh et al., 2006), reduces migration (Gao et al., 2017a, Duan et al., 2019) Inhibits metastasis (Zhou et al., 2017a)	LNCaP, JCA-1 (Chen et al., 2001) HePG2, SMMC-7721 (Yu et al., 2015)	P_e 0.0455 \times 10 ⁻⁶ cm/s when tested in artificial PAMPA BBB model using 200 μ M of the compound (Tarragó et al., 2008) P_{app} 3.89 \times 10 ⁻⁶ \pm 0.48 cm/s in Caco-2 monolayer using 23.7 μ M of the compound (Li et al., 2012)	BCRP inhibitor (Kalapos-Kovács et al., 2015a) MRP-2 inhibitor (Akao et al., 2007, Li et al., 2012)
Curcumin	Apoptosis, suppression of cell proliferation, invasion, and migration (Anand et al., 2008,	HepG2 (Fan et al., 2014, Cao et al., 2008) A549 (Liu et al., 2017, Chen, 2009) HT29 (Sharma, 2009)	NR	BCRP inhibitor (Shukla et al., 2009b) MDR-3 inhibitor (Wen et al., 2019)

	Kunnumakkara et al., 2017)	HeLa (Cai et al., 2012, Shang et al., 2016)		
Naringin	Inhibit cell proliferation, chemosensitizer, Induce Apoptosis (Erdogan et al., 2018, Memariani et al., 2020, Ghanbari-Movahed et al., 2021, Camargo et al., 2012)	HT-29 (Krajka-Kuzniak et al., 2017) PC-3 (Erdogan et al., 2018)	NR	P-gp inhibitor (Mohana et al., 2016)
Naringenin	reduce Cell migration, Induce Apoptosis (Chang et al., 2017, Shi et al., 2021, Memariani et al., 2020)	A549 (Chang et al., 2017) TCC (Ghanbari-Movahed et al., 2021)	NR	P-gp inhibitor (de Castro et al., 2007, de Castro et al., 2008) BCRP inhibitor (Ahmed-Belkacem et al., 2005b, Takahata et al., 2008)
Hesperidin	Induce apoptosis, reduce angiogenesis, chemoresistance, metastasis (Aggarwal et al., 2020, Ahmadi and Shadboorestan, 2016)	HePG2 (Banjerdpongchai et al., 2016) HeLa (Wang et al., 2015)	$P_{app} 3.78 \times 10^{-6} \pm 0.32$ cm/s in Caco-2 monolayer using 50 μ M of the compound (Yang et al., 2014)	P-gp inhibitor (Mohana et al., 2016)
α-Naphthoflavone	Induces apoptosis (Yu et al., 2019)	MCF-7 (Merchant et al., 1993)	NR	P-gp inhibitor (Datta et al., 2015)

	Chemosensitizer (Datta et al., 2015)			
Biochanin A	Induce apoptosis, inhibit cell migration (Li et al., 2018b, Bhardwaj et al., 2014, Szliszka et al., 2013, Jain et al., 2015)	PANC1(Bhardwaj et al., 2014) A549 (Li et al., 2018b)	NR	P-gp inhibitor (Zhang and Morris, 2003) BCRP inhibitor (Zhang et al., 2004a, Pick et al., 2011)
Benzo (a) pyrene	Carcinogenic Tumorigenic (Gelboin, 1980, Goyal et al., 2010)	WHCO-1 (Dzobo et al., 2018) MCF-7, HePG2 (Hockley et al., 2006)	NR	NR
Fisetin	Induce apoptosis Inhibit invasion and migration and cell proliferation (Imran et al., 2021, Mukhtar et al., 2016, Mukhtar et al., 2015)	HT-29 (Suh et al., 2009) U266 (Jang et al., 2012) BT549 (Li et al., 2018a) PANC1 (Jia et al., 2019)	NR	BCRP inhibitor (Yarla and Ganapaty, 2013a) P-gp inhibitor (Mohana et al., 2016)

NR: Not Reported.

2.2 Aims and objectives

Given the ability of flavonoids to initiate apoptosis and attenuate the functional activity of BCRP at the BBB and within glioblastoma cells, our aim for this chapter was to examine the impact of flavonoids on BCRP functional transporter activity and expression in LN229 cells and their dual role as apoptosis and reactive oxygen species inducing agents. To achieve the aims for this chapter, the overall objectives were to utilise the LN229 GBM cellular model:

- To assess the cytotoxicity of phytochemicals and anti-cancer agents
- To assess the ability of phytochemicals to modulate the efflux action of BCRP
- To assess the effect of phytochemicals to modulate the expression of BCRP
- To assess the effect of phytochemicals on cellular migration
- To assess the effect of flavonoids and anti-cancer agents on reactive oxygen species generation
- To assess the effect of flavonoids and anti-cancer agents on the activation of caspases

2.3 Materials

Dulbecco's modified essential media with 4.5 g/L glucose (DMEM), Antibiotic-Antimycotic® were obtained from Biosera (Sussex, UK); Ko143, RIPA lysis buffer system, Tris Buffered Saline with Tween 20 (TBST) 20X were obtained from Santa Cruz Biotechnology (Texas, USA); TruPAGE™ Precast gels 4-8%; TruPAGE™ TEA-Tricine SDS Running Buffer, TruPAGE™ TEA-Tricine SDS transfer buffer were obtained from Sigma-Aldrich (UK); monoclonal ABCG2 antibody (BXP-21) (#sc-58222) and β -actin C4 HRP (#sc-47778) were obtained from Santa Cruz Biotechnology (Texas, USA), goat anti-mouse IgG (H+L) secondary antibody (#62-6520) was obtained from Thermofisher (Oxford, UK); curcumin was obtained from Cayman Chemicals (Cambridge, UK); and all other chemicals were sourced from Sigma (Dorset, UK) and are HPLC grade.

For this chapter, the following modulators/flavonoids were considered α -naphthoflavone; baicalin; benzo-a-pyrene; biochanin A; curcumin; estrone; fisetin; hesperidin; hesperetin; naringin; naringenin; quercetin and rutin. Stock solutions of all test compounds were prepared in dimethyl sulfoxide (DMSO) and stored at $-80\text{ }^{\circ}\text{C}$ until use.

2.4 Methods

2.4.1 Culture of LN229 human glioblastoma cells

The immortalised human glioblastoma cell line LN229 (ATCC: CRL-2611) were cultured in media containing 1% FBS, 1% v/v antibiotic-antimycotic and DMEM. Cells were seeded in an uncoated T75 flask and grown for 4-5 days until confluency. Thereafter, 1 mL 0.25% w/v trypsin-EDTA was added to the flask for 3 minutes and then neutralised with an equal amount of growth media. The cell suspension was then placed into T25 flasks, 24-well and 96-well plates for further experiments.

2.4.2 Methyl thiazolyl diphenyl tetrazolium bromide (MTT) assay.

In order to assess the impact of the phytochemicals of interest on cellular viability and determine the 50% cellular growth inhibitory concentration (IC₅₀), a MTT assay was conducted. A sterile stock solution of MTT was prepared by dissolving 5 mg/mL MTT powder in DMSO and stored at -20 °C. This was diluted to a working concentration (1:10) in sterile serum free growth media on the day of experiment. In each well of the 96-well plates, 50,000 LN229 cells were seeded and incubated for 24 hours at 37 °C, 5% CO₂. The cells were treated with a 6-fold concentration range of modulators (0.001-100 µM) and were incubated for an additional 24 hours. The media was subsequently removed, and the cells were washed with pre-warmed PBS. The cells were incubated with MTT working solution (0.5 mg/mL) in the dark for 4 hours. Thereafter, the MTT solution was removed, and the formed purple formazan crystals were dissolved using 100 µL/well DMSO. After gentle shaking for 15 minutes, the absorbance was measured at 362 nm and the percentage viability calculated according to equation (2).

$$\% \text{ Cellular viability} = \frac{\text{UV absorbance in treated cells}}{\text{UV absorbance in control cells}} \times 100 \quad (2)$$

2.4.3 Intracellular accumulation of the fluorescent BCRP probe substrate, Hoescht-33342

To assess the impact of modulators on BCRP functional activity, changes in the intracellular accumulation of the BCRP fluorescent substrate, Hoescht-33342 (H33342), were assessed in the presence and absence of the modulators (Kaur and Badhan, 2015, Kaur and Badhan, 2017). Into each well of 96-well plates, 50,000 LN229 cells were seeded and incubated for 24 hours at 37 °C and 5% CO₂. Cells were then pre-incubated with phytochemicals over a 6-fold concentration range of flavonoids, 0.001-100 µM, for 1 hour. Thereafter the cells were incubated for an additional 1 hour with identical phytochemicals concentrations in addition to 10 µM H33342. The media was then removed, and the cells were washed twice with ice cold PBS, 20 µL of PBS was added to each well before being frozen at -80 °C for 20 minutes. The cells were then removed

from the clear plate into a black 96-well plate by scraping. The fluorescence of H33342 was measured (Tecan Spark 10M[®]) at an excitation and emission wavelength of 360 nm and 489 nm respectively.

2.4.4 Cellular migration assay

This assay was conducted to examine the effect of the flavonoids on the cellular migration properties of LN229 cells (Sharma et al., 2007b, Jonkman et al., 2014). Into each well of a 24-well plate, 70,000 LN229 cells were seeded and incubated for 24 hours (at least 90% confluence). The cells were subsequently incubated for an additional 24 hours in serum free growth media (Sharma et al., 2007b, Jonkman et al., 2014). Thereafter, vertical and horizontal scratches were made in the middle of each well using a 20 μ L pipette tip. The cells were then washed with pre-warmed PBS to remove any cell debris. Based on the results of the MTT assay, a non-toxic concentration of each flavonoid was incubated in addition to untreated wells within the incubation chamber of an optimal imaging microscope capable of automated looped imagery of each well (Cell-IQ[®]) (CM Technologies, Finland). Images were captured every 30 minutes for a 24-hour period. The percentage of wound closure was calculated using the Cell-IQ[®] analyser[™] software according to the differences between initially scratched area and new closure area following the incubation period. In order to compare effectiveness, a minimum cut-off of 50% inhibition of cellular migration was utilised.

2.4.5 The impact of phytochemicals on the expression of BCRP using Western blotting

Western blotting was carried to assess the effect of the phytochemicals on the expression of BCRP in LN229 cells. LN229 cells were seeded into T25 flasks at a density of 50,000 cells/flask to achieve 80% confluence. The cells were then incubated with the phytochemicals at a concentration of 50 μ M for a further 24 hours. Thereafter, the flasks were washed with ice cold PBS and removed from the surface of the flask using a cell scraper. The cells suspension was centrifuged at 3000 rpm (Hettich MIKRO 200) for 5 minutes at 4 °C. The supernatant was then discarded, and the pellet was resuspended with 50 μ L of RIPA buffer and

homogenised three times by passing through a 29G needle at 4 °C. The lysed cell suspension was centrifugated at 13,500 rpm for 25 minutes at 4 °C. The total protein in each sample was determined using Thermo scientific Pierce® Microplate BCA Protein Assay Kit. Thereafter, 40 µg of protein from each flavonoid exposed sample was prepared for SDS-PAGE by the addition of 2.5 µL LDS 4X sample buffer, 1 µL DTT 10X sample reducer to a final total volume of 30 µL with sterile filtered water. The samples were heated at 70 °C for 10 minutes before being transferred into wells of a TruPAGE™ Precast SDS-PAGE gel (4-8 %).

A Bio-Rad Mini Trans-Blot® system was used for electrophoresis and run using a TruPAGE™ TEA-Tricine SDS Running Buffer (1:50) at 180 V for at least 40 minutes or until the blue dye approached the end of the cassette. Thereafter, the gel was washed with ultrapure water and placed on to a PVDF membrane for protein blotting. The PVDF membrane was pre-activated prior to use, in methanol for 10 minutes and soaked in transfer TruPAGE™ TEA-Tricine SDS transfer Buffer 20X (1:50 dilution) with 20% methanol. The membrane was then submerged within the cassette into the gel tank with ice cold transfer buffer and blotting commenced at 50 V for 2 hours and 45 minutes. The membrane was then washed with ultrapure water and exposed to Ponceau stain (0.1% w/v Ponceau S in 5% v/v acetic acid) for one minute to allow for the visualisation of the transferred proteins on the membrane. The membrane was then washed with TBST for 15 minutes until the dye was removed, followed by blocking in 5% w/v skimmed powdered milk blocking buffer for 6 hours.

Thereafter, the membrane was incubated with the monoclonal *ABCG2* antibody (BXP-21) (1:200 dilution) overnight at 4 °C. The blots were then washed three times for 5 minutes each in TBST, before being incubated with goat anti-mouse IgG (H+L) secondary antibody (1:15000 dilution) for 2 hours. The membrane was subsequently washed three times in TBST buffer for 5 minutes each time, before being incubated with Clarity™ Western ECL Substrate for 1 minute. Thereafter, the membrane was placed on transparent film and transferred to a developing cassette then developed using a CL-X Posure™ X-ray film. Following visualisation, membranes were stripped using a mild stripping agent (glycine

15 g, SDS 1 g, Tween-20 10 mL, ultrapure water up to 1 L) (Abcam, 2020) and subsequently blocked for 3 hours at room temperature in 10% w/v skimmed powdered milk blocking buffer before being incubated with β -actin C4 HRP (1:8000 dilution) for 1 hour at room temperature and developed and visualised as described above.

2.4.6 Radical oxygen species (ROS) detection assay

To assess the potential for optimal flavonoids to activate ROS pathways in LN229 cells, 25,000 cells/well were seeded into a 96-well black clear bottom plates and allowed to attach for 24 hours. To detect intracellular ROS production, a fluorescent probe 2',7'-dichlorofluorescein diacetate (DCF-DA) cellular ROS Detection assay kit (Ab113851, Abcam Cambridge, UK) was utilised. Once DCF-DA diffuses into the cell, it undergoes deacetylation by esterase to a non-fluorescent compound. ROS has the ability to oxidize this non-fluorescent compound to a highly fluorescent 2' 7' dichlorofluorescein (DCF).

The cells were washed with 1X buffer and treated with 25 μ M DCF-DA and incubated for 45 minutes at 37 °C, 5% CO₂. Thereafter, the cells were treated with the selected optimal flavonoids and control anti-cancer agents methotrexate and temozolomide all at 10 μ M, 100 μ M and 500 μ M, for 2 hours. The fluorescence of DCF was then detected (Tecan Spark 10M®) at an excitation and emission wavelengths of 485 nm and 535 nm respectively. The increase in fluorescence intensity was used to assess the generation of net intracellular ROS when compared to control (un-treated cells).

2.4.7 The activation of Caspase-3/7 pathways

In order to assess the ability of the flavonoids to activate apoptosis in LN229 cells, the detection of caspase activity was assessed using a fluorescence Caspase-3/7 assay kit (Cayman Chemicals, 10009135, USA). This assay kit utilises a specific substrate, N-Ac-DEVD-N'-MC-R110, which can be cleaved by active caspase-3 or caspase-7, to generate a product which is highly fluorescent, and

can be detected at an excitation and emission wavelengths of 485 and 535 nm, respectively.

LN229 cells were seeded at a 40,000 cells/well into a 96-well plate and incubated for 24 hours. Thereafter the cells were treated with selected optimal flavonoids and control anti-cancer agents methotrexate and temozolomide, all at 10 μ M and 100 μ M for 4 hours. The plate was subsequently centrifuged at 800 g for 5 minutes and the media was aspirated, followed by addition of 200 μ L/well of assay buffer. The plate was then centrifuged for further 5 minutes at 800 g, before the supernatant was removed and 100 μ L/well of cell lysis buffer was added and then incubated under gentle shaking at room temperature for 30 minutes. Thereafter, the plate was centrifuge for an additional 10 minutes at 800 g followed by the transfer of 90 μ L into the corresponding wells of a black 96-well plate. Into each well, 10 μ L of assay buffer and 100 μ L of the caspase-3/7 substrate solution were also added. The plate was then incubated for 90 minutes at 37 °C, 5% CO₂. The resulting florescence of the cleaved DEVD substrate was measured at an excitation and emission wavelengths of 485 nm and 535 nm respectively (Tecan Spark 10M®).

2.5 Statistical Analysis

All data is presented as mean \pm standard deviation, with experiments being conducted in at least 3 replicate independent experiment unless otherwise stated. Where appropriate, statistical analyses was performed in GraphPad Prism 9 (La Jolla, California, USA), with t-tests and one-way ANOVA used to determine differences between the mean values. A significance p-value of <0.05 was considered as statistically significant.

2.6 Results

2.6.1 Assessing the cellular toxicity of the phytochemicals in LN229 cells.

In order to investigate the cellular toxicity towards LN229 cells, a MTT cytotoxicity assay was conducted across a 6-fold concentration (0.001-100 μM) range of the modulators for 24 hours. All the modulators displayed limited toxicity up to 100 μM , with an IC_{50} determined only for biochanin A (113.4 μM [CI: 64.39-199.8 μM]) and benzo-a-pyrene (40.2 μM [CI: 18.03-87.94 μM]) (Figure 2.1).

2.6.2 Cellular toxicity of methotrexate and temozolomide towards LN229 cells.

To further investigate the cytotoxicity of the anti-cancer agents methotrexate and temozolomide as a baselines for comparison, LN229 cells were exposed to a 6-fold concentration range, 0.001-100 μM , of anti-cancer agents for 24 hours (Figure 2.2). Temozolomide demonstrated an IC_{50} , 302.3 μM [CI: 165.9-708.6 μM] and methotrexate demonstrated IC_{50} , 639.7 μM [CI: 460.8-881].

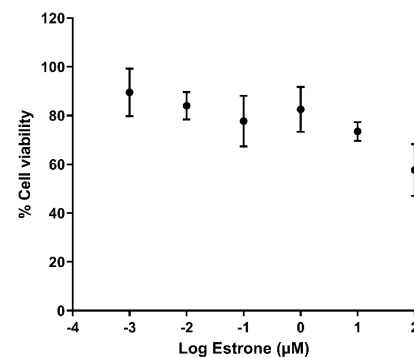
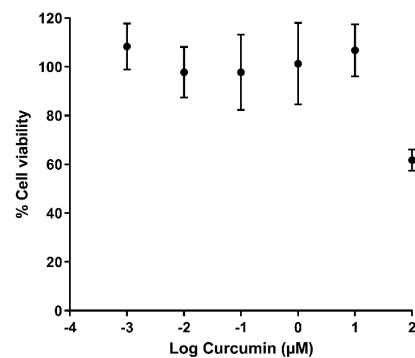
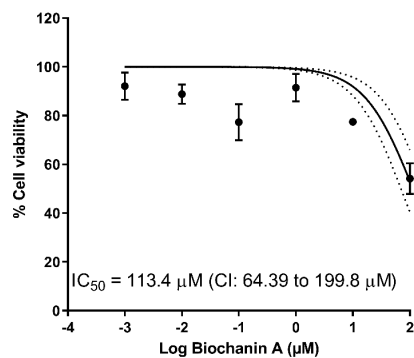
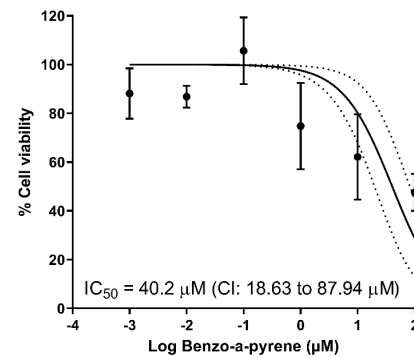
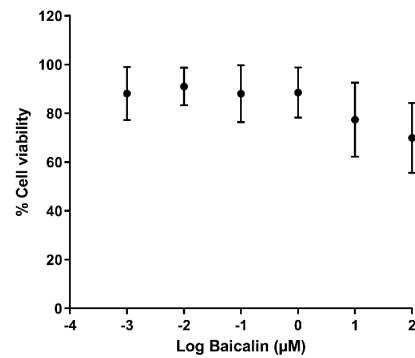
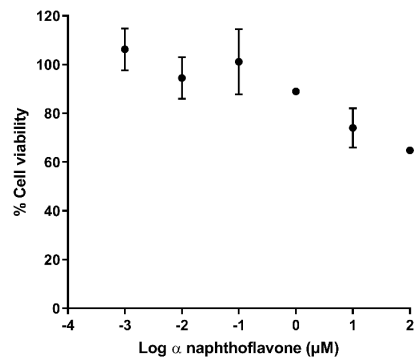


Figure 2.1 Cellular cytotoxicity of modulators of BCRP in LN229 cells.

Cells were seeded and grown on 96 well plate for 24 hrs prior to exposure to modulators over a concentration range of 0.001-100 μM for 24 hours. Thereafter, 20 μL /well (0.5 mg/mL) of MTT was added into each well and the plate was incubated for 4 hours. The media was aspirated and a 100 μL /well of DMSO was added before absorbance was measured for each well at 570 nm.

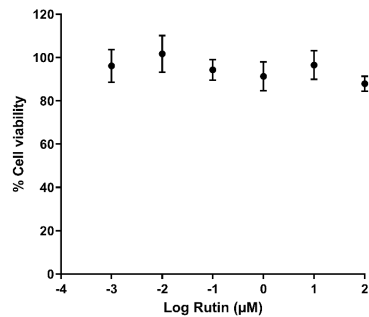
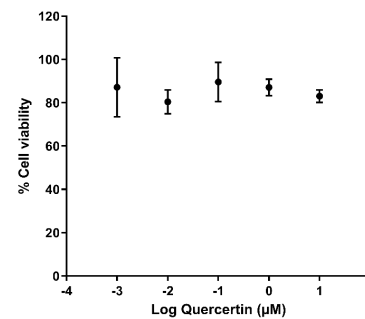
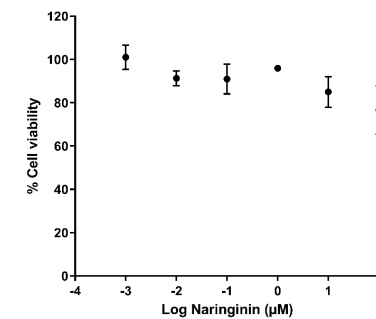
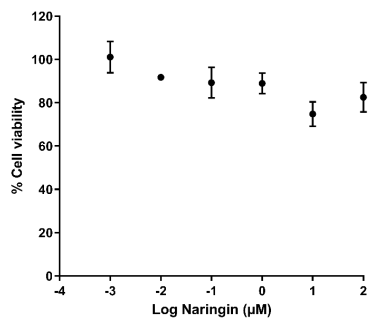
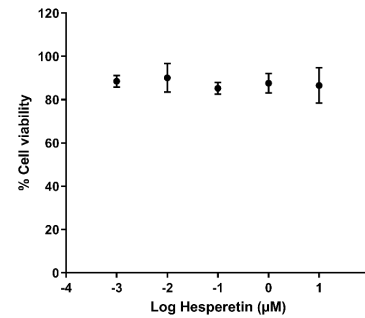
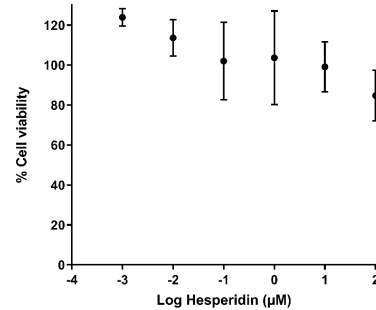
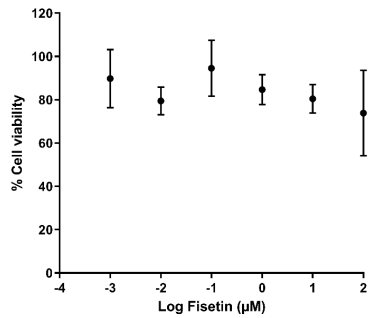


Figure 2.1 Cellular cytotoxicity of modulators of BCRP in LN229 cells (Cont.)

Cells were seeded and grown on 96 well plate for 24 hrs prior to exposure to modulators over a concentration range of 0.001-100 µM for 24 hours. Thereafter, 20 µL/well (0.5 mg/mL) of MTT was added into each well and the plate was incubated for 4 hours. The media was aspirated and a 100 µL/well of DMSO was added before absorbance was measured for each well at 570 nm.

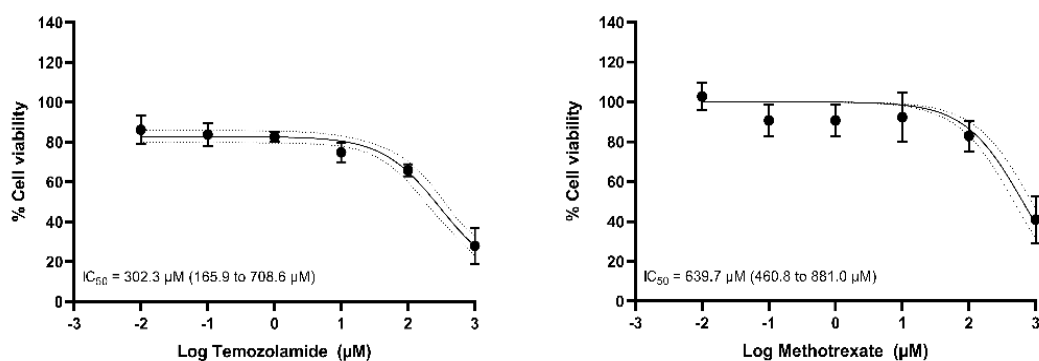


Figure 2.2 Cellular cytotoxicity of methotrexate and temozolomide in LN229

Cells were seeded and grown on 96 well plate for 24 hours prior to exposure to anti-cancer agents over concentration range of 0.001-1000 µM for 24 hours. subsequently, 20 µl/ well (0.5 mg/mL) of MTT was added and the plates were incubated for 24 hours. The media was aspirated and 100 µL/well of DMSO was added before absorbance was measured for each well at 570 nm.

2.6.3 Modulator mediated inhibition of BCRP efflux function in a H33342 intracellular accumulation assay

To assess the ability of the modulators to inhibit BCRP efflux function in LN229 cells, the intracellular accumulation of H33342, a fluorescent BCRP probe substrate, was assessed in the absence and presence of modulators across 6 fold concentration range, (0.001-100 µM) (Figure 2.3). Estrone, naringin, α -naphthoflavone demonstrated no significant increase in intracellular H33342 at all concentrations studied. Biochanin-a and the non-flavonoid carcinogen benzo-a-pyrene demonstrated statistically significant increases at 100 µM only ($P \leq 0.001$). Using the commercially available BCRP modulator Ko143 demonstrated a statically significant increase (1.5-1.55-fold) in intracellular accumulation of H33342 over concentration range (1,10 µM). The greatest increase in H33342 intracellular accumulation was demonstrated with baicalin (1.8-2.2-fold) and hesperetin (2.5-2.8-fold) over the range of (1-100 µM) (Figure 2.3).

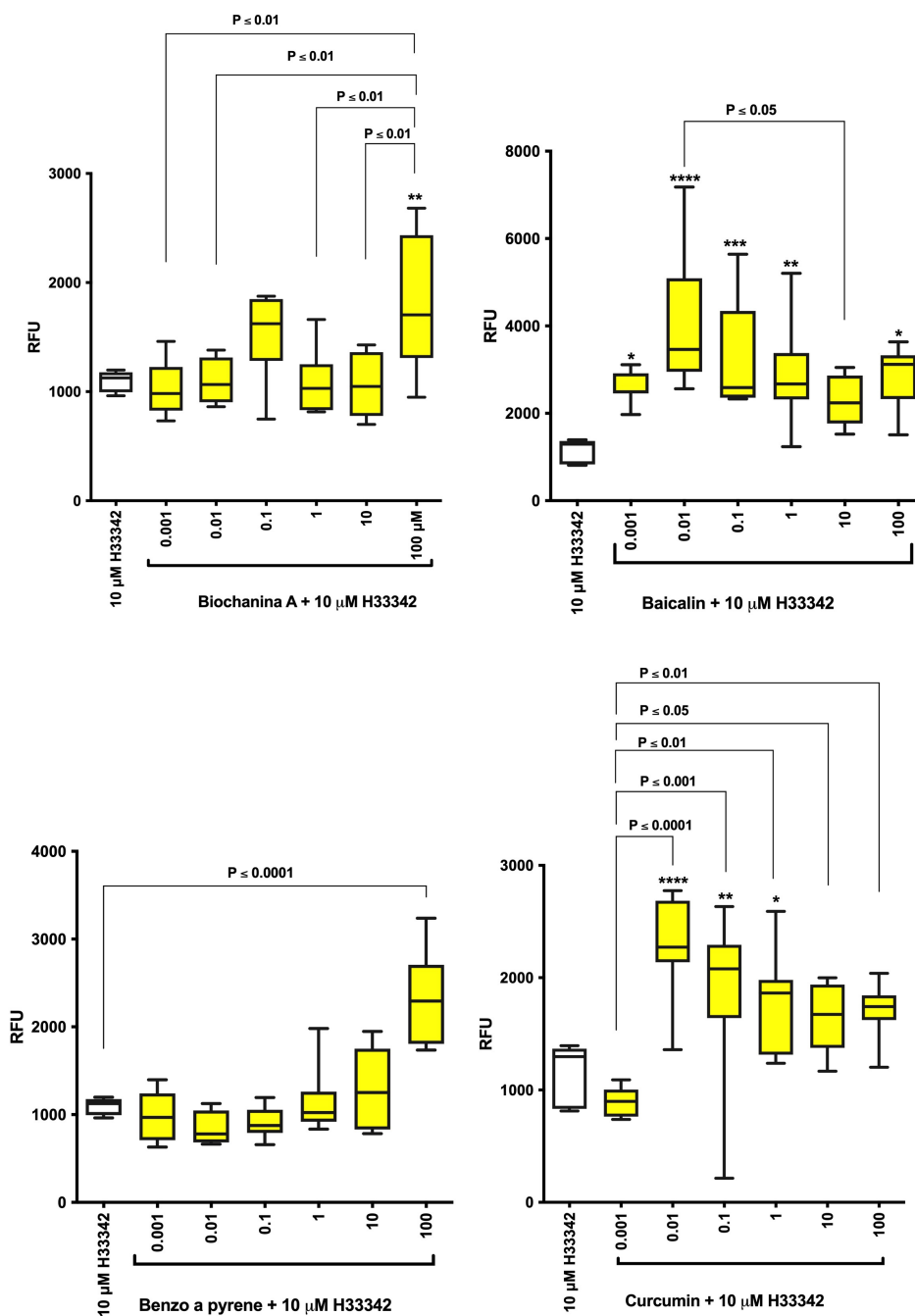
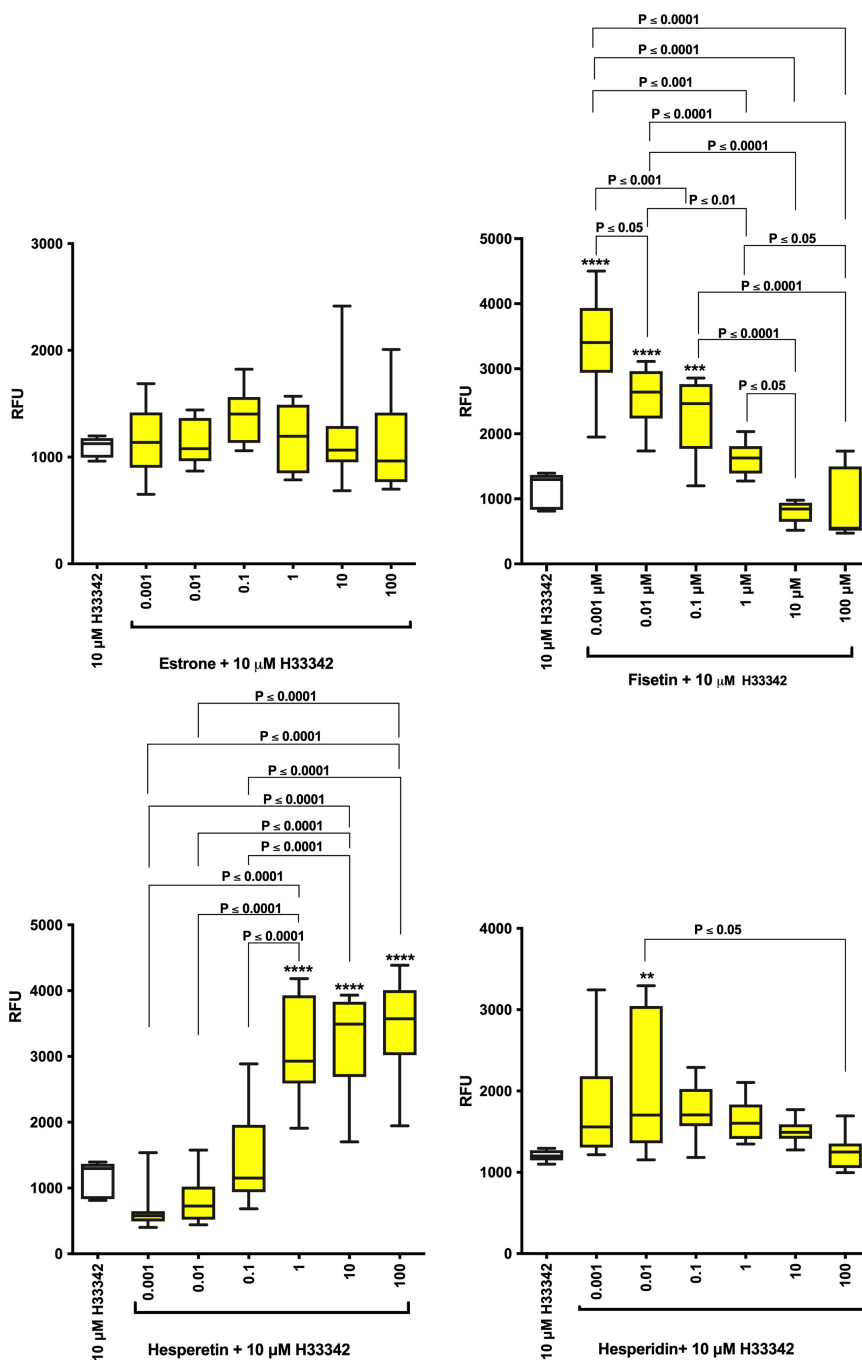


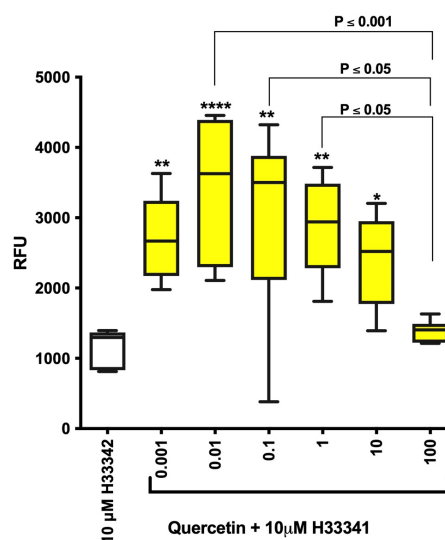
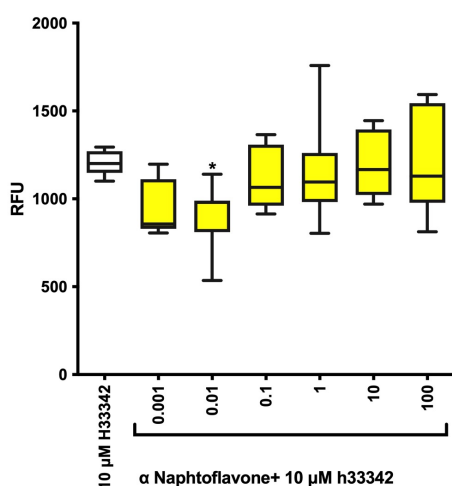
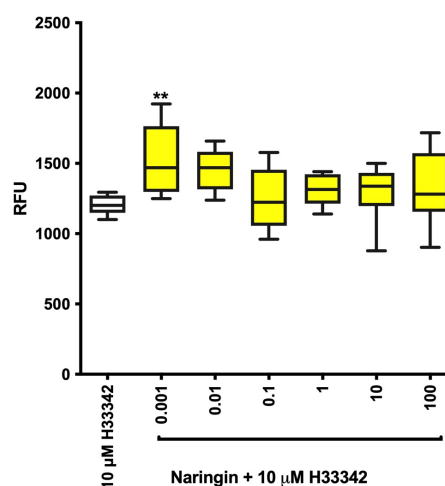
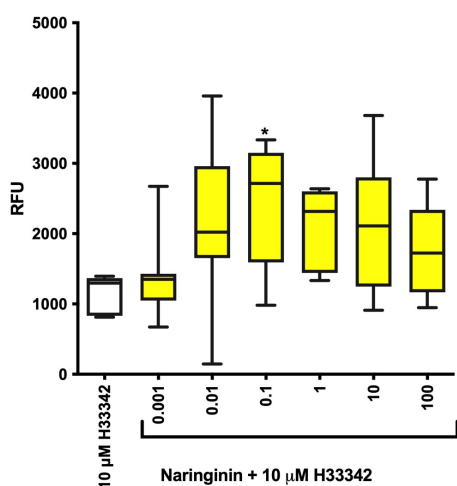
Figure 2.3 H33342 accumulation assay for BCRP function in LN229 cells.

Cells were grown in 96-well plates for 24 hours prior to incubation and subsequently washed with pre-warmed PBS prior to being pre-incubated for 1 hour with BCRP modulators over a concentration range of 0.001- 100 μM in blank media. Thereafter the cells were incubated with the same modulator concentrations in addition to 10 μM H33342 for 1 hour. The cells were washed with cold PBS and stored in -80°C for 20 minutes. Thereafter, the cells were moved to an opaque bottom plate and fluorescence was measured on a multi-plate reader at excitation and emission wavelengths 355 nm and 460 nm respectively. Statistical significance was conducted relative to control. * P ≤ 0.05, ** P ≤ 0.01, *** P ≤ 0.001 and **** P ≤ 0.0001.



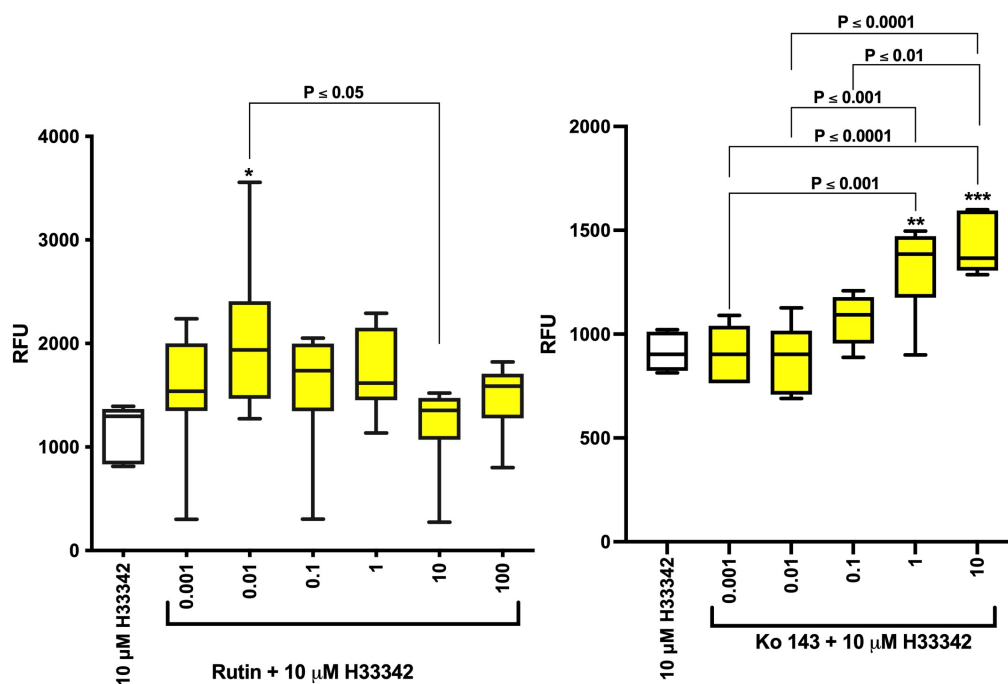
H33342 accumulation assay for BCRP function in LN229 cells (cont).

Cells were grown in 96-well plates for 24 hours prior to incubation and subsequently washed with pre-warmed PBS prior to being pre-incubated for 1 hour with BCRP modulators over a concentration range of 0.001- 100 μM in blank media. Thereafter the cells were incubated with the same modulator concentrations in addition to 10 μM H33342 for 1 hour. The cells were washed with cold PBS and stored in -80°C for 20 minutes. Thereafter, the cells were moved to an opaque bottom plate and fluorescence was measured on a multi-plate reader at excitation and emission wavelengths 355 nm and 460 nm respectively. Statistical significance was conducted relative to control. * P ≤ 0.05, ** P ≤ 0.01, *** P ≤ 0.001 and **** P ≤ 0.0001.



H33342 accumulation assay for BCRP function in LN229 cells (cont).

Cells were grown in 96-well plates for 24 hours prior to incubation and subsequently washed with pre-warmed PBS prior to being pre-incubated for 1 hour with BCRP modulators over a concentration range of 0.001- 100 μM in blank media. Thereafter the cells were incubated with the same modulator concentrations in addition to 10 μM H33342 for 1 hour. The cells were washed with cold PBS and stored in -80°C for 20 minutes. Thereafter, the cells were moved to an opaque bottom plate and fluorescence was measured on a multi-plate reader at excitation and emission wavelengths 355 nm and 460 nm respectively. Statistical significance was conducted relative to control. * P≤ 0.05, ** P ≤ 0.01, *** P ≤ 0.001 and **** P ≤ 0.0001.



H33342 accumulation assay for BCRP function in LN229 cells (cont).

Cells were grown in 96-well plates for 24 hours prior to incubation and subsequently washed with pre-warmed PBS prior to being pre-incubated for 1 hour with BCRP modulators over a concentration range of 0.001- 100 μM in blank media. Thereafter the cells were incubated with the same modulator concentrations in addition to 10 μM H33342 for 1 hour. The cells were washed with cold PBS and stored in -80°C for 20 minutes. Thereafter, the cells were moved to an opaque bottom plate and fluorescence was measured on a multi-plate reader at excitation and emission wavelengths 355 nm and 460 nm respectively. Statistical significance was conducted relative to control. * P ≤ 0.05, ** P ≤ 0.01, *** P ≤ 0.001 and **** P ≤ 0.0001.

2.6.4 Cellular migration of LN229 in the presence of flavonoids

In order to examine the ability of the modulators to inhibit cellular migration of human glioblastoma cells LN229, a wound healing assay was conducted where the migration of cells within a scratch was quantified over 24 hours in the presence of 50 μM of the modulators (Figure 2.4). Incubation with all modulators resulted in a statistically significant decreases in cellular migration compared to control (P ≤ 0.0001), except for naringin, naringenin and rutin (Figure 2.4A).

Biochanin-a and curcumin demonstrated < 2% migration following 24 hours with the overall order of migration (Figure 2.4A) being: untreated > naringin > rutin > naringenin > hesperidin > quercetin > fisetin > estrone > benzo-a-pyrene > baicalin > α -naphthoflavone > hesperetin > curcumin > biochanin-a (Figure 2.4 A and B).

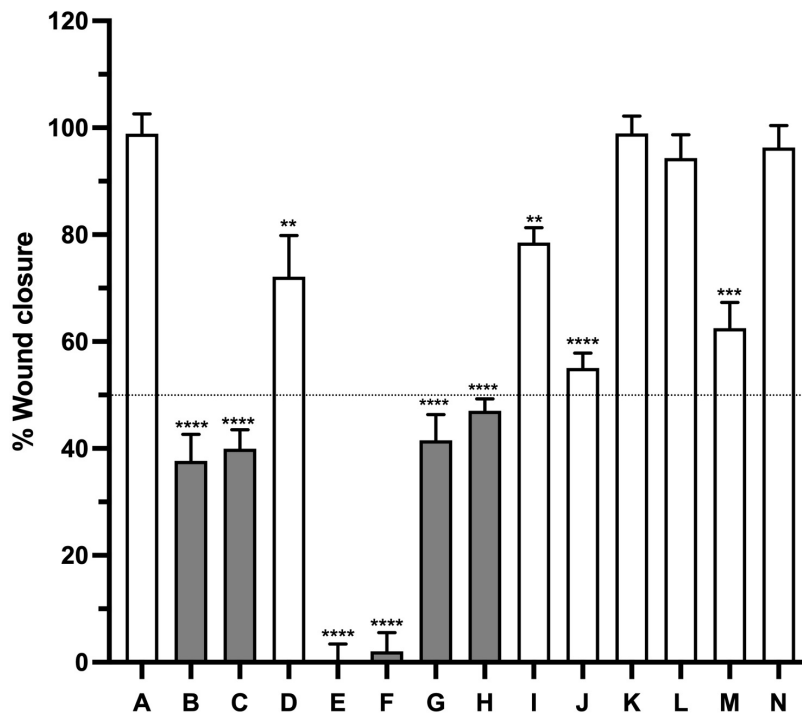
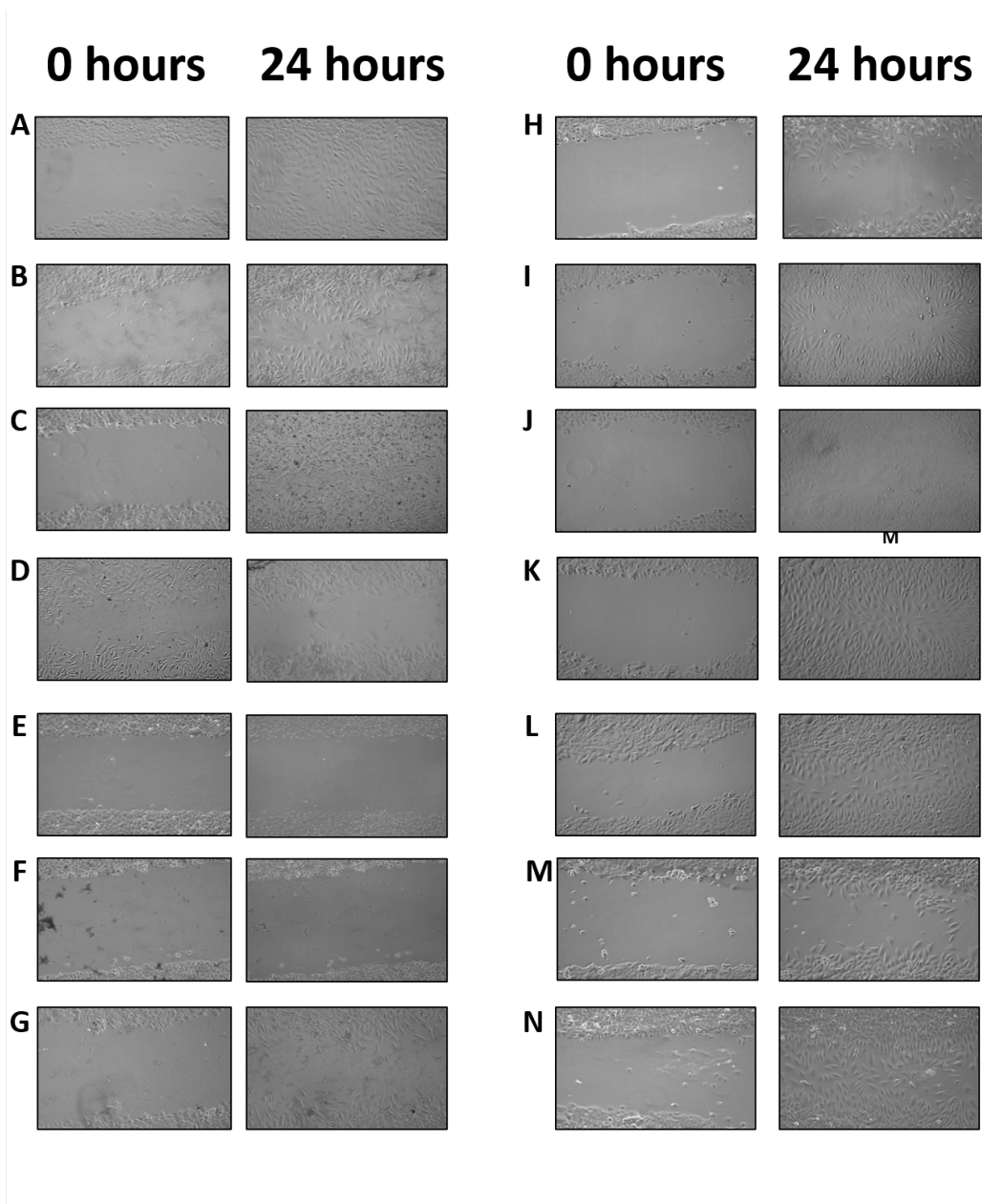


Figure 2.4 Cellular migration assay

(A) percentage closure of LN229 cells following scratches made to the plate surface. Cells were incubated with serum free media containing 50 μ M of the modulators for 24 hours within a Cell-IQ incubator. Automated looped images were taken prior to incubation and after 24 hours of incubation with the horizontal dashed line represent a 50% closure cut-off. A: untreated; B: α -naphthoflavone; C: baicalin; D: benzo-a-pyrene; E: biochanin A; F: curcumin; G: estrone; H: fisetin; I: hesperidin; J: hesperetin; K: naringin; L: naringenin; M: quercetin; N: rutin. Statistical significance was conducted relative to control (A). ** $P \leq 0.01$ and **** $P \leq 0.0001$.



Cellular migration assay(cont.)

(B) images of the wound at 0 and 24 hours of LN229 cells following scratches made to the plate surface. Cells were incubated with serum free media containing 50 μ M of the modulators for 24 hours within a Cell-IQ incubator. Automated looped images were taken prior to incubation A: untreated; B: α -naphthoflavone; C: baicalin; D: benzo-a-pyrene; E: biochanin A; F: curcumin; G: estrone; H: fisetin; I: hesperidin; J: hesperetin; K: naringin; L: naringenin; M: quercetin; N: rutin.

2.6.5 The effect of the modulators on the expression of BCRP

To assess the impact of modulators on BCRP protein expression, LN229 cells were incubated with 50 μ M modulators for 24 hours and western blot analysis was conducted (Figure 2.5). Hesperetin demonstrated the highest statistically significant downregulation in BCRP protein expression, -2.56 ± 0.45 -fold ($P \leq 0.0001$), followed by curcumin -0.65 ± 0.1 -fold ($P \leq 0.01$) and biochanin A -1.4 ± 0.01 -fold (Figure 2.6). All the other modulators lead to an increase in the expression of BCRP in the following order: rutin > quercetin > benzo-a-pyrene > fisetin > naringenin > baicalin > naringin > α -naphthoflavone > estrone > hesperidin (Figure 2.6).

Based upon the studies so far, baicalin and hesperetin were selected as optimal modulators for further experiments

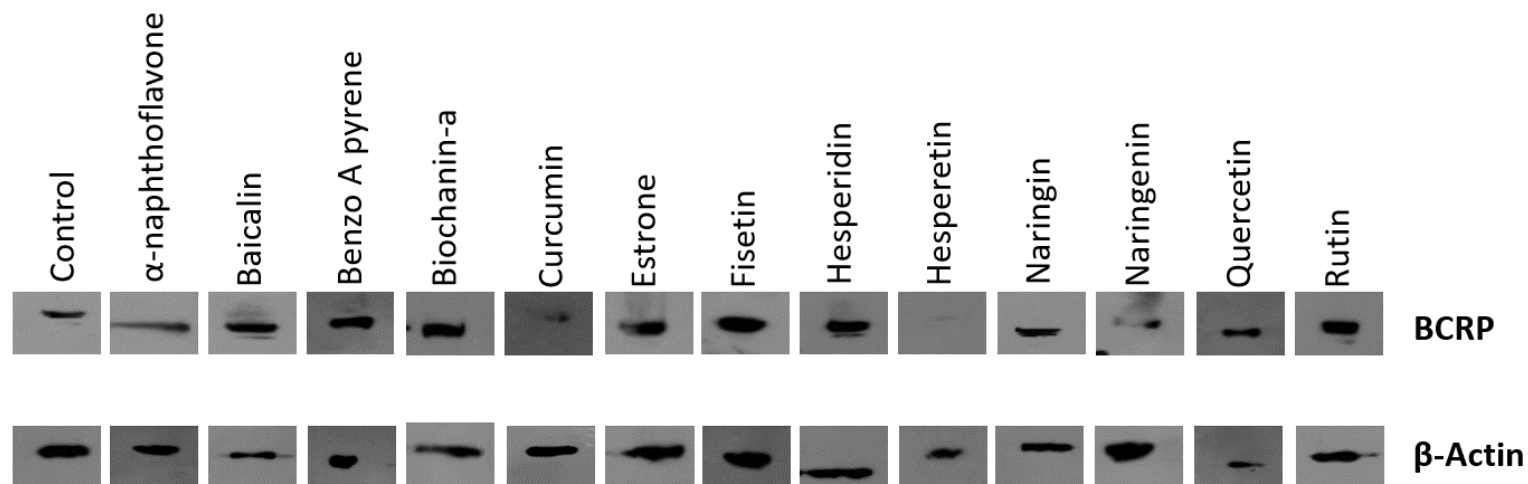


Figure 2.5 Changes on BCRP expression after 24-hour incubation with the modulators

Cells were seeded in T25 flasks and incubated with 50 μ M of the modulators once confluent for 24 hours. cells protein extraction was conducted using RIPA buffer. 40 μ g of the protein was loaded on a 4%-8% SDS PAGE gel to separate the bands, the gel was then transferred to a PVDF membrane and incubated with BXP21 (Santa Cruz,USA) for 24 hours at 4 C, then incubated with mouse anti-rabbit IgG (Themofisher,UK). ECL (Bio-RAD, UK) detection was conducted. Control presents the absence of modulators.

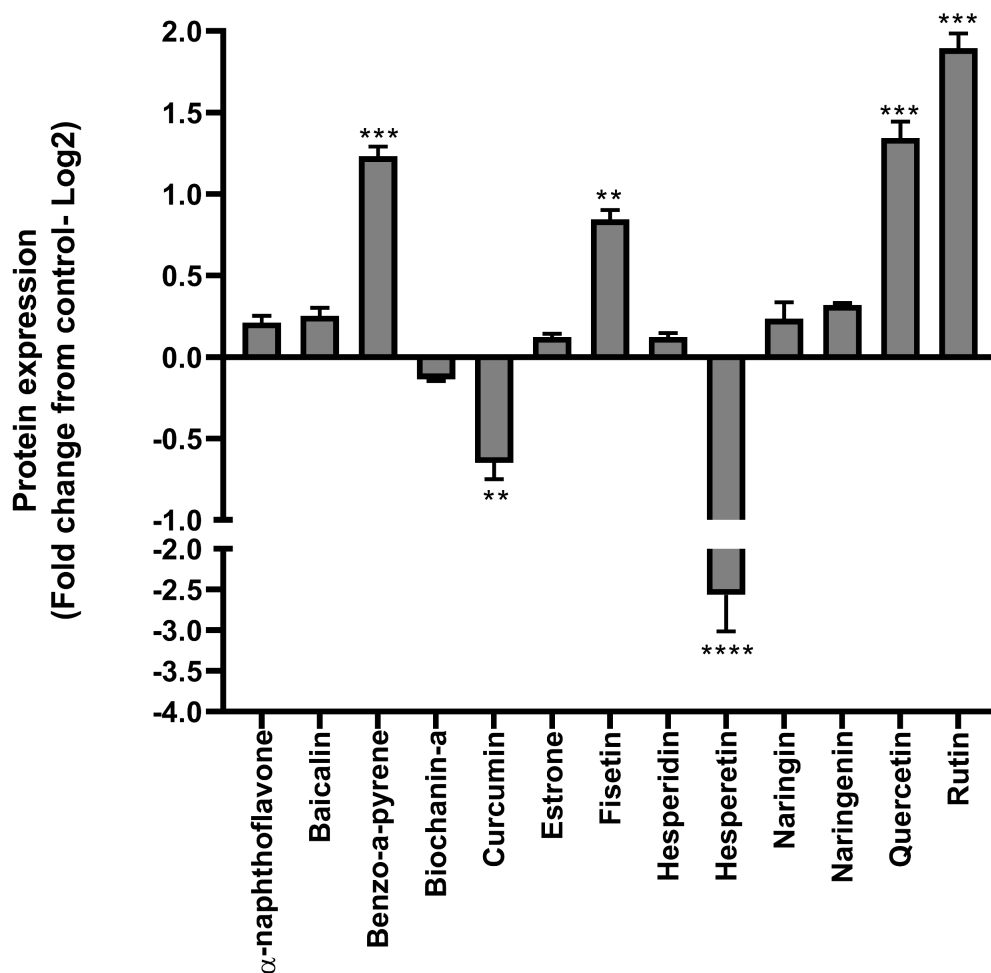


Figure 2.6 Fold change in BCRP expression

Cells were seeded in T25 flasks and incubated with 50 μ M of the modulators once confluent for 24 hours. cells protein extraction was conducted using RIPA buffer. 40 μ g of the protein was loaded on a 4%-8% SDS PAGE gel to separate the bands, the gel was then transferred to a PVDF membrane and incubated with BXP21 (Santa Cruz,USA) for 24 hours at 4 $^{\circ}$ C, then incubated with mouse anti-rabbit IgG (Themofisher,UK). ECL (Bio-RAD, UK) detection was conducted. Significant difference in protein expression is shown relative to control. * $P \leq 0.05$; ** $P \leq 0.01$; *** $P \leq 0.001$; **** $P \leq 0.0001$

2.6.6 The impact of flavonoids in modulating ROS pathways

In order to assess the ability of baicalin and hesperetin, and current therapeutic anti-cancer agents methotrexate and temozolomide to activate ROS pathways in human glioblastoma LN229 cells, a ROS assay was conducted at 10 μM , 100 μM and 500 μM of each compound. Methotrexate 10 μM resulted in the largest ROS detection, 5.16 \pm 2.44-fold with both modulators demonstrated at least a 3-fold increase (all statistically significant) in ROS production when compared to untreated cells (Figure 2.7).

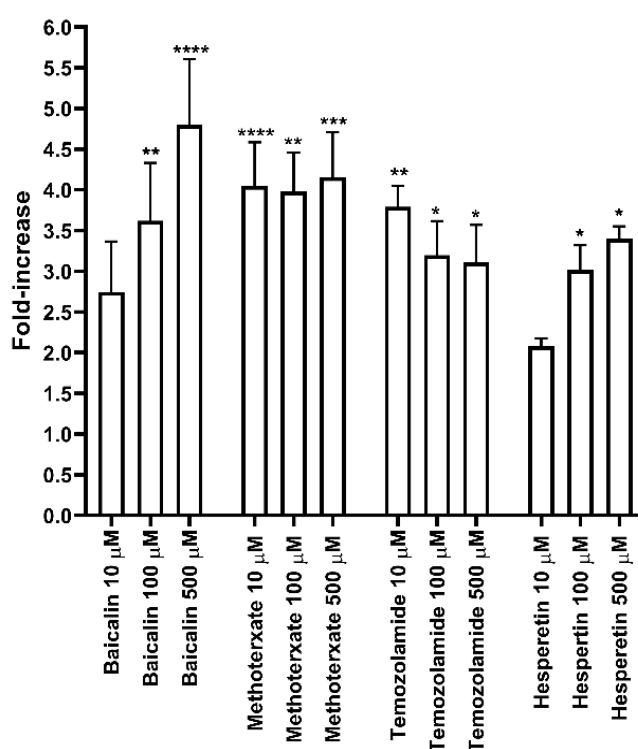


Figure 2.7 Radical oxygen species detection assay

LN229 cells were grown in 96-well plates for 24 hours prior to being washed with 1X buffer. The cells were treated with 25 μM DCF-DA and incubated for 45 minutes. Thereafter, the cells were treated with baicalin, hesperetin, methotrexate and temozolomide (10 μM , 100 μM , 500 μM) for 1 hour. DCF-DA fluorescence was measured at excitation and emission 485 nm and 535 nm. Results are presented normalised against untreated cells. * $P \leq 0.05$; ** $P \leq 0.01$; *** $P \leq 0.001$; **** $P \leq 0.0001$.

2.6.7 The impact of flavonoids to modulate Caspase-3/7 activity

The activation of caspase 3 and 7 is known to be the functional endpoint of the apoptotic cascade and hence are used as a marker for apoptosis. A caspase-3/7 fluorometric assay was utilised to assess activation of apoptosis pathways through the cleavage of N-Ac-DEVD-N'-MC-R11 to a fluorescent product. Flavonoid modulators resulted in an excess of a 9-fold increase in caspase activity compared to control at both 10 μ M and 100 μ M (Figure 2.8). Furthermore, temozolomide demonstrated an approximately 8-fold increase and methotrexate 10.5-12 fold increase at both 10 μ M and 100 μ M (Figure 2.8).

Both flavonoids demonstrated a statistically significant increase in caspase activity when compared to untreated cells ($P < 0.0001$). Furthermore, a statistically significant ($P < 0.01$) higher caspase activity (compared to untreated control), was noted for hesperetin 100 μ M (10.23 ± 0.37 fold) and baicalin 10 μ M (11.12 ± 1.51 fold) than temozolomide at 10 μ M (7.91 ± 0.53 fold) and 100 μ M (8.24 ± 0.32 fold) (Figure 2.8).

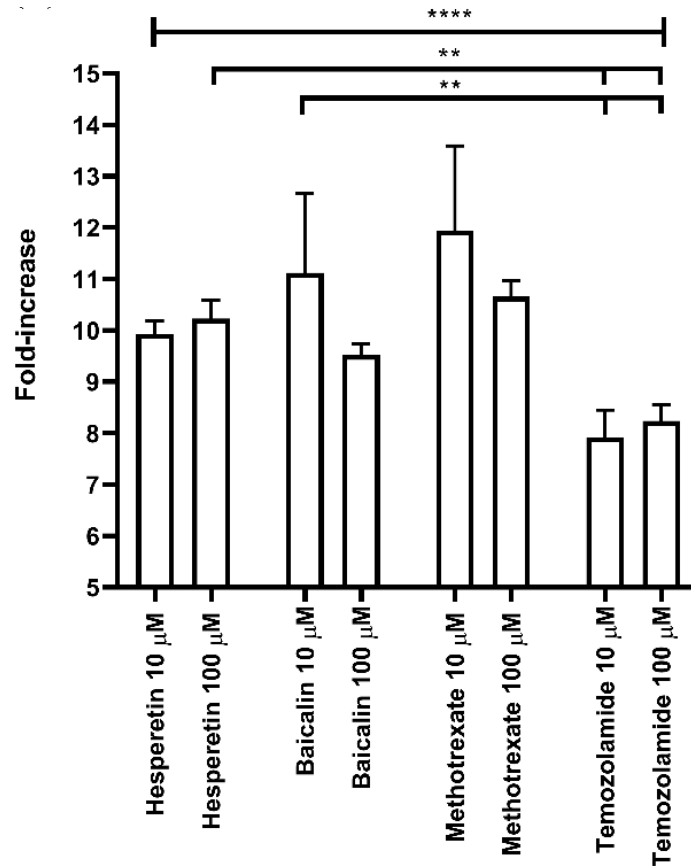


Figure 2.8 Caspase-3/7 assay

LN229 cells were seeded in 96 well plates for 24 hours followed by incubation with 10 μM and 100 μM of each compound (baicalin, hesperetin, methotrexate and temozolomide) for 4 hours. The resulting N-Ac-DEVD-N'-MC-R110 parent was cleaved by cellular Caspases to a fluorescent product, detected at an excitation and emission 485 nm and 535 nm. Results are presented normalised against untreated cells. * $P \leq 0.05$; ** $P \leq 0.01$; *** $P \leq 0.001$; **** $P \leq 0.0001$.

2.7 Discussion

Increasing evidence now suggests that flavonoids may play a role as modulators of BCRP, potentially leading to an enhancing intracellular accumulation of substrate molecules (Dei et al., 2019, Fan et al., 2019, Imai et al., 2004b, Kalapos-Kovács et al., 2015b, Kaur and Badhan, 2015, Kaur and Badhan, 2017, Mao and Unadkat, 2015, Peña-Solórzano et al., 2017, Pick et al., 2011, Santos et al., 2015, Sowndhararajan et al., 2017, Tiwari et al., 2011, Toyoda et al., 2019, Xu et al., 2018). In the context of brain cancers, the localisation of BCRP and other ABC transporters at the BBB and BTB offer a novel target to enhance intracellular accumulation of anti-cancer agents. Previously, we demonstrated the impact of flavonoids on the modulation of BCRP at the BBB (Kaur and Badhan, 2017) and blood-CSF-barrier (Kaur and Badhan, 2015). In this chapter we examined the potential of flavonoids to modulate BCRP function in human glioblastoma LN229 cells, in addition to examining the role of flavonoids in initiating ROS-production, activation of Caspase apoptosis cascade and hindering cellular migration, as potential adjunct agents in oncology.

2.7.1 Cellular toxicity of modulators towards LN229 cells.

13 modulators were screened for their cytotoxicity towards LN229 across a 6-fold log-concentration range. The majority of modulators displayed limited toxicity up to 150 μM , with biochanin-a and the non-flavonoid carcinogen benzo-a-pyrene displaying a cell viability IC_{50} of $\leq 150 \mu\text{M}$ (Figure 2.1). Previous studies have utilised biochanin-a at concentrations below the calculated IC_{50} in LN229 cells (Habicht et al., 2014). Furthermore, benzo-a-pyrene is a known polycyclic aromatic hydrocarbon carcinogen and used as a positive control and has been reported to demonstrate an IC_{50} of $\sim 10 \mu\text{M}$ in human brain microvascular endothelial cells (Jeong et al., 2019). The lack of significant cellular toxicity for most flavonoids concurs with the typical concentrations reported for many flavonoids within the brain, namely $\sim 50 \mu\text{M}$ (Peng et al., 1998, Youdim et al., 2003, Youdim et al., 2004b). Toxicity of the anti-cancer compounds towards the LN229 cells, were not what was expected. With reported IC_{50} values (Figure 2.2) slightly higher than those reported in other

cancer cell lines. This might be due mutated p53 and PTEN that is resembles human GBM reported to be expressed in the LN229 cells line (Ishii et al., 1999). This would suggest that the LN229 cells might have been obtained from a high-grade glioblastoma However, there are no reports or additional information from ATCC to support that claim.

2.7.2 Hoechst-33342 intracellular accumulation assay

The fluorescent BCRP probe substrate H33342 was used as a tool to assess BCRP efflux function in the presence of modulators. Our results demonstrated a range of responses over a phytochemical concentration range of 0.001-100 μM , with the greatest increase in H33342 intracellular accumulation demonstrated with baicalin (1.8-2.2-fold) and hesperetin (2.5-2.8-fold) over the range of 1-100 μM which was more than that demonstrated by the commercially available BCRP modulator Ko143 (1.5-fold) across 1-10 μM (Figure 2.3). Both baicalin and hesperetin have been previously demonstrated to inhibit BCRP efflux at a low IC_{50} of < 50 μM (Cooray et al., 2004b, Kalapos-Kovács et al., 2015b, Sowndhararajan et al., 2017). The exact mechanism of this interaction is thought to occur at the level of the cytosolic ATPase element of the transporter (Peña-Solórzano et al., 2017) or the transmembrane binding sites (Fan et al., 2019).

2.7.3 Cellular migration assay

A main feature of glioblastomas are their ability to invade their surrounding microenvironment, migrate and metastasise (Johansen et al., 2016).

Moreover, BCRP plays a role In the ability of cancer cells to migrate where, BCRP was reported to regulate the transport of active substrates such as extracellular matrix adhesion molecules which are critical for the ability of cancer cells' migration and invasion (Lye et al., 2019). It has been demonstrated that pharmacological modulation BCRP reduces migration in U251 stem cells glioma (Gong et al., 2014) and PANC-1 pancreatic cancer cells (Wang et al., 2010b).

The majority of modulators demonstrated an ability to hinder cellular migration with fisetin, estrone, benzo-a-pyrene, baicalin, hesperetin, curcumin and

biochanin-A demonstrating a 50% or greater inhibition of migration at concentration 50 μ M (Figure 2.4). Previous reports have highlighted a similar ability to modulate metastasis in different tumour cell lines for fisetin and curcumin (Ham et al., 2015), baicalin (Gao et al., 2017b, Zhu et al., 2018a), hesperetin (Zhang et al., 2017) and biochanin A (Zhao et al., 2018). This inhibitory mechanism is thought to occur through inhibition of the activity of metalloproteases such as MMP-2 and MMP-9, previously elucidated for baicalin (Wang et al., 2010c, Zhu et al., 2018b) and hesperetin (Mao et al., 2017, Demuth and Berens, 2004, Singh et al., 2010, Santos et al., 2015).

2.7.4 Effect of the modulators on the expression of BCRP

In order to further assess the effect of the modulators on the expression of BCRP in LN229 cells, western blot was conducted following incubating LN229 cells for 24 hours with 50 μ M flavonoids (Figure 2.5). Hesperetin demonstrated the largest down regulation in BCRP expression, -2.56 ± 0.45 -fold ($P \leq 0.0001$), followed by curcumin and biochanin-A (Figure 2.6). The remaining modulators increased the expression of BCRP.

The transcriptional regulation of BCRP, as with many ABC transporters, is thought to be governed by a range of nuclear hormone receptors (Wang and Negishi, 2003, Xu et al., 2005) and the interference of these signalling pathways under physiological and pathophysiological conditions provides a new approach to modulate BCRP function at the CNS barriers (Mahringer and Fricker, 2010, Hartz and Bauer, 2011, Bauer et al., 2006). Many members of the nuclear receptor superfamily are known to regulate drug transporters this includes the pregnane-X-receptor (PXR), the constitutive androstane receptor (CAR) and the aryl hydrocarbon receptor (AhR) (Jacob et al., 2011, Xu et al., 2005, Dauchy et al., 2008b, Granberg et al., 2003). The regulation of many of the transporter proteins is controlled by endogenous and exogenous compounds, some of which are thought to be flavonoids, which act to activate the receptors and subsequently leads to changes in transporter gene and protein expression (Mahringer and Fricker, 2010, Hartz and Bauer, 2011, Bauer et al., 2006).

Based on the cellular toxicity, accumulation, migration assay, and Western blot, baicalin and hesperetin were selected as two candidates to take forward, in part due to their lower cellular toxicity, significant increase in intracellular H33342 accumulation, inhibition effects on cellular migration and downregulation of BCRP, when compared to other modulators.

2.7.5 Ability of hesperetin and baicalin to induce ROS production

Whilst many flavonoids are known to modulate ABC transporter function, their role as potential anti-cancer agents, namely metastatic inhibitors and apoptosis inducers were further investigated using a ROS production assay and caspase-activation assay. Flavonoids are well known as free radical scavengers, but also demonstrated to function as pro-oxidatives leading to cytotoxicity, possibly due to the generation of ROS and leading to induction of apoptosis (Miura et al., 1998, Kuntz et al., 1999). With a disproportional increase in intracellular ROS, cancer cell cycle arrest, senescence and apoptosis will often follow. This often is a result of opening of mitochondrial permeability transition pores which releases cytochrome-c and thereby causing the activation of caspase. The switch to pro-oxidant behaviour can often occurs under certain conditions, such as high concentrations of transition metal ions, an alkali pH environment and the presence of oxygen molecules (Blokhina et al., 2003). When assessing the impact of flavonoids and anti-cancer agents to enhance intracellular ROS, we demonstrated that methotrexate 10 μ M caused a significant increase in ROS (5.16 ± 2.44 -fold) with all other modulators demonstrated at least a 3-fold increase (all statistically significant) in ROS production when compared to untreated cells (Figure 2.7).

Reports have indicated baicalin as possessing pro-oxidant properties in both human glioma and breast cancer cells (Gao et al., 2016, Zhu et al., 2018b), possibly with a role for endogenous copper (or other transition metals), controlling its pro-oxidant properties and modulation of cell growth (Liu et al., 2019). It has been reported that baicalin is capable of forming a complex with intracellular copper which is then able to initiate the redox cycling to increase ROS production and mitochondrial-dependent apoptosis cell death (Liu et al., 2019). Additionally,

it has been demonstrated that flavonoids which include a structural phenol B ring are capable of forming phenoxy radicals which can then oxidise NADH and leading to free radical oxygen activation (Chan et al., 1999).

2.7.5.1 Ability of hesperetin and baicalin to activate caspase pathways

Programmed cell death (apoptosis) is responsible for vital biological functions such as elimination of unwanted damaged cells and maintenance of homeostasis. Irregularities in occurrence of apoptosis plays a part in tumour formation, progression and developing anticancer drug resistance (Ziegler and Groscurth, 2004, Ghobrial et al., 2005). Subsequently, triggering apoptosis has emerged a primary means in cancer drug development (Goldar et al., 2015). One of the mechanisms through which cellular apoptosis can be mediated is through the caspase's family of specific cysteine proteases, which are otherwise inactive within the cytosol. Upon activation, they play a primary role in the cellular apoptosis process and are an attractive target for glioblastoma treatments (Fulda, 2018). Flavonoids have been demonstrated to activate the caspase molecular pathways in human glioblastoma cells (Das et al., 2009, Kong et al., 2019, Souza et al., 2018, Ghobrial et al., 2005)

The active caspase-3/7 substrate, N-Ac-DEVD-N'-MC-R110, was utilised given its ability, upon cleavage by caspase enzymes, to yield a fluorescent compound capable of being detected. Different caspases have distinctive but overlapping cleavage sights, for example caspase -3/7 have the same cleavage sight where cleavage occurs after the second Asp (Asp-Glu-Val-Asp). The cleavage of caspase-3/7 is a functional end point for the apoptosis process (Ghavami et al., 2009). Baicalin and hesperetin were subsequently assessed for the impact on this pathway at 10 μ M and 100 μ M (Figure 2.8). At both concentrations, a 9-fold increase in caspase activity was observed compared to control at both 10 μ M and 100 μ M (Figure 2.8) in addition to increases in activity for both temozolomide and methotrexate.

Flavonoids have been reported on as having pro-apoptotic properties *in-vitro* (Braganhol et al., 2006, Nguyen et al., 2004) as well as temozolomide in U251 cells (Li et al., 2015) and methotrexate in RIE-1 (Papaconstantinou et al., 2001).

In-vitro, baicalin has been shown to reduce cell proliferation of myeloma cell lines (NCI-H929 and U266), lymphoma cell lines (NCEB1) and lymphatic leukaemia cell lines (HL-60 and THP-1) (Kumagai et al., 2007). In addition, studies have reported its apoptotic effects in T24 human bladder cancer (Lin et al., 2013) A549 lung cancer cell line (JJ et al., 2017) and HeLa cervical cancer cells (Yong et al., 2015). Moreover, baicalin was shown to activate caspase-3 in U937 lymphoma cell line, however, the study showed that the baicalin's effect was concentration dependent where, a high dose of baicalin has to be used in order to produce the desired apoptotic effect (Zakki et al., 2018), the same study also reported that baicalin was able to suppress anti-oxidant enzymes and increase ROS generation (Zakki et al., 2018). In a further study, conducted in human osteosarcoma cells, baicalin was able to initiate substantial generation of ROS and was able to induce apoptosis through the activation of caspase -3 and -9 and inhibition of Bcl-2 proteins responsible for regulation of cell death (Wan and Ouyang, 2017).

Previous research reported that hesperetin can induce apoptosis in rats with colon cancer (Aranganathan and Nalini, 2013), as well as in *in-vitro* cancer models such as HT-29 colorectal adenocarcinoma cells (Rajamanickam et al., 2012), gastric cancer (Zhang et al., 2015a), MCF-7 breast cancer cell line (Palit et al., 2015), PC-3 prostate cancer cell line (Sambantham et al., 2013) and SiHa cervical tumour cell lines (Alshatwi, 2012). Furthermore, hesperetin was shown to trigger apoptosis by increasing ROS generation in SGC-7901 human gastric cancer cell lines (Zhang et al., 2015b).

Much like baicalin, hesperetin also inhibited Bcl-2 and induced caspase-3, caspase-9 (Green and Kroemer, 2004, Chen and Lesnefsky, 2011) and caspase-7 (Palit et al., 2015). The apoptotic action of hesperetin in various cell lines involves the formation of an oxidant/antioxidant imbalance as hesperetin possess both pro-oxidative and anti-oxidant properties (Haidari et al., 2009), such that it

is able to reduce activities of anti-oxidants such as superoxide dismutase (SOD) and catalase (Zhang et al., 2015b, Sivagami et al., 2012).

2.8 Conclusion

To conclude, the expression of the efflux transporter BCRP at the BTB in glioblastoma is a major contributor in MDR, which results in sub-optimal concentration of anti-cancer drugs at the tumour site. In this study, we screened 13 phytochemicals in human glioblastoma cells LN229 for their cytotoxicity, ability to modulate the efflux function and expression of BCRP and reduce cancer cell migration.

Based on the results obtained, we have identified two optimal flavonoids hesperetin and baicalin and have demonstrated their ability to modulate the action and expression of BCRP as well as pro-oxidant and apoptosis inducing properties within LN229 glioblastoma cell line.

This chapter highlights the potential for these two flavonoids to be further investigated as pro-oxidant agents alone or in combination with existing anticancer agents susceptible to BCRP efflux at the BBB and/or BTB. In the following chapter, hesperetin was selected as the optimal flavonoid to assess its ability to permeate across an *in-vitro* BBB model and modulate the efflux action of BCRP at the BBB and therefore enhance the permeability of anti-cancer substrate drugs methotrexate and mitoxantrone.

Chapter 3

Enhancing the permeability of anti-cancer agents across an in-vitro BBB model by modulation of BCRP using hesperetin

Elements of this chapter have been published in the following manuscripts:

Elbakary, B. and R. K. S. Badhan (2020). "A dynamic perfusion based blood-brain barrier model for cytotoxicity testing and drug permeation." Scientific Reports **10**(1): 1-12.

Elbakary, B. and R. K. S. Badhan (2021). " Phytochemical mediated modulation of breast cancer resistance protein in human glioblastoma cells." Brain Research **submitted 11/02/21**

3.1 Background

The blood brain barrier (BBB) constitutes a significant obstacle to drug delivery for brain tumours, primarily as a result of the presence of tight junctions localised between the cells of the BBB endothelium which renders the intercellular endothelial space shut (Gomez-Zepeda et al., 2019, Brazil, 2017).

This is further augmented by the presence of ABC efflux transporters, such as BCRP, which plays a major role in the MDR phenotype (Tiwari et al., 2011). BCRP has been shown to play a significant role in limiting the penetration of many structurally unrelated anti-cancer agents such as methotrexate, mitoxantrone, doxorubicin and topotecan amongst others (Ni et al., 2010, Wijnholds et al., 2000, Cisternino et al., 2004, Breedveld et al., 2005, Toyoda et al., 2019). With glioblastoma reported to be the deadliest form of brain cancer (Tan et al., 2020), permeation of anti-cancer drugs across the BBB becomes a critical pre-requisite for successful drug delivery to gliomas.

The role of BCRP in limiting brain delivery of anticancer agents has been extensively demonstrated. For example, the correlation between the expression of BCRP and poor response to 5-fluorouracil has been reported in breast cancer patients (Burger et al., 2003, Yuan et al., 2008). In non-small cell lung cancer patients, the expression of BCRP was also reported to be linked with resistance to platinum-based chemotherapeutic agent vinorelbine and poor survival (Yoh et al., 2004).

Regarding glioblastoma, the expression of BCRP at the BTB as well as the BBB has been reported to correlate with poor response to GBM therapy (Mao and Unadkat, 2005, Wang et al., 2019). Wild type BCRP knockout mice with oncogene induced glioblastoma were found to demonstrate an up to 3-fold increase in the concentration of dasatinib in the core of the tumour upon its dissection (Agarwal et al., 2012). Moreover, gefitinib permeability across the BBB was found to be hindered by the presence of BCRP *in-vitro* in MDCK II cells as well as *in-vivo* in mice (Agarwal et al., 2010). Furthermore, vandetanib penetration across the BBB and into mice brains was shown to be limited by the expression of BCRP (Minocha et al., 2012).

Modulation and inhibition of BCRP was proposed to overcome its efflux function and increase permeability of substrates across the BBB (Mao and Unadkat, 2015, Ni et al., 2010). Many BCRP modulators have come to light as inhibitors of BCRP efflux function. These include fumitremorgin C (FTC) (Rabindran and LM, 2000), GF120918 (Duan and You, 2009, Suzuki and Watanabe, 2019) and Ko143 (Giri et al., 2008). However, their cytotoxicity and lack of selectivity limits their widespread clinical use (Zhang et al., 2004b).

Interest in naturally occurring phytochemicals has increased over the past decade, due to their potent anti-cancer activities (Prakash et al., 2013) and ability to modulate the efflux function of BCRP (Zhang et al., 2004c, Gao et al., 2017b, An and Morris, 2010). Studies have demonstrated the effect of various phytochemicals in modulating BCRP (Kaur and Badhan, 2017). This is achievable at low concentrations, such as biochanin-a, benzoflavone, and chrysin at 30 μ M, were able to inhibit BCRP in breast cancer cell line MCF-7 and increase influx of mitoxantrone. In the same cell line, hesperetin, quercetin and resveratrol were also able to increase intracellular accumulation of mitoxantrone by inhibiting BCRP (Cooray et al., 2004b, Pick et al., 2011). In human leukaemia cells line K-562, naringenin and genistein have also shown to modulate efflux function of BCRP (Imai et al., 2004a). Moreover, quercetin and curcumin were found to modulate the function of BCRP and down regulate its expression in porcine microvascular endothelial cell line (Kaur and Badhan, 2017)

Methotrexate is used in treating primary CNS lymphoma and glioblastoma (Zhu et al., 2009, Sane et al., 2014). Methotrexate formally known as amethopterin is a folate derivative that is used in lower doses to manage autoimmune diseases such as rheumatoid arthritis and psoriasis. It is administered at higher doses to treat a number cancers such as head and neck, brain, breast, lung and bladder cancer (Sane et al., 2014). Studies have shown that methotrexate has limited distribution into the brain where rodent brain interstitial fluid was assessed for accumulation using brain micro-dialysis with a brain-to-plasma ratio of 0.051 ± 0.32 (Devineni et al., 1996). A similar study was performed in humans which displayed an even lower brain-to-plasma methotrexate ratio, 0.032 ± 0.094

(Blakeley et al., 2009). A primary cause of the limited distribution into the brain is the role of BCRP in effluxing methotrexate (Sane et al., 2014, Agarwal et al., 2010). An additional often used treatment for tumours is mitoxantrone. Mitoxantrone is a type II topoisomerase inhibitor that is used in regimens to treat acute myeloid leukaemia, breast cancer, non-Hodgkin's lymphoma, and liver cancer. In addition, it is used as a TRAIL sensitising agent in glioblastoma cell lines (Senbabaoglu et al., 2016, Taylor et al., 2011). Mitoxantrone is a known BCRP substrate (Nakanishi and Ross, 2012, Özvegy et al., 2001) and resistance to mitoxantrone has been strongly correlated to the efflux function of BCRP (Doyle et al., 1998, Higgins, 1995, Miyata et al., 1999).

In this chapter, temozolomide was replaced with mitoxantrone due to conflicting studies reporting on the effect of BCRP as a contributor to MDR towards temozolomide where, knockdown of BCRP did not have an effect on the sensitivity of temozolomide (Wijaya et al., 2017), while others stated that BCRP was a contributor in reducing temozolomide sensitivity in treating glioblastoma (Chua et al., 2008, Bleau et al., 2009). In addition, HPLC detection issues were encountered during the method development for temozolomide which is suspected to be due to compound degradation (Kapçak and Şatana Kara, 2018). Further, it was decided to focus on one optimal flavonoid, hesperetin, as it displayed stronger abilities in modulating the expression of BCRP at the BBB.

3.2 Aims and objectives

Utilising results from the previous chapter, the focus of this study was on hesperetin and its ability to modulate BCRP efflux function in a BBB *in-vitro* model. The aims were to assess the ability of hesperetin to permeate across the BBB, in addition to modulating the efflux function of BCRP in an *in-vitro* BBB model. Subsequently, our goal was to enhance the transport of methotrexate and mitoxantrone across the BBB.

In order to achieve those aims, the objectives were to:

- Optimise collagen culture surface coating using PBMEC/C12 cells

- Develop and characterise an *in-vitro* BBB model using primary porcine brain cells
- Assess the cytotoxicity of hesperetin, methotrexate and mitoxantrone within primary porcine brain cells
- Demonstrate the efflux function of BCRP using the substrates methotrexate and mitoxantrone
- Assess the permeability of hesperetin across the BBB model
- Demonstrate the ability of hesperetin to modulate the efflux action of BCRP and enhance drug permeation across the BBB

3.3 Materials

Dulbecco's modified essential media with 4.5 g/L glucose (DMEM), minimum essential media (MEM), phenol red free DMEM 4.5 g/L, new born calf serum (NCS), foetal bovine serum (FBS), Leibovitz-15 (L-15), Hams F12, Antibiotic-Antimycotic® were obtained from Biosera (Sussex, UK); Rat tail-1 collagen 1 g solution and plasma derived bovine serum (PDBS) (Firstlink, UK); Ko143 was obtained from Santa Cruz Biotechnology (Texas, USA); HEPES buffer solution and 0.25% trypsin-EDTA were obtained from (Gibco, UK); bovine collagen type-1 50 µg/mL was obtained from (Thermo fisher, UK); ZO-1 1A12 monoclonal antibody, goat anti-mouse IgG H+L: super clonal secondary antibody were obtained from (Thermofisher, UK); Phalloidin-iFluor 488 reagent (ab176753) was obtained from (Abcam, UK); Thincerts® were obtained from Greiner Bio-One (Stonehouse, UK); all other chemicals were sourced from Sigma (Dorset, UK) and are HPLC grade. Stock solutions of all test compounds were prepared in dimethyl sulfoxide (DMSO) and stored at -20°C until use.

3.4 Methods

3.4.1 Development of an *in-vitro* permeable insert BBB model

3.4.1.1 Culture of C6 rat astrocytes

C6 rat astrocytes are typically used to obtain astrocyte conditioned media (ACM) utilised in the development of the PBMEC system (Patabendige et al., 2013). C6 cells were obtained from Cell Line Services (Germany). Cryopreserved cells were

thawed and resuspended in a T75 flask containing media prepared from Hams F12:DMEM (50:50), 7.5% v/v new-born calf serum, 5 µg/mL transferrin, 0.5 U/mL heparin, 0.5% v/v antibiotic/antimycotic and 7 mM L-glutamine.

The cells were grown in an uncoated T75 flask at 37 °C, 5% CO₂ for 3 days. At 80% confluency, the cells were washed with calcium and magnesium free PBS, followed by the addition of 2 mL 0.25% w/v trypsin-EDTA for 5 minutes. Thereafter, the cell suspension was resuspended in 10 mL C6 media and centrifuged for 5 minutes at 1500 rpm, 4 °C. The resultant cell pellet was then resuspended in C6 media and split into two T75 flasks. The used media from the C6 cells was aspirated, changed daily and filtered through a 0.22 µm filter and stored at 4 °C and used within one week of collection. The media obtained is termed astrocyte conditioned media (ACM).

3.4.1.2 Culture of immortalised PBMEC/C12

Cells, *in-vivo*, are not packed tightly together to form tissues, rather the majority of the tissue volume is made up of a meshwork of proteins called the extracellular matrix (ECM). The ECM is made up of proteins such as collagen, fibronectin, elastin and laminin which are secreted by fibroblasts (Lodish et al., 2000). These function to support the cellular cytoskeleton and facilitate cellular communication as well as regulate cell growth and proliferation (Frantz et al., 2010). Collagen is the most abundant protein in mammals making up 25% of the total protein mass (Alberts et al., 2002) and its use in tissue culture pertains to its function to support cellular growth, proliferation and differentiation (Heino, 2007, Kleinman et al., 1981). The type of culture surface coating greatly affects cell behaviour and the response observed is reliant on both cell culture type and coating used as a substrate (Kleinman et al., 1987, Frantz et al., 2010).

Herein, we aimed to assess the impact of species-specific collagen to develop an optimal *in-vitro* BBB model, using the rapidly growing immortalised PBMEC/C12 model, prior to utilising primary cells. PBMEC/C12 cells were obtained from Dr. M. Teifel (institute für Biochemie, Technische Hochschule Darmstadt, Germany). A T75 flask was coated with 1% w/v gelatine and cells seeded and grown in C6 growth media: ACM media (1:1). Cells achieved

confluency within 3-5 days post seeding. At 90% confluency, cells were washed with calcium and magnesium free PBS and 2 mL 0.25% w/v trypsin-EDTA was added to the flask and placed in the incubator for 5 minutes thereafter the cell suspension was placed in 10 mL fresh media and centrifuged for 5 minutes at 1500 rpm, 4 °C. The formed cell pellet was then resuspended in 1 mL media and counted using a haemocytometer for seeding in 24-well inserts.

3.4.1.3 The impact of species-specific collagen on the formation of a robust BBB model

In order to assess the impact of species-specific collagen on barrier formation, 50,000 PBMEC/C1-2 were seeded into 24-well inserts coated with a combination of bovine collagen (50 µg/mL) and fibronectin (7.5 µg/ml) or rat tail collagen (200 µL/mL) and fibronectin (7.5 µg/mL). PBMEC/C12 media is made up of a 50:50 C6 media and ACM was supplemented with 1 µg/mL fibronectin to enhance attachment. The transepithelial electrical resistance (TEER) was measured for 5 days using a chopstick electrode (STX2) and voltmeter (EVOM) (World Precision Instrument). The TEER was calculated according to equation (3):

$$\text{TEER Values } (\Omega \cdot \text{cm}^2) = (R_{\text{Cell monolayer}} - R_{\text{Blank insert}}) \times \text{SA} \quad (3)$$

Where SA is the surface area of the permeable insert (cm²), $R_{\text{Cell monolayer}}$ is the resistance across permeable insert with cells (Ω) and $R_{\text{Blank insert}}$ is the resistance across coated insert without cells.

3.4.2 Isolation of porcine brain capillaries

Porcine brain endothelial cells were isolated according to the methods reported by (Cantrill et al., 2012, Patabendige et al., 2013) with adaptations (Elbakary and Badhan, 2020, Kaur and Badhan, 2017). Porcine brain hemispheres were obtained from a local abattoir (Long Compton, Oxford, UK) within 30 minutes of slaughter and transported on ice cold Leibovitz-15 (L-15) media supplemented with 1% v/v penicillin and streptomycin. Hemispheres were placed into a sterile

beaker containing PBS with 1% v/v penicillin and streptomycin and washed to remove the meninges, blood vessels, choroid plexus and capillaries. The white matter was removed, and the grey matter excised and placed into a sterile beaker containing MEM supplemented with 10 mM HEPES and 1% v/v penicillin and streptomycin. The grey matter was chopped into smaller pieces using a sterile scalpel and passed through a 50 mL syringe into a T75 flask containing 50 mL MEM supplemented with 10 mM HEPES and 1% v/v penicillin and streptomycin.

Thereafter 15 mL of the tissue suspension was transferred into a 40 mL Dounce tissue homogeniser containing 25 mL MEM supplemented with 10 mM HEPES and 1% v/v penicillin and streptomycin. The tissue suspension was homogenised with a loose (“A”) pestle gently for 15 strokes, followed by 15 strokes using the tight (“B”) pestle. Thereafter, tissue homogenates were transferred into a sterile T175 flask and the process was repeated for the remaining tissue suspension.

The collected tissue homogenate was subsequently filtered through a 150 µm nylon mesh (Plastok Limited, UK), the collected filtrate was then filtered again through a 60 µm nylon mesh and filters were kept separately. The filters were placed into a petri dish containing 80 mL of digest mix consisting of M199 media containing DNase I (2108 U/mg); trypsin (211 U/mg); collagenase (223 U/mg) (Worthington Biochemical, NJ, USA); 10% v/v FCS and 1% v/v penicillin and streptomycin. Petri dishes were labelled as 150s and 60s and incubated at 37 °C for 1 hour on an orbital shaker at 150 rpm. Thereafter the filters were carefully washed, and the digest mix moved to 50 mL centrifuge tubes and centrifuged at 4 °C for 5 minutes at 5000 rpm, before being suspended in fresh MEM supplemented with 1% v/v penicillin and streptomycin and 10 mM HEPES. This process was repeated three times before the pellets were resuspended in cryopreservation media (10% v/v DMSO and 90% v/v FCS) for long-term storage in liquid nitrogen and labelled as ‘150s’, suitable for gene/protein expression/functional activity, and ‘60s’ suitable for drug permeability studies.

3.4.3 Growth of PBMEC cells

A T75 flask was coated with bovine collagen (50 µg/mL) prior to addition of cells from a thawed ‘150s or 60s’. Thawed cells were suspended in full PBMEC media:

phenol red free DMEM, 10% v/v plasma derived bovine serum (PBDS), 1% v/v antibiotic-antimycotic, 125 µg/mL heparin and 1% v/v L-glutamine. Cells were grown for 2 days before the addition of 4 µg/mL puromycin for 2 days, to eradicate pericyte contamination. Thereafter, PBMEC cells were maintained in ACM collected from the growth of rat C6 astrocytes (See Section 3.4.1.1), in a 1:1 (PBMEC:ACM), until confluence (8–10 days post seeding) and are referred to as passage 0. Following trypsinisation, PBMEC cells were subsequently seeded on 24 well, 96 well coated with bovine collagen (50 µg/mL) to contact further experiments.

3.4.4 Development of a PBMEC *in-vitro* BBB model

Following trypsinisation, PBMEC cells were subsequently seeded at a density of 80×10^3 cells/cm² into 1.12 cm² permeable inserts (Greiner BioOne transparent ThinCerts® 12 well) coated with bovine collagen (50 µg/mL) and fibronectin (7.5 µg/mL) and maintained in PBMEC:ACM and considered as passage 1.

Barrier integrity and formation was assessed through the determination of TEER, which was measured every 2 days using a chop-stick electrode (World Precision Instruments STX2). Tight-junction formation was enhanced through the addition of 250 µM cAMP, 17.5 µM RO 20–1724 and 550 nM hydrocortisone 24-hours prior to the initiation of an assay, with TEER values used to assess barrier integrity (Patabendige et al., 2013). The media was changed on the day a TEER measurement was carried out and measured every two days up to 10 days post seeding. Monolayer formation was monitored by measuring the TEER using a chopstick electrode (STX2) and voltammeter (EVOM) (World Precision Instrument) TEER was calculated according to equation (3).

Control measurements were made using filters without cells (blank filter). The PBMEC model is considered suitable for transport/permeability assays when TEER > 400 Ω.cm² is achieved (Patabendige et al., 2013, Yang et al., 2017, Gaillard and de Boer, 2000).

3.4.4.1 Immunostaining detection of ZO-1 and F-actin in PBMECs *in-vitro* BBB model

On the day peak TEER value was recorded typically 24 hours following the addition of barrier additives, the bottoms of the inserts were carefully peeled and washed with cold PBS and fixed in cold paraformaldehyde 4% w/v for 10 minutes. Thereafter the inserts were prepared for ZO-1 or F-actin visualisation.

Zona occludin-1 (ZO-1) is a tight junction protein used to determine the integrity of BBB *in-vitro* models (Cantrill et al., 2012, Patabendige et al., 2013). In addition to using TEER measurements and lucifer yellow leakage in order to assess the barrier integrity, tight junction protein ZO-1 was visualised when peak TEER values were observed.

Following fixing, the cells were washed three times with cold PBS and permeabilised using 0.02% w/v saponin for 10 minutes, followed by an additional cycle of washing with PBS. The cells were then blocked in 6% v/v goat serum overnight. Thereafter, inserts were incubated with ZO-1 primary antibody (ZO-1 1A12 monoclonal) prepared in blocking buffer of 1% v/v goat serum (1:100 PBS) and incubated overnight at 4 °C. The inserts were then washed with cold PBS three times prior to being incubated with secondary antibody (0.5 µg/mL goat anti-mouse IgG H+L super clonal secondary Alexa 488) for 2 hours on an orbital shaker (150 rpm) at room temperature. Cells were then washed with PBS and mounted on a coverslip using Flourosshield (containing DAPI). ZO-1 Tight junction formation was assessed using an upright confocal microscope Leica SP5 TCS II MP (Leica microscope systems (UK) Ltd, Milton Keynes, UK) using a 40x oil immersion lens. The images were obtained with an argon laser at 494 nm and a helium neon laser for DAPI visualisation at 461 nm.

F-actin was visualised to ensure that the *in-vitro* model possessed an appropriate cytoskeleton formation which is essential for cell stability, cell proliferation and morphogenesis (Dominguez and Holmes, 2011). Following fixing, the cells were washed with cold PBS three times and permeabilised for 10 minutes using 0.2% w/v saponin. Thereafter, the inserts were washed with ice cold PBS 3 times; the

inserts were then blocked in 1% w/v BSA for 1 hour then washed three times with ice cold PBS. The cells were then incubated with Phalloidin-iFluor 488 (1:50) for 20 minutes. The inserts were then washed and mounted on microscope slides using Fluoroshield (containing DAPI). F-actin filaments were assessed using upright confocal microscope Leica SP5 TCS II MP (Leica microscope systems (UK) Ltd, Milton Keynes, UK) using a 40x oil immersion lens. The images were obtained with an argon laser at 517 nm and a helium neon laser for DAPI visualisation at 493 nm.

3.4.5 Cellular toxicity in PBMECs

The cellular toxicity of hesperetin, methotrexate and mitoxantrone were assessed using a MTT assay, as previously detailed in Section 2.4.2.

3.4.6 Transport of methotrexate, mitoxantrone and hesperetin across PBMECs *in-vitro* BBB model

24 hours following the addition of barrier forming additives (See Section 3.4.4), a transport assay was conducted to determine the ability of methotrexate, mitoxantrone and hesperetin to permeate across the developed *in-vitro* BBB model. 50 μ M methotrexate was prepared in serum free PBMEC media containing 25 mM HEPES and added to the apical (for AB flux) or basolateral (for BA flux) compartments with sampling taking place from the opposite compartment. Samples (100 μ L) were withdrawn at intervals between 15–90 minutes and replaced with an equal amount fresh pre-warmed serum free PBMEC media containing 25 mM HEPES. Each sample was placed in a 2 mL HPLC autosampler amber vial and stored at 4 °C until the end of the assay. Methotrexate concentrations were analysed using HPLC-UV detection (Agilent 1200 series) (detailed in the subsequent section). The apparent permeability (P_{app}) was calculated using equation (4):

$$P_{app} = \frac{dQ/dt}{C_0 \times A} \quad (4)$$

where dQ/dt represents the amount of drug permeated per unit time, calculated from the regression line of time points of sampling; C_0 the initial drug

concentration in the donor compartment; A (cm²) is the insert surface area (1.12 cm²). Efflux ratios were calculated according to equation (5):

$$ER = \frac{P_{appBA}}{P_{appAB}} \quad (5)$$

where P_{app BA} is the apparent permeability from basolateral to apical, and P_{app AB} is the apparent permeability from apical to basolateral.

This method was used to assess the permeability of 50 μM mitoxantrone and 50 μM hesperetin:

(i) Mitoxantrone: samples detected using a fluorescent plate reader (Tecan Spark 10M®) with an excitation wavelength of 488 nm and an emission wavelength of 670 nm.

(ii) Hesperetin: samples detected using UV-HPLC detection (Agilent 1200 series).

3.4.6.1 Lucifer yellow permeability assay

Lucifer yellow (LY) is a fluorescent dye routinely used as a marker to assess the formation of monolayers and barrier integrity since it is transported paracellularly (Zhao et al., 2019b, Yang et al., 2017). PBEMC were grown on inserts and were incubated with 100 μM Lucifer yellow (LY) prepared in serum free media with added 25mM HEPES. Samples for LY measurements were transferred into an opaque plate and fluorescence was measured at excitation and emission wavelength 428 nm and 540 nm respectively using fluorescent multiplate reader (Tecan spark 10M®). The percentage transfer of LY was determined using equation (6):

$$\% \text{ Lucifer yellow transported} = 100 \times (1 - \frac{RFU \text{ basolateral}}{RFU \text{ apical}}) \quad (6)$$

where RFU basolateral is the relative fluorescence measurements of the sample taken from the basolateral side, RFU apical is the relative fluorescence measurement taken from the apical side.

Inserts with LY transport exceeding 1% were excluded from further experiments.

3.4.7 High pressure liquid chromatography detection of compounds

3.4.7.1 HPLC-UV detection of hesperetin

An isocratic HPLC method was utilised for the HPLC-UV detection of hesperetin (Arya et al., 2015). HPLC analysis was conducting using a 1200 Infinity II LC Agilent system. Analysis of hesperetin was performed using a reversed phase C18 column 150 x 4.6 mm (Phenomenex, UK) with a mobile phase consisting of (45:55:0.1) acetonitrile: water: acetic acid with a flowrate of 1 mL/min at 25 °C, injection sample volume 20 µL/sample and UV detection wavelength of 288 nm. Samples were examined over a concentration range of 0.1-50 µM. The method was validated by evaluating limit of detection (LOD) (Equation 7) and limit of quantification (LOQ) (Equation 8). A calibration curve for hesperetin was developed over the concentration range of 0.1-50 µM, which was used to determine linearity. The standards were prepared in quadruplicate and r^2 was determined using the calibration curve generated from running this standard.

$$LOD = 3.3 \left(\frac{\sigma}{S} \right) \quad (7)$$

$$LOQ = 10 \left(\frac{\sigma}{S} \right) \quad (8)$$

where σ is the standard deviation and S is the slope of the calibration curve.

A linear regression analysis was conducted with the standards to calculate the standard deviation and the slope.

3.4.7.2 HPLC-UV detection for methotrexate

An isocratic HPLC method was utilised for the HPLC-UV detection of methotrexate (Karami et al., 2019). Analysis of methotrexate was conducted using reversed phase C18 column 150 x 4.6 mm (Phenomenex, UK) with a mobile phase consisting of 89:11 50 mM acetate buffer: acetonitrile. The mobile phase was acidified using HCl to obtain a final pH of 3.6 before it was filtered using a 0.4 µm filter. The flow rate was fixed at 1.5 mL/min, with an injection volume of 40 µL/sample and UV-detection spectrum at 307 nm. Samples were

examined over a concentration range of 0.1-50 μM . The method was validated by evaluating limit of detection (LOD) (Equation 7) and limit of quantification (LOQ) (Equation 8). A calibration curve for methotrexate was developed over the concentration range of 0.1-50 μM , which was used to determine linearity. The standards were prepared in quadruplicate and r^2 was determined using the calibration curve generated from running this standard.

3.4.8 Fluorescence detection of mitoxantrone

A fluorescent multi-plate reader was used for detection of mitoxantrone due to the unavailability of a UV-visible light detector (over 400 nm). Mitoxantrone was detected using a fluorescent multi-plate reader (Tecan spark 10 M®) at an excitation wavelength of 607 nm and emission wavelength of 684 nm. A calibration curve for mitoxantrone was developed over the concentration range of 0.1- 50 μM , which was used to determine linearity. The standards were prepared in quadruplicates and r^2 was determined from the calibration curve obtained from running the standard.

3.5 Statistical analysis

All data is presented as mean and standard deviation, with experiments being conducted in at least 3 replicate independent experiment unless otherwise stated. Where appropriate, statistical analyses were performed in GraphPad Prism 9 (La Jolla, California, USA), with t-tests used to determine differences between the mean values. A significance p-value of <0.05 was considered as statistically significant.

3.6 Results

3.6.1 The impact of species-specific collagen on the formation of a robust BBB model.

To assess the impact of species-specific ECM (rat or bovine collagen) on barrier formation, PBMEC/C12 cells were grown on permeable inserts coated with either rat or bovine collagen and their effect on TEER values determined.

The use of bovine collagen coated inserts resulted in higher TEER values throughout the study when compared to rat tail collagen coated inserts (Figure 3.1). The peak TEER occurring on day 3 post seeding, with a 1.8-fold higher mean TEER for cells grown on bovine collagen (Bovine: $46.5 \Omega \cdot \text{cm}^2 \pm 2.1 \Omega \cdot \text{cm}^2$; Rat: $26 \Omega \cdot \text{cm}^2 \pm 5.6 \Omega \cdot \text{cm}^2$) ($P < 0.0001$).

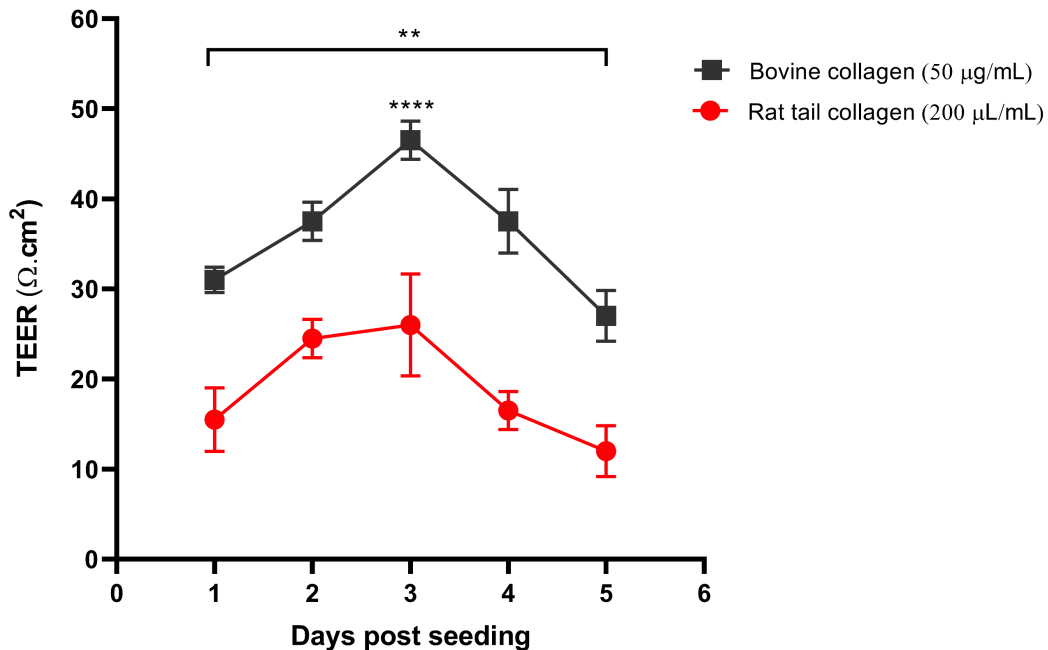


Figure 3.1 TEER measurements following growth of PBMEC1/2 on permeable cell culture inserts

50,000 PBMEC C1/2 cells were seeded on either bovine 50 µg/mL and fibronectin 7.5 µg/mL coated inserts (black) or rat tail collagen 200 µg/mL and fibronectin 7.5 µg/mL coated inserts (red). TEER values were measured every day for five days. Symbols represent the mean measurement for each day ($n=12$ inserts in 4 independent experiments for each day). Vertical lines indicate the standard deviation (SD). Statistical analysis compared the TEER at day 3 (peak) ($**** P < 0.0001$) and paired t-tests for each day ($** P < 0.01$ for all days).

3.6.2 Cellular morphology and culturing of primacy brain microvascular endothelial cells (PBMEC)

Based on the results obtained from the previous section, the culturing method for PBMECs was adapted to grow cells on bovine coated (50 µg/mL) plastic surfaces. Following addition of puromycin (4 µg/mL) to the culturing media to remove pericyte contamination (Figure 3.2A), a confluent robust layer formed by day 10 (Figure 3.2B).

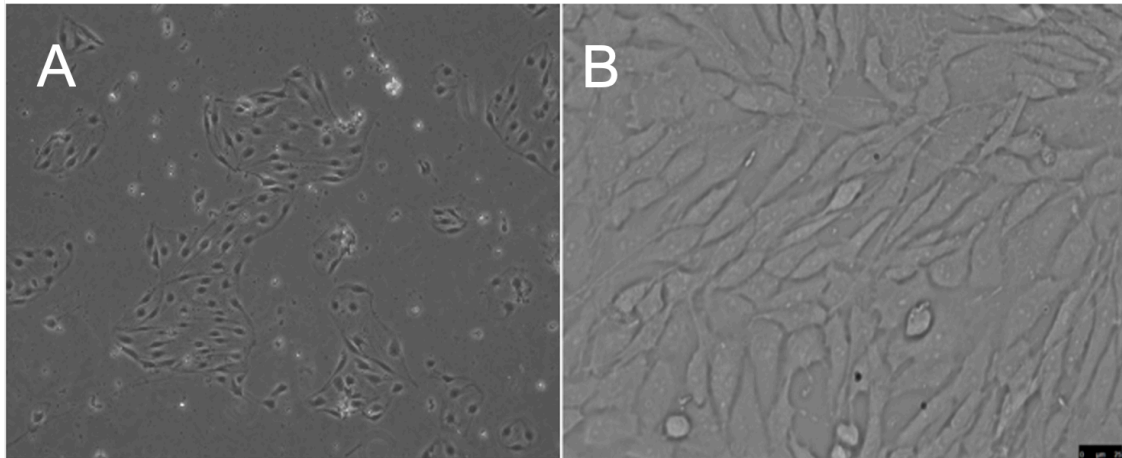


Figure 3.2 Morphology of PBMEC cultured on bovine collagen coated plasticware

PBMECs were grown in a T75 flask coated with 50 $\mu\text{g}/\text{mL}$ bovine collagen and incubated for 10 days at 37 $^{\circ}\text{C}$, 5% CO_2 . (A) PBMECs on day 2 using x10 prior to treatment with perimycin lens (B) confluent PBMECs on day 10 using x40 lens.

3.6.3 Development of a PBMEC *in-vitro* BBB model.

The formation of a PBMEC monolayers, when grown on 12-well permeable inserts, was assessed by measuring TEER values every other day post-seeding. TEER values demonstrated a steady increase after the addition of barrier forming additives on day 2 post seeding (Figure 3.3). TEER values peaked to a maximum of $1428.56 \pm 270.4 \Omega.\text{cm}^2$ on day 4 ($P \leq 0.0001$) when compared to TEER values on day 2 ($61.89 \pm 6.8 \Omega.\text{cm}^2$). Transport studies were conducted on the day of the highest recorded TEER (Day 4).

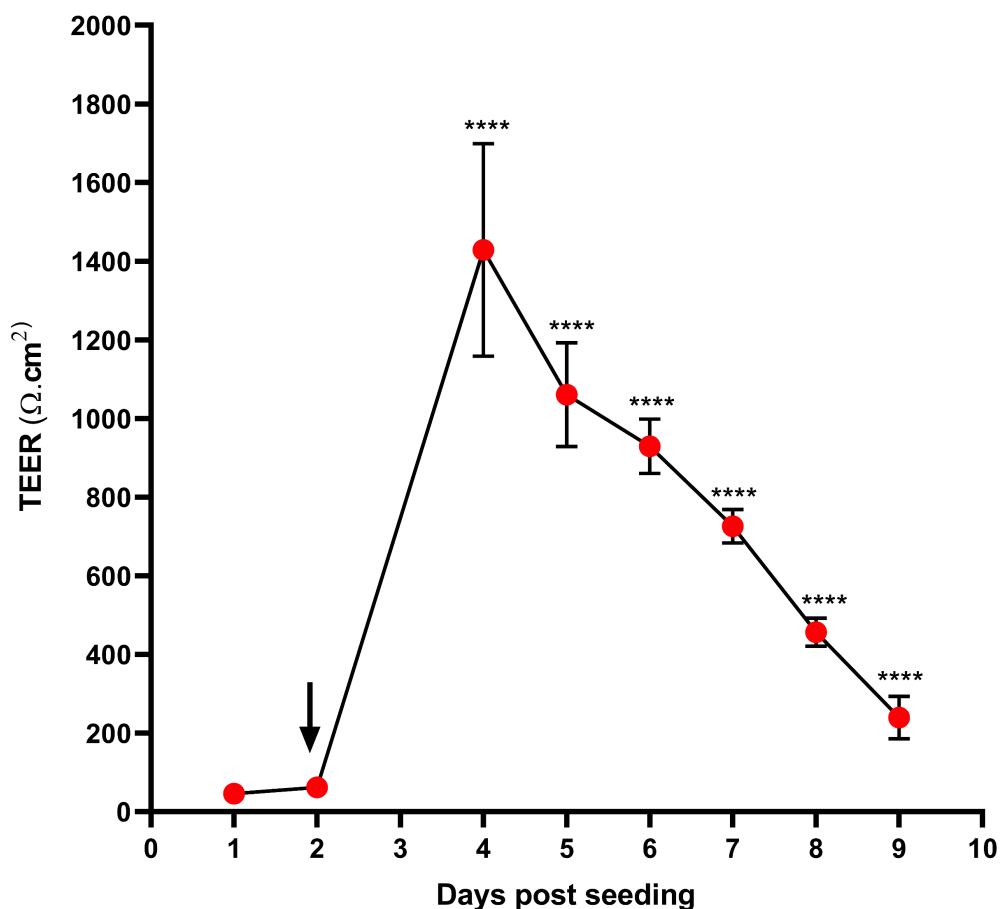


Figure 3.3 TEER measurement of PBMECs on 12 well permeable insert

80,000 cells were seeded on permeable cell culture inserts (12-well, 1.12 cm²) coated with bovine collagen (50 µg/mL) and fibronectin (7.5 µg/mL). The arrow indicates the day barrier forming agents (250 µM cAMP, 17.5 µM RO 20–1724 and 550 nM hydrocortisone) were added. Statistical analysis compares TEER at day 2 to all other data points. ****P ≤ 0.0001. Red circles indicate the mean measurement for each day (n=12 inserts in 4 independent experiments for each day). Black lines indicate the standard deviation (SD).

3.6.3.1 Lucifer yellow permeability assay

To assess the formation of a suitable cellular monolayer, the paracellular permeability marker lucifer yellow (LY) was used. Coated inserts lacking cells displayed a lucifer yellow permeability of 97% ± 2.6% (P < 0.0001), while inserts seeded with PBMEC displayed an average of 0.88% ± 0.17% LY permeation (Figure 3.4).

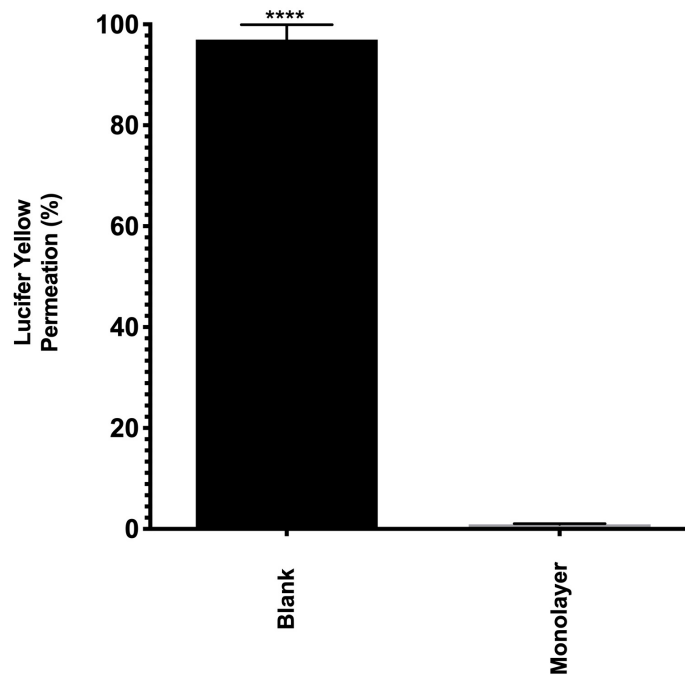


Figure 3.4 Lucifer yellow permeability assay

80,000 PMBECs were seeded in 12-well inserts. On day 4 post seeding, LY assay was conducted. Leakage of 100 μ M LY across PBMEC was assessed over 15-90 minutes assay. LY fluorescence was detected in the samples using Tecan spark 10M[®]). Vertical black lines represent the standard deviation. Unpaired t-test analysis was conducted between the mean measurements of the blank inserts and the inserts containing a monolayer of cells (**** < P 0.0001).

3.6.3.2 Immunocytochemistry of tight junction protein ZO-1 and F-actin

The expression of the tight junction protein ZO-1 was assessed using immunostaining of PBMEC grown on permeable inserts (Figure 3.5). Confocal laser microscopy was used to validate clear presence of ZO-1 in PBMEC *in-vitro* BBB model. Furthermore, to assess the integrity of PBMEC cytoskeleton, the expression of filamentous F-actin was validated using immunostaining of PBMEC grown on permeable inserts (Figure 3.6).

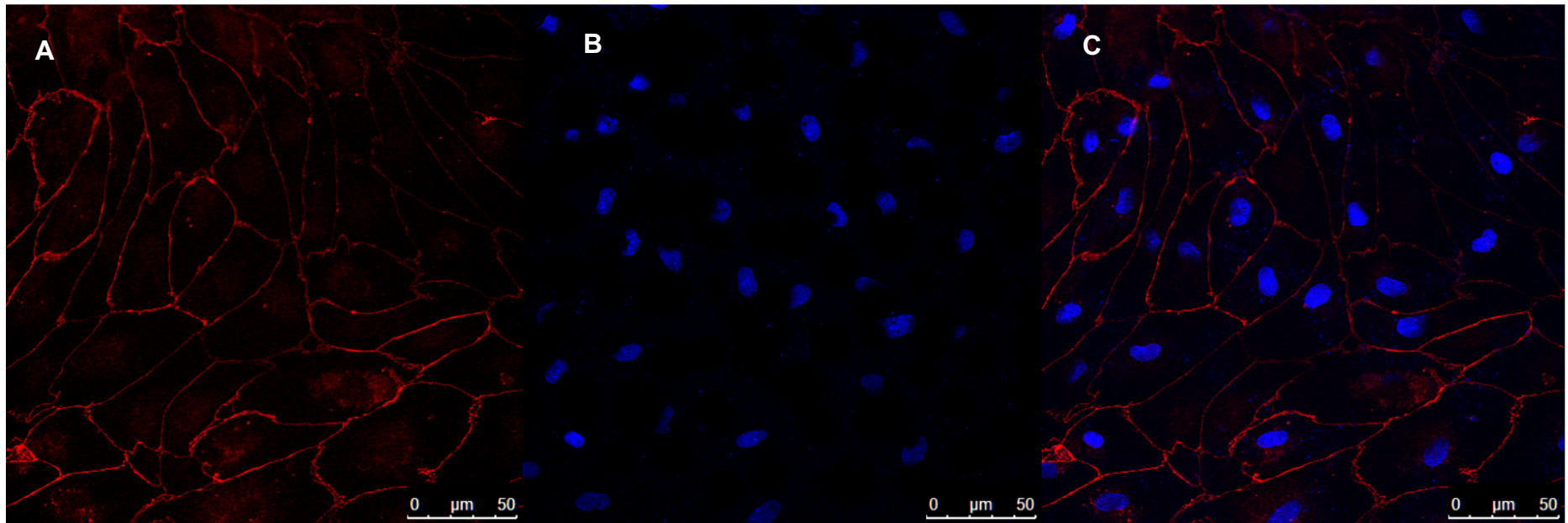


Figure 3.5 ZO1 Immunocytochemistry images for PBMEC

PBMECs were grown on permeable inserts, following adding the barrier enhancing additives on day 4, the peeled inserts were stained for (A) ZO-1, (B) DAPI, and (C) merged. Images were taken using Lecia SP5TCS II MP confocal microscope

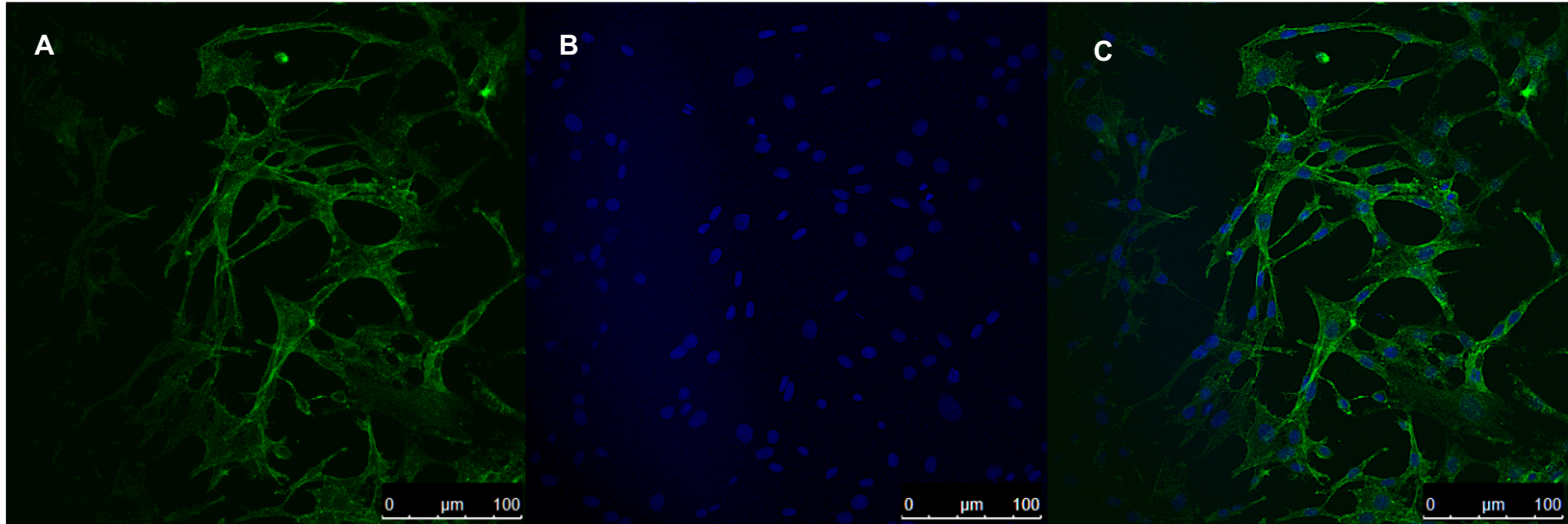


Figure 3.6 F-Actin Immunocytochemistry images for PBMEC

PBMECs were grown on permeable inserts, following adding the barrier enhancing additives on day 4, the peeled inserts were stained for (A) F-actin, (B) DAPI, and (C) merged. Images were taken using Lecia SP5TCS II MP confocal microscope

3.6.4 Cytotoxicity assays

3.6.4.1 Cellular toxicity of methotrexate towards PBMEC

In order to determine the level of cytotoxicity of methotrexate and determine IC_{50} for further studies, a MTT cytotoxicity assay was conducted in PBMEC across a 6-fold concentration range, 0.001-100 μ M. The IC_{50} was calculated to be 138.6 μ M (CI: 99.47-193.1) (Figure 3.7).

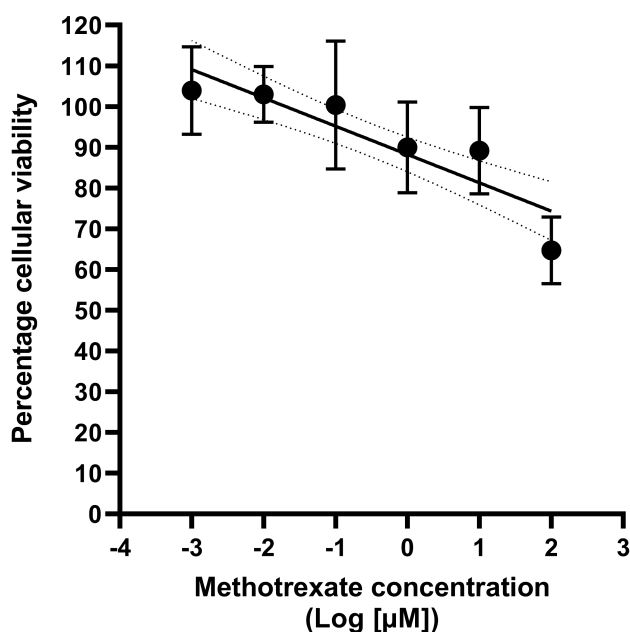


Figure 3.7 Cellular toxicity of methotrexate

50,000 cells were seeded in a 96 well plate and incubated until confluent. PBMEC were then incubated with methotrexate, 0.001-100 μ M, for 24 hours. PBMEC were washed with PBS and incubated with MTT (0.5 mg/mL) for 4 hours. Thereafter, DMSO (100 μ L/well) was added and absorbance was measured at 570 nm. Data is presented from 8 replicates per experiment repeated in three independent experiments. Vertical black lines indicate the standard deviation. Shaded dashed lines indicate confidence interval of regression line.

3.6.4.2 Cellular cytotoxicity of mitoxantrone

In order to determine the level of cytotoxicity of mitoxantrone and determine IC_{50} for further studies, a MTT toxicity assay was conducted using PBMEC across a 6-fold concentration range, 0.001-100 μ M. The IC_{50} was determined to be 243.3 μ M (CI: 141.3-496.5) (Figure 3.8).

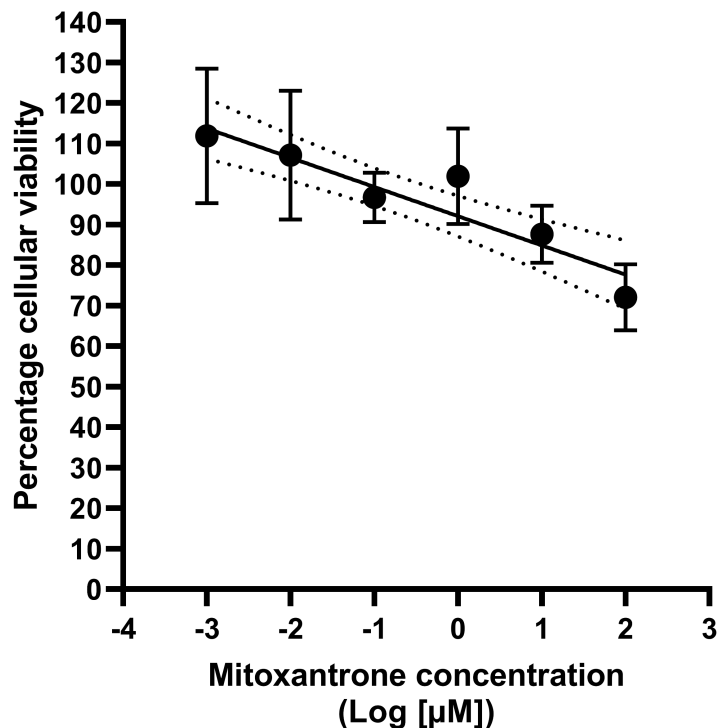


Figure 3.8 Cellular toxicity of mitoxantrone

50,000 cells were seeded in a 96 well plate and incubated until confluent. PBMEC were then incubated with mitoxantrone, 0.001-100 µM, for 24 hours. PBMEC were washed with PBS and incubated with MTT (0.5 mg/mL) for 4 hours. Thereafter, DMSO (100 µL/well) was added and absorbance was measured at 570 nm. Data is presented from 8 replicates per experiment repeated in three independent experiments. Vertical black lines indicate the standard deviation. Shaded dashed lines indicate confidence interval of regression line.

3.6.4.3 Cellular cytotoxicity of hesperetin

In order to determine the level of cytotoxicity of hesperetin and determine IC₅₀ for further studies, a MTT toxicity assay was conducted using PBMEC across a 6-fold concentration range, 0.001-100 µM. The IC₅₀ was determined to be 298.9 µM (CI: 200.2 - 494.2) (Figure 3.9).

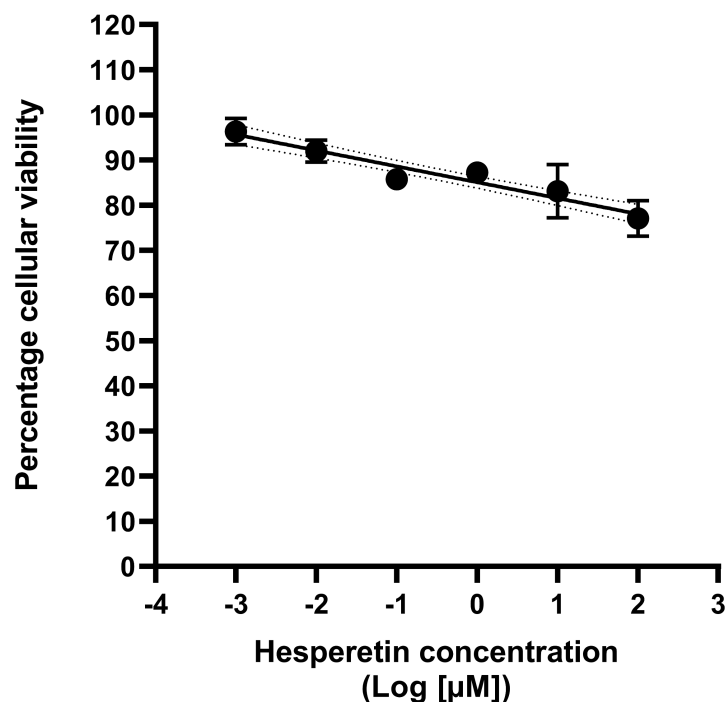


Figure 3.9 Cellular toxicity of hesperetin

50,000 cells were seeded in a 96 well plate and incubated until confluent. PBMEC were then incubated with hesperetin, 0.001-100 µM, for 24 hours. PBMEC were washed with PBS and incubated with MTT (0.5 mg/mL) for 4 hours. Thereafter, DMSO (100 µL/well) was added and absorbance was measured at 570 nm. Data is presented from 8 replicates per experiment repeated in three independent experiments. Vertical black lines indicate the standard deviation. Shaded dashed lines indicate confidence interval of regression line.

3.6.4.4 Cellular toxicity of methotrexate in the presence of hesperetin

In order to assess the impact of hesperetin on altering the cellular toxicity of methotrexate at the BBB, using the PBMEC model, cellular toxicity was determined using this combination. A MTT assay was conducted using a fixed hesperetin concentration 50 µM, with 3 concentrations of methotrexate (1, 10 and 100 µM) (Figure 3.10). The percentage cellular viability obtained for each concentration was high, 97.5% ± 1.4% (1 µM), 90.01% ± 1.3% (10 µM) and 84.4% ± 2.3% (100 µM). No statistically significant differences were determined with control.

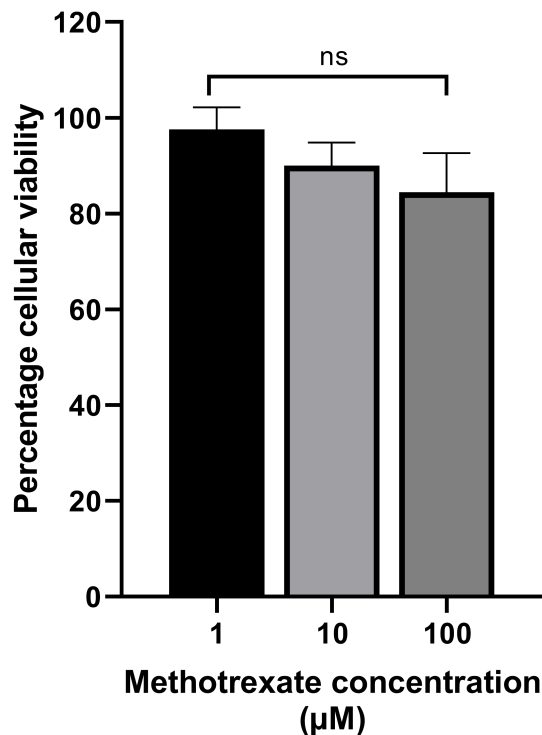


Figure 3.10 Cellular cytotoxicity of methotrexate in combination with hesperetin

Methotrexate (1, 10, 100 µM) was added to the cells, in combination with 50 µM hesperetin per each concentration and incubated with 24 hours at 37 °C, 5% CO₂. PBMECs were washed with PBS and incubated with MTT (0.5 mg/mL) for 4 hours. Thereafter, DMSO (100 µL/well) was added and absorbance was measured at 570 nm. Black vertical lines indicate the standard deviation. ns: no significant difference between samples (One-way ANOVA) and no significant difference between each concentration and control (Paired t-test).

3.6.4.5 Cytotoxicity of mitoxantrone in combination with hesperetin

In order to assess the impact of hesperetin on altering the cellular toxicity of mitoxantrone at the BBB, using the PBMEC model, cellular toxicity was determined using this combination. A MTT assay was conducted using a fixed hesperetin concentration 50 µM, with 3 concentrations of mitoxantrone (1, 10 and 100 µM) (Figure 3.11). The percentage cellular viability obtained for each concentration was high, 90.5% ± 1.1%, (1 µM), 87.4% ± 1.3 (10 µM) and 80.3% ± 2.4% (100 µM). No statistically significant differences were determined with control.

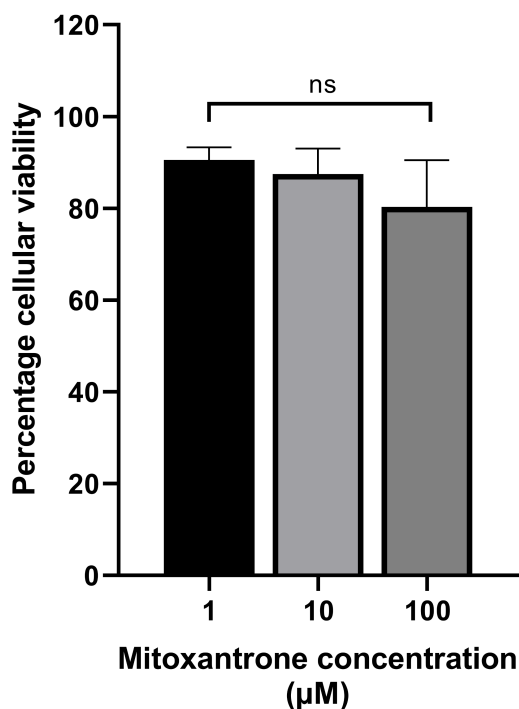


Figure 3.11 Cellular cytotoxicity mitoxantrone in combination with hesperetin

Mitoxantrone (1, 10, 100 µM) was added to the cells, in combination with 50 µM hesperetin per each concentration and incubated with 24 hours at 37 °C, 5% CO₂. PBMECs were washed with PBS and incubated with MTT (0.5 mg/mL) for 4 hours. Thereafter, DMSO (100 µL/well) was added and absorbance was measured at 570 nm. Black vertical lines indicate the standard deviation. ns: no significant difference between samples (One-way ANOVA) and no significant different between each concentration and control (Paired t-test).

3.6.5 HPLC-UV detection for hesperetin

An isocratic HPLC method was utilised in order to allow the detection of hesperetin during cellular permeability assays. Samples were prepared from a hesperetin stock solution (10 mM) in PBS containing 25 mM HEPES. Hesperetin was detected at a constant retention time of 3.4 minutes (Figure 3.12) with a solvent front peak appearing at 1.4 minutes.

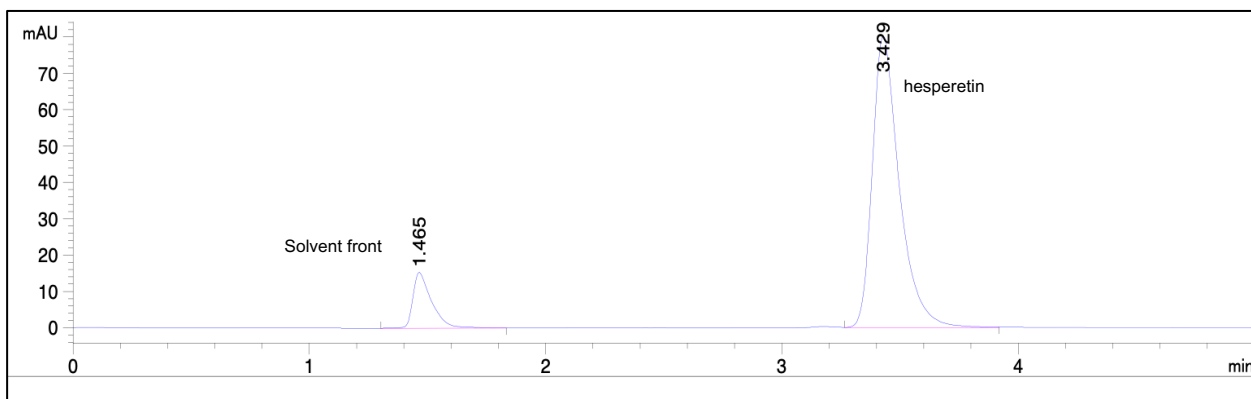


Figure 3.12 HPLC chromatogram for hesperetin

Hesperetin was detected with a retention time 3.4 minutes using reversed phase C18 column and a mobile phase containing 45:44:0.1 acetonitrile: water: acetic acid at 1 mL/min flow rate.

In order to account for system precision, 6 injections from the same hesperetin stock solution were analysed and the peak area was calculated (Table 3.1). The standard deviation was 0.19 and the relative standard deviation was less than 1% indicating that the system precision is within an acceptable range. For method precision, 6 samples were prepared from the same stock solution and analysed (Table 3.1). The relative standard deviation was less than 1% indicating that the method precision is within an acceptable range.

Table 3.1 System precision and method precision for UV-HPLC detection of hesperetin

System precision		Method precision	
Injection number	AUC (mAU)	Vial number	AUC (mAU)
1	110.7	1	111.4
2	110.6	2	111.5
3	110.5	3	111.2
4	110.5	4	111.4
5	110.6	5	111.4
6	110.1	6	109.9
Mean	110.55	Mean	111.4
SD	0.19	SD	0.61
% RSD	0.17	% RSD	0.55

The linearity of the HPLC method used for detection of hesperetin was determined by formulating a calibration curve using concentration range 0.09 μM -50 μM (Figure 3.13). The area under the curve (AUC) was linearly regressed under the concentration range used. The correlation coefficient (r^2) was 0.9995, the slope and intercept were 0.2772 $\text{mAU}\cdot\mu\text{M}$ and 5.334 mAU respectively. The LOD and LOQ were found to be 0.91 μM and 0.93 μM respectively.

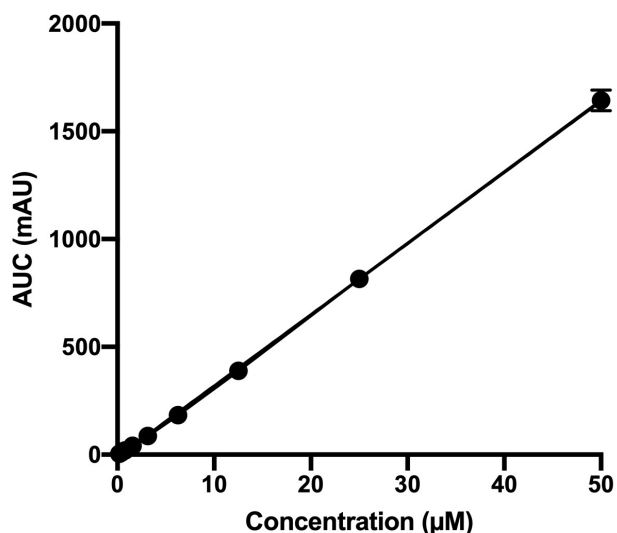


Figure 3.13 HPLC linearity calibration plot for hesperetin

A HPLC calibration curve for the detection of hesperetin. A concentration range of 0.09-50 μM was prepared in PBS containing 25 mM HEPES. The HPLC was injected with a volume of 20 μL of each concentration and the AUC was obtained. LOD and LOQ were calculated using regression analysis.

3.6.6 HPLC-UV detection for methotrexate

An isocratic HPLC method was utilised for the detection of methotrexate. Samples were prepared in PBS containing 25 mM HEPES from a 5 mM stock solution. Methotrexate was detected at a constant retention time of 5.7 minutes (Figure 3.14) with a solvent front peak appearing at 1.4 minutes.

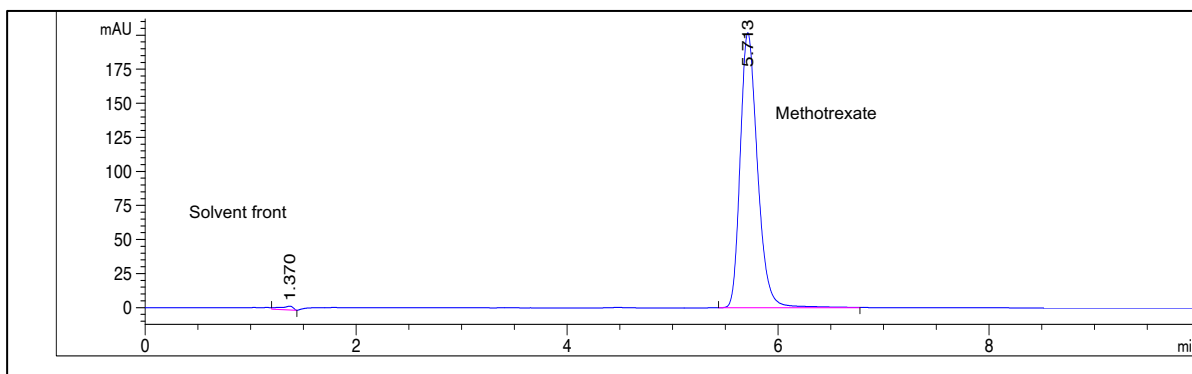


Figure 3.14 HPLC chromatogram for methotrexate

Methotrexate was detected with a retention time 5.7 minutes using reversed phase C18 column and a mobile phase containing 89:11 acetate buffer: water (pH= 3.6) at a constant 1.5 mL/min flow rate.

In order to account for system precision, 6 injections from the same methotrexate stock solution were analysed and the peak area was calculated (Table 3.2). The relative standard deviation was less than 1% indicating that the system precision is within an acceptable range. For method precision, 6 samples were prepared from the same stock solution and analysed (Table 3.2). the standard deviation was 0.3 and the relative standard deviation was less than 1% indicating that the method precision is within an acceptable range.

Table 3.2 System precision and method precision for UV-HPLC detection of methotrexate

System precision		Method precision	
Injection number	AUC (mAU)	Vial number	AUC (mAU)
1	68	1	67.8
2	68.1	2	68
3	67.9	3	68
4	67.8	4	68.4
5	68	5	68.6
6	68	6	68
Mean	68	Mean	68
SD	0.10	SD	0.30
%RSD	0.15	%RSD	0.44

The linearity of the HPLC method used for detection of methotrexate was determined by formulating a calibration curve using concentration range 0.09 μM -50 μM (Figure 3.15). The area under the curve (AUC) was linearly regressed under the concentration range used. The correlation coefficient (r^2) was 0.9998, the slope and intercept were 0.2178 $\text{mAU}\cdot\mu\text{M}$ and 3.976 mAU respectively. The LOD and LOQ were found to be 2.03 μM and 2.7 μM respectively (Figure 3.15).

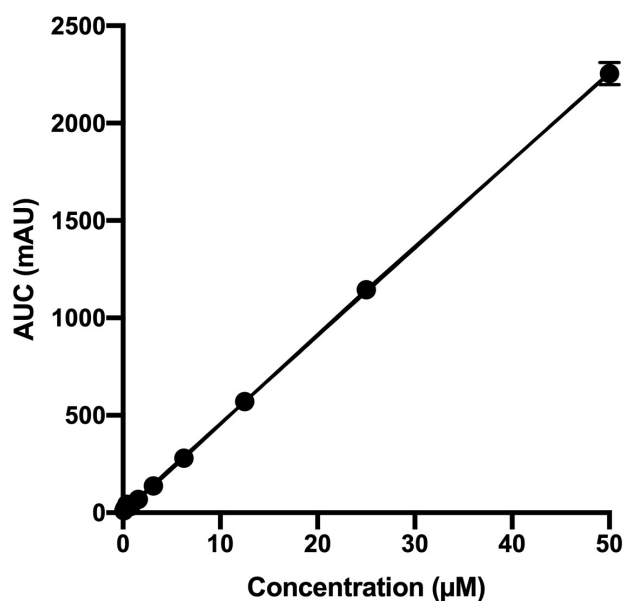


Figure 3.15 HPLC linearity calibration plot for methotrexate

A HPLC calibration curve for the detection of methotrexate. A concentration range of 0.09-50 μM was prepared in PBS containing 25 mM HEPES. The HPLC was injected with a volume of 40 μL of each concentration and the AUC was obtained. LOD and LOQ were calculated using regression analysis.

3.6.7 Fluorescence detection of mitoxantrone

Mitoxantrone was detected in the samples using a fluorescence multiplate reader at excitation and emission 607 nm and 684 nm respectively. Mitoxantrone samples, 0.09–50 μM , were prepared in PBS containing 5 mM HEPES from a 10 mM stock. The correlation coefficient (r^2) was 0.9880, the slope and intercept were 14.61 $\text{RFU}\cdot\mu\text{M}$ and 266.8 RFU respectively. LOD and LOQ were calculated using regression analysis (Figure 3.16).

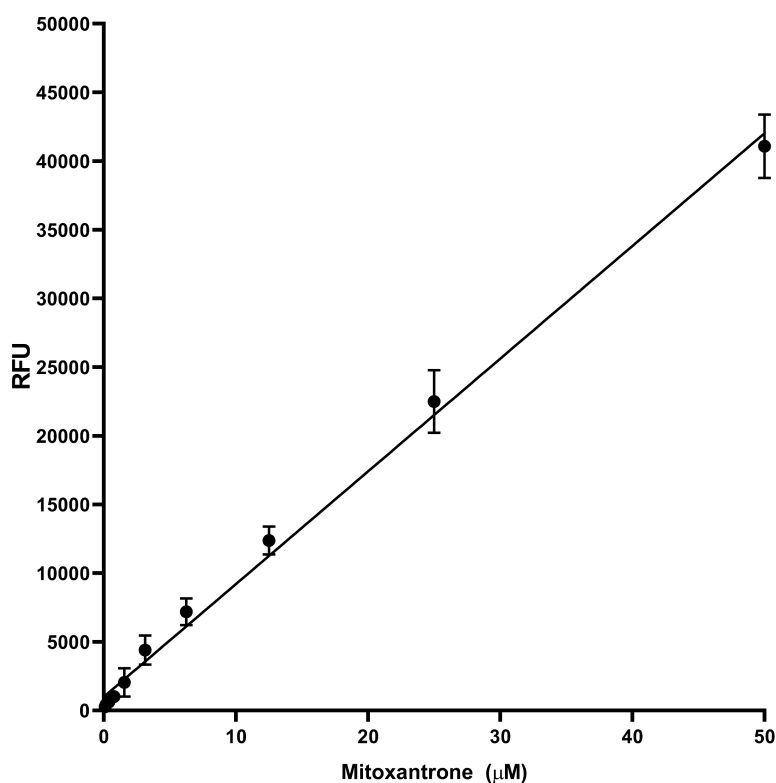


Figure 3.16 Fluorescence detection linearity calibration plot for mitoxantrone

A fluorescence detection calibration curve for the detection of mitoxantrone, 0.09-50 μM , prepared in PBS containing 25 mM HEPES. 100 μL samples were placed into a well sample of a black 96-well plate and the fluorescence measured at an excitation wavelength of 607 nm and emission wavelength of 684 using Tecan Spark 10M[®] multiplate reader.

3.6.8 Modulating the efflux action of BCRP to enhance the permeability of methotrexate and mitoxantrone across an *in-vitro* BBB model

The results obtained from the previous chapter demonstrated the ability of hesperetin to modulate the efflux action of BCRP in LN229 cells. Herein, the ability of hesperetin to permeate through the BBB was first assessed. Secondly, its ability to modulate the efflux function of BCRP in a PBMECs *in-vitro* BBB model was evaluated and subsequently compared the permeability of methotrexate and mitoxantrone in the presence and absence of hesperetin.

3.6.8.1 Methotrexate permeability across an *in-vitro* BBB model

The permeability of methotrexate was assessed across an *in-vitro* PBMEC BBB model (Figure 3.17). The flux of methotrexate from the apical to basolateral direction (AB) $P_{app\ AB}$ was determined with an apparent permeability of $1.05 \times 10^{-6} \text{ cm/s} \pm 2.72 \times 10^{-6} \text{ cm/s}$ with a basolateral to apical (BA) $P_{app\ BA}$ apparent permeability of $1.64 \times 10^{-6} \text{ cm/s} \pm 2.05 \times 10^{-6} \text{ cm/s}$, resulting in an efflux ratio of 1.6.

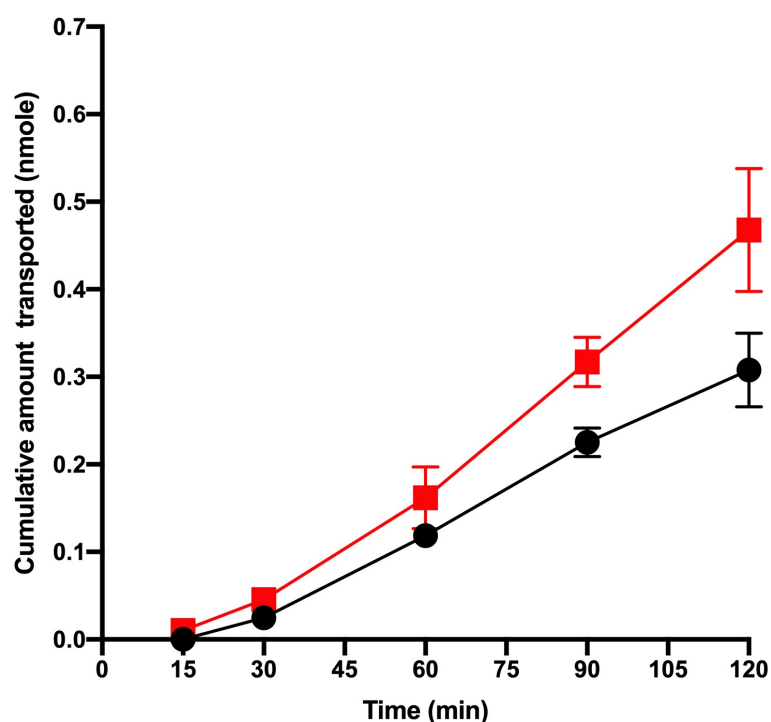


Figure 3.17 The permeability of methotrexate across an *in-vitro* BBB model established with PBMEC grown on permeable inserts

80,000 PBMECs were seeded onto 12-well permeable inserts. On day 3 post seeding, barrier forming additives were added to the media. Transport of methotrexate, 50 μM , across the formed monolayer was evaluated by determining the flux from apical to basolateral (AB) (black) and basolateral to apical (BA) (red). Methotrexate was detected using UV-HPLC. Each data point represents the mean measurement for each day (n=16 inserts in 4 independent experiments for each day).

3.6.8.2 Hesperetin permeability across an *in-vitro* BBB model

The permeability of hesperetin was assessed across an *in-vitro* PBMEC BBB model (Figure 3.18). The flux of methotrexate from the apical to basolateral direction (AB) ($P_{app\ AB}$) was determined with an apparent permeability of $4.68 \times 10^{-6} \text{ cm/s} \pm 5.6 \times 10^{-7} \text{ cm/s}$ with a basolateral to apical (BA) ($P_{app\ BA}$) apparent permeability of $4.59 \times 10^{-6} \text{ cm/s} \pm 4.73 \times 10^{-7} \text{ cm/s}$, resulting in an efflux ratio of 0.98.

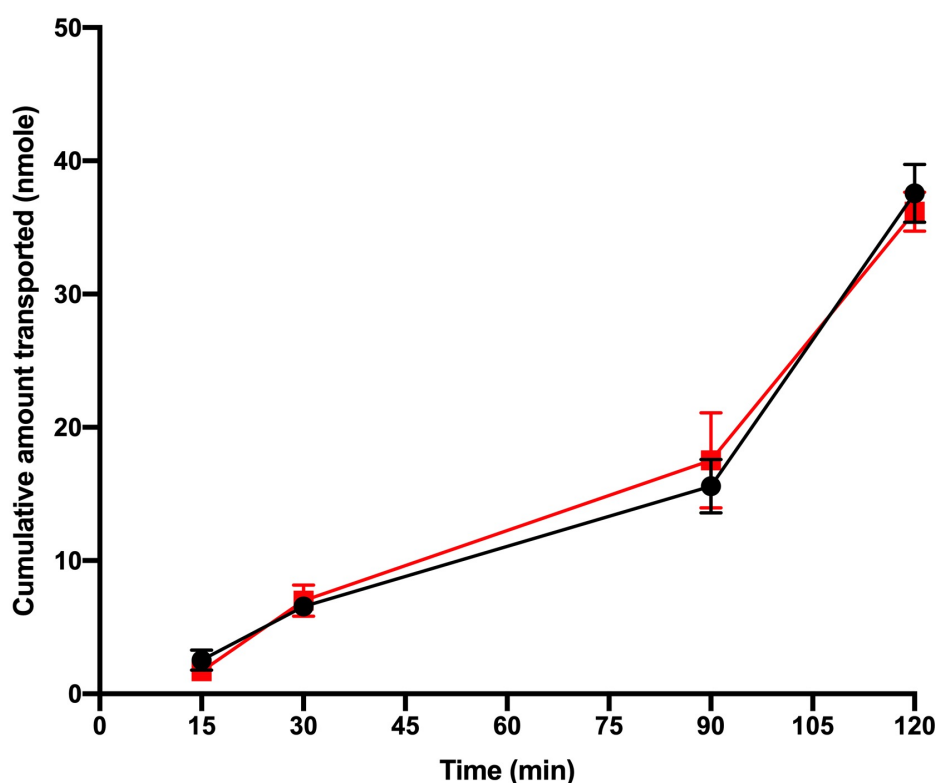


Figure 3.18 The permeability of hesperetin across an *in-vitro* BBB model established with PBMEC grown on permeable inserts

80,000 PBMECs were seeded onto 12-well permeable inserts. On day 3 post seeding, barrier forming additives were added to the media. Transport of hesperetin, $50 \mu\text{M}$, across the formed monolayer was evaluated by determining the flux from apical to basolateral (AB) (black) and basolateral to apical (BA) (red). Hesperetin was detected using UV-HPLC. Each data point represents the mean measurement for each day ($n=12$ inserts in 4 independent experiments for each day).

3.6.8.3 Assessing the impact of hesperetin on the modulating the permeability of methotrexate across an *in-vitro* BBB model.

In order to assess the ability of hesperetin to modulate the flux of methotrexate across an *in-vitro* BBB model, PBMECs were incubated with 50 μ M hesperetin 30 minutes prior to incubation with methotrexate. The inclusion of hesperetin resulted in an increased AB flux of methotrexate with an apparent permeability ($P_{app\ AB}$) of 2.85×10^{-6} cm/s \pm 1.35×10^{-7} cm/s and basolateral to apical flux ($P_{app\ BA}$) of 2.43×10^{-6} cm/s \pm 5.5×10^{-7} cm/s (Figure 3.19). The efflux ratio for the transport of methotrexate in the presence of hesperetin was 0.85.

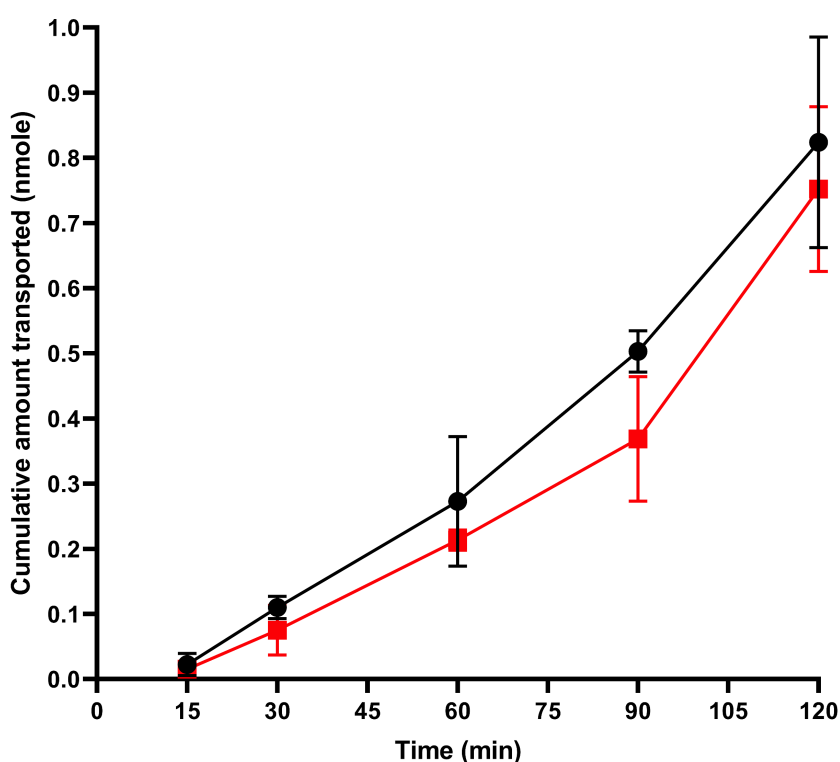


Figure 3.19 The permeability of methotrexate across an *in-vitro* BBB model established with PBMEC grown on permeable inserts

80,000 PBMECs were seeded onto 12-well permeable inserts. On day 3 post seeding, barrier forming additives were added to the media. Transport of methotrexate, 50 μ M, across the formed monolayer was evaluated by determining the flux from apical to basolateral (AB) (black) and basolateral to apical (BA) (red). Inserts were pre-incubated with hesperetin 50 μ M prior to the addition of methotrexate. The study was conducted in the presence of both methotrexate and hesperetin. Methotrexate was detected using HPLC-UV. Each data point represents the mean measurement for each day (n=16 inserts in 4 independent experiments for each day).

3.6.8.4 Mitoxantrone permeability across an *in-vitro* BBB model

The permeability of mitoxantrone was assessed across an *in-vitro* PBMEC BBB model (Figure 3.20). The flux of mitoxantrone from the apical to basolateral direction (AB) $P_{app\ AB}$ was determined with an apparent permeability of $1.59 \times 10^{-7} \text{ cm/s} \pm 3.5 \times 10^{-8} \text{ cm/s}$ with a basolateral to apical (BA) $P_{app\ BA}$ apparent permeability of $7.11 \times 10^{-7} \text{ cm/s} \pm 1.8 \times 10^{-8} \text{ cm/s}$, resulting in an efflux ratio of 4.47.

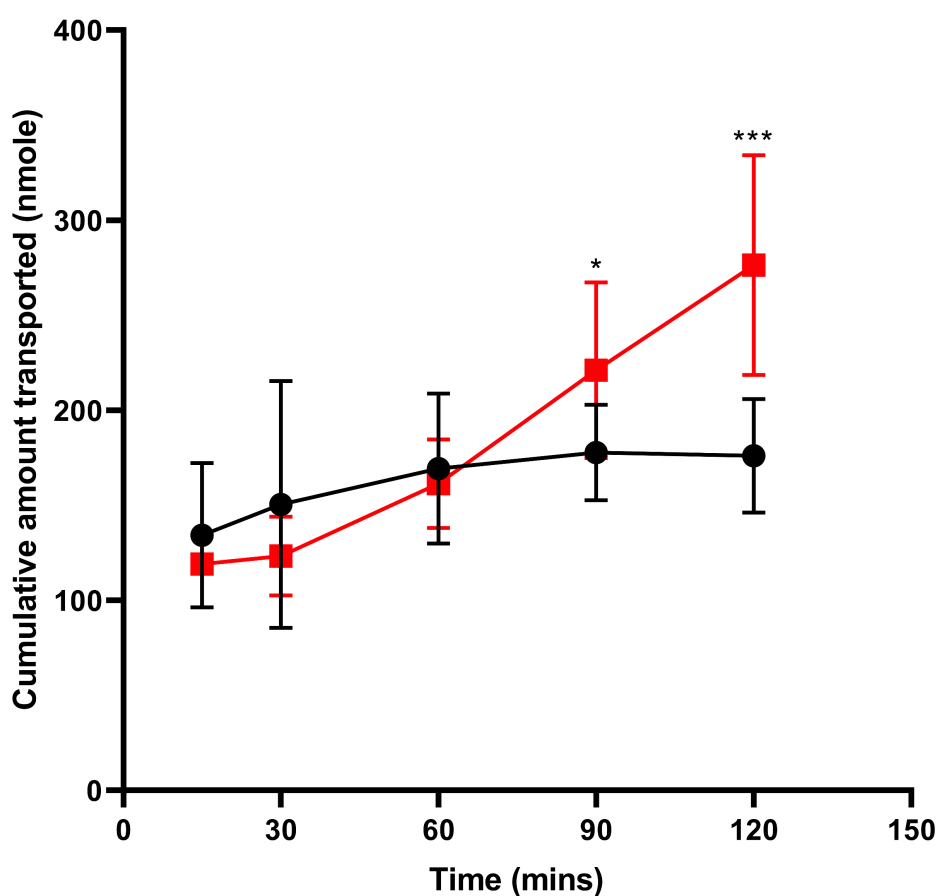


Figure 3.20 The permeability of mitoxantrone across an *in-vitro* BBB model established with PBMEC grown on permeable inserts

80,000 PBMECs were seeded onto 12-well permeable inserts. On day 3 post seeding, barrier forming additives were added to the media. Transport of mitoxantrone, 50 μM , across the formed monolayer was evaluated by determining the flux from apical to basolateral (AB) (black) and basolateral to apical (BA) (red). Mitoxantrone was detected using fluorescence detection. Each data point represents the mean measurement for each day ($n=12$ inserts in 4 independent experiments for each day). * $P < 0.05$; *** $P < 0.001$.

3.6.8.5 Assessing the impact of hesperetin on the modulating the permeability of mitoxantrone across an *in-vitro* BBB model

In order to assess the ability of hesperetin to modulate the flux of mitoxantrone across an *in-vitro* BBB model, PBMECs were incubated with 50 μ M hesperetin 30 minutes prior to incubation with mitoxantrone. The inclusion of hesperetin resulted in an increased AB flux of mitoxantrone with an apparent permeability ($P_{app\ AB}$) of 3.7×10^{-7} cm/s \pm 3.36×10^{-8} cm/s and basolateral to apical flux ($P_{app\ BA}$) of 4.79×10^{-7} cm/s \pm 2.3×10^{-8} cm/s. (Figure 3.21). The efflux ratio for the transport of mitoxantrone in the presence of hesperetin was 1.29.

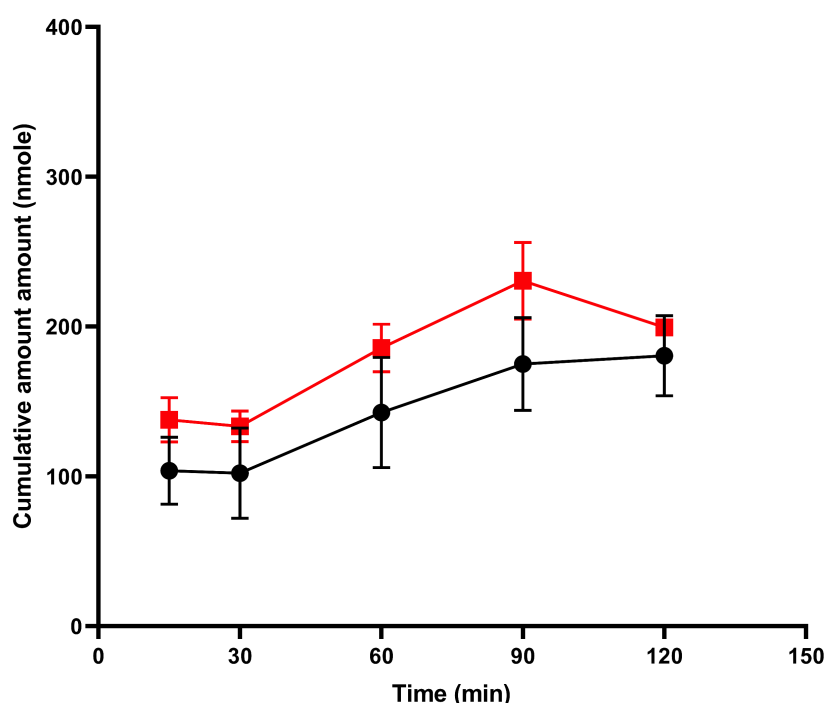


Figure 3.21 The permeability of mitoxantrone across an *in-vitro* BBB model established with PBMEC grown on permeable insert, in the presence of hesperetin

80,000 PBMECs were seeded onto 12-well permeable inserts. On day 3 post seeding, barrier forming additives were added to the media. Transport of mitoxantrone, 50 μ M, across the formed monolayer was evaluated by determining the flux from apical to basolateral (AB) (black) and basolateral to apical (BA) (red). Inserts were pre-incubated with hesperetin 50 μ M prior to the addition of mitoxantrone. The study was conducted in the presence of both mitoxantrone and hesperetin. Mitoxantrone was detected using fluorescence detection. Each data point represents the mean measurement for each day (n=12 inserts in 4 independent experiments for each day).

3.6.8.6 Changes in the basolateral to apical flux of anti-cancer agents in the presence of hesperetin

In the presence of hesperetin, methotrexate $P_{app\ BA}$ was $2.43 \times 10^{-6} \pm 5.5 \times 10^{-6}$ cm/s and in absence of hesperetin the reported $P_{app\ BA}$ was $1.64 \times 10^{-6} \pm 2.05 \times 10^{-7}$ cm/s, resulting in the demonstrated increase in $P_{app\ BA}$ for methotrexate was 48% (Figure 3.22A). However, the reported ER of methotrexate in the presence and absence of hesperetin were 0.85 and 1.6 respectively (* $P \leq 0.05$) (Figure 3.22.B), an overall reduction in ER by 46.9%.

In the presence and absence of hesperetin, the reported $P_{app\ BA}$ of mitoxantrone was $0.5 \times 10^{-6} \pm 2.3 \times 10^{-8}$ cm/s and $0.7 \times 10^{-6} \pm 1.8 \times 10^{-8}$ cm/s (* $P \leq 0.05$) respectively (Figure 3.22A). The demonstrated reduction in $P_{app\ BA}$ was 32.6%. The reported ER in the presence and absence of hesperetin were 1.29 and 4.47 respectively (** $P \leq 0.001$) (Figure 3.22B), which is an overall reduction of ER by 71.1%.

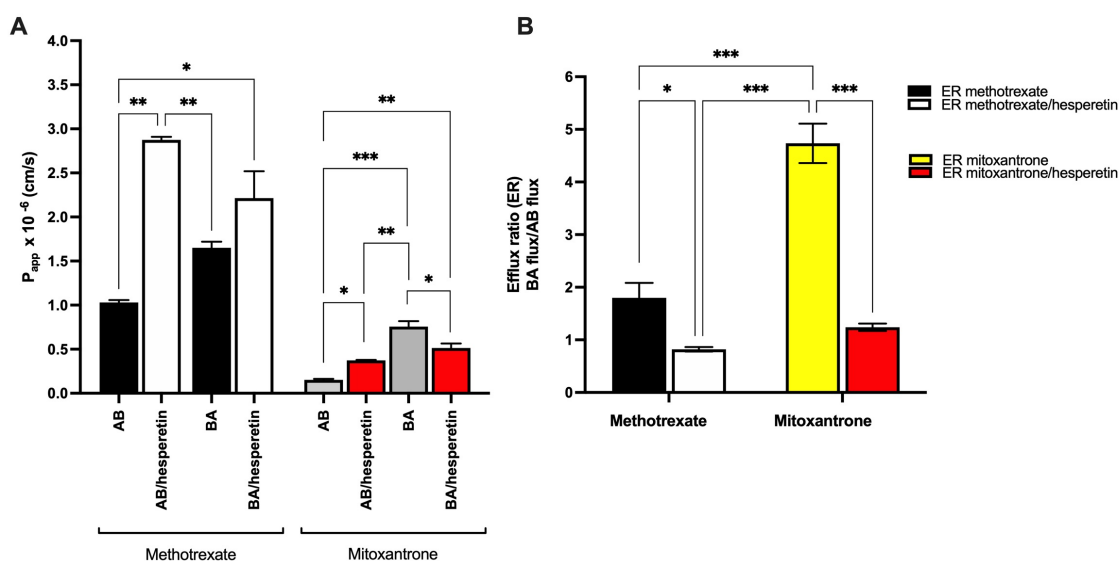


Figure 3.22 The apparent permeability (A) and efflux ratio (B) of methotrexate and me mitoxantrone in the absence and presence of hesperetin

(A) Apparent permeability of methotrexate (black, white) and mitoxantrone (grey, red) in the presence and absence of hesperetin. **(B)** the efflux ratio of methotrexate (black, white) and hesperetin (yellow, red) in the presence and absence of hesperetin. * $P \leq 0.05$, ** $P \leq 0.01$ and *** $P \leq 0.001$.

3.7 Discussion

Glioblastomas are a common form of primary brain tumours which are known to affect 0.02% of the global population which constitutes to approximately 1.6 million cases (Hanif and Muzaffar, 2017, Ersoz et al., 2019). Glioblastomas are considered rare, however, due to poor survival rates they represent a critical public health issue (Zhang et al., 2020). The standard treatment for glioblastoma is usually surgical removal of the tumour mass followed by chemotherapy treatment and/or radiotherapy. Yet, with a survival rate of less than 15 month, it's clear that the current treatment regimens are not efficient enough (Bi and Beroukhim, 2014).

Methotrexate has been used as a part of the treatment regime for glioblastoma (Zhu et al., 2009, Sane et al., 2014) with studies reporting its limited distribution into the brain due to the role of BCRP at the BBB and BTB hindering access to GBM (Sane et al., 2014, Agarwal et al., 2010, Devineni et al., 1996). On the other hand, mitoxantrone has been used in the treatment of glioblastoma (Ferroli and Broggi, 2006) and as a TRAIL sensitising agent in GBM (Senbabaoglu et al., 2016). With studies correlating its MDR to the efflux function of BCRP (Doyle et al., 1998, Higgins, 1995, Miyata et al., 1999).

Key to delivery of anticancer agents to gliomas, is the permeation across the BBB. Many anti-cancer agents such as mitoxantrone and methotrexate amongst others have limited permeability across the BBB due to the presence of ABC efflux transporters such as BCRP (Ni et al., 2010, Wijnholds et al., 2000, Cisternino et al., 2004, Breedveld et al., 2005, Toyoda et al., 2019). Breast cancer resistance protein (BCRP) itself is known to bind to and restrict the permeability of many CNS active anti-cancer agents, which leads to lowered therapeutic concentrations at the intended target (Dei et al., 2019). However, flavonoids from the phytochemicals group of chemicals, have emerged as potential novel agents possessing the ability to modulate the efflux function of BCRP and other ABC transporters (Kaur and Badhan, 2017, Zhang et al., 2004c, Gao et al., 2017b, An and Morris, 2010).

The results obtained from the previous chapter identified the ability of hesperetin to modulate the expression and function of BCRP in LN229 cells, in addition to hindering cellular migration, inducing ROS and activating Caspase-3/7 pathways. For this chapter we aimed to develop an *in-vitro* blood brain barrier model using primary PBMEC and assess the ability of hesperetin to permeate across the BBB model and to modulate the action of BCRP efflux transporter function to enhance the permeability of the anti-cancer agents methotrexate and mitoxantrone across the BBB.

3.7.1 The impact of species-specific collagen on immortalised PBMEC/C12 growth

The effects of using an appropriate extra cellular matrix as a coating surface on endothelial cell biology and integrity, cell adhesion and the cellular cytoskeleton have been well established (Carey et al., 2012, Levy-Mishali et al., 2009, Aurand et al., 2012, Antoine et al., 2014).

Reports have noted that the extraction process of the collagen from an animal tissue affects the composition of fibrils of the collagen and subsequently would affect the interaction of cells with it when grown *in-vitro* (Kreger et al., 2010, Antoine et al., 2014). Type-1 rat tail collagen is a minimally crosslinked collagen usually sourced from tendons and is usually extracted by acid solubilisation (Antoine et al., 2014), while for highly crosslinked collagens from bovine and porcine, sourced from the dermis, the extraction process entails a mixture of neutral salt solution with proteolytic digestion (Walters and Stegemann, 2014, Parenteau-Bareil et al., 2010).

Therefore, we decided to assess the impact of species-specific collagen using immortalised PBMEC/C12 cells, in order to conclude differences in TEER values under type-1 bovine collagen and type-1 rat-tail collagen. PBMEC/C12 cells were used rather than PBMEC for their rapid growth for initial screening. The results demonstrated that the use of bovine collagen resulted in higher TEER values throughout the study with a 1.8-fold higher mean TEER values for cells

grown on bovine coated inserts ($P < 0.0001$) (Figure 3.1). Based on these studies, we adopted type-1 bovine collagen for all future studies when using the primary PBMEC cell model.

3.7.2 Developing an *in-vitro* BBB permeable insert model

There is no consensus on a single best cellular model for use within *in-vitro* BBB research. A variety of cell lines are being utilised as BBB *in-vitro* models such as human cerebral cell line (hCMEC/D3) (Weksler et al., 2013), mouse models (bEND.5,b.END.3) (Schuhmann and Fluri, 2017) and bovine models (BCEC) (Helms et al., 2016). However, these produce suboptimal TEER values $< 300 \Omega \cdot \text{cm}^2$ (based on 12-well measurements) when the goal is to study drug transport (Weksler et al., 2013). Models such as iPSC-derived cells (Workman and Svendsen, 2020) can produce TEER values up to $3000 \Omega \cdot \text{cm}^2$, but the reproducibility of the model is poor due to the nature of stem cells and being cost ineffective (Gorecka et al., 2019, Liang and Zhang, 2013)

Primary porcine brain microvascular endothelial cells (PBMEC) have been characterised and used in BBB *in-vitro* research for a number of years (Cantrill et al., 2012, Abbott, 2005, Patabendige et al., 2013, Elbakary and Badhan, 2020). The key benefits of using primary porcine cells are affordability, high yield, and maintenance of morphological and cellular characteristics after extraction (Patabendige et al., 2013). Pig brains are relatively easy to obtain shortly following slaughter, as they are a byproduct of the meat industry, therefore there is no need for a specialised animal breeding facility. In addition, porcine endothelial cells can retain crucial BBB features after isolation and the rate of loss of BBB phenotypes is less than that of bovine or rodent (Deli et al., 2005). They can produce a tight BBB model with high TEER values ($\sim 800 \Omega \cdot \text{cm}^2$) based on 12-well insert measurements (Patabendige et al., 2013). Furthermore, the anatomy, genome and physiology of pigs reflect more closely to human than many established laboratory animals (Walters et al., 2011).

PBMEC were isolated from brain hemispheres following a detailed method that was reported in (Patabendige et al., 2013). Cells were grown in bovine coated

flasks (50 µg/mL) and started growing in cluster formation (Figure 3.2.A), becoming confluent within 8-10 days (Figure 3.2.B). The barrier integrity was enhanced by adding 250 µM CPT-cAMP, 17.5 µM RO20-1724 and 500 nM of hydrocortisone on day 3 post seeding which results in a spike in TEER values from $61.89 \Omega \cdot \text{cm}^2 \pm 6.8 \Omega \cdot \text{cm}^2$ to $1428.56 \Omega \cdot \text{cm}^2 \pm 270.4 \Omega \cdot \text{cm}^2$ (Figure 3.3).

CMT-cAMP enhances intracellular cAMP which is known to enhance cell differentiation in different cell types (Tilling et al., 1998, Patabendige et al., 2013). The use of cAMP for this model is based on its use in a bovine model which resulted in enhancement in monolayer formation (Rubin et al., 1991). Furthermore, the addition of hydrocortisone is known to improve and sustain barrier tightness (Hoheisel et al., 1998, Förster et al., 2008) and is utilised by cell lines such as hCMEC/D3 cells to enhance barrier formation and increase TEER value (Weksler et al., 2013). When combined with growing cells in a 50:50 mixture of ACM, parodies the native endothelial/astrocyte basement membrane microenvironment (Haseloff et al., 2005).

The highest TEER value obtained was $1428.6 \Omega \cdot \text{cm}^2 \pm 270.4 \Omega \cdot \text{cm}^2$ (Figure 3.3), which was higher than those reported by Patabendige *et al.* (Patabendige et al., 2013), $\sim 800 \Omega \cdot \text{cm}^2$. This may be a result of the use of bovine collagen due to the phylogenetic similarities *sus scrofa* have with *bos taurus* rather than *rattus* (Tejedor et al., 2011). However, there is a paucity in published studies comparing the interaction of porcine cells with bovine collagen.

Nevertheless, using bovine collagen rather than rat tail collagen, significantly enhanced BBB formation and represents a novel extra cellular matrix enhancing cell proliferation, adhesion and polarity (Lu et al., 2011, Yue, 2014). To ensure barrier integrity and formation of tight junctions, the permeation of LY across the monolayer was used as a further marker and was detected at less than 1% (Figure 3.4). LY is routinely used as a paracellular permeability marker in testing barrier integrity and proper monolayer formation (Zhao et al., 2019b).

We stained for tight junction protein ZO-1 on day 4, 24-hours following addition of barrier forming additives, and peak TEER value was recorded (Figure 3.5). We demonstrated complete cell-to-cell tight junction formation, which supports

the increase in TEER that was recorded. To ensure that actin is present within the cytoskeleton of the cells, we stained for F-actin (Figure 3.6). F-actin is a significant protein for maintenance of cell function and morphology (Dominguez and Holmes, 2011). The presence of F-actin is merely a confirmation of healthy viable morphologically correct cells which in turns would form a robust *in-vitro* BBB model.

3.7.3 Assessing the cytotoxicity of methotrexate, mitoxantrone and hesperetin in PBMECs

In order to carry out transport studies, cellular toxicity studies were conducted to identify a non-toxic concentration range of hesperetin, methotrexate and mitoxantrone for use in the PBMEC model. Over the concentration range studied hesperetin displayed limited cellular toxicity, with the highest concentration (100 μM) displaying 78% viability (Figure 3.9). Methotrexate demonstrated a greater degree of toxicity, where 100 μM exposure resulted in 64% cellular viability and an IC_{50} value of 138.6 μM (CI: 99.47-193.1) (Figure 3.7). Mitoxantrone demonstrated a higher IC_{50} of 243.3 μM (CI: 141.3- 496.5) (Figure 3.8).

Previous reports have demonstrated limited toxicity of methotrexate at higher concentrations than those used in our studies, for example exposure to human renal cells to 100 μM of methotrexate after 24 hour exposure in serum free media resulted in ~80% viability (Caetano-Pinto et al., 2017). Whereas hesperetin has been reported to demonstrated an IC_{50} of 592 μM in human lymphoid cancer cells and IC_{50} of 500 μM in human myeloid cancer cells after 24 hours exposure (Sak, 2014). Mitoxantrone was reported to have an IC_{50} of 139 μM when exposed to MCF-7 across a concentration range of 0-1000 μM for 24 hours (An and Morris, 2010).

In order to conduct further permeability studies using hesperetin in combination with methotrexate and mitoxantrone, the cytotoxic effects of the combinations on PBMEC were assessed. Methotrexate at 1, 10 and 100 μM , was combined with 50 μM hesperetin (Figure 3.10) with the viability remaining at $80.4\% \pm 2.3\%$ at the highest methotrexate concentration. Mitoxantrone displayed similar toxicity

profile when combined with hesperetin (Figure 3.11), with cellular viability at $70.3\% \pm 2.4\%$ at 100 μM mitoxantrone.

The combination of hesperetin with each anti-cancer agents resulted in slight changes in cellular viability, but this was not statistically significant. This may be due to the low concentrations used in the assays and consequently, their cytotoxic effect wasn't fully realised. Additionally, this might suggest that hesperetin does not hinder the toxicity of the anti-cancer compounds at the BBB when it inhibits BCRP. Moreover, this would also suggest that hesperetin, much like other phytochemicals, has the ability to preserve normal healthy BBB cellular viability in the presence of anti-cancer agents, possibly due to the inherent anti-oxidant properties (Xiao et al., 2011, Ren et al., 2003, Perez-Vizcaino and Fraga, 2018).

3.7.4 Assessing the permeability of methotrexate and mitoxantrone in the presence and absence of hesperetin.

Hesperetin has been demonstrated to modulate the efflux action of BCRP (Zhang et al., 2004c). When combining hesperetin with two anti-cancer agents that were reported to be effluxed by BCRP, namely methotrexate (Breedveld et al., 2004) and mitoxantrone (Mahringer et al., 2009). Here forth the aim was to enhance the permeability of these compound across the PBMEC *in-vitro* BBB model.

The results demonstrated that hesperetin was able to permeate across the *in-vitro* BBB model with reported $P_{\text{app AB}}$ of $4.68 \times 10^{-6} \text{ cm/s} \pm 5.6 \times 10^{-7} \text{ cm/s}$ and $P_{\text{app BA}}$ of $4.59 \times 10^{-6} \text{ cm/s} \pm 4.73 \times 10^{-7} \text{ cm/s}$ (Figure 3.18).

It is important to note that hesperetin has a high reported AB flux with a reported $P_{\text{app AB}}$ value of $4.68 \times 10^{-6} \text{ cm/s} \pm 5.6 \times 10^{-7} \text{ cm/s}$ (Figure 3.18), which is 29.4-fold higher than that of mitoxantrone (Figure 3.20) and 4.5-fold higher than that of methotrexate (Figure 3.17). The reported ER of hesperetin is 0.98, which is in line with other flavonoids which have been reported to have demonstrated an ER ranging over 0.8-1.5 (Shen et al., 2015, Youdim et al., 2004a, Fang et al., 2017). Furthermore, P_{app} values of more than or equal $5 \times 10^{-6} \text{ cm/s}$ indicate a high

permeability compound (Volpe et al., 2008) suggesting that hesperetin undergoes transcellular passive diffusion as it is the case of many flavonoid aglycons (Nait Chabane et al., 2009, Nielsen et al., 2006, Shen et al., 2015). Other studies have also reported the permeability of hesperetin across the BBB *in-vivo* in rats brains when 50 mg/kg was administered intravenously (Tung-Hu and Mei-Chun, 2004).

On the other hand, methotrexate demonstrated a lower AB flux and higher BA flux, with an efflux ratio of 1.6 (Figure 3.17). This is in line with a study reporting the ER of methotrexate in MDCK canine cells, ER=1.8, with a reported $P_{app\ AB}$ of $0.11 \times 10^{-6} \text{ cm/s} \pm 0.02 \times 10^{-6} \text{ cm/s}$ and $P_{app\ BA}$ of $0.2 \times 10^{-6} \text{ cm/s} \pm 0.02 \times 10^{-6} \text{ cm/s}$ (Wang et al., 2005a). Under the combination of methotrexate with hesperetin, the resultant AB flux of methotrexate increased by 1.8-fold, with a 1.9-fold reduction of ER was reported (Figure 3.22).

The change in AB and BA flux may, in part, be due to the modulatory effect hesperetin on BCRP (Kaur and Badhan, 2017, Kaur and Badhan, 2015), in addition to its ability to modulate the action and downregulate the expression of BCRP in LN229 glioblastoma cells as demonstrated in the previous chapter. A study reported that hesperetin 30 μM had the greatest inhibitory effect when tested in MCF-7 cells and produced results similar to that of ko 143 10 μM but with far less toxicity (Cooray et al., 2004b). Furthermore, hesperetin was able to modulate the action of BCRP in porcine cells PBMEC C1/2 cells at a concentration 1 μM and increase the intracellular accumulation of BCRP fluorescent substrate H33342 (Kaur and Badhan, 2017).

When the apparent permeability of mitoxantrone was assessed in the PBMEC BBB model, the reported $P_{app\ AB}$ was $1.59 \times 10^{-7} \text{ cm/s} \pm 3.5 \times 10^{-8} \text{ cm/s}$ and $P_{app\ BA}$ was $7.11 \times 10^{-7} \text{ cm/s} \pm 1.8 \times 10^{-8} \text{ cm/s}$ (Figure 3.20). This suggests that mitoxantrone is a low permeability compound with a reported ER of 4.47. This is consistent with studies that reported the mitoxantrone was a low permeability compound with an $P_{app\ AB}$ of $0.49 \times 10^{-7} \pm 0.3 \times 10^{-7} \text{ cm/s}$ and $P_{app\ BA} = 1.04 \times 10^{-8} \pm 0.37 \times 10^{-8} \text{ cm/s}$ with an efflux ratio of 2.19 assessed in Caco-2 cells (Li et al., 2017). Furthermore, an ER of 2.65 was reported using MDCK canine cells, with

a reported $P_{app\ AB}$ of $2.14 \times 10^{-7} \pm 0.81 \times 10^{-7}$ cm/s and a $P_{app\ BA}$ of $5.68 \times 10^{-7} \pm 0.86 \times 10^{-7}$ cm/s (An and Morris, 2010).

When combining mitoxantrone with hesperetin, the reported AB flux increased by 3.5-fold (Figure 3.21) and BA flux reduced by 1.5-fold in the presence of hesperetin, with a concomitant reduction in ER of 3.5-fold reduction (Figure 3.22) This is in accordance with a study that successfully utilised hesperetin amongst other flavonoids to enhance permeability of mitoxantrone in MCF-7 breast cancer cells (Zhang et al., 2004b).

To summarise, we developed a primary PBMEC BBB *in-vitro* model which was validated as a model suitable for drug permeability studies by the recorded high TEER values, less than 1% LY leakage and the presence of tight junction protein ZO-1.

Using this model, we were able to assess the ability of hesperetin to permeate across an *in-vitro* BBB model as well as its ability to modulate the efflux function of BCRP expressed in PBMECs and subsequently enhance the permeability of BCRP substrate anti-cancer agents methotrexate and mitoxantrone. combining hesperetin with methotrexate lead to a 2.7-fold increase in AB flux. More notably, combining hesperetin with mitoxantrone lead to a 3.5-fold increase in AB flux and a 1.5-fold decrease in BA flux.

3.8 Conclusion:

To conclude, in this chapter hesperetin was used as a BCRP modulator in *in-vitro* PBMECs BBB model to enhance the permeability of BCRP substrate anti-cancer agents methotrexate and mitoxantrone. Our results demonstrated that hesperetin was able to permeate across an *in-vitro* BBB model, and was able to modulate the efflux action of BCRP and significantly increase the AB flux of both methotrexate and mitoxantrone and decrease the BA flux of mitoxantrone. Hesperetin is therefore a potentially viable candidate for use in further studies, in combination with BCRP substrate anti-cancer agents and may enhance intracellular brain and GBM uptake of anti-cancer agents.

Chapter 4

A dynamic perfusion-based *in-vitro* model to enhance BBB characteristics

This chapter has been published in the following manuscript:

Elbakary, B. and R. K. S. Badhan (2020). "A dynamic perfusion based blood-brain barrier model for cytotoxicity testing and drug permeation." Scientific Reports **10**(1): 1-12.

4.1 Background:

The blood-brain barrier (BBB) represents a restrictive barrier for the delivery of therapeutic agents for a wide range of central nervous system (CNS) disorders. Penetration through the restrictive brain microvascular endothelial cell barrier is often hindered by the presence of a network of intra-cellular tight junction proteins, in addition to a network of membrane localised active transporter proteins and enzymatic metabolism processes.

The development and maintenance of an appropriate restrictive *in-vitro* BBB model is critical when assessing the potential for small molecule transport. Despite the rise in the use of *in-vivo* models for assessing BBB structure and function, *in-vitro* models are still widely used and have been developed from a range of species. However, a consensus on the most appropriate cellular system has still not been achieved, particularly in the context of assessing drug permeation and inherent barrier properties.

For example, the human immortalised hCMEC/D3 cells, when grown in co-culture with astrocytes, yields low TEER values of approximately 140 $\Omega\cdot\text{cm}^2$ (Hatherell et al., 2011) and those from primary endothelial cells from rodents yield TEER values of approximately 300 $\Omega\cdot\text{cm}^2$ (Abbott et al., 2010). Higher TEER values have been obtained with stem cell-based systems (iPSC-derived endothelial cells) and neuronal progenitor cells, when exposed to chemical treatment to promote BBB formation, resulting in values of 3000-4000 $\Omega\cdot\text{cm}^2$ (Lippmann et al., 2015), however, these often require specialised and costly methods to culture. Although human brain tissue derived *in-vitro* BBB models are ideal for BBB studies, the lack of appropriate monolayer formation and reproducibility *in-vitro* has led to other cellular models being attractive options.

The use of a porcine primary cell culture system, PBMEC, reporting high TEER without the need for co-culture with astrocytes, are a potentially viable high purity, high resistance and reproducible *in-vitro* blood brain barrier model (Cantrill et al., 2012, Patabendige et al., 2013, Kaur and Badhan, 2017, Elbakary and Badhan, 2020).

However, a critical feature of the BBB endothelium missing in many current *in-vitro* models, is the exposure of cells to laminar shear stress. Shear stress is an indirect force caused by flow of blood across the surface of endothelial cells. This flow modulates upregulation/downregulation of genes, and that in turn impacts BBB characteristics and functions (Cucullo et al., 2011).

When comparing gene analysis results from human brain microvascular endothelial cells (HBMEC) grown under static (traditional flask culture methods) and dynamic perfusion conditions (under constant media flow) have shown elevated RNA levels of tight junction proteins such as claudin-3, cadherins and zonula occludens-1 (ZO-1) under dynamic conditions (Schnittler, 1998). The importance of this response to shear stress is very evident in the structural integrity and tightness of the endothelial vascular bed. Endothelial cells cultured under flow formed a much tighter barrier (TEER $\approx 700 \Omega \cdot \text{cm}^2$) in comparison to its static counterpart (TEER $\approx 100 \Omega \cdot \text{cm}^2$). The 'tightness' of the barrier also affects its selectivity and consequently affects permeation of drug molecules (Cucullo et al., 2011).

Brain endothelial cells are exposed to rapid blood perfusion (750 mL/min) to which they act in response by cellular re-alignment in the direction of the flow, rearrangement of cell fibres, in addition to functional remodelling (Ando and Yamamoto, 2009) and increased life span and proliferation (Cucullo et al., 2011, Di and Kerns, 2015). Further, there is an underrated mechanical stimulus that also affects endothelial cells in the brain, that stimulus is shear stress (Cucullo et al., 2011).

Gene array analysis of key tight junction proteins showed that expression of proteins such as occludin, claudin-5 and cadherin-1 in flow models were upregulated compared to static models (Wong et al., 2013). Exposure to shear stress also increased the RNA expression levels of a range of ABC transporter proteins such as *ABCB1*, *ABCC2*, and *ABCC5* (Doan et al., 2002) and CYP450 enzymes such as CYP1, CYP2 and CYP3 families (Dauchy et al., 2008a). Furthermore, shear stress also enhances response of pro-inflammatory stimuli by facilitating endothelial-leukocyte cross talk and T-lymphocyte migration by

upregulating expression levels of ICAM-1, VCAM-1 and PECAM-1 (Wong, 2007, Steiner et al., 2010). Furthermore, shear stress stimulates the endothelial expression of ion channels and specialised transport systems such glucose transporter family (GLUT-1, GLUT-2, GLUT-3 and GLUT-5), Acetyl-CoA transporter (SLC33A1) and organic anions and cations transporters amongst many others (Cucullo et al., 2011).

Modern dynamic cell culture *in-vitro* models can mimic the physiological interactions between tissues connected by bloodstream. These models have immense capabilities as they enable studies on specific organ-organ and tissue interactions. A range of approaches have been used to simulate shear stress across brain endothelial cells, from microfluidic systems (Wang et al., 2017, Brown et al., 2015) to hollow fibre constructs (Neuhaus et al., 2006).

Recently, a novel cell culture flow-based chamber technology was developed and commercialised (Vozzi et al., 2008, Sbrana and Ahluwalia, 2012) this technology is called the QuasiVivo[®] system (Kirstall, Sheffield, UK). The QuasiVivo[®] system utilises a flow model that is able to simulate blood flow between different cell culture chambers which represent tissues (Haycock, 2014).

This novel perfusion cell culture system was designed to be used alongside permeable inserts (QV600 and QV900) often developed with *in-vitro* barrier models such as the lung (Chandorkar et al., 2017) and the BBB (Elbakary and Badhan, 2020) and, for the first time, allowed direct modelling of the impact of perfusion on cell differentiation and barrier formation. The QV600 system allows for the application of various flow rates depending on the cell type which provides the cells with a constant nutrient return (Mazzei et al., 2010). The QV600 system consists of 1) PDSM chamber that is 15 mm in width and can hold up to 4 mL liquid, 2) connectors through which the chambers are linked, 3) a reservoir bottle that can hold up to 30 mL of media, 4) a peristaltic pump that can be housed in the incubator (Figure 1.13).

The advantages of using QV600 as opposed to other dynamic *in-vitro* cell culture models are:

- Continuous use of media across all cell cultures
- Easy to run and set up
- Easy to clean (can be autoclave up to 3 times)
- Steady level of liquid within the chamber- no risk of cells drying.

The QV600 was successfully used in the development of *in-vitro* organ models. A 3D lung model to study fungal infection was developed using QV600. This study demonstrated that growing normal human bronchial cells NHBE under an air-liquid interface (ALI) resulted in a significant increase in mucous production on day 7 in the perfusion model compared to day 21 under static conditions (Chandorkar et al., 2017).

Furthermore, the QV600 system was used with epithelial Caco-2 cells. The results displayed an enhancement of barrier integrity which was validated by an increase in the expression of tight junction protein ZO-1 as well as an increase in the reported TEER values $1800 \Omega \cdot \text{cm}^2$ after growing the cells under static conditions for 20 days followed by a 48 hour exposure to flow (Giusti et al., 2014).

4.2 Aims and objectives

The aim for this chapter was to assess the effect of shear stress on the *in-vitro* PBMEC BBB model cellular morphology and characteristics following the application of laminar flow using the QV600 system.

In order to attain these aims, the objectives were to:

- Create a blood brain barrier model using PBMEC grown in 24-well inserts for use in the QV600 chamber
- Determine the optimal flow rate suitable for PBMEC growth
- Examine the effect of shear stress on cell proliferation
- Examine the effect of shear stress on TEER values
- Examine the effect of shear stress on ZO-1 tight junction protein expression
- Assess the permeability of mitoxantrone and hesperetin across the BBB model, following exposure to shear stress

4.3 Materials:

See section 3.3 for a list of materials. The Quasi Vivo® chamber, connectors and the peristaltic pump were obtained from Kirkstall (Rotherham, UK); all other chemicals were sourced from Sigma (Dorset, UK).

Stock solutions of all test compounds were prepared in dimethyl sulfoxide (DMSO) and stored at -20°C until use.

4.4 Methods

In order to examine the effect shear stress on the characteristics of an *in-vitro* BBB model, PBMEC were grown in permeable inserts and subjected to low and high shear stress in the form of laminal flow.

4.4.1 Isolation of porcine brain capillaries

The PBMEC model was isolated as described in Section 3.4.2.

4.4.2 Development of PBMEC *in-vitro* BBB model under static conditions

The PBMEC model was developed as described in Section 3.4.4. Here, we utilised 24 well/0.33 cm² permeable inserts (Greiner BioOne transparent ThinCerts® 24 well), a lower seeding density 3x10⁴ cells/cm² was used to accommodate the small size of the inserts used within the QV600 chambers.

4.4.3 Preparation of the QV600 perfusion system

To model dynamic perfusion of media within the cell culturing environment, the QV600 interconnected chamber system was utilised. This allows for the use of permeable inserts and coverslips within chambers. The QV600 consists of chambers, a media reservoir, a peristaltic pump and associated tubing connectors (Figure 4.1A). In order to utilise permeable inserts, the media level within each chamber was raised by increasing the height of the reservoir bottle by 5 cm with luer-locks sealing the upper chambers (Figure 4.1B). Prior to use,

the QV600 system was sterilised by submerging in 70% v/v ethanol for 24 hours, followed by exposed to UV light for 6 hours and flushed for 1 hour with PBS supplemented with 1% v/v penicillin and streptomycin.

Each peristaltic pump provided two independent channels, which were used with 3 chambers each. To assess shear stress, we considered flow rates within a range of 0-600 $\mu\text{L}/\text{min}$ ($0-11.0 \times 10^{-6}$ Pa or $0-110 \times 10^{-6}$ dyne/cm²) or flow speed of $0-1.69 \times 10^{-6}$ m/s, with shear stress (Pa) and flow speed (m/s) as described by (Miranda-Azpiazu et al 2018).

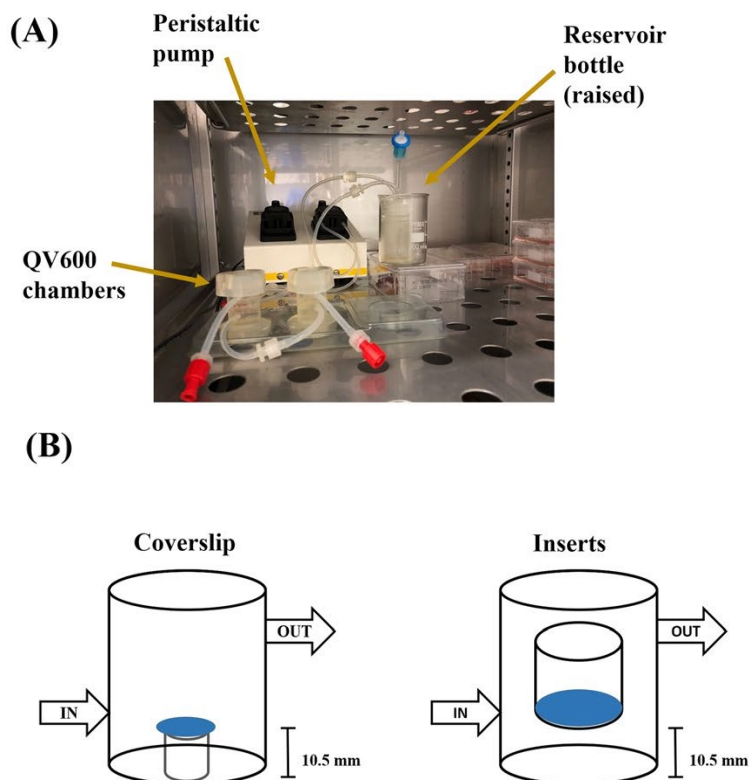


Figure 4.1 Diagrammatical representation of the QuasiVivo® 600

(A) The setup of the QV600 in the incubator showing peristaltic pump, a raised reservoir bottle, two interconnected chambers were 24-well inserts are fitted; (B) A schematic representation of the exposure to the raised coverslips to the flow compared to the bottom of a 24-well permeable insert.

4.4.4 Determination of optimal flow rate

Circular cover slips (13 mm) were coated with bovine collagen (50 µg/mL) and fibronectin (7.5 µg/mL) prior to seeding with 3×10^4 cells (from passage 1) and grown in 24-well plates in PBMEC:ACM. On day 3, coverslips were carefully transferred to QV600 chambers and raised by 10.5 mm using an inverted standing insert (Millicell, 12 mm insert) (Figure 4.1B), to match the height of the permeable insert membrane when seated within the QV600 chamber (Figure 4.1A).

Following optimisation of initial flow rates, cells were subjected to flow at 275 µL/min and 550 µL/min for 48 hours. The choice of the flow rate was based on previous findings that endothelial cells can withstand flow rates over 300 µL/min (Miranda-Azpiazu et al., 2018)

Thereafter, cell morphology was assessed using light microscopy followed by assessment of tight junction formation through immunocytochemistry. Coverslips were washed with ice cold PBS three times and fixed in 4% w/v paraformaldehyde for 10 minutes. The coverslips were then washed three times with PBS and cells permeabilised using 0.02% w/v saponin for 10 minutes followed by a further cycle of washing in PBS three times.

Cells were subsequently blocked with 6% v/v goat serum (Sigma, UK) for 5 hours, prior to incubation with the ZO-1 primary antibody (ZO-1 1A12 monoclonal) prepared in blocking buffer at a 1:100 dilution overnight at 4 °C. Thereafter, the coverslips were washed three times with ice cold PBS followed by the addition of the secondary antibody (0.5 µg/ml goat anti-mouse IgG H+L superclonal secondary Alexa 488®) for 2 hours at room temperature. The cells were then washed with ice cold PBS three times and mounted on a microscope slides using Fluoroshield (containing DAPI). Tight junction formation was subsequently assessed using an upright confocal microscope (Leica SP5 TCS II MP) and visualised with a 40× oil immersion objective. Images were acquired with an argon laser at 494 nm and a helium–neon laser to visualise DAPI at 461 nm.

4.4.5 Cellular viability in the presence of shear stress

In order to assess the impact of shear stress on the viability of the cells, a 3-(4,5-dimethylthiazol-2-yl)-2,5-diphenyltetrazolium bromide (MTT) assay was conducted using PBMEC grown on cover slips that were subjected to laminar flow for 48 hours (at an optimal flow rate determined previously) and under static conditions. Thereafter, the coverslips were placed in 24-well plates and washed once with pre-warmed PBS prior to being incubated with 0.5 mg/mL MTT for 4 hours at 37 °C, 5% CO₂. The resulting formazan crystals were dissolved in DMSO (100 µL/coverslip) for 15 minutes, before being transferred to a clear 96 well plate and with the UV-absorbance of the formazan crystals measured at 570 nm (Tecan Spark 10M®).

4.4.6 The impact of shear stress on the BBB *in-vitro* model

PBMEC grown on 24-well permeable inserts intended for use in the QV600, were first seeded and grown on inserts under static conditions, within 24-well plates, and grown for 3 days prior to transfer into the QV600 chambers (n=20 inserts in total over 5 independent experiments). An acceptable monolayer formation under static and shear stress was determined using the TEER value (EVOM, World Precision Instruments, USA) and corrected for background resistance (coated inserts without cells) and by the surface area of the insert (0.33 cm²). TEER was assessed by transferring the inserts into 24-well plates for TEER measurement, before returning to the QV600 chambers. Furthermore, tight junction formation was assessed using immunocytochemical methods as described previously in Section 3.4.4.1.

4.4.7 Permeability of mitoxantrone across the *in-vitro* BBB model, developed under shear stress

PBMECs were grown on permeable inserts and exposed to high flow (550 µL/min) for 48 hours using the QV600. Thereafter, inserts were removed and placed into a 24-well cell culture plate. Mitoxantrone (50 µM) was prepared in serum free PBMEC media containing 25 mM HEPES and added to the apical (AB

flux) or basolateral (BA flux) compartments with sampling taking place from the opposite compartment, which contained serum free PBMEC media containing 25 mM HEPES.

Samples were taken at intervals between 15-90 minutes and replaced with equal amount fresh warm serum free PBMEC media containing 25 mM HEPES. Mitoxantrone concentrations were analysed using a fluorescent plate reader (Tecan Spark 10M[®]) at an excitation wavelength of 488 nm and emission wavelength of 670 nm. The apparent permeability (P_{app}) was calculated (Equation 4, see Section 3.4.5).

4.4.8 Permeability of hesperetin across the *in-vitro* BBB model, developed under shear stress

PBMECs were grown on permeable inserts and exposed to high flow (550 μ L/min) for 48 hours using the QV600. Thereafter, inserts were removed and placed into a 24-well cell culture plate. hesperetin (50 μ M) was prepared in serum free PBMEC media containing 25 mM HEPES and added to the apical (AB flux) or basolateral (BA flux) compartments with sampling taking place from the opposite compartment, which contained serum free PBMEC media containing 25 mM HEPES.

The hesperetin transport assay and subsequent detection was detailed in Sections 3.4.6.1 and 3.6.8.2.

4.5 Statistical analysis

All data is presented as mean \pm standard deviation, with experiments being conducted in at least replicate independent experiment unless otherwise stated. Where appropriate, statistical analyses was performed in Graphpad Prism (La Jolla, California, USA), with t-tests used to determine differences between the mean values. A significance p-value of <0.05 was considered as statistically significant

4.6 Results

4.6.1 Identification of optimal shear stress

In order to identify optimal shear stress for use with PBMECs, coverslips were raised and exposed to low (275 $\mu\text{L}/\text{min}$) and high (550 $\mu\text{L}/\text{min}$) flow rates and compared to matching coverslips grown under static conditions and subsequently stained for ZO-1. Under static conditions, limited cell-to-cell ZO-1 formation is evident (Figure 4.2). When the flow rate was applied at low (275 $\mu\text{L}/\text{min}$) (Figure 4.3) and high (550 $\mu\text{L}/\text{min}$) (Figure 4.4), cellular reorganisation was evident with the cell-to-cell ZO-1 protein formation. However, the translocation of ZO-1 to the cytoplasm was also evident under low and high flow rates.

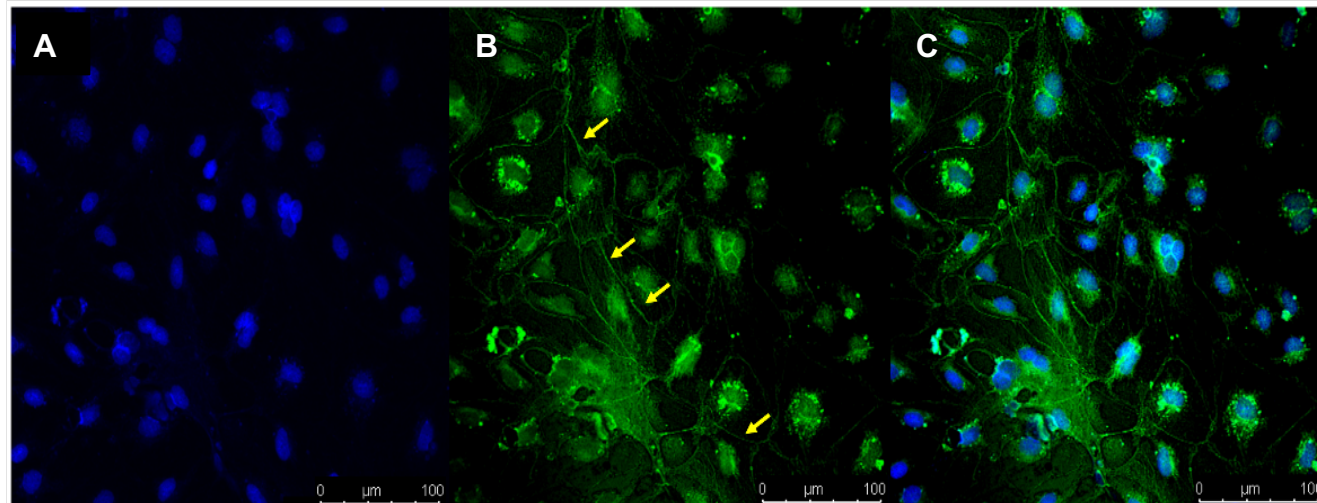


Figure 4.2 Immunocytochemistry images obtained following ZO-1 staining under static conditions on coverslips

PBMEC grown on collagen (50 $\mu\text{g}/\text{mL}$) and fibronectin (7.5 $\mu\text{g}/\text{mL}$) coated coverslips under static conditions. Images were taken using a Leica SP5 TCS II MP confocal microscope. (A) for DAPI, (B) for ZO-1 and (C) for merged. Yellow arrows indicate formation of tight junctions.

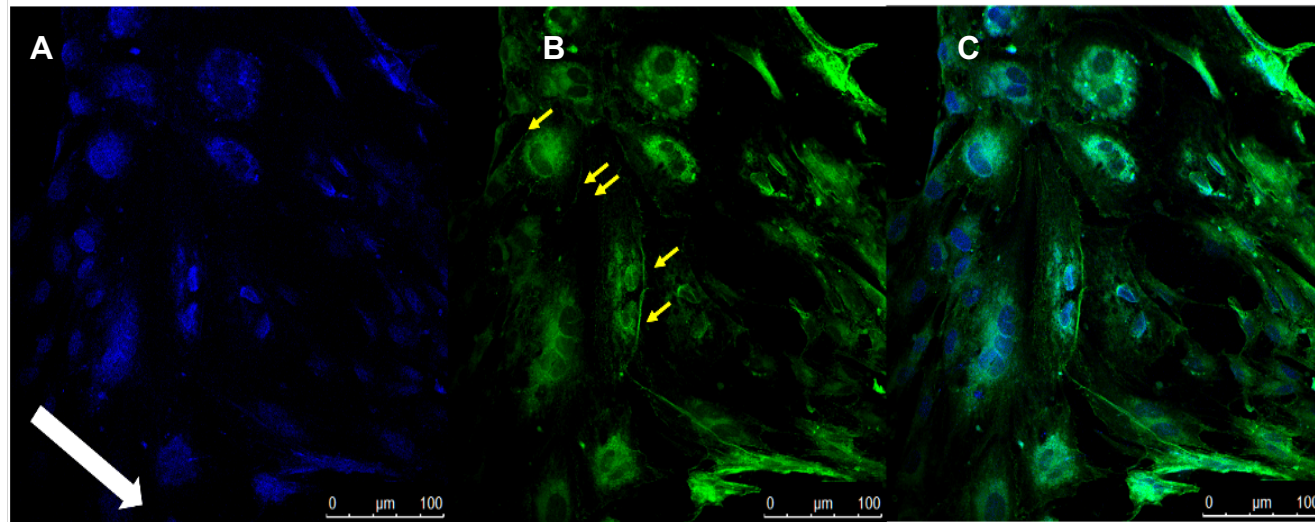


Figure 4.3 Immunocytochemistry images obtained following ZO-1 staining following exposure to low flow rate on coverslips

PBMECs grown on bovine collagen (50 $\mu\text{g}/\text{mL}$) and fibronectin (7.5 $\mu\text{g}/\text{mL}$) coated coverslips. PBMEC exposed to low flow (275 $\mu\text{L}/\text{min}$) for 48 hours in the QV600 system. (A) for DAPI, (B) for ZO-1 and (C) for merged . Images were taken using a Leica SP5 TCS II MP confocal microscope. The white arrow indicates the direction of flow and the yellow arrows indicate formation of tight junctions.

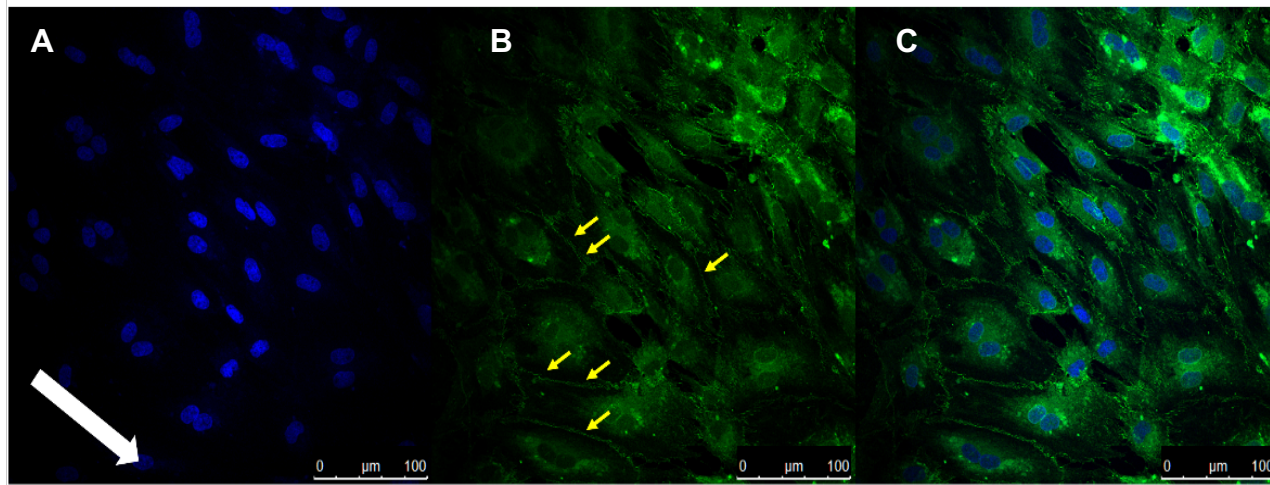


Figure 4.4 Immunocytochemistry images obtained following ZO-1 staining following exposure to high flow rate on coverslips

PBMECs grown on bovine collagen (50 µg/mL) and fibronectin (7.5 µg/mL) coated coverslips. PBMEC were exposed to high flow (550 µL/min) for 48 hours using the QV600. (A) for DAPI, (B) for ZO-1 and (C) for merged. Images were taken using a Leica SP5 TCS II MP confocal microscope. The white arrow indicates the direction of flow and yellow arrows indicate formation of tight junctions.

4.6.2 Cellular viability under shear stress

To assess the impact of shear stress on PBMEC cellular viability, high flow (550 $\mu\text{L}/\text{min}$) was applied for 96 hours and cellular viability of PBMECs (grown on raised coverslips) was assessed using a MTT cellular viability assay. The presence of high flow for 4 days did not reduce the viability of PBMEC cells, with a nominal, but significant ($P < 0.05$) increase in viability for dynamic shear stress (Figure 4.5).

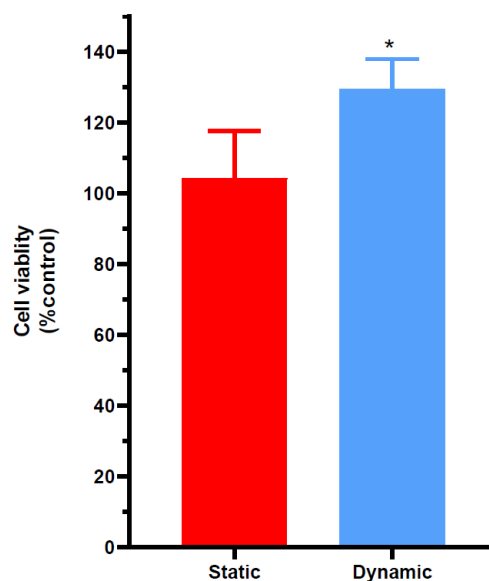


Figure 4.5 Cellular viability of PBMECs grown in static and dynamic conditions

Cellular viability of PBMEC grown on coverslips under static media and dynamic high flow (550 $\mu\text{L}/\text{min}$) for 96 hours, using a MTT assay. Dynamic results were normalised to the mean of the static results. $n=9$ coverslips in 3 independent experiment. * $P \leq 0.05$.

4.6.3 Assessment of the impact of shear stress on the TEER of PBMEC *in-vitro* BBB model

To investigate the formation of a high resistance barrier, the TEER from monolayers of '60s' grown on semi-permeable inserts (24-well, 0.33 cm^2) were determined under static conditions and under dynamic shear stress.

To assess whether shear stress is capable of inducing barrier formation, PBMEC were grown on semi-permeable inserts and subjected to flow at 550 $\mu\text{L}/\text{min}$, without the addition of any barrier forming additives. At 4 days post-seeding, inserts exposed to flow demonstrated a significantly higher TEER ($35.7 \Omega\cdot\text{cm}^2 \pm 5.1 \Omega\cdot\text{cm}^2$) compared by those maintained in static culture conditions ($21 \Omega\cdot\text{cm}^2 \pm 1.5 \Omega\cdot\text{cm}^2$) ($P \leq 0.001$), which was maintained through to day 7 post seeding (Figure 4.6A).

To further assess the ability of shear stress to induce barrier formation, static and dynamic inserts were exposed to endothelial tight junction inducing agents on day 3 post seeding for 24 hours only. On day 4, TEER values significantly increased under both static media, to $306.3 \Omega\cdot\text{cm}^2 \pm 41.9 \Omega\cdot\text{cm}^2$, and dynamic flow to $448.1 \Omega\cdot\text{cm}^2 \pm 11.3 \Omega\cdot\text{cm}^2$ ($P \leq 0.0001$), which was maintained to day 7 (Figure 4.6B).

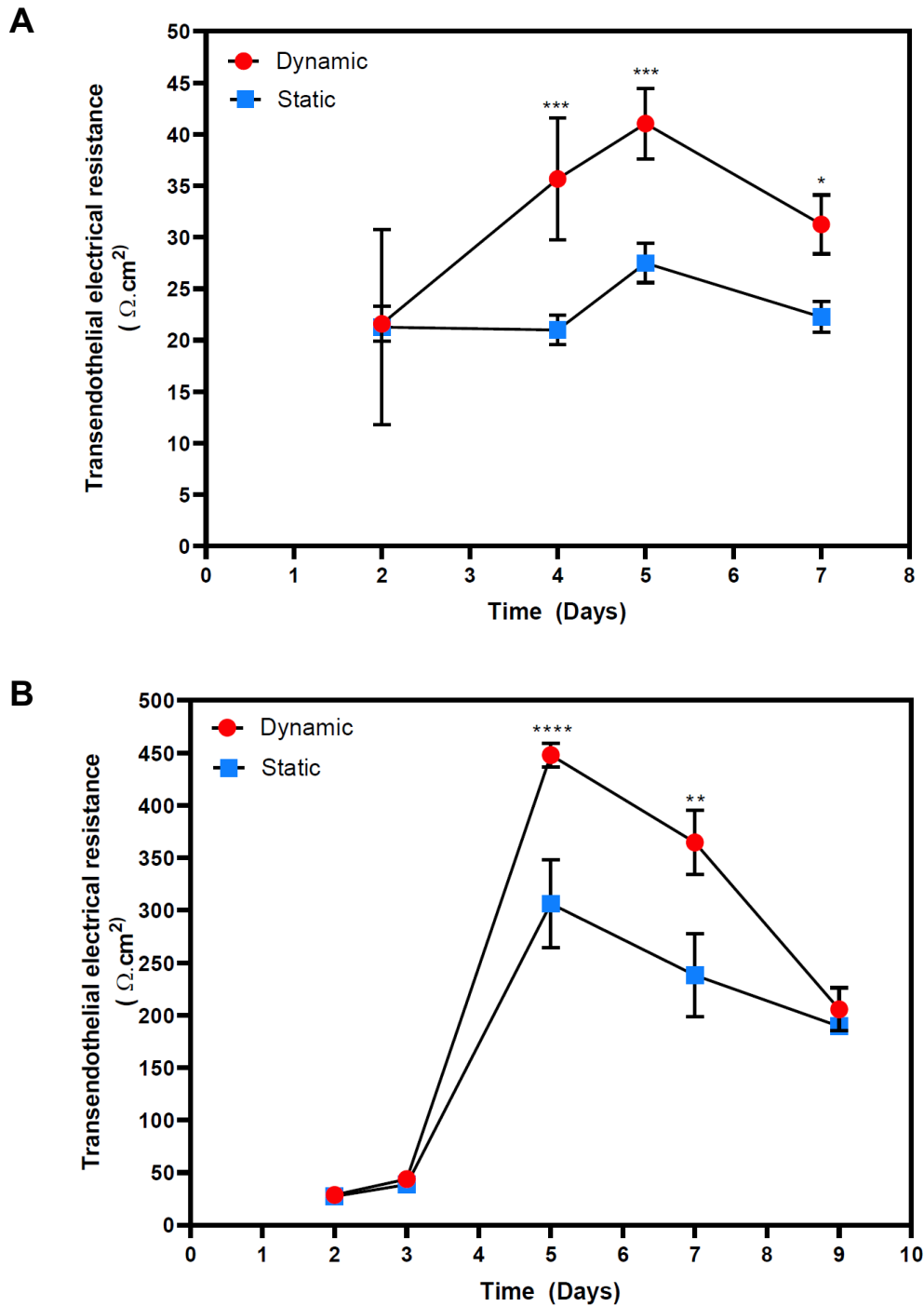


Figure 4.6 TEER measurements under static and dynamic conditions

TEER measured following growth of PBMEC cells on permeable cell culture inserts (24-well, 0.33 cm²) under static and dynamic (550 μL/min) conditions. TEER of PBMEC were measured when grown on permeable inserts in the **(A)** absence and **(B)** presence of barrier forming additives. * P ≤ 0.05, ** P ≤ 0.01, *** P ≤ 0.001 and **** P ≤ 0.0001. n=12 in replicates of 3 in 4 independent experiments.

4.6.4 Tight junction formation and cellular reorganisation under shear stress

The expression of the tight junction protein ZO-1 was assessed using immunocytochemistry on semi-permeable inserts maintained in either static media or exposed to shear stress (550 $\mu\text{L}/\text{min}$). In the absence (Figure 4.7) and presence (Figure 4.8 and 4.9) of shear stress, cellular labelling with ZO-1 antibody demonstrated the ability of PBMECs to form tight junctions. Under static conditions (Figure 4.7), the cellular morphology was indiscriminately organised with a discontinuous serrated pattern. However, under shear stress, linear realignment of the PBMECs was particularly visible following 24-hours (Figure 4.8) and 48-hours (Figure 4.9) of shear stress exposure and was largely localised to the intracellular junctions of cells, with limited discontinuous tight junction formation.

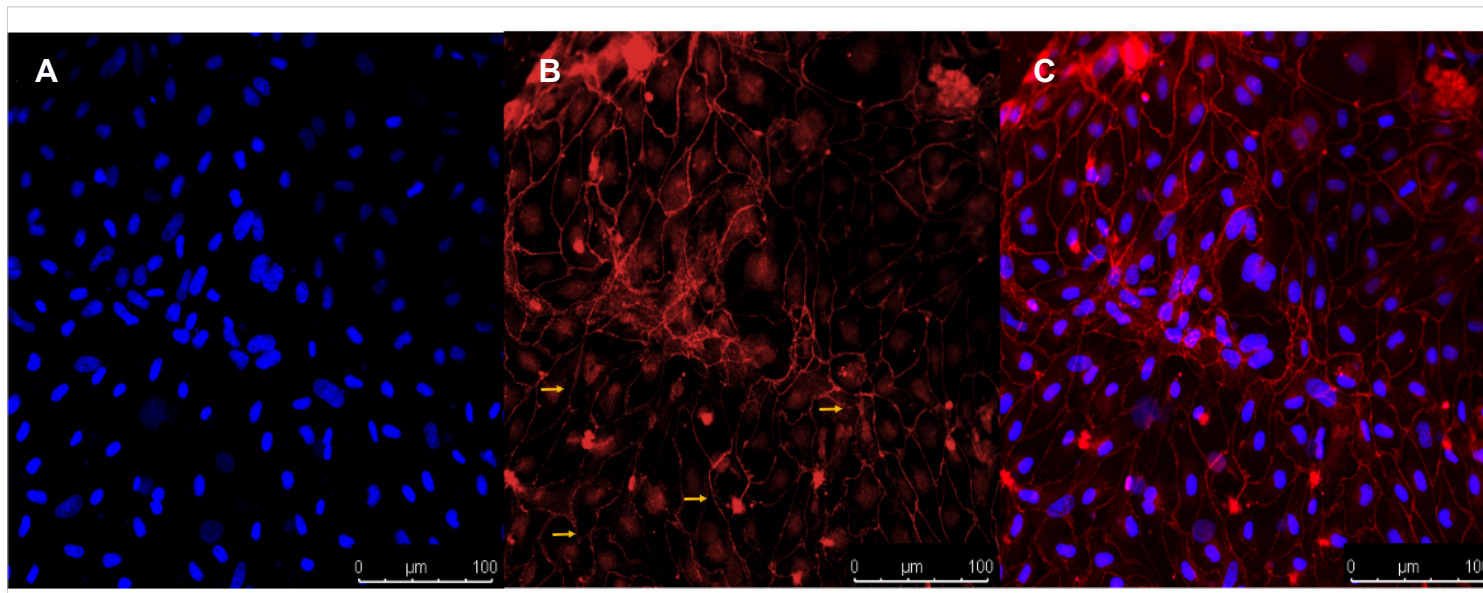


Figure 4.7 Immunocytochemistry images obtained following ZO-1 staining under static conditions in inserts

Immunocytochemistry images obtained following PBMEC staining for (A) DAPI, (B) ZO-1 and (C) merged. PBMECs were grown on permeable inserts under static media conditions. Images were taken using a Leica SP5 TCS II MP confocal microscope. The yellow arrows indicate disrupted tight junction.

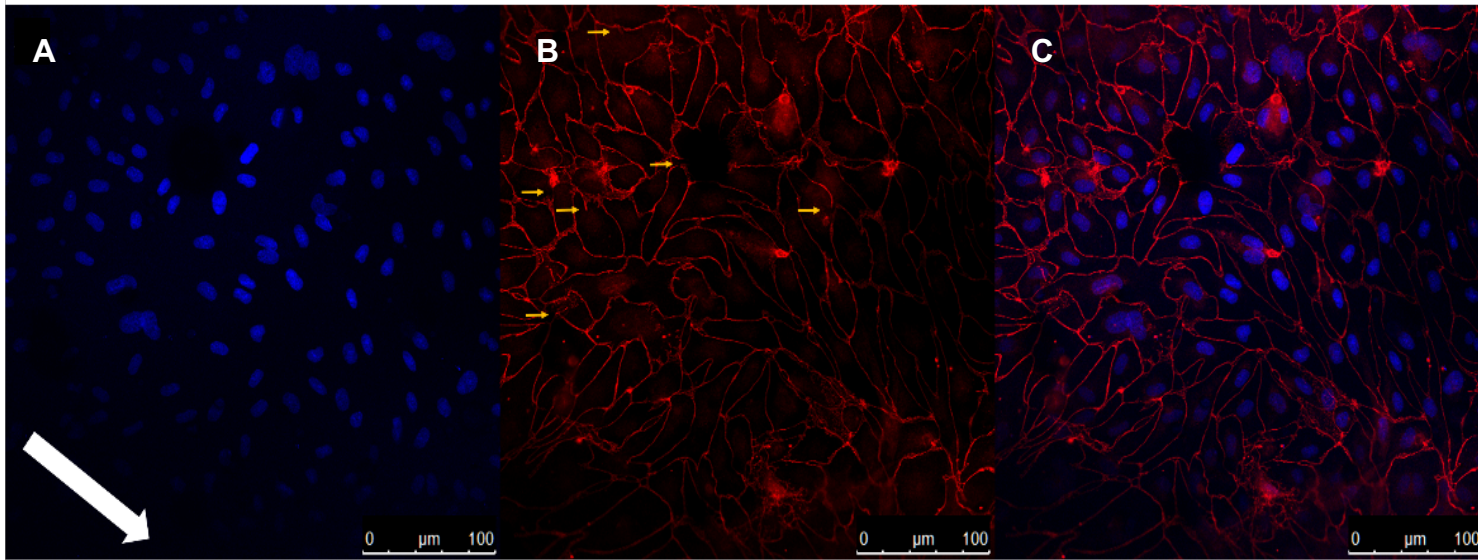


Figure 4.8 Immunocytochemistry images obtained following ZO-1 staining following exposure to high flow in inserts for 24 hours

Immunocytochemistry images obtained following PBMEC staining for (A) DAPI, (B) ZO-1 and (C) merged. PBMECs were grown on permeable inserts under high flow (550 $\mu\text{L}/\text{min}$) for 24 hours using the QV600. Images were taken using a Leica SP5 TCS II MP confocal microscope. The white arrow indicates the direction of flow; and the yellow arrows indicate disrupted tight junction.

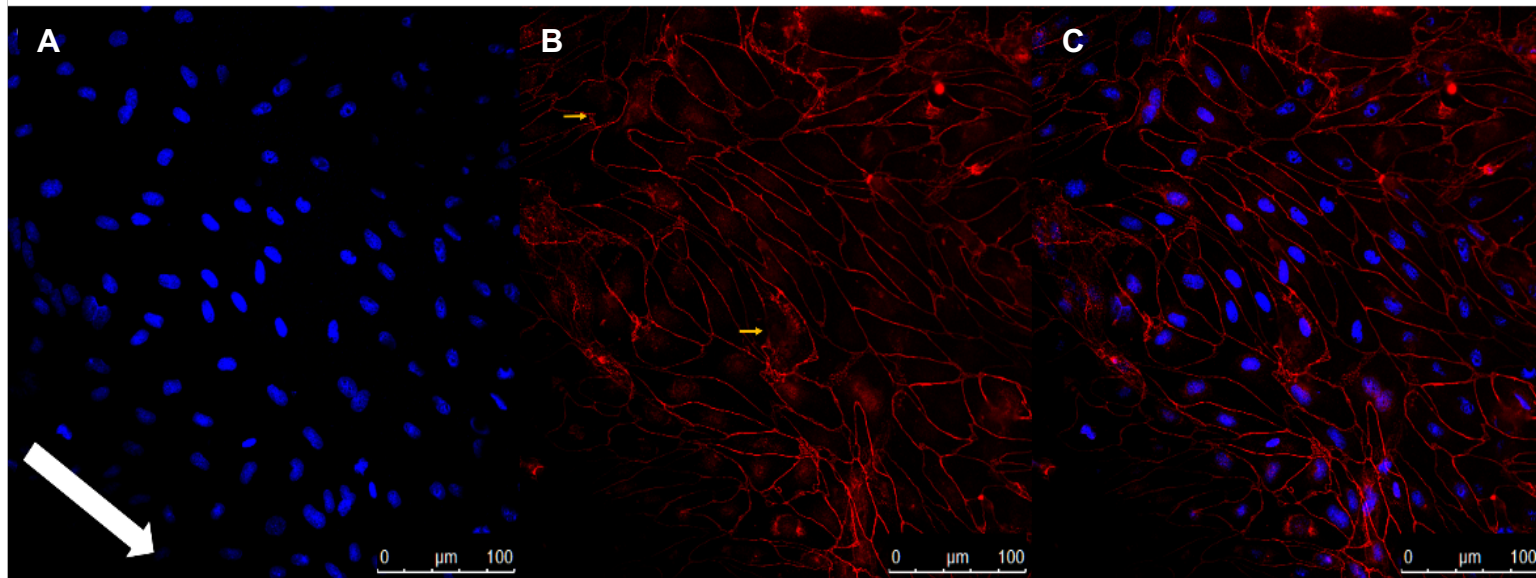


Figure 4.9 Immunocytochemistry images obtained following ZO-1 staining following exposure to high flow in inserts for 48 hours

Immunocytochemistry images obtained following PBMEC staining for (A) DAPI, (B) ZO-1 and (C) merged. . PBMECs were grown on permeable inserts under high flow (550 $\mu\text{L}/\text{min}$) for 48 hours using the QV600. Images were taken using a Leica SP5 TCS II MP confocal microscope. The white arrow indicates the direction of flow; and the yellow arrows indicate disrupted tight junction.

Furthermore, the ZO-1 junctional intensity was significantly higher following 48-hours exposure to flow (1.52 ± 0.11 fold) than in static control ($P \leq 0.05$). In addition, there was a statistically significant greater junctional intensity at 48-hours when compared to 24-hours exposure (1.12 ± 0.18 fold) ($P \leq 0.05$) (Figure 4.10).

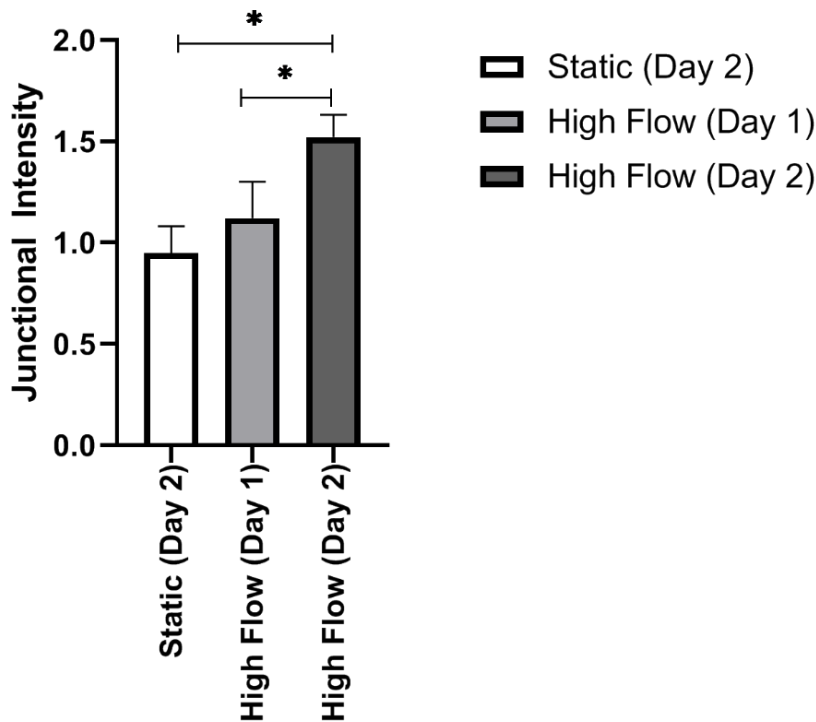


Figure 4.10 ZO-1 junctional fluorescence intensity

ZO-1 junctional fluorescence intensity as quantified by junctional regions and when normalised to static controls. * $P < 0.05$.

4.6.5 Mitoxantrone permeability across PBEMC BBB *in-vitro* model under static and dynamic conditions

To demonstrate the functional impact of dynamic media flow on BBB properties, the permeability of the anti-cancer agent mitoxantrone was assessed across PBMECs grown on permeable inserts, in the absence (Figure 4.11A) and presence of flow (Figure 4.11B).

When compared to static conditions, the impact of shear stress resulted in a significant increase in the cumulative amount transported in the BA direction (Figure 4.11B) when compared to the AB direction (Figure 4.11A). In the absence of flow, $P_{app AB}$ was $0.84 \times 10^{-6} \text{ cm/s} \pm 0.16 \times 10^{-6} \text{ cm/s}$ and $P_{app BA}$ was $1.35 \times 10^{-6} \text{ cm/s} \pm 0.23 \times 10^{-6} \text{ cm/s}$, resulting in an efflux ratio of 1.6.

However, under the exposure of flow, there was a significant increase in efflux ratio to 3.6 with a significantly reduced $P_{app AB}$ ($0.48 \times 10^{-6} \text{ cm/s} \pm 0.09 \times 10^{-6} \text{ cm/s}$) ($P \leq 0.01$) and significantly increased $P_{app BA}$ ($1.74 \times 10^{-6} \text{ cm/s} \pm 0.08 \times 10^{-6} \text{ cm/s}$) ($P \leq 0.05$), (Figure 4.11C).

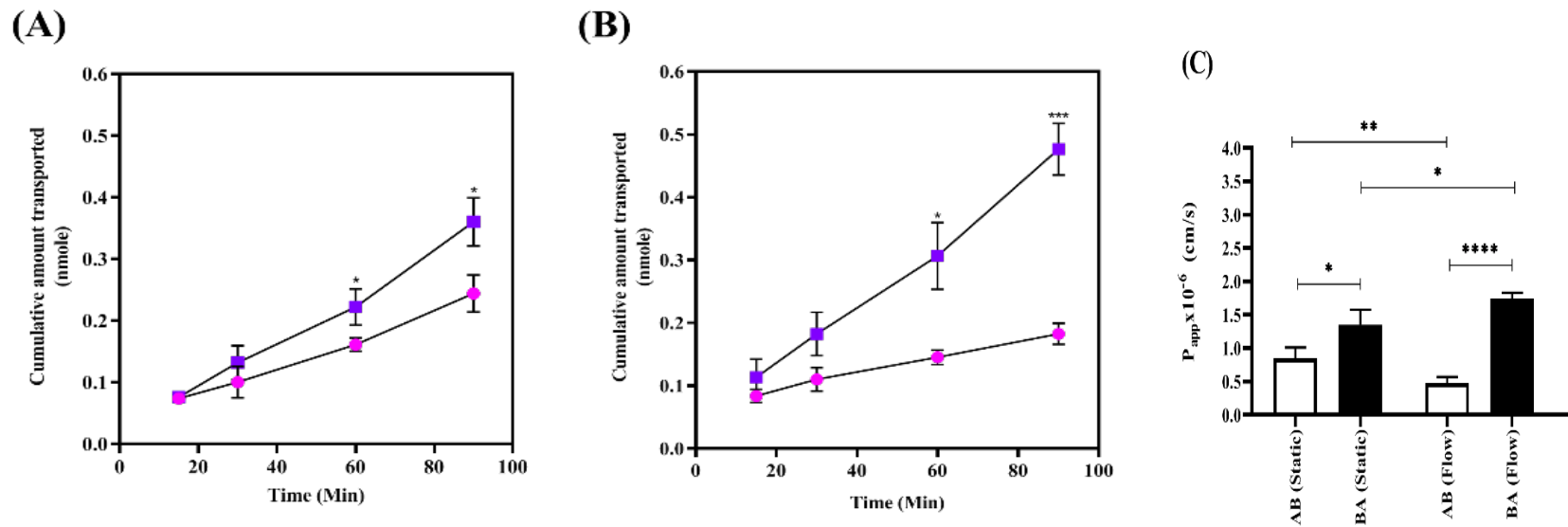


Figure 4.11 Mitoxantrone flux across PBMEC grown on permeable insets

Mitoxantrone transport in apical-to-basolateral (AB) (circles) or basolateral-to-apical (BA) (squares) under (A) static media or (B) when exposed to high flow (550 μ L/min) for 48 hours with associated apparent membrane permeability (P_{app}) values in the AB or BA directions (C). * $P \leq 0.05$, ** $P \leq 0.01$, *** $P \leq 0.001$ and **** $P \leq 0.0001$. $n = 16$ for static and dynamic, in 4 independent experiments

4.6.6 Hesperetin permeability across a PBEMC *in-vitro* BBB model, under static and dynamic conditions

To further confirm the ability of hesperetin to permeate across a physiologically relevant *in-vitro* BBB model, its permeability was assessed in the perfusion based PBMEC *in-vitro* model (Figure 4.12). When compared to static conditions, the impact of shear stress resulted in an increase in the cumulative amount transported in the BA direction (Figure 4.12B) when compared to the AB direction (Figure 4.12A). In the absence of flow, $P_{app\ AB}$ was $4.67 \times 10^{-6} \text{ cm/s} \pm 1 \times 10^{-7} \text{ cm/s}$ and $P_{app\ BA}$ was $7.19 \times 10^{-6} \text{ cm/s} \pm 2 \times 10^{-7} \text{ cm/s}$, which resulted in an efflux ratio of 1.53.

However, under the exposure of flow, there was a slight but insignificant increase in efflux ratio to 1.54 with increased $P_{app\ AB}$ of $4.89 \times 10^{-6} \text{ cm/s} \pm 1 \times 10^{-7} \text{ cm/s}$ and $P_{app\ BA}$ of $7.57 \times 10^{-6} \text{ cm/s} \pm 4 \times 10^{-7} \text{ cm/s}$ (Figure 4.12C) .

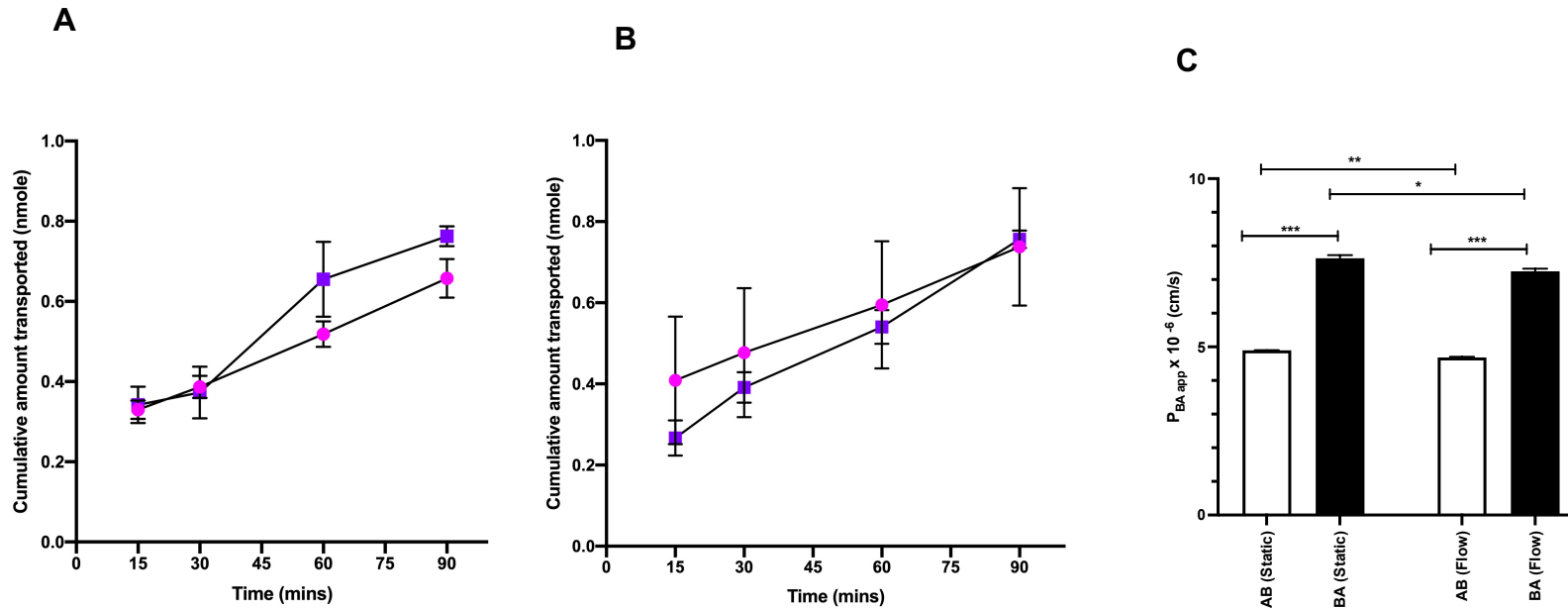


Figure 4.12 Hesperetin flux across PBMEC grown on permeable inserts

Hesperetin transport in apical-to-basolateral (AB) (circles) or basolateral-to-apical (BA) (squares) under (A) static media or (B) when exposed to high flow (550 µL/min) for 48 hours. with associated apparent membrane permeability (P_{app}) values in the AB or BA directions (C). n = 16 for static and dynamic, in 4 independent experiments. * $P \leq 0.05$, ** $P \leq 0.01$ and *** $P \leq 0.001$.

4.7 Discussion

The development and maintenance of an *in-vitro* BBB model is critical when assessing the potential for small molecule transport, with the ability to form a coherent and robust barrier being paramount. Critical to the establishment of models, is the maintenance of appropriate *in-vitro* culturing conditions.

A key component to the formation of the BBB *in-vivo*, is the presence of circumferential stress on the walls of the brain microvasculature, which plays an important role in the morphology and functional capacity of endothelial cells, along with governing signalling and transport processes within the neurovascular unit (Chien, 2007, Johnson et al., 2011, Conway and Schwartz, 2012, Krizanac-Bengez et al., 2004, Cucullo et al., 2011). The average shear stress within the arterial circulation is 4–30 dyne cm² and 1–4 dyne cm² in the venous circulation (Wong et al., 2013). BBB models which have incorporated laminar shear stress have demonstrated the lowest permeability to sucrose and mannitol tracers, highlighting the critical role that laminar shear plays in stimulating a stable BBB phenotype (Santaguida et al., 2006, Stanness et al., 1997).

Given the low TEER and complexity in culturing approaches, we adopted the use of a primary porcine brain microvascular endothelial cell culture system (PBMEC) reporting high TEER without the need for co-culture with astrocytes (Kaur and Badhan, 2017, Patabendige et al., 2013, Cantrill et al., 2012).

4.7.1 The effect of shear stress on the morphology and viability of PBMEC grown on coverslips

We first aimed to assess the impact of shear stress on PBMEC when grown on coverslips and evaluated both changes in cellular morphology along with cellular viability. The location of the coverslip within the QV600 chamber is critical when assessing the impact of shear stress on cellular viability, given that there is at least a 200 to 300-fold decrease in shear stress when approaching the base of the chamber (Mazzei et al., 2010). Furthermore, the use of permeable inserts to develop a BBB monolayer places the cell layer within the vicinity of the chamber inlet/outlet (Wilkinson, 2017). To this end, PBMEC were seeded on coverslips

and raised to the equivalent height of the filter membrane of the permeable inserts (Figure 4.1B), prior to exposure to low (275 $\mu\text{L}/\text{min}$) and high (550 $\mu\text{L}/\text{min}$) flow rates.

The impact of shear stress on PBMECs morphology was evident at both low and high flow rates, with significant reorientation under flow in addition to improved clarity of cell-to-cell tight junction formation (Figure 4.3 and 4.4) when compared to cells grown under static conditions (Figure 4.2).

Given that PBMEC have not been previously used within the QV system, the present study attempted to first identify an appropriate flow rate for use within PBMECs. Drawing on work conducted previously by Miranda-Azpiazu *et al.*, we selected a flow rate of 550 $\mu\text{L}/\text{min}$ to assess cellular viability. Miranda-Azpiazu *et al.* utilised a maximum flow rate of 300 $\mu\text{L}/\text{min}$ and suggested higher flow rates are sustainable for endothelial cells within the same perfusion-based system we used. Furthermore, the flow rates chosen were within the range suggested to ensure laminar flow within the perfusion system (Mazzei *et al.*, 2010). This would mimic the haemodynamic flow and forces within the broad linear regions of the endothelial structure as opposed to the branched regions where non-linear/disturbed flow would be more apparent (Chiu and Chien, 2011). Given that morphological alterations were evident under both low and high flow rates (Figure 4.3 and 4.4) we focussed upon the high flow rate (550 $\mu\text{L}/\text{min}$) for a comparison of cellular viability between static and dynamic conditions.

This higher flow rate did not adversely affect cellular viability, but rather resulted in a 28.2 % increase ($P = 0.031$) in viability when exposed for 4 days to high flow (Figure 4.5). The increase in viability reported herein was not to the same extent as those reported by Mazzei *et al.*, > 50% increase, who utilised astrocytes cultured on coverslips and exposed to flow within the QV500 system without raising the height of the coverslips to achieve more representative shear stress (Mazzei *et al.*, 2010).

4.7.2 The impact of shear stress on the development PBMEC *in-vitro* BBB characteristics

Having established that higher flow rates can sustain the growth of PBMEC within the QV600 system, we next assessed the impact of sheer stress on barrier formulation when PBEMC were grown on permeable inserts. A benefit of the PBMEC system is the reproducible nature of the high TEER small vessels isolated from fresh porcine hemispheres (Patabendige et al., 2013, Cantrill et al., 2012, Kaur and Badhan, 2017) which can reach in excess of $800 \Omega \cdot \text{cm}^2$ (in 1.1 cm^2 , 12-well permeable inserts).

In the absence of barrier forming additives, sheer stress resulted in a statistically significant ($P < 0.05$) increase in TEER throughout the study period of 7 days, when compared to inserts grown under static conditions (Figure 4.6A). A peak TEER of $35.7 \Omega \cdot \text{cm}^2 \pm 5.1 \Omega \cdot \text{cm}^2$ was determined when compared to that of static conditions, $21 \Omega \cdot \text{cm}^2 \pm 1.5 \Omega \cdot \text{cm}^2$ ($P \leq 0.001$) highlighting the positive impact sheer stress had on barrier formation, despite the absence of media supplementation.

With the addition of supplementation, we noted a 12.8-fold increase in peak TEER under shear stress when compared to its absence, with TEER under shear stress significantly higher from day 5 onwards (Figure 4.6B). The peak TEER under flow, $448.1 \Omega \cdot \text{cm}^2 \pm 11.3 \Omega \cdot \text{cm}^2$, is higher than those conducted in other cells lines (Daniels et al., 2013, Abbott, 2013, Lippmann et al., 2015). However, it should be noted that the QV600 accepts only 24-well multiplate inserts with a surface area of 0.33 cm^2 . PBMECs established in the previous chapter as well as by other groups typically utilise 12-well multiplate inserts (1.1 cm^2) (Cantrill et al., 2012, Patabendige et al., 2013).

In the QV600, the insert is used in such a way that the flow of media attempts to mimic human brain interstitial flow, reported to be $<500 \mu\text{L}/\text{min}$ in human brain (Faghieh and Sharp, 2018, Hladky and Barrand, 2014). The role of sheer stress under these conditions are difficult to conceptualise. However, it is known that shear stress can exert a mechanism strain and pressure effect on cells, impacting upon cell differentiation and growth (Gayer and Basson, 2009, Diresta et al.,

2005, Sun et al., 2013). With flow in the basolateral side of the membrane, the porous nature of the membrane would allow this pressure differential, which would enhance both the transfer of small molecules such as oxygen and CO₂ in addition to providing physical forces to the cell monolayer (Pörtner et al., 2005). This is critical as increased dissolved CO₂ concentrations (Kimura, 1996, Gray et al., 1996) can reduce the intracellular pH and thereby affect cell metabolism (Madhus, 1988), in addition to high levels of dissolved CO₂ reducing cellular growth rates (Pattison et al., 2000, Dezenogita et al., 1998).

Furthermore, the increase in TEER may also be a direct result of the rearrangement of cellular morphology of the cells, which is commonplace and the defining feature of laminar flow within the vascular network. For example, within atherosclerotic-prone regions of the endothelia, there is a strong correlation with the failure of endothelial cells to elongate and align (Davies et al., 1997, Davies, 2009, Nerem, 1981, Flaherty et al., 1972, Wang et al., 2013). A similar increase in TEER was noted by others when using the QV600 to develop an *in-vitro* pulmonary model cultured on permeable inserts (Chandorkar et al., 2017).

To examine morphological changes under flow, permeable inserts were subsequently assessed for the formation and localisation of tight junction protein marker ZO-1. Under static conditions, the localisation of ZO-1 was presented with a discontinuous pattern of formation (Figure 4.7). In the presence of shear stress, clear realignment of the cells was evident, with more pronounced TJ formation after 48-hours (Figure 4.9) rather than 24-hours (Figure 4.8) of exposure of shear stress. The fluorescent intensity of the junction protein expression was further assessed and demonstrated that 48 hours of exposure yielded statistically significant ($P \leq 0.05$) higher levels of ZO-1 when compared to static PBMEC (Figure 4.10). Further, the solidity of the tight junctions was greater at 48-hours compared to 24-hours when compared to static conditions ($P \leq 0.05$). Although the decrease in solidity at 24-hours, may be a result of realignment of junctional morphology (Figure 4.6). This increasing expression of tight junction markers has been previously demonstrated, albeit under higher shear stress in alternative hollow-system bioreactors (Cucullo et al., 2011, Garcia-Polite et al., 2017) and in QV500.

4.7.3 The impact of shear stress on small molecule transport

In the scope of developing a BBB, the use of permeable inserts allows for the monitoring of monolayer formation and small molecular transport. To assess the impact of shear stress on these processes, we assess the permeation of the anti-cancer agent mitoxantrone across PBMEC grown under static and shear stress-exposed inserts. mitoxantrone undergoes active transport partly through *ACBG2* and *ABCB1* (Ross et al., 1999, Morrow et al., 2006) and is classified as a low permeability compound (Volpe et al., 2008)

Under static conditions, the resultant apparent permeability in the BA direction, when compared to the AB direction, (i.e. the efflux ratio) was 1.6-fold greater and statistically significant ($P < 0.05$) suggesting an active efflux process (Figure 4.11A) However, in the presence of shear stress, this increased to 3.6-fold (Figure 4.11B) with a concomitant reduction in $P_{app, AB}$ suggesting a tighter barrier formation limiting mitoxantrone flux (Figure 4.11C).

To further assess the impact of shear stress on the permeability of molecules, we assessed the permeability of hesperetin in this system. The changes noted in the absence and presence of shear stress were small but significant. A 4.7% decrease (** $P \leq 0.01$) was recorded for A to B flux and 5.3% decrease (* $P \leq 0.05$) in B to A flux after exposure of the model to flow (Figure 4.12C).

The insignificant changes obtained when assessing permeability of hesperetin in static and dynamic models may be due to the fact that hesperetin is a high permeability compound, and static PBMEC *in-vitro* blood brain barrier model produces a restrictive model and hence there wasn't a significant change in flux or efflux. This further confirms the claim made in the previous chapter regarding the ability of hesperetin to permeate across the BBB since it was able to permeate across a more restrictive barrier formed as result of exposure to shear stress.

To summarise, in the present study we applied the PBMEC model system (Patabendige et al., 2013) within the Kirkstall QuasiVivo® (Mazzei et al., 2010) interconnected chambers system QV600 (Figure 1.13) which can accommodate both cells grown on coverslips (13 mm diameter) and permeable inserts (24-well

plate, 13 mm diameter) in an attempt to determine whether the impact of localised perfusion on PBMECs would enhance barrier formation, as measured by the TEER (Patabendige et al., 2013, Nakagawa et al., 2007, Nakagawa et al., 2009). The presence of hemodynamic shear stress is an important element within endothelial cells which is absent in cells cultured on inserts under static conditions and contributes to the polarisation of the brain endothelium structure as well as governing the expression and localisation of drug transporter systems (Björnmalm et al., 2016).

The QV600 chambers are connected in series or parallel, with perfusion within all chambers from a central perfusion pump (Figure 4.1A). The key advantage is the rapid perfusion of media and oxygen transport. Whilst the QuasiVivo® system has been used by other groups to assess the benefit of dynamic media flow within an interconnected system of chambers with different cell cultures (Miranda-Azpiazu et al., 2018) its use with BBB cell types grown on permeable inserts has been limited, particularly with high TEER primary origin cell lines.

Furthermore, whilst the use of human origin cells in microfluidic systems has gained traction, these remain a novel and niche research tool (Wang et al., 2017, Brown et al., 2015) which often fail to represent macroscale environments and make it difficult for research with established techniques, such as permeable insert barrier systems, to easily adopt such systems (Cucullo et al., 2011).

4.8 Conclusion

To conclude, for the first time we have demonstrated the impact of the novel application of sheer stress to an easy to isolate, cost-effective and highly reproducible TEER BBB model derived from porcine brain micro-vascular endothelial cells (PBMEC) when grown on routinely utilised permeable inserts culturing system. The use of this well-established culturing approach provides an ability to incorporate, with ease, BBB *in-vitro* models into the commercially available QuasiVivo® perfusion system platform without the necessary complications of other perfusion-based systems, such as microfluidic platforms.

Microfluidic systems have gained some traction but still remain a niche research tool for perfusion based cell culture systems, given that the vast majority of research groups working on barrier models are still using permeable-inserts such as Transwell® systems (Ohshima et al., 2019, Bayir et al., 2019, Zhao et al., 2019a, Puech et al., 2018, Oda et al., 2018) for assessment of the impact of perfusion on the functional activity of barrier due to commercial availability, high-throughput potential and ease of use. Several well documented challenges and limitations have been reported with micro-fluidics systems, for example the lack of standardised parameters and critical experiment factors such as: (i) the use of an appropriate shear stress; (ii) defining an appropriate TEER cut-off for monolayer formation, which are typically low ($<250 \Omega \cdot \text{cm}^2$) (Tang et al., 2018, Deosarkar et al., 2015) and (iii) appropriate application of paracellular permeability markers (Gastfriend et al., 2018, Helms et al., 2016, Musafargani et al., 2020).

These limitations make comparison to well established BBB models such as, permeable insert models challenging. Further, the well cited scalability issues and specialised microfluidics fabrication equipment severely limit the use and validation of such models across the wider scientific community (Musafargani et al., 2020) In comparison, the proposed model system we implemented is commercially available and well validated, utilising existing and well-established permeable insert systems for barrier formation. Further, using a simplistic PBMEC system from porcine hemispheres, we were able to demonstrate significantly higher TEER in traditional inserts in addition to enhanced TEER using a commercially available perfusion system, with the benefits of being reproducible and requiring little technical knowledge when compared to microfluidic systems.

The novelty herein is the fact that we have, for the first time, highlighted the application of the easy to isolate and cost-effective PBMEC BBB model within the QuasiVivo® system, which for the first time demonstrated a resultant impact on TEER and BBB phenotype enhancement. Further, we demonstrated higher TEER values in the absence or presence of perfusion, when compared to other microfluidic systems employing rodent or human derived BBB models, alongside

further demonstrated the functional consequence of shear stress on small-molecule transport. Our results highlight an apparent change in both cellular morphology and enhanced barrier formation, providing a valuable research tool to assess both the neurotoxicity of molecules at the BBB but also their permeability across widely utilised permeable insert-based BBB monolayer systems.

Chapter 5

Conclusions and future work

5.1 Conclusion

The overall aim of this work was to enhance permeability and drug delivery of anti-cancer agents into brain tumours by modulating the action of BCRP at the BBB and the BTB using phytochemical modulators, in addition to assessing the anti-cancer properties of phytochemicals as possible adjunct therapy with routinely used anti-cancer agents.

The theory behind the order of the work presented within this thesis was to commence from the tumour site and progress towards the BBB. This was based on previous studies conducted by our group demonstrating that some phytochemicals are permeable across the BBB. Our goal was to screen phytochemicals for their anti-cancer properties and their ability to modulate BCRP expressed in the GMB *in-vitro* cell culture model LN229 cells, before examining their permeability through the BBB and their ability to modulate BCRP in the BBB and hence enhance the permeability of BCRP substrate anti-cancer drugs.

In Chapter 2, a total of 13 modulators were assessed and screened, for the first time, for their cytotoxicity and ability to modulate the efflux function of BCRP, in addition to their ability to reduce LN229 cellular migration and their effects on the expression of BCRP in LN229 cells. Based on the results obtained, two candidates were selected for further investigation, namely hesperetin and baicalin. Further studies assessed their ability to activate apoptosis through ROS production and the activation of caspase pathways, with both methotrexate and temozolomide used as reference compounds.

Our findings highlighted that both hesperetin and baicalin were able to increase ROS production and activate caspase -3/7 in addition to their ability to modulate BCRP efflux function. Furthermore, we demonstrated the action of hesperetin in downregulating the expression of BCRP in LN229 cells.

Based on the findings we observed in the second chapter, we selected hesperetin for further testing using the primary PBMECs *in-vitro* BBB model. In Chapter 3,

we were able to develop an *in-vitro* BBB model using PBMECs. This model possessed BBB characteristics comparable to published studies and achieved comparable TEER values along with the presence of ZO-1 tight junction proteins and F-actin expression. We demonstrated, for the first time, the ability of hesperetin to permeate across the PBMEC BBB model in addition to the permeability of methotrexate and mitoxantrone. Further, the impact of hesperetin in modulating BCRP at the BBB was demonstrated by an increase in both methotrexate and mitoxantrone $P_{app\ AB}$ flux and reduced $P_{app\ BA}$ flux when studied in combination with hesperetin.

In order to provide more evidence on the ability of hesperetin to permeate across the BBB, in Chapter 4 we developed a more realistic perfusion based PBMEC *in-vitro* BBB model which was determined to be a more restrictive model, displaying better BBB characteristics when compared to BBB models grown in static conditions. The impact of shear stress on the PBMEC *in-vitro* BBB model was assessed where, the cells responded to the flow by rearranging and changing in morphology. In addition, higher TEER values were recorded, and ZO-1 was formed with fewer interruptions which indicates the formation of a more restrictive model. Next, we assessed the permeability of hesperetin and mitoxantrone across the perfusion-based model compared to a static counterpart. In these studies, hesperetin demonstrated higher permeabilities when compared to those reported under static conditions, however, the permeability of mitoxantrone was significantly reduced.

Limitations of this study were (I) using porcine cells instead of human cells to create a BBB model and (II) differences in transporter expression due to homologic differences between pigs and humans. This might become a hindrance when extrapolating the data obtained for human pharmacokinetics studies. That said, primary human brain cells are difficult to obtain and characterise, in addition, commercially available human cell lines express low TEER values ($<250\ \Omega\cdot\text{cm}^2$) and wouldn't have been suitable for small molecule drug transport studies. Moreover, similar to human brain endothelial cells, BCRP in PBMECs was reported to be the most abundant efflux transporter. (III) some of the anti-cancer compounds and phytochemicals that were used might interact

with other efflux transporters expressed in the cells that we utilised mainly P-gp. Nevertheless, in both PBMECs and LN229 cells, BCRP is more abundantly expressed than p-gp, therefore, the compounds used were likely to interact with BCRP over p-gp. However, in future studies using a P-gp modulator such as verapamil should be taken in consideration to ensure that any compounds used would only interact with BCRP. (IV) utilising a 2D cancer cell line. Using patient derived primary tumour cells in a 3D culture would have been a better representation of human *in-vitro* solid tumours. Still, using 2D cell lines remain a necessary preliminary step for screening of novel compounds before proceeding to using patient derived tumour cells and 3D culture as these more technically challenging and time consuming to optimise.

To summarise, this thesis has identified hesperetin as being a viable candidate phytochemical agent which possess both pro-oxidant properties towards LN229 human glioblastoma cells, in addition to being capable of inhibiting BCRP. It therefore represents a viable dual-purpose candidate for further studies to assess its impact on GBM *in-vivo* in conjunction with anti-cancer agents.

5.2 Future work

Whilst we examined some flavonoids, future work should examine other groups of flavonoids, more specifically phenolic acids and stilbenes for their modulatory effect on BCRP as well as P-gp and MRP-1 which were reported to be expressed in LN229 cells and their effect on cell migration and apoptosis. Further, evaluating the potential of using two or more flavonoids in combination, would allow for multiple avenues to explore such as the ability to modulate a range of drug transporter proteins and their resultant synergistic and/or antagonistic effects towards therapeutic interventions in oncology.

In Chapter 3, we explored the role of the ECM in enhancing barrier formation. This should further explore the impact and causes of bovine-specific ECM on *in-vitro* cell growth and characteristics. However, due to the commercial unavailability of medical grade porcine collagen, a method could be devised to extract porcine collagen from porcine skin, in a similar fashion to that routinely conducted for rat tail collagen, in order to better assess its effect on BBB model formation. Additionally, assessing the permeability of other flavonoids that displaying optimal anti-cancer properties and BCRP inhibitory effects in LN229 cells.

Moreover, throughout our cell culture models, we did not consider co-culturing with LN229 cells. Future work should examine combining an *in-vitro* glioblastoma model with the already established PBMEC BBB *in-vitro* model to examine the effect the tumour cells may have on the integrity of the BBB model, and to assess the resulting impact on drug permeability across both the BBB and BTB. Furthermore, applying shear stress to the *in-vitro* glioblastoma model alone and in combination with the established *in-vitro* BBB perfusion model would allow an opportunity to study the effect of the tumour formation and progression under an optimised extracellular environmental condition.

References

- ABACI, H. E., SHEN, Y.-I., TAN, S. & GERECHT, S. 2015. Recapitulating physiological and pathological shear stress and oxygen to model vasculature in health and disease. *Scientific Reports*, 4.
- ABBOTT, N. 2005. Dynamics of CNS barriers: evolution, differentiation, and modulation. *Cellular and molecular neurobiology*, 25.
- ABBOTT, N., RÖNNBÄCK, L. & HANSSON, E. 2006. Astrocyte-endothelial interactions at the blood-brain barrier. *Nature reviews. Neuroscience*, 7.
- ABBOTT, N. J. 2013. Blood–brain barrier structure and function and the challenges for CNS drug delivery. *Journal of Inherited Metabolic Disease*, 36, 437-449.
- ABBOTT, N. J., PATABENDIGE, A. A. K., DOLMAN, D. E. M., YUSOF, S. R. & BEGLEY, D. J. 2010. Structure and function of the blood–brain barrier. *Neurobiology of Disease*, 37, 13-25.
- ABBRUZZESE, C., MATTEONI, S., SIGNORE, M., CARDONE, L., NATH, K., GLICKSON, J. D. & PAGGI, M. G. 2017. Drug repurposing for the treatment of glioblastoma multiforme. *Journal of Experimental & Clinical Cancer Research*, 36.
- ABCAM. 2020. *Western blot membrane stripping for restaining protocol* | Abcam [Online]. Available: <https://www.abcam.com/protocols/western-blot-membrane-stripping-for-restaining-protocol> [Accessed].
- ABOTALEB, M., SAMUEL, S., VARGHESE, E., VARGHESE, S., KUBATKA, P., LISKOVA, A. & BÜSSELBERG, D. 2018. Flavonoids in Cancer and Apoptosis. *Cancers*, 11, 28.
- ACHROL, A., RENNERT, R., C, A., R, S., MS, A., L, N., S, P., ND, A., GR, H., PS, S. & SD, C. 2019. Brain metastases. *Nature reviews. Disease primers*, 5.
- AGARWAL, S., MITTAPALLI, R., DM, Z., JL, G., R, D., C, S., SA, D., KS, S., JL, P., JN, S., WF, E. & JR, O. 2012. Active efflux of Dasatinib from the brain limits efficacy against murine glioblastoma: broad implications for the clinical use of molecularly targeted agents. *Molecular cancer therapeutics*, 11.
- AGARWAL, S., SANE, R., GALLARDO, J. L., OHLFEST, J. R. & ELMQUIST, W. F. 2010. Distribution of Gefitinib to the Brain Is Limited by P-glycoprotein (ABCB1) and Breast Cancer Resistance Protein (ABCG2)-Mediated Active Efflux. *Journal of Pharmacology and Experimental Therapeutics*, 334, 147-155.
- AGGARWAL, V., TULI, H., THAKRAL, F., P, S., D, A., S, S., A, P., K, S., M, V., MA, K. & G, S. 2020. Molecular mechanisms of action of hesperidin in cancer: Recent trends and advancements. *Experimental biology and medicine (Maywood, N.J.)*, 245.
- AHMADI, A. & SHADBOORESTAN, A. 2016. Oxidative stress and cancer; the role of hesperidin, a citrus natural bioflavonoid, as a cancer chemoprotective agent. *Nutrition and cancer*, 68.
- AHMED-BELKACEM, A., MACALOU, S., BORRELLI, F., CAPASSO, R., FATTORUSSO, E., TAGLIALATELA-SCAFATI, O. & DI PIETRO, A. 2007. Nonprenylated rotenoids, a new class of potent breast cancer resistance protein inhibitors. *J Med Chem*, 50, 1933-8.

- AHMED-BELKACEM, A., POZZA, A., MUNOZ-MARTINEZ, F., BATES, S. E., CASTANYS, S., GAMARRO, F., DI PIETRO, A. & PEREZ-VICTORIA, J. M. 2005a. Flavonoid structure-activity studies identify 6-prenylchrysin and tectochrysin as potent and specific inhibitors of breast cancer resistance protein ABCG2. *Cancer Res*, 65, 4852-60.
- AHMED-BELKACEM, A., POZZA, A., MUÑOZ-MARTÍNEZ, F., SE, B., S, C., F, G., A, D. P. & JM, P.-V. 2005b. Flavonoid structure-activity studies identify 6-prenylchrysin and tectochrysin as potent and specific inhibitors of breast cancer resistance protein ABCG2. *Cancer Research*, 65, 4852-4860.
- AKAO, T., HANADA, M., SAKASHITA, Y., K, S., M, M. & T, I. 2007. Efflux of baicalin, a flavone glucuronide of Scutellariae Radix, on Caco-2 cells through multidrug resistance-associated protein 2. *The Journal of pharmacy and pharmacology*, 59.
- ALBERTS, B., JOHNSON, A. J. L., RAFF, M., ROBERTS, K. & WALTER, P. 2002. *Molecular Biology of the Cell*, Garland Science.
- ALSHATWI, A. R., E. PARIASAMY, V.S. SUBASH-BABU, P. 2012. *The apoptotic effect of hesperetin on human cervical cancer cells is mediated through cell cycle arrest, death receptor, and mitochondrial pathways - Alshatwi - 2013 - Fundamental & Clinical Pharmacology - Wiley Online Library*.
- ALVAREZ, A. I., REAL, R., PÉREZ, M., MENDOZA, G., PRIETO, J. G. & MERINO, G. 2010. Modulation of the activity of ABC transporters (P-glycoprotein, MRP2, BCRP) by flavonoids and drug response. *Journal of Pharmaceutical Sciences*, 99, 598-617.
- AMIN, M. L. 2013. P-glycoprotein Inhibition for Optimal Drug Delivery. *Drug Target Insights*, 7, DTI.S12519.
- AN, G. & MORRIS, M. E. 2010. Effects of Single and Multiple Flavonoids on BCRP-Mediated Accumulation, Cytotoxicity and Transport of Mitoxantrone In Vitro. *Pharmaceutical Research*, 27, 1296-1308.
- ANAND, P., SUNDARAM, C., JHURANI, S., AB, K. & BB, A. 2008. Curcumin and cancer: an "old-age" disease with an "age-old" solution. *Cancer letters*, 267.
- ANDO, J. & YAMAMOTO, K. 2009. Vascular Mechanobiology. *Circulation Journal*, 73, 1983-1992.
- ANFUSO, C., MOTTA, C., G, G., V, A., M, A. & G, L. 2014. Endothelial PKC α -MAPK/ERK-phospholipase A2 pathway activation as a response of glioma in a triple culture model. A new role for pericytes? *Biochimie*, 99.
- ANTOINE, E. E., VLACHOS, P. P. & RYLANDER, M. N. 2014. Review of Collagen I Hydrogels for Bioengineered Tissue Microenvironments: Characterization of Mechanics, Structure, and Transport. *Tissue Engineering Part B: Reviews*, 20, 683-696.
- ARANGANATHAN, S. & NALINI, N. 2013. Antiproliferative efficacy of hesperetin (citrus flavanoid) in 1,2-dimethylhydrazine-induced colon cancer. *Phytotherapy Research : PTR*, 27, 999-1005.
- ARMULIK, A., GENOVÉ, G., .MÄE, M., NISANCIOGLU, M., E, W., C, N., L, H., J, N., P, L., K, S., BR, J. & C, B. 2010. Pericytes regulate the blood-brain barrier. *Nature*, 468.
- ARONICA, E., GORTER, J., S, R., EA, V. V., M, R., GL, S., RJ, S., P, V. D. V., S, L., JC, B., WG, S. & D, T. 2005. Localization of breast cancer

- resistance protein (BCRP) in microvessel endothelium of human control and epileptic brain. *Epilepsia*, 46.
- ARVANITIS, C., FERRARO, G. & JAIN, R. 2020a. The blood-brain barrier and blood-tumour barrier in brain tumours and metastases. *Nature reviews. Cancer*, 20.
- ARVANITIS, C. D., FERRARO, G. B. & JAIN, R. K. 2020b. The blood–brain barrier and blood–tumour barrier in brain tumours and metastases. *Nature Reviews Cancer*, 20, 26-41.
- ARYA, A., KHANDELWAL, K., SINGH, A., AHMAD, H., AGRAWAL, S., KHATIK, R., MITTAPELLY, N. & DWIVEDI, A. K. 2015. Validation of RP-HPLC Method for Simultaneous Quantification of Bicalutamide and Hesperetin in Polycaprolactone-Bicalutamide-Hesperetin-Chitosan Nanoparticles. *Journal of Chromatographic Science*, 53, 1485-1490.
- ASAI, A., MIYAGI, Y., A, S., M, G., SH, H., S, T., K, N., M, M., K, T. & Y, K. 1994. Negative effects of wild-type p53 and s-Myc on cellular growth and tumorigenicity of glioma cells. Implication of the tumor suppressor genes for gene therapy. *Journal of neuro-oncology*, 19.
- AURAND, E., LAMPE, K. & KB, B. 2012. Defining and designing polymers and hydrogels for neural tissue engineering. *Neuroscience research*, 72.
- AUSTIN DOYLE, L. & ROSS, D. D. 2003. Multidrug resistance mediated by the breast cancer resistance protein BCRP (ABCG2). *Oncogene*, 22, 7340-7358.
- AWAD, H., BOERSMA, M., S, B., PJ, V. B., J, V. & IM, R. 2002. The regioselectivity of glutathione adduct formation with flavonoid quinone/quinone methides is pH-dependent. *Chemical research in toxicology*, 15.
- AZIMI, T., LOIZIDOU, M. & DWEK, M. V. 2020. Cancer cells grown in 3D under fluid flow exhibit an aggressive phenotype and reduced responsiveness to the anti-cancer treatment doxorubicin. *Scientific Reports*, 10.
- AZZARITI, A., PORCELLI, L., GM, S., AE, Q., NA, C., F, B., R, P., M, Z., M, D. I., JM, X. & A, P. 2010. Tyrosine kinase inhibitors and multidrug resistance proteins: interactions and biological consequences. *Cancer chemotherapy and pharmacology*, 65.
- BACAC, M. & STAMENKOVIC, I. 2008. Metastatic cancer cell. *Annual review of pathology*, 3.
- BAGCHI, S., CHHIBBER, T., LAHOOTI, B., VERMA, A., BORSE, V. & JAYANT, R. D. 2019. <p>In-vitro blood-brain barrier models for drug screening and permeation studies: an overview</p>. *Drug Design, Development and Therapy*, Volume 13, 3591-3605.
- BALAGURU, U. M., SUNDARESAN, L., MANIVANNAN, J., MAJUNATHAN, R., MANI, K., SWAMINATHAN, A., VENKATESAN, S., KASIVISWANATHAN, D. & CHATTERJEE, S. 2016. Disturbed flow mediated modulation of shear forces on endothelial plane: A proposed model for studying endothelium around atherosclerotic plaques. *Scientific Reports*, 6, 27304.
- BALÇA-SILVA, J., MATIAS, D., AD, C., AB, S.-R., MC, L. & V, M.-N. 2019. Cellular and molecular mechanisms of glioblastoma malignancy: Implications in resistance and therapeutic strategies. *Seminars in cancer biology*, 58.

- BALÇA-SILVA, J., MATIAS, D., DO CARMO, A., DUBOIS, L. G., GONÇALVES, A. C., GIRÃO, H., SILVA CANEDO, N. H., CORREIA, A. H., DE SOUZA, J. M., SARMENTO-RIBEIRO, A. B., LOPES, M. C. & MOURA-NETO, V. 2017. Glioblastoma entities express subtle differences in molecular composition and response to treatment. *Oncology Reports*, 38, 1341-1352.
- BANERJEE, S. & BHAT, M. 2007. Neuron-Glial Interactions in Blood-Brain Barrier Formation. <http://dx.doi.org/10.1146/annurev.neuro.30.051606.094345>.
- BANIK, N., RAY, S. & LAJTHA, A. 2010. *Handbook of Neurochemistry and Molecular Neurobiology | ABEL LAJTHA | Springer*.
- BANJERDPONGCHAI, R., WUDTIWAI, B., KHAW-ON, P., RACHAKHOM, W., DUANGNIL, N. & KONGTAWELERT, P. 2016. Hesperidin from Citrus seed induces human hepatocellular carcinoma HepG2 cell apoptosis via both mitochondrial and death receptor pathways. *Tumor Biology*, 37, 227-237.
- BANKS, W. 2016. From blood-brain barrier to blood-brain interface: new opportunities for CNS drug delivery. *Nature reviews. Drug discovery*, 15.
- BATES, S. E., BAKKE, S., KANG, M., ROBEY, R. W., ZHAI, S., THAMBI, P., CHEN, C. C., PATIL, S., SMITH, T., STEINBERG, S. M., MERINO, M., GOLDSPIEL, B., MEADOWS, B., STEIN, W. D., CHOYKE, P., BALIS, F., FIGG, W. D. & FOJO, T. 2004. A phase I/II study of infusional vinblastine with the P-glycoprotein antagonist valspodar (PSC 833) in renal cell carcinoma. *Clinical Cancer Research: An Official Journal of the American Association for Cancer Research*, 10, 4724-4733.
- BAUER, B., YANG, X., HARTZ, A. M., OLSON, E. R., ZHAO, R., KALVASS, J. C., POLLACK, G. M. & MILLER, D. S. 2006. In vivo activation of human pregnane X receptor tightens the blood-brain barrier to methadone through P-glycoprotein up-regulation. *Mol Pharmacol*, 70, 1212-9.
- BAYIR, E., CELTIKOGLU, M. & SENDEMIR, A. 2019. The use of bacterial cellulose as a basement membrane improves the plausibility of the static in vitro blood-brain barrier model. *International journal of biological macromolecules*, 126.
- BAYRAKÇEKEN, F., AKTAŞ, S., TOPTAN, M. & ÜNLÜGEDİK, A. 2003. High resolution electronic absorption spectra of anisole and phenoxy radical. *Spectrochimica Acta Part A: Molecular and Biomolecular Spectroscopy*, 59, 135-138.
- BEAUCHESNE, P. 2010. Intrathecal chemotherapy for treatment of leptomeningeal dissemination of metastatic tumours. *The Lancet. Oncology*, 11.
- BEHIN, A., HOANG-XUAN, K., CARPENTIER, A. F. & DELATTRE, J.-Y. 2003. Primary brain tumours in adults. *The Lancet*, 361, 323-331.
- BENDA, P., LIGHTBODY, J., G, S., L, L. & W, S. 1968. Differentiated rat glial cell strain in tissue culture. *Science (New York, N.Y.)*, 161.
- BENSON, K., CRAMER, S. & GALLA, H.-J. 2013. Impedance-based cell monitoring: barrier properties and beyond. *Fluids and Barriers of the CNS*, 10, 5.
- BERTOUT, J. A., PATEL, S. A. & SIMON, M. C. 2008. The impact of O₂ availability on human cancer. *Nature reviews. Cancer*, 8, 967-975.

- BHARDWAJ, V., TADINADA, S., JAIN, A., V, S., CK, D., JC, L. & A, B. 2014. Biochanin A reduces pancreatic cancer survival and progression. *Anti-cancer drugs*, 25.
- BHATIA, P. 2013. *Identification and Characterization of Transporters in Human Gliomas*. Phd, university of sunderland.
- BHATIA, P., BERNIER, M., SANGHVI, M., MOADDEL, R., SCHWARTING, R., RAMAMOORTHY, A. & WAINER, I. W. 2012. Breast cancer resistance protein (BCRP/ABCG2) localises to the nucleus in glioblastoma multiforme cells. *Xenobiotica*, 42, 748-755.
- BI, W. L. & BEROUKHIM, R. 2014. Beating the odds: extreme long-term survival with glioblastoma. *Neuro-Oncology*, 16, 1159-1160.
- BIEMANS, E. A. L. M., JÄKEL, L., DE WAAL, R. M. W., KUIPERIJ, H. B. & VERBEEK, M. M. 2017. Limitations of the hCMEC/D3 cell line as a model for A β clearance by the human blood-brain barrier. *Journal of Neuroscience Research*, 95, 1513-1522.
- BJÖRNMALM, M., FARIA, M., CHEN, X., CUI, J. & CARUSO, F. 2016. Dynamic Flow Impacts Cell-Particle Interactions: Sedimentation and Particle Shape Effects. *Langmuir*, 32, 10995-11001.
- BLAKELEY, J. O., OLSON, J., GROSSMAN, S. A., HE, X., WEINGART, J. & SUPKO, J. G. 2009. Effect of blood brain barrier permeability in recurrent high grade gliomas on the intratumoral pharmacokinetics of methotrexate: a microdialysis study. *Journal of Neuro-Oncology*, 91, 51-58.
- BLEAU, A., HAMBARDZUMYAN, D., OZAWA, T., EI, F., JT, H., CW, B. & EC, H. 2009. PTEN/PI3K/Akt pathway regulates the side population phenotype and ABCG2 activity in glioma tumor stem-like cells. *Cell stem cell*, 4.
- BLOKHINA, O., VIROLAINEN, E. & FAGERSTEDT, K. V. 2003. Antioxidants, oxidative damage and oxygen deprivation stress: a review. *Ann Bot*, 91 Spec No, 179-94.
- BOCK, K., ECKLE, T., M, O. & S, F.-G. 2000. Coordinate induction by antioxidants of UDP-glucuronosyltransferase UGT1A6 and the apical conjugate export pump MRP2 (multidrug resistance protein 2) in Caco-2 cells. *Biochemical pharmacology*, 59.
- BOOTH, R. & KIM, H. 2012. Characterization of a microfluidic in vitro model of the blood-brain barrier (μ BBB). *Lab on a chip*, 12.
- BOUMENDJEL, A., BOIS, F., C, B., AM, M., G, C. & A, D. P. 2001. B-ring substituted 5,7-dihydroxyflavonols with high-affinity binding to P-glycoprotein responsible for cell multidrug resistance. *Bioorganic & medicinal chemistry letters*, 11.
- BOWMAN, P. D., BETZ, A. L., AR, D., WOLINSKY, J. S., PENNEY, J. B., SHIVERS, R. R. & GOLDSTEIN, G. W. 1981. Primary culture of capillary endothelium from rat brain. *In Vitro*, 17, 353-362.
- BRAGANHOL, E., ZAMIN, L. L., CANEDO, A. D., HORN, F., TAMAJUSUKU, A. S. K., WINK, M. R., SALBEGO, C. & BATTASTINI, A. M. O. 2006. Antiproliferative effect of quercetin in the human U138MG glioma cell line. *Anti-Cancer Drugs*, 17, 663-671.
- BRAND, W., OOSTERHUIS, B., KRAJCSI, P., BARRON, D., DIONISI, F., BLADEREN, P. J., RIETJENS, I. M. C. M. & WILLIAMSON, G. 2011. Interaction of hesperetin glucuronide conjugates with human BCRP,

- MRP2 and MRP3 as detected in membrane vesicles of overexpressing baculovirus-infected Sf9 cells. *Biopharmaceutics & Drug Disposition*, 32, 530-535.
- BRAZIL, R. 2017. A barrier to progress: getting drugs to the brain.
- BREEDVELD, P., BEIJNEN, J. H. & SCHELLENS, J. H. M. 2006. Use of P-glycoprotein and BCRP inhibitors to improve oral bioavailability and CNS penetration of anticancer drugs. *Trends in Pharmacological Sciences*, 27, 17-24.
- BREEDVELD, P., PLUIM, D., G, C., P, W., O, V. T., AH, S. & JH, S. 2005. The effect of Bcrp1 (Abcg2) on the in vivo pharmacokinetics and brain penetration of imatinib mesylate (Gleevec): implications for the use of breast cancer resistance protein and P-glycoprotein inhibitors to enable the brain penetration of imatinib in patients. *Cancer research*, 65.
- BREEDVELD, P., ZELCER, N., PLUIM, D., SÖNMEZER, Ö., TIBBEN, M. M., BEIJNEN, J. H., SCHINKEL, A. H., VAN TELLINGEN, O., BORST, P. & SCHELLENS, J. H. M. 2004. Mechanism of the Pharmacokinetic Interaction between Methotrexate and Benzimidazoles. *Cancer Research*, 64, 5804-5811.
- BREGY, A., SHAH, A., MV, D., HE, P., PL, A., D, D. & RJ, K. 2013. The role of Gliadel wafers in the treatment of high-grade gliomas. *Expert review of anticancer therapy*, 13.
- BRONGER, H., KÖNIG, J., KOPFLOW, K., STEINER, H.-H., AHMADI, R., HEROLD-MENDE, C., KEPPLER, D. & NIES, A. T. 2005. ABCG2 Drug Efflux Pumps and Organic Anion Uptake Transporters in Human Gliomas and the Blood-Tumor Barrier. *Cancer Research*, 65, 11419-11428.
- BROWN, J. A., PENSABENE, V., MARKOV, D. A., ALLWARDT, V., NEELY, M. D., SHI, M., BRITT, C. M., HOILETT, O. S., YANG, Q., BREWER, B. M., SAMSON, P. C., MCCAWLEY, L. J., MAY, J. M., WEBB, D. J., LI, D., BOWMAN, A. B., REISERER, R. S. & WIKSWO, J. P. 2015. Recreating blood-brain barrier physiology and structure on chip: A novel neurovascular microfluidic bioreactor. *Biomicrofluidics*, 9, 054124.
- BUDANOV, A. 2014. The role of tumor suppressor p53 in the antioxidant defense and metabolism. *Sub-cellular biochemistry*, 85.
- BURDA, S. & OLESZEK, W. 2001. Antioxidant and antiradical activities of flavonoids. *Journal of agricultural and food chemistry*, 49.
- BURGER, H., FOEKENS, J., MP, L., ME, M.-V. G., JG, K., EA, W., G, S. & K, N. 2003. RNA expression of breast cancer resistance protein, lung resistance-related protein, multidrug resistance-associated proteins 1 and 2, and multidrug resistance gene 1 in breast cancer: correlation with chemotherapeutic response. *Clinical cancer research : an official journal of the American Association for Cancer Research*, 9.
- CAETANO-PINTO, P., JAMALPOOR, A., HAM, J., GOUMENOU, A., MOMMERSTEEG, M., PIJNENBURG, D., RUIJTENBEEK, R., SANCHEZ-ROMERO, N., VAN ZELST, B., HEIL, S. G., JANSEN, J., WILMER, M. J., VAN HERPEN, C. M. L. & MASEREEUW, R. 2017. Cetuximab Prevents Methotrexate-Induced Cytotoxicity in Vitro through Epidermal Growth Factor Dependent Regulation of Renal Drug Transporters. *Molecular Pharmaceutics*, 14, 2147-2157.

- CAI, W., ZHANG, B., DUAN, D., WU, J. & FANG, J. 2012. Curcumin targeting the thioredoxin system elevates oxidative stress in HeLa cells. *Toxicology and applied pharmacology*, 262.
- CAMARGO, C., GOMES-MARCONDES, M., WUTZKI, N. & H, A. 2012. Naringin inhibits tumor growth and reduces interleukin-6 and tumor necrosis factor α levels in rats with Walker 256 carcinosarcoma. *Anticancer research*, 32.
- CANDOLFI, M., CURTIN, J., WS, N., AG, M., GD, K., GE, P., EA, M., JR, O., AB, F., PF, M., J, L., PR, L. & MG, C. 2007. Intracranial glioblastoma models in preclinical neuro-oncology: neuropathological characterization and tumor progression. *Journal of neuro-oncology*, 85.
- CANO, C. E., GOMMEAUX, J., PIETRI, S., CULCASI, M., GARCIA, S., SEUX, M., BARELIER, S., VASSEUR, S., SPOTO, R. P., PÉBUSQUE, M.-J., DUSETTI, N. J., IOVANNA, J. L. & CARRIER, A. 2009. Tumor protein 53-induced nuclear protein 1 is a major mediator of p53 antioxidant function. *Cancer Research*, 69, 219-226.
- CANTRILL, C. A., SKINNER, R. A., ROTHWELL, N. J. & PENNY, J. I. 2012. An immortalised astrocyte cell line maintains the in vivo phenotype of a primary porcine in vitro blood–brain barrier model. *Brain Research*, 1479, 17-30.
- CAO, G., SOFIC, E. & PRIOR, R. L. 1997. Antioxidant and prooxidant behavior of flavonoids: structure-activity relationships. *Free Radical Biology & Medicine*, 22, 749-760.
- CAO, J., LIU, Y., JIA, L., JIANG, L., GENG, C., XF, Y., Y, K., BN, J. & LF, Z. 2008. Curcumin attenuates acrylamide-induced cytotoxicity and genotoxicity in HepG2 cells by ROS scavenging. *Journal of agricultural and food chemistry*, 56.
- CAPARICA, R., JÚLIO, A., ARAÚJO, M. E. M., BABY, A. R., FONTE, P., COSTA, J. G. & SANTOS DE ALMEIDA, T. 2020. Anticancer Activity of Rutin and Its Combination with Ionic Liquids on Renal Cells. *Biomolecules*, 10, 233.
- CAPPA, M., BIZZARRI, C., VOLLONO, C., A, P. & S, B. 2011. Adrenoleukodystrophy. *Endocrine development*, 20.
- CAREY, S., KRANING-RUSH, C., RM, W. & CA, R.-K. 2012. Biophysical control of invasive tumor cell behavior by extracellular matrix microarchitecture. *Biomaterials*, 33.
- CARMELIET, P. & JAIN, R. K. 2011. Molecular mechanisms and clinical applications of angiogenesis. *Nature*, 473, 298-307.
- CHAFFER, C. & WEINBERG, R. 2011. A perspective on cancer cell metastasis. *Science (New York, N.Y.)*, 331.
- CHAMBERS, A., GROOM, A. & IC, M. 2002. Dissemination and growth of cancer cells in metastatic sites. *Nature reviews. Cancer*, 2.
- CHAN, T., GALATI, G. & PJ, O. B. 1999. Oxygen activation during peroxidase catalysed metabolism of flavones or flavanones. *Chemico-biological interactions*, 122.
- CHANDORKAR, P., POSCH, W., ZADERER, V., BLATZER, M., STEGER, M., AMMANN, C. G., BINDER, U., HERMANN, M., HÖRTNAGL, P., LASS-FLÖRL, C. & WILFLINGSIEDER, D. 2017. Fast-track development of an in vitro 3D lung/immune cell model to study Aspergillus infections. *Scientific Reports*, 7.

- CHANG, H.-L., CHANG, Y.-M., LAI, S.-C., CHEN, K.-M., WANG, K.-C., CHIU, T.-T., CHANG, F.-H. & HSU, L.-S. 2017. Naringenin inhibits migration of lung cancer cells via the inhibition of matrix metalloproteinases-2 and -9. *Experimental and Therapeutic Medicine*, 13, 739-744.
- CHEN 2009. Curcumin induces apoptosis in human lung adenocarcinoma A549 cells through a reactive oxygen species-dependent mitochondrial signaling pathway. *Oncology Reports*, 23.
- CHEN, H., MIAO, Q., GENG, M., LIU, J., HU, Y., TIAN, L., PAN, J. & YANG, Y. 2013. Anti-Tumor Effect of Rutin on Human Neuroblastoma Cell Lines through Inducing G2/M Cell Cycle Arrest and Promoting Apoptosis. *The Scientific World Journal*, 2013, 1-8.
- CHEN, J., KANG, J., DA, W. & OU, Y. 2004. Combination with water-soluble antioxidants increases the anticancer activity of quercetin in human leukemia cells. *Die Pharmazie*, 59.
- CHEN, Q. & LESNEFSKY, E. J. 2011. Blockade of electron transport during ischemia preserves bcl-2 and inhibits opening of the mitochondrial permeability transition pore. *FEBS Letters*, 585, 921-926.
- CHEN, S., RUAN, Q., BEDNER, E., DEPTALA, A., WANG, X., HSIEH, T. C., TRAGANOS, F. & DARZYNKIEWICZ, Z. 2001. Effects of the flavonoid baicalin and its metabolite baicalein on androgen receptor expression, cell cycle progression and apoptosis of prostate cancer cell lines. *Cell Proliferation*, 34, 293-304.
- CHEN, Y., MICKLEY, L., AM, S., EM, A., JL, H. & AT, F. 1990. Characterization of adriamycin-resistant human breast cancer cells which display overexpression of a novel resistance-related membrane protein. *The Journal of biological chemistry*, 265.
- CHEN, Z., ROBEY, R., BELINSKY, M., I, S., XQ, R., Y, S., DD, R., SE, B. & GD, K. 2003. Transport of methotrexate, methotrexate polyglutamates, and 17beta-estradiol 17-(beta-D-glucuronide) by ABCG2: effects of acquired mutations at R482 on methotrexate transport. *Cancer research*, 63.
- CHENG, L., HUANG, Z., W, Z., Q, W., S, D., JK, L., X, F., AE, S., Y, M., JD, L., W, M., RE, M., JN, R. & S, B. 2013. Glioblastoma stem cells generate vascular pericytes to support vessel function and tumor growth. *Cell*, 153.
- CHIANG, J. 2013. Bile acid metabolism and signaling. *Comprehensive Physiology*, 3.
- CHICOINE, M. & SILBERGELD, D. 1995. Invading C6 glioma cells maintaining tumorigenicity. *Journal of Neurosurgery*, 83.
- CHIEN, S. 2006. Molecular basis of rheological modulation of endothelial functions: importance of stress direction. *Biorheology*, 43.
- CHIEN, S. 2007. Mechanotransduction and endothelial cell homeostasis: the wisdom of the cell. *American Journal of Physiology-Heart and Circulatory Physiology*, 292, H1209-H1224.
- CHIU, J.-J. & CHIEN, S. 2011. Effects of Disturbed Flow on Vascular Endothelium: Pathophysiological Basis and Clinical Perspectives. *Physiological Reviews*, 91, 327-387.
- CHOBOT, V. & HADACEK, F. 2011. Exploration of pro-oxidant and antioxidant activities of the flavonoid myricetin. *Redox Report*, 16, 242-247.

- CHOI, E. 2007. Hesperetin induced G1-phase cell cycle arrest in human breast cancer MCF-7 cells: involvement of CDK4 and p21. *Nutrition and cancer*, 59.
- CHOU, Y., KHUON, S., H, H. & RD, G. 2003. Nestin promotes the phosphorylation-dependent disassembly of vimentin intermediate filaments during mitosis. *Molecular biology of the cell*, 14.
- CHOWDHARY, S., RYKEN, T. & HB, N. 2015. Survival outcomes and safety of carmustine wafers in the treatment of high-grade gliomas: a meta-analysis. *Journal of neuro-oncology*, 122.
- CHUA, C., ZAIDEN, N., KH, C., SJ, S., MC, W., BT, A. & C, T. 2008. Characterization of a side population of astrocytoma cells in response to temozolomide. *Journal of neurosurgery*, 109.
- CHUNG, F., SANTIAGO, J., MF, J., CV, T. & MF, S. 2016. Disrupting P-glycoprotein function in clinical settings: what can we learn from the fundamental aspects of this transporter? *American journal of cancer research*, 6.
- CISTERNINO, S., MERCIER, C., F, B., F, R. & JM, S. 2004. Expression, up-regulation, and transport activity of the multidrug-resistance protein Abcg2 at the mouse blood-brain barrier. *Cancer research*, 64.
- CLAY, A. S., F. 2013. Lipid bilayer properties control membrane partitioning, binding, and transport of p-glycoprotein substrates. *Biochemistry*, 52.
- COHEN, G. M. 1997. Caspases: the executioners of apoptosis. *Biochemical Journal*, 326, 1-16.
- COHEN, N. & WELLER, R. 2007. *WHO Classification of Tumours of the Central Nervous System*.
- COHEN, T. & PRINCE, A. 2012. Cystic fibrosis: a mucosal immunodeficiency syndrome. *Nature medicine*, 18.
- COLLINS, K., JACKS, T. & PAVLETICH, N. P. 1997. The cell cycle and cancer. *Proceedings of the National Academy of Sciences*, 94, 2776-2778.
- CONSEIL, G., BAUBICHON-CORTAY, H., DAYAN, G., JAULT, J. M., BARRON, D. & DI PIETRO, A. 1998. Flavonoids: a class of modulators with bifunctional interactions at vicinal ATP- and steroid-binding sites on mouse P-glycoprotein. *Proceedings of the National Academy of Sciences of the United States of America*, 95, 9831-9836.
- CONWAY, D. & SCHWARTZ, M. A. 2012. Lessons from the endothelial junctional mechanosensory complex. *F1000 Biology Reports*, 4.
- COORAY, H. C., JANVILISRI, T., VAN VEEN, H. W., HLADKY, S. B. & BARRAND, M. A. 2004a. Interaction of the breast cancer resistance protein with plant polyphenols. *Biochemical and Biophysical Research Communications*, 317, 269-275.
- COORAY, H. C., JANVILISRI, T., VAN VEEN, H. W., HLADKY, S. B. & BARRAND, M. A. 2004b. Interaction of the breast cancer resistance protein with plant polyphenols. *Biochem Biophys Res Commun*, 317, 269-75.
- COS, P., YING, L., CALOMME, M., JP, H., K, C., B, V. P., L, P., AJ, V. & D, V. B. 1998. Structure-activity relationship and classification of flavonoids as inhibitors of xanthine oxidase and superoxide scavengers. *Journal of natural products*, 61.
- COUSSENS, L. M. & WERB, Z. 1996. Matrix metalloproteinases and the development of cancer. *Chemistry & Biology*, 3, 895-904.

- CUCULLO, L., HOSSAIN, M., PUVENNA, V., MARCHI, N. & JANIGRO, D. 2011. The role of shear stress in Blood-Brain Barrier endothelial physiology. *BMC Neuroscience*, 12, 40.
- CUCULLO, L., HOSSAIN, M., TIERNEY, W. & JANIGRO, D. 2013. A new dynamic in vitro modular capillaries-venules modular system: Cerebrovascular physiology in a box. *BMC Neuroscience*, 14, 18.
- CUCULLO, L., MCALLISTER, M., K, K., L, K.-B., M, M., MR, M., KA, S. & D, J. 2002. A new dynamic in vitro model for the multidimensional study of astrocyte-endothelial cell interactions at the blood-brain barrier. *Brain research*, 951.
- DA SILVA, A., CERQUEIRA, C. P., DAS NEVES, O., JL, O., JA, O. A., KC, D. S., JRP, S., BPS, P., C, D. S. S., GP, D. F. L., VDA, D. S., M, D. F. D. C., MP, J., H, C., V, M.-N. & SL, C. 2020. The flavonoid rutin and its aglycone quercetin modulate the microglia inflammatory profile improving antiangioma activity. *Brain, behavior, and immunity*, 85.
- DANG, C. V., KIM, J.-W., GAO, P. & YUSTEIN, J. 2008. The interplay between MYC and HIF in cancer. *Nature Reviews. Cancer*, 8, 51-56.
- DANIELS, B., CRUZ-ORENGO, L., PASIEKA, T., PO, C., IA, R., B, W., JA, C., TL, D. & RS, K. 2013. Immortalized human cerebral microvascular endothelial cells maintain the properties of primary cells in an in vitro model of immune migration across the blood brain barrier. *Journal of neuroscience methods*, 212.
- DAS, A., BANIK, N. L. & RAY, S. K. 2009. Flavonoids activated caspases for apoptosis in human glioblastoma T98G and U87MG cells but not in human normal astrocytes. *Cancer*, NA-NA.
- DASH, R., JAYACHANDRA, B. R. & NR, S. 2017. Therapeutic Potential and Utility of Elacridar with Respect to P-glycoprotein Inhibition: An Insight from the Published In Vitro, Preclinical and Clinical Studies. *European journal of drug metabolism and pharmacokinetics*, 42.
- DATTA, A., BHASIN, N., KIM, H., RANJAN, M., RIDER, B., ABD ELMAGEED, Z. Y., MONDAL, D., AGRAWAL, K. C. & ABDEL-MAGEED, A. B. 2015. Selective targeting of FAK–Pyk2 axis by alpha-naphthoflavone abrogates doxorubicin resistance in breast cancer cells. *Cancer Letters*, 362, 25-35.
- DAUCHY, S., DUTHEIL, F., WEAVER, R. J., CHASSOUX, F., DAUMAS-DUPOINT, C., COURAUD, P.-O., SCHERRMANN, J.-M., DE WAZIERS, I. & DECLÈVES, X. 2008a. ABC transporters, cytochromes P450 and their main transcription factors: expression at the human blood-brain barrier. *Journal of Neurochemistry*, 107, 1518-1528.
- DAUCHY, S., DUTHEIL, F., WEAVER, R. J., CHASSOUX, F., DAUMAS-DUPOINT, C., COURAUD, P. O., SCHERRMANN, J. M., DE WAZIERS, I. & DECLEVES, X. 2008b. ABC transporters, cytochromes P450 and their main transcription factors: expression at the human blood-brain barrier. *J Neurochem*, 107, 1518-28.
- DAVIES, P. F. 2009. Hemodynamic shear stress and the endothelium in cardiovascular pathophysiology. *Nature Clinical Practice Cardiovascular Medicine*, 6, 16-26.
- DAVIES, P. F., BARBEE, K. A., VOLIN, M. V., ROBOTENSKYJ, A., CHEN, J., JOSEPH, L., GRIEM, M. L., WERNICK, M. N., JACOBS, E., POLACEK, D. C., DEPAOLA, N. & BARAKAT, A. I. 1997. SPATIAL RELATIONSHIPS IN EARLY SIGNALING EVENTS OF FLOW-

- MEDIATED ENDOTHELIAL MECHANOTRANSDUCTION. *Annual Review of Physiology*, 59, 527-549.
- DE CASTRO, W., MERTENS-TALCOTT, S., DERENDORF, H. & V, B. 2007. Grapefruit juice-drug interactions: Grapefruit juice and its components inhibit P-glycoprotein (ABCB1) mediated transport of talinolol in Caco-2 cells. *Journal of pharmaceutical sciences*, 96.
- DE CASTRO, W., MERTENS-TALCOTT, S., DERENDORF, H. & V, B. 2008. Effect of grapefruit juice, naringin, naringenin, and bergamottin on the intestinal carrier-mediated transport of talinolol in rats. *Journal of agricultural and food chemistry*, 56.
- DE GOOIJER, M., DE VRIES, N., T, B., LCM, B., JH, B., W, B. & O, V. T. 2018. Improved Brain Penetration and Antitumor Efficacy of Temozolomide by Inhibition of ABCB1 and ABCG2. *Neoplasia (New York, N.Y.)*, 20.
- DE VITA, V. & LAWRENCE, T. 2011. *Cancer: Principles & Practice of Oncology*, 2011, Lippincott.
- DE VRIES, H., KOOIJ, G., D, F., S, G., A, M. & D, J. 2012. Inflammatory events at blood-brain barrier in neuroinflammatory and neurodegenerative disorders: implications for clinical disease. *Epilepsia*, 53 Suppl 6.
- DE VRIES, N., BEIJNEN, J. & O, V. T. 2009. High-grade glioma mouse models and their applicability for preclinical testing. *Cancer treatment reviews*, 35.
- DEAN, M., RZHETSKY, A. & ALLIKMETS, R. 2001. The human ATP-binding cassette (ABC) transporter superfamily. *Genome Research*, 11, 1156-1166.
- DEI, S., BRACONI, L., ROMANELLI, M. N. & TEODORI, E. 2019. Recent advances in the search of BCRP- and dual P-gp/BCRP-based multidrug resistance modulators. *Cancer Drug Resistance*, 2, 710-743.
- DELI, M. A., ÁBRAHÁM, C. S., KATAOKA, Y. & NIWA, M. 2005. Permeability Studies on In Vitro Blood–Brain Barrier Models: Physiology, Pathology, and Pharmacology. *Cellular and Molecular Neurobiology*, 25, 59-127.
- DELSING, L., HERLAND, A., FALK, A., HICKS, R., SYNNERGREN, J. & ZETTERBERG, H. 2020. Models of the blood-brain barrier using iPSC-derived cells. *Molecular and Cellular Neuroscience*, 107, 103533.
- DEMUTH, T. & BERENS, M. E. 2004. Molecular mechanisms of glioma cell migration and invasion. *Journal of Neuro-Oncology*, 70, 217-228.
- DEOSARKAR, S. P., PRABHAKARPANDIAN, B., WANG, B., SHEFFIELD, J. B., KRYNSKA, B. & KIANI, M. F. 2015. A Novel Dynamic Neonatal Blood-Brain Barrier on a Chip. *PLOS ONE*, 10, e0142725.
- DERADA TROLETTI, C., DE GOEDE, P., KAMERMANS, A. & DE VRIES, H. E. 2016. Molecular alterations of the blood–brain barrier under inflammatory conditions: The role of endothelial to mesenchymal transition. *Biochimica et Biophysica Acta (BBA) - Molecular Basis of Disease*, 1862, 452-460.
- DERMAUW, W. & VAN LEEUWEN, T. 2014. The ABC gene family in arthropods: Comparative genomics and role in insecticide transport and resistance. *Insect Biochemistry and Molecular Biology*, 45, 89-110.
- DESAI, S., MARRONI, M., L, C., L, K.-B., MR, M., MT, H., GG, G. & D, J. 2002. Mechanisms of endothelial survival under shear stress. *Endothelium : journal of endothelial cell research*, 9.
- DEVINENI, D., KLEIN-SZANTO, A. & JM, G. 1996. In vivo microdialysis to characterize drug transport in brain tumors: analysis of methotrexate

- uptake in rat glioma-2 (RG-2)-bearing rats. *Cancer chemotherapy and pharmacology*, 38.
- DEZENGOTITA, V. M., KIMURA, R. & MILLER, W. M. 1998. *Cytotechnology*, 28, 213-227.
- DHAR, I. & PRASAD, K. 2014. Oxidative Stress as a Mechanism of Added Sugar-Induced Cardiovascular Disease. *International Journal of Angiology*, 23, 217-226.
- DHERMAIN, F., HAU, P., H, L., AH, J. & MJ, V. D. B. 2010. Advanced MRI and PET imaging for assessment of treatment response in patients with gliomas. *The Lancet. Neurology*, 9.
- DHILLON, H., CHIKARA, S. & REINDL, K. M. 2014. Piperlongumine induces pancreatic cancer cell death by enhancing reactive oxygen species and DNA damage. *Toxicology Reports*, 1, 309-318.
- DI, L. & KERNS, E. 2015. *Blood-Brain Barrier in drug discovery*.
- DI PIETRO, A., CONSEIL, G., PÉREZ-VICTORIA, J. M., DAYAN, G., BAUBICHON-CORTAY, H., TROMPIER, D., STEINFELS, E., JAULT, J.-M., DE WET, H., MAITREJEAN, M., COMTE, G., BOUMENDJEL, A., MARIOTTE, A.-M., DUMONTET, C., MCINTOSH, D. B., GOFFEAU, A., CASTANYS, S., GAMARRO, F. & BARRON, D. 2002. Modulation by flavonoids of cell multidrug resistance mediated by P-glycoprotein and related ABC transporters. *Cellular and Molecular Life Sciences CMLS*, 59, 307-322.
- DIAO, W., TONG, X., YANG, C., ZHANG, F., BAO, C., CHEN, H., LIU, L., LI, M., YE, F., FAN, Q., WANG, J. & OU-YANG, Z.-C. 2019. Behaviors of Glioblastoma Cells in in Vitro Microenvironments. *Scientific Reports*, 9.
- DIRESTA, G. R., NATHAN, S. S., MANOSO, M. W., CASAS-GANEM, J., WYATT, C., KUBO, T., BOLAND, P. J., ATHANASIAN, E. A., MIODOWNIK, J., GORLICK, R. & HEALEY, J. H. 2005. Cell Proliferation of Cultured Human Cancer Cells are Affected by the Elevated Tumor Pressures that Exist In Vivo. *Annals of Biomedical Engineering*, 33, 1270-1280.
- DISERENS, A., DE TRIBOLET, N., A, M.-A., AC, G., JF, S. & S, C. 1981. Characterization of an established human malignant glioma cell line: LN-18. *Acta neuropathologica*, 53.
- DOAN, K. H., JE.WEBSTER, LO., SA, W., LJ, S., CJ, S.-S., KK, A. & JW, P. 2002. Passive permeability and P-glycoprotein-mediated efflux differentiate central nervous system (CNS) and non-CNS marketed drugs. *The Journal of pharmacology and experimental therapeutics*, 303.
- DOBLAS, S., HE, T., D, S., J, P., J, H., N, S., M, L. & RA, T. 2010. Glioma morphology and tumor-induced vascular alterations revealed in seven rodent glioma models by in vivo magnetic resonance imaging and angiography. *Journal of magnetic resonance imaging : JMRI*, 32.
- DOMINGUEZ, R. & HOLMES, K. C. 2011. Actin Structure and Function. *Annual Review of Biophysics*, 40, 169-186.
- DOYLE, L. A., YANG, W., ABRUZZO, L. V., KROGMANN, T., GAO, Y., RISHI, A. K. & ROSS, D. D. 1998. A multidrug resistance transporter from human MCF-7 breast cancer cells. *Proceedings of the National Academy of Sciences*, 95, 15665-15670.
- DRÉAN, A., ROSENBERG, S., LEJEUNE, F.-X., GOLI, L., NADARADJANE, A. A., GUEHENNEC, J., SCHMITT, C., VERREAULT, M., BIELLE, F.,

- MOKHTARI, K., SANSON, M., CARPENTIER, A., DELATTRE, J.-Y. & IDBAIH, A. 2018. ATP binding cassette (ABC) transporters: expression and clinical value in glioblastoma. *Journal of Neuro-Oncology*, 138, 479-486.
- DUAN, P. & YOU, G. 2009. Novobiocin Is a Potent Inhibitor for Human Organic Anion Transporters. *Drug Metabolism and Disposition*, 37, 1203-1210.
- DUAN, X., GUO, G., PEI, X., WANG, X., LI, L., XIONG, Y. & QIU, X. 2019. Baicalin Inhibits Cell Viability, Migration and Invasion in Breast Cancer by Regulating miR-338-3p and MORC4. *OncoTargets and Therapy*, Volume 12, 11183-11193.
- DUBOIS, L. G., CAMPANATI, L., RIGHY, C., ANDREA-MEIRA, I., SPOHR, T. C. L. D. S. E., PORTO-CARREIRO, I., PEREIRA, C. M., BALANÇA-SILVA, J., KAHN, S. A., DOSSANTOS, M. F., OLIVEIRA, M. D. A. R., XIMENES-DA-SILVA, A., LOPES, M. C., FAVERET, E., GASPARETTO, E. L. & MOURA-NETO, V. 2014. Gliomas and the vascular fragility of the blood brain barrier. *Frontiers in Cellular Neuroscience*, 8.
- DUCHEMIN, S., BOILY, M., SADEKOVA, N. & H, G. 2012. The complex contribution of NOS interneurons in the physiology of cerebrovascular regulation. *Frontiers in neural circuits*, 6.
- DURIEU-TRAUTMANN, O., FOIGNANT-CHAVEROT, N., PERDOMO, J., GOUNON, P., STROSBURG, A. D. & COURAUD, P. O. 1991. Immortalization of brain capillary endothelial cells with maintenance of structural characteristics of the blood-brain barrier endothelium. *In Vitro Cellular & Developmental Biology - Animal*, 27, 771-778.
- DWIVEDI, S., MALIK, C. & CHHOKAR, V. 2017. Molecular Structure, Biological Functions, and Metabolic Regulation of Flavonoids. *Plant Biotechnology: Recent Advancements and Developments*. Springer Singapore.
- DZOBO, K., HASSEN, N., SENTHEBANE, D., THOMFORD, N., ROWE, A., SHIPANGA, H., WONKAM, A., PARKER, M., MOWLA, S. & DANDARA, C. 2018. Chemoresistance to Cancer Treatment: Benzo- α -Pyrene as Friend or Foe? *Molecules*, 23, 930.
- EBERT, B., SEIDEL, A. & LAMPEN, A. 2006. Phytochemicals Induce Breast Cancer Resistance Protein in Caco-2 Cells and Enhance the Transport of Benzo[a]pyrene-3-sulfate. *Toxicological Sciences*, 96, 227-236.
- EDENHARDER, R., VON PETERSDORFF, I. & RAUSCHER, R. 1993. Antimutagenic effects of flavonoids, chalcones and structurally related compounds on the activity of 2-amino-3-methylimidazo[4,5-f]quinoline (IQ) and other heterocyclic amine mutagens from cooked food. *Mutation Research*, 287, 261-274.
- EISENBLÄTTER, T., HÜWEL, S. & HJ, G. 2003. Characterisation of the brain multidrug resistance protein (BMDP/ABCG2/BCRP) expressed at the blood-brain barrier. *Brain research*, 971.
- EJENDAL, K. F. K., DIOP, N. K., SCHWEIGER, L. C. & HRYCYNA, C. A. 2006. The nature of amino acid 482 of human ABCG2 affects substrate transport and ATP hydrolysis but not substrate binding. *Protein Science*, 15, 1597-1607.
- ELBAKARY, B. & BADHAN, R. K. S. 2020. A dynamic perfusion based blood-brain barrier model for cytotoxicity testing and drug permeation. *Sci Rep*, 10, 3788.

- EMANUELI, C., SCHRATZBERGER, P., KIRCHMAIR, R. & MADEDDU, P. 2003. Paracrine control of vascularization and neurogenesis by neurotrophins. *British journal of pharmacology*, 140.
- EMUSS, V. 2006. The Molecular Biology of Cancer. *British journal of cancer*, 95.
- ERDOGAN, S., DOGANLAR, O., DOGANLAR, Z. B. & TURKEKUL, K. 2018. Naringin sensitizes human prostate cancer cells to paclitaxel therapy. *Prostate International*, 6, 126-135.
- ERSOZ, M., ERDEMIR, A., DURANOGLU, D., UZUNOGLU, D., ARASOGLU, T., DERMAN, S. & MANSUROGLU, B. 2019. Comparative evaluation of hesperetin loaded nanoparticles for anticancer activity against C6 glioma cancer cells. *Artificial Cells, Nanomedicine, and Biotechnology*, 47, 319-329.
- ESCH, M., SUNG, J., YANG, J., C, Y., J, Y., JC, M. & ML, S. 2012. On chip porous polymer membranes for integration of gastrointestinal tract epithelium with microfluidic 'body-on-a-chip' devices. *Biomedical microdevices*, 14.
- FAGHIH, M. M. & SHARP, M. K. 2018. Is bulk flow plausible in perivascular, paravascular and paravenous channels? *Fluids and Barriers of the CNS*, 15.
- FAN, H., TIAN, W. & MA, X. 2014. Curcumin induces apoptosis of HepG2 cells via inhibiting fatty acid synthase. *Targeted oncology*, 9.
- FAN, T.-J., HAN, L.-H., CONG, R.-S. & LIANG, J. 2005. Caspase Family Proteases and Apoptosis. *Acta Biochimica et Biophysica Sinica*, 37, 719-727.
- FAN, X., BAI, J., ZHAO, S., HU, M., SUN, Y., WANG, B., JI, M., JIN, J., WANG, X., HU, J. & LI, Y. 2019. Evaluation of inhibitory effects of flavonoids on breast cancer resistance protein (BCRP): From library screening to biological evaluation to structure-activity relationship. *Toxicology in Vitro*, 61, 104642.
- FANG, Y., CAO, W., XIA, M., PAN, S. & XU, X. 2017. Study of Structure and Permeability Relationship of Flavonoids in Caco-2 Cells. *Nutrients*, 9, 1301.
- FANG, Y., LU, Y., ZANG, X., WU, T., QI, X., PAN, S. & XU, X. 2016. 3D-QSAR and docking studies of flavonoids as potent Escherichia coli inhibitors. *Scientific Reports*, 6, 23634.
- FANTINI, M., BENVENUTO, M., L, M., GV, F., I, T., A, M. & R, B. 2015. In vitro and in vivo antitumoral effects of combinations of polyphenols, or polyphenols and anticancer drugs: perspectives on cancer treatment. *International journal of molecular sciences*, 16.
- FARDEL, O., LECUREUR, V. & A, G. 1993. Regulation by dexamethasone of P-glycoprotein expression in cultured rat hepatocytes. *FEBS letters*, 327.
- FERRALI, M., SIGNORINI, C., B, C., L, S., L, C., D, G. & M, C. 1997. Protection against oxidative damage of erythrocyte membrane by the flavonoid quercetin and its relation to iron chelating activity. *FEBS letters*, 416.
- FERROLI, P. & BROGGI, M. 2006. Surgifoam and Mitoxantrone in the Glioblastoma Multiforme Postresection Cavity The First Step of Locoregional Chemotherapy through an Ad Hoc-placed Catheter: Technical Note. *Neurosurgery*, 59.

- FERRY, D., TRAUNECKER, H. & KERR, D. 1996. Clinical trials of P-glycoprotein reversal in solid tumours. *European journal of cancer (Oxford, England : 1990)*, 32A.
- FIGLEY, C. & STROMAN, P. 2011. The role(s) of astrocytes and astrocyte activity in neurometabolism, neurovascular coupling, and the production of functional neuroimaging signals. *The European journal of neuroscience*, 33.
- FINKEL, T. 2011. Signal transduction by reactive oxygen species. *Journal of Cell Biology*, 194, 7-15.
- FLAHERTY, J. T., PIERCE, J. E., FERRANS, V. J., PATEL, D. J., TUCKER, W. K. & FRY, D. L. 1972. Endothelial Nuclear Patterns in the Canine Arterial Tree with Particular Reference to Hemodynamic Events. *Circulation Research*, 30, 23-33.
- FOURNET, J., MAYAUD, C., DE LONLAY, P., MS, G.-M., V, V., M, C., M, D., J, R., F, B., JJ, R., C, N.-F., JM, S. & C, J. 2001. Unbalanced expression of 11p15 imprinted genes in focal forms of congenital hyperinsulinism: association with a reduction to homozygosity of a mutation in ABCC8 or KCNJ11. *The American journal of pathology*, 158.
- FRANKE, H., GALLA, H. & CT, B. 1999. An improved low-permeability in vitro-model of the blood-brain barrier: transport studies on retinoids, sucrose, haloperidol, caffeine and mannitol. *Brain research*, 818.
- FRANKE, H. G., H. BEUCKMANN, CT. 2000. Primary cultures of brain microvessel endothelial cells: a valid and flexible model to study drug transport through the blood-brain barrier in vitro. *Brain research. Brain Research Protocols*, 5, 248-256.
- FRANTZ, C., STEWART, K. M. & WEAVER, V. M. 2010. The extracellular matrix at a glance. *Journal of Cell Science*, 123, 4195-4200.
- FRIEDEMANN, U. 1942. BLOOD-BRAIN BARRIER. <https://doi.org/10.1152/physrev.1942.22.2.125>.
- FRIEDLANDER, R. M. 2003. Apoptosis and Caspases in Neurodegenerative Diseases. *New England Journal of Medicine*, 348, 1365-1375.
- FULDA, S. 2018. Cell death-based treatment of glioblastoma. *Cell Death & Disease*, 9, 121.
- FÖRSTER, C., BUREK, M., IA, R., B, W., PO, C. & D, D. 2008. Differential effects of hydrocortisone and TNFalpha on tight junction proteins in an in vitro model of the human blood-brain barrier. *The Journal of physiology*, 586.
- GAILLARD, F. 2021. WHO classification of CNS tumours [Online]. @radiopaedia. Available: <https://radiopaedia.org/articles/who-classification-of-cns-tumours-1?lang=gb> [Accessed].
- GAILLARD, P. & DE BOER, A. 2000. Relationship between permeability status of the blood-brain barrier and in vitro permeability coefficient of a drug. *European journal of pharmaceutical sciences : official journal of the European Federation for Pharmaceutical Sciences*, 12.
- GAILLARD, P. J., VOORWINDEN, L., JL, N., A, I., R, A., H, E., C, R., AG, D. B. & DD, B. 2001. Establishment and functional characterization of an in vitro model of the blood-brain barrier, comprising a co-culture of brain capillary endothelial cells and astrocytes. *European journal of pharmaceutical sciences : official journal of the European Federation for Pharmaceutical Sciences*, 12.

- GALATI, G., CHAN, T., B, W. & PJ, O. B. 1999. Glutathione-dependent generation of reactive oxygen species by the peroxidase-catalyzed redox cycling of flavonoids. *Chemical research in toxicology*, 12.
- GALATI, G., SABZEVARI, O., JX, W. & PJ, O. B. 2002. Prooxidant activity and cellular effects of the phenoxyl radicals of dietary flavonoids and other polyphenolics. *Toxicology*, 177.
- GANESHPURKAR, A. & SALUJA, A. K. 2017. The Pharmacological Potential of Rutin. *Saudi Pharmaceutical Journal*, 25, 149-164.
- GANIPINENI, L. P., DANHIER, F. & PRÉAT, V. 2018. Drug delivery challenges and future of chemotherapeutic nanomedicine for glioblastoma treatment. *Journal of Controlled Release*, 281, 42-57.
- GAO, C., ZHOU, Y., LI, H., CONG, X., JIANG, Z., WANG, X., CAO, R. & TIAN, W. 2017a. Antitumor effects of baicalin on ovarian cancer cells through induction of cell apoptosis and inhibition of cell migration in vitro. *Molecular Medicine Reports*, 16, 8729-8734.
- GAO, C., ZHOU, Y., LI, H., CONG, X., JIANG, Z., WANG, X., CAO, R. & TIAN, W. 2017b. Antitumor effects of baicalin on ovarian cancer cells through induction of cell apoptosis and inhibition of cell migration in vitro. *Molecular medicine reports*, 16, 8729-8734.
- GAO, Y., SNYDER, S. A., SMITH, J. N. & CHEN, Y. C. 2016. Anticancer properties of baicalein: a review. *Med Chem Res*, 25, 1515-1523.
- GARCIA-POLITE, F., MARTORELL, J., DEL REY-PUECH, P., MELGAR-LESMES, P., O'BRIEN, C. C., ROQUER, J., OIS, A., PRINCIPE, A., EDELMAN, E. R. & BALCELLS, M. 2017. Pulsatility and high shear stress deteriorate barrier phenotype in brain microvascular endothelium. *Journal of Cerebral Blood Flow & Metabolism*, 37, 2614-2625.
- GASTFRIEND, B. D., PALECEK, S. P. & SHUSTA, E. V. 2018. Modeling the blood–brain barrier: Beyond the endothelial cells. *Current Opinion in Biomedical Engineering*, 5, 6-12.
- GAYER, C. & BASSON, M. 2009. The effects of mechanical forces on intestinal physiology and pathology. *Cellular signalling*, 21.
- GELBOIN, H. 1980. Benzo[alpha]pyrene metabolism, activation and carcinogenesis: role and regulation of mixed-function oxidases and related enzymes. *Physiological reviews*, 60.
- GHANBARI-MOVAHED, M., JACKSON, G., FARZAEI, M. & A, B. 2021. A Systematic Review of the Preventive and Therapeutic Effects of Naringin Against Human Malignancies. *Frontiers in pharmacology*, 12.
- GHAVAMI, S., HASHEMI, M., SR, A., B, Y., W, X., M, E., CJ, B., K, K., E, W., AJ, H. & M, L. 2009. Apoptosis and cancer: mutations within caspase genes. *Journal of medical genetics*, 46.
- GHOBRIL, I. M., WITZIG, T. E. & ADJEI, A. A. 2005. Targeting apoptosis pathways in cancer therapy. *CA Cancer J Clin*, 55, 178-94.
- GIAKOUMETTIS, D., KRITIS, A. & N, F. 2018. C6 cell line: the gold standard in glioma research. *Hippokratia*, 22.
- GIBELLINI, L., PINTI, M., NASI, M., DE BIASI, S., ROAT, E., BERTONCELLI, L. & COSSARIZZA, A. 2010. Interfering with ROS Metabolism in Cancer Cells: The Potential Role of Quercetin. *Cancers*, 2, 1288-1311.
- GIERYNG, A., PSZCZOLKOWSKA, D., BOCIAN, K., DABROWSKI, M., RAJAN, W. D., KLOSS, M., MIECZKOWSKI, J. & KAMINSKA, B. 2017.

- Immune microenvironment of experimental rat C6 gliomas resembles human glioblastomas. *Scientific Reports*, 7.
- GIL-MARTINS, E., BARBOSA, D., V, S., F, R. & R, S. 2020. Dysfunction of ABC transporters at the blood-brain barrier: Role in neurological disorders. *Pharmacology & therapeutics*, 213.
- GIMENEZ-BONAFE, P., GUILLEN CANOVAS, A., AMBROSIO, S., TORTOSA, A. & PEREZ-TOMAS, R. J. K. R. S. 2008. Multidrug Resistance: Biological and Pharmaceutical Advance in the Antitumour Treatment.
- GINGUENÉ, C., CHAMPIER, J., MAALLEM, S., STRAZIELLE, N., JOUVET, A., FÈVRE-MONTANGE, M. & GHERSI-EGEA, J. F. J. B. P. 2010. P-glycoprotein (ABCB1) and Breast Cancer Resistance Protein (ABCG2) Localize in the Microvessels Forming the Blood-Tumor Barrier in Ependymomas. 20, 926-935.
- GIRI, N., SHAIK, N., PAN, G., TERASAKI, T., MUKAI, C., KITAGAKI, S., MIYAKOSHI, N. & ELMQUIST, W. F. 2008. Investigation of the Role of Breast Cancer Resistance Protein (Bcrp/Abcg2) on Pharmacokinetics and Central Nervous System Penetration of Abacavir and Zidovudine in the Mouse. *Drug Metabolism and Disposition*, 36, 1476-1484.
- GIUSTI, S., SBRANA, T., M, L. M., V, D. P., V, M., A, T., C, D. & A, A. 2014. A novel dual-flow bioreactor simulates increased fluorescein permeability in epithelial tissue barriers. *Biotechnology journal*, 9.
- GLORIA, L., KARLO, B., MANISHA, R., PRAT, A., WOSIK, K. & BENDAYAN, R. 2007. Expression of the ATP-binding Cassette Membrane Transporter, ABCG2, in Human and Rodent Brain Microvessel Endothelial and Glial Cell Culture Systems. *Pharmaceutical Research*, 24, 1262-1274.
- GOLDAR, S., KHANIANI, M., SM, D. & B, B. 2015. Molecular mechanisms of apoptosis and roles in cancer development and treatment. *Asian Pacific journal of cancer prevention : APJCP*, 16.
- GOLDMANN, E. 1912. The late The professor Edwin Goldmann's investigations on the central nervous system by vital staining. *Med J*.
- GOMEZ-ZEPEDA, D., TAGHI, M., SCHERRMANN, J.-M., DECLEVES, X. & MENET, M.-C. 2019. ABC Transporters at the Blood–Brain Interfaces, Their Study Models, and Drug Delivery Implications in Gliomas. *Pharmaceutics*, 12, 20.
- GONG, W., WANG, Z., Y, W., L, S. & Y, Z. 2014. Downregulation of ABCG2 protein inhibits migration and invasion in U251 glioma stem cells. *Neuroreport*, 25.
- GORECKA, J., KOSTIUK, V., FEREDDOONI, A., GONZALEZ, L., LUO, J., DASH, B., ISAJI, T., ONO, S., LIU, S., LEE, S. R., XU, J., LIU, J., TANIGUCHI, R., YASTULA, B., HSIA, H. C., QYANG, Y. & DARDIK, A. 2019. The potential and limitations of induced pluripotent stem cells to achieve wound healing. *Stem Cell Research & Therapy*, 10, 1-10.
- GORLACH, S., FICHNA, J. & U, L. 2015. Polyphenols as mitochondria-targeted anticancer drugs. *Cancer letters*, 366.
- GOYAL, P., VERMA, P., SHARMA, P., PARMAR, J. & A, A. 2010. Evaluation of anti-cancer and anti-oxidative potential of *Syzygium Cumini* against benzo[a]pyrene (BaP) induced gastric carcinogenesis in mice. *Asian Pacific journal of cancer prevention : APJCP*, 11.

- GRAF, G., YU, L., LI, W., GERARD, R., PL, T., JC, C. & HH, H. 2003. ABCG5 and ABCG8 are obligate heterodimers for protein trafficking and biliary cholesterol excretion. *The Journal of biological chemistry*, 278.
- GRANBERG, L., OSTERGREN, A., BRANDT, I. & BRITTEBO, E. B. 2003. CYP1A1 and CYP1B1 in blood-brain interfaces: CYP1A1-dependent bioactivation of 7,12-dimethylbenz(a)anthracene in endothelial cells. *Drug Metab Dispos*, 31, 259-65.
- GRAY, D. R. C., SU., HOWARTH, W., INLOW, D. & MAIORELLA, B. L. 1996. CO₂ in large-scale and high-density CHO cell perfusion culture. *Cytotechnology*, 22, 65-78.
- GREEN, D. R. & KROEMER, G. 2004. The Pathophysiology of Mitochondrial Cell Death.
- GRIEP, L. M., WOLBERS, F., DE WAGENAAR, B., TER BRAAK, P. M., WEKSLER, B. B., ROMERO, I. A., COURAUD, P. O., VERMES, I., VAN DER MEER, A. D. & VAN DEN BERG, A. 2013. BBB ON CHIP: microfluidic platform to mechanically and biochemically modulate blood-brain barrier function. *Biomedical Microdevices*, 15, 145-150.
- GRIVENNIKOVA, V. G. & VINOGRADOV, A. D. 2013. Mitochondrial production of reactive oxygen species. *Biochemistry (Moscow)*, 78, 1490-1511.
- GROOTHUIS, D. 2000. The blood-brain and blood-tumor barriers: a review of strategies for increasing drug delivery. *Neuro-oncology*, 2.
- GUO, Q., GRIMMIG, T., GONZALEZ, G., GIOBBIE-HURDER, A., BERG, G., CARR, N., WILSON, B. J., BANERJEE, P., MA, J., GOLD, J. S., NANDI, B., HUANG, Q., WAAGA-GASSER, A. M., LIAN, C. G., MURPHY, G. F., FRANK, M. H., GASSER, M. & FRANK, N. Y. 2018. ATP-binding cassette member B5 (ABCB5) promotes tumor cell invasiveness in human colorectal cancer. *Journal of Biological Chemistry*, 293, 11166-11178.
- GUOHUA, A., JORGE, G. & MORRIS, M. E. 2011. The Bioflavonoid Kaempferol Is an Abcg2 Substrate and Inhibits Abcg2-Mediated Quercetin Efflux.
- GUPTA, S. C., PATCHVA, S. & AGGARWAL, B. B. 2013. Therapeutic Roles of Curcumin: Lessons Learned from Clinical Trials. *The AAPS Journal*, 15, 195-218.
- HABICHT, K. L., SINGH, N. S., KHADEER, M. A., SHIMMO, R., WAINER, I. W. & MOADDEL, R. 2014. Characterization of a multiple endogenously expressed adenosine triphosphate-binding cassette transporters using nuclear and cellular membrane affinity chromatography columns. *Journal of chromatography. A*, 1339, 80-85.
- HADI, S., ASAD, S., SINGH, S. & AHMAD, A. 2000. Putative mechanism for anticancer and apoptosis-inducing properties of plant-derived polyphenolic compounds. *IUBMB life*, 50.
- HAENEN, G., PAQUAY, J., RE, K. & A, B. 1997. Peroxynitrite scavenging by flavonoids. *Biochemical and biophysical research communications*, 236.
- H Aidari, F., Ali Keshavarz, S., Reza Rashidi, M. & Mohammad Shahi, M. 2009. Orange Juice and Hesperetin Supplementation to Hyperuricemic Rats Alter Oxidative Stress Markers and Xanthine Oxidoreductase Activity. *Journal of Clinical Biochemistry and Nutrition*, 45, 285-291.

- HAKKARAINEN, J., RILLA, K., M, S., M, R. & MM, F. 2014. Re-evaluation of the role of P-glycoprotein in in vitro drug permeability studies with the bovine brain microvessel endothelial cells. *Xenobiotica; the fate of foreign compounds in biological systems*, 44.
- HAM, S. L., NASROLLAHI, S., SHAH, K. N., SOLTISZ, A., PARUCHURI, S., YUN, Y. H., LUKER, G. D., BISHAYEE, A. & TAVANA, H. 2015. Phytochemicals potently inhibit migration of metastatic breast cancer cells. *Integrative biology : quantitative biosciences from nano to macro*, 7, 792-800.
- HANAHAH, D. & WEINBERG, A., ROBERT 2011. Hallmarks of Cancer: The Next Generation. *Cell*, 144, 646-674.
- HANAHAH, D. & WEINBERG, R. A. 2000. The Hallmarks of Cancer. *Cell*, 100, 57-70.
- HANASAKI, Y., OGAWA, S. & S, F. 1994. The correlation between active oxygens scavenging and antioxidative effects of flavonoids. *Free radical biology & medicine*, 16.
- HANIF, F. & MUZAFFAR, K. 2017. Glioblastoma Multiforme: A Review of its Epidemiology and Pathogenesis through Clinical Presentation and Treatment. *Asian Pacific journal of cancer prevention : APJCP*, 18.
- HARADA, M., KAN, Y., NAOKI, H., FUKUI, Y., KAGEYAMA, N., NAKAI, M., MIKI, W. & KISO, Y. 1999. Identification of the major antioxidative metabolites in biological fluids of the rat with ingested (+)-catechin and (-)-epicatechin. *Bioscience, Biotechnology, and Biochemistry*, 63, 973-977.
- HARTZ, A. & BAUER, B. 2011. ABC transporters in the CNS—an inventory. *Curr. Pharm. Biotechnol*, 12, 656-673.
- HASELOFF, R., BLASIG, I., BAUER, H. & BAUER, H. 2005. In search of the astrocytic factor(s) modulating blood-brain barrier functions in brain capillary endothelial cells in vitro. *Cellular and molecular neurobiology*, 25.
- HATHERELL, K., COURAUD, P.-O., ROMERO, I. A., WEKSLER, B. & PILKINGTON, G. J. 2011. Development of a three-dimensional, all-human in vitro model of the blood–brain barrier using mono-, co-, and tri-cultivation Transwell models. *Journal of Neuroscience Methods*, 199, 223-229.
- HATTORI, K., NAGURO, I., RUNCHEL, C. & ICHIJO, H. 2009. The roles of ASK family proteins in stress responses and diseases. *Cell Communication and Signaling*, 7, 9.
- HAYASHI, H. & SUGIYAMA, Y. 2013. Bile salt export pump (BSEP/ABCB11): trafficking and sorting disturbances. *Current molecular pharmacology*, 6.
- HAYCOCK, I. A., ARTI. WILKINSON, MALCOLM. 2014. *Cellular In Vitro Testing: Methods and Protocols*, Jenny Stanford.
- HAZAI, E. & BIKÁDI, Z. 2008. Homology modeling of breast cancer resistance protein (ABCG2). *Journal of structural biology*, 162.
- HEIM, K., TAGLIAFERRO, A. & DJ, B. 2002. Flavonoid antioxidants: chemistry, metabolism and structure-activity relationships. *The Journal of nutritional biochemistry*, 13.
- HEINO, J. 2007. The collagen family members as cell adhesion proteins. *BioEssays : news and reviews in molecular, cellular and developmental biology*, 29.

- HELMS, H. C., ABBOTT, N. J., BUREK, M., CECHELLI, R., COURAUD, P.-O., DELI, M. A., FÖRSTER, C., GALLA, H. J., ROMERO, I. A., SHUSTA, E. V., STEBBINS, M. J., VANDENHAUTE, E., WEKSLER, B. & BRODIN, B. 2016. In vitro models of the blood–brain barrier: An overview of commonly used brain endothelial cell culture models and guidelines for their use. *Journal of Cerebral Blood Flow & Metabolism*, 36, 862-890.
- HERNÁNDEZ, I., ALEGRE, L., F, V. B. & S, M.-B. 2009. How relevant are flavonoids as antioxidants in plants? *Trends in plant science*, 14.
- HIGGINS, C. 1995. The ABC of channel regulation. *Cell*, 82.
- HIGGINS, C. 2001. ABC transporters: physiology, structure and mechanism--an overview. *Research in microbiology*, 152.
- HIGGINS, C. & LINTON, K. 2004. The ATP switch model for ABC transporters. *Nature Structural & Molecular Biology*, 11, 918-926.
- HIRSCH, H. A., ILIOPOULOS, D., TSICHLIS, P. N. & STRUHL, K. 2009. Metformin Selectively Targets Cancer Stem Cells, and Acts Together with Chemotherapy to Block Tumor Growth and Prolong Remission. *Cancer Research*, 69, 7507-7511.
- HLADKY, S. B. & BARRAND, M. A. 2014. Mechanisms of fluid movement into, through and out of the brain: evaluation of the evidence. *Fluids and Barriers of the CNS*, 11, 26.
- HOCKLEY, S. L., ARLT, V. M., BREWER, D., GIDDINGS, I. & PHILLIPS, D. H. 2006. Time- and concentration-dependent changes in gene expression induced by benzo(a)pyrene in two human cell lines, MCF-7 and HepG2. *BMC Genomics*, 7.
- HOHEISEL, D., NITZ, T., FRANKE, H., WEGENER, J., HAKVOORT, A., TILLING, T. & GALLA, H.-J. 1998. Hydrocortisone Reinforces the Blood–Brain Barrier Properties in a Serum Free Cell Culture System. *Biochemical and Biophysical Research Communications*, 244, 312-316.
- HOLLAND, E. C. 2000. Glioblastoma multiforme: The terminator.
- HONJO, Y., HRYCYNA, C., YAN, Q., WY, M.-P., RW, R., A, V. D. L., T, L., M, D. & SE, B. 2001. Acquired mutations in the MXR/BCRP/ABCP gene alter substrate specificity in MXR/BCRP/ABCP-overexpressing cells. *Cancer research*, 61.
- HOSOYA, K., HORI, S., OHTSUKI, S. & TERASAKI, T. 2004. A new in vitro model for blood-cerebrospinal fluid barrier transport studies: an immortalized choroid plexus epithelial cell line derived from the tsA58 SV40 large T-antigen gene transgenic rat. *Advanced drug delivery reviews*, 56.
- HUSAIN, S., BEHARI, N., RJ, K., I, P. & RK, P. 1998. Complete regression of established human glioblastoma tumor xenograft by interleukin-4 toxin therapy. *Cancer research*, 58.
- HUWYLER, J., DREWE, J., C, K. & G, F. 1996. Evidence for P-glycoprotein-modulated penetration of morphine-6-glucuronide into brain capillary endothelium. *British journal of pharmacology*, 118.
- HUYNH, T., NORRIS, M. D., HABER, M. & HENDERSON, M. J. 2012. ABCC4/MRP4: a MYCN-regulated transporter and potential therapeutic target in neuroblastoma. *Frontiers in Oncology*, 2.
- HYDE, S., EMSLEY, P., HARTSHORN, M., MM, M., U, G., SR, P., MP, G., DR, G., RE, H. & CF, H. 1990. Structural model of ATP-binding proteins

- associated with cystic fibrosis, multidrug resistance and bacterial transport. *Nature*, 346.
- IMAI, Y., TSUKAHARA, S., ASADA, S. & SUGIMOTO, Y. 2004a. Phytoestrogens/flavonoids reverse breast cancer resistance protein/ABCG2-mediated multidrug resistance. *Cancer Res*, 64, 4346-52.
- IMAI, Y., TSUKAHARA, S., ASADA, S. & SUGIMOTO, Y. J. C. R. 2004b. Phytoestrogens/flavonoids reverse breast cancer resistance protein/ABCG2-mediated multidrug resistance. 64, 4346-4352.
- IMRAN, M., SAEED, F., GILANI, S. A., SHARIATI, M. A., IMRAN, A., AFZAAL, M., ATIF, M., TUFAIL, T. & ANJUM, F. M. 2021. Fisetin: An anticancer perspective. *Food Science & Nutrition*, 9, 3-16.
- IORI, E., VINCI, B., MURPHY, E., MARESCOTTI, M. C., AVOGARO, A. & AHLUWALIA, A. 2012. Glucose and Fatty Acid Metabolism in a 3 Tissue In-Vitro Model Challenged with Normo- and Hyperglycaemia. *PLoS ONE*, 7, e34704.
- IORIO, A., ROS, M., O, F., M, L., L, F., A, S., S, B., M, G., C, F., MD, M., L, G. & I, S. 2016. Blood-Brain Barrier and Breast Cancer Resistance Protein: A Limit to the Therapy of CNS Tumors and Neurodegenerative Diseases. *Anti-cancer agents in medicinal chemistry*, 16.
- ISHII, N., MAIER, D., MERLO, A., M, T., Y, S., AC, D. & EG, V. M. 1999. Frequent co-alterations of TP53, p16/CDKN2A, p14ARF, PTEN tumor suppressor genes in human glioma cell lines. *Brain pathology (Zurich, Switzerland)*, 9.
- JACOB, A., HARTZ, A. M., POTIN, S., COUMOUL, X., YOUSIF, S., SCHERRMANN, J. M., BAUER, B. & DECLEVES, X. 2011. Aryl hydrocarbon receptor-dependent upregulation of Cyp1b1 by TCDD and diesel exhaust particles in rat brain microvessels. *Fluids Barriers CNS*, 8, 23.
- JAIN, A., LAI, J. & BHUSHAN, A. 2015. Biochanin A inhibits endothelial cell functions and proangiogenic pathways: implications in glioma therapy. *Anti-cancer drugs*, 26.
- JAMES, B. D. & ALLEN, J. B. 2018. Vascular Endothelial Cell Behavior in Complex Mechanical Microenvironments. *ACS Biomaterials Science & Engineering*, 4, 3818-3842.
- JANG, K., JEONG, S., KIM, S., JUNG, J., JH, K., W, K., CY, C. & SH, K. 2012. Activation of reactive oxygen species/AMP activated protein kinase signaling mediates fisetin-induced apoptosis in multiple myeloma U266 cells. *Cancer letters*, 319.
- JANIGRO, D., LEAMAN, S. & STANNESS, K. 1999. Dynamic modeling of the blood-brain barrier: a novel tool for studies of drug delivery to the brain. *Pharmaceutical Science & Technology Today*, 2, 7-12.
- JEONG, J.-H., AN, J. Y., KWON, Y. T., RHEE, J. G. & LEE, Y. J. 2009. Effects of low dose quercetin: Cancer cell-specific inhibition of cell cycle progression. *Journal of cellular biochemistry*, 106, 73-82.
- JEONG, K.-H., LEE, H. J., PARK, T.-S. & SHIM, S.-M. 2019. Catechins Controlled Bioavailability of Benzo[a]pyrene (B[a]P) from the Gastrointestinal Tract to the Brain towards Reducing Brain Toxicity Using the In Vitro Bio-Mimic System Coupled with Sequential Co-Cultures. *Molecules (Basel, Switzerland)*, 24, 2175.

- JIA, S., XU, X., ZHOU, S., CHEN, Y., DING, G. & CAO, L. 2019. Fisetin induces autophagy in pancreatic cancer cells via endoplasmic reticulum stress- and mitochondrial stress-dependent pathways. *Cell Death & Disease*, 10.
- JJ, M. M., UNIVERSIDAD NACIONAL DEL CHACO AUSTRAL - COMANDANTE FERNÁNDEZ 755, C. P. R. S. P., CHACO, ARGENTINA., LG, N., CEQUINOR, C. U., FACULTAD DE CIENCIAS EXACTAS, UNIVERSIDAD NACIONAL DE LA PLATA, BV. 120 N° 1465, 1900 LA PLATA, ARGENTINA., AL, P., DEPARTAMENTO DE FÍSICA, F. D. B. Y. C. B.-U. N. D. L., CIUDAD UNIVERSITARIA-PARAJE EL POZO, 3000 SANTA FE, ARGENTINA., A, R., EG, F., PAM, W. & WILLIAMS@QUIMICA.UNLP.EDU.AR 2017. Antioxidant and anticancer effects and bioavailability studies of the flavonoid baicalin and its oxidovanadium(IV) complex. *Journal of Inorganic Biochemistry*, 166, 150-161.
- JOHANSEN, M. D., ROCHAT, P., LAW, I., SCHEIE, D., POULSEN, H. S. & MUHIC, A. 2016. Presentation of Two Cases with Early Extracranial Metastases from Glioblastoma and Review of the Literature. *Case reports in oncological medicine*, 2016, 8190950-8190950.
- JOHNSON, B. D., MATHER, K. J. & WALLACE, J. P. 2011. Mechanotransduction of shear in the endothelium: Basic studies and clinical implications. *Vascular Medicine*, 16, 365-377.
- JOHNSON, D. & O'NEILL, B. 2012. Glioblastoma survival in the United States before and during the temozolomide era. *Journal of neuro-oncology*, 107.
- JONKMAN, J. E. N., CATHCART, J. A., XU, F., BARTOLINI, M. E., AMON, J. E., STEVENS, K. M. & COLARUSSO, P. 2014. An introduction to the wound healing assay using live-cell microscopy. *Cell Adhesion & Migration*, 8, 440-451.
- JUILLERAT-JEANNERET, L. 2008. The targeted delivery of cancer drugs across the blood–brain barrier: chemical modifications of drugs or drug-nanoparticles? *Drug Discovery Today*, 13, 1099-1106.
- JULIANO, R. & LING, V. 1976. A surface glycoprotein modulating drug permeability in Chinese hamster ovary cell mutants. *Biochimica et biophysica acta*, 455.
- JÄKEL, S. & DIMOU, L. 2017. Glial Cells and Their Function in the Adult Brain: A Journey through the History of Their Ablation. *Frontiers in Cellular Neuroscience*, 11.
- KACHADOURIAN, R. & DAY, B. J. 2006. Flavonoid-induced glutathione depletion: potential implications for cancer treatment. *Free Radical Biology & Medicine*, 41, 65-76.
- KAISAR, M. A., SAJJA, R. K., PRASAD, S., ABHYANKAR, V. V., LILES, T. & CUCULLO, L. 2017. New experimental models of the blood-brain barrier for CNS drug discovery. *Expert Opinion on Drug Discovery*, 12, 89-103.
- KALAPOPOS-KOVÁCS, B., MAGDA, B., JANI, M., FEKETE, Z., PT, S., I, A., P, K. & I, K. 2015a. Multiple ABC Transporters Efflux Baicalin. *Phytotherapy research : PTR*, 29.
- KALAPOPOS-KOVÁCS, B., MAGDA, B., JANI, M., FEKETE, Z., SZABÓ, P. T., ANTAL, I., KRAJCSI, P. & KLEBOVICH, I. 2015b. Multiple ABC Transporters Efflux Baicalin. *Phytother Res*, 29, 1987-90.

- KANG, T. & LIANG, N. 1997. Studies on the inhibitory effects of quercetin on the growth of HL-60 leukemia cells. *Biochemical pharmacology*, 54.
- KANWAR, J., TASKEEN, M., I, M., C, H., TH, C. & QP, D. 2012. Recent advances on tea polyphenols. *Frontiers in bioscience (Elite edition)*, 4.
- KAPÇAK, E. & ŞATANA KARA, E. H. 2018. Development and full validation of a stability-indicating RP-LC method for the determination of anticancer drug Temozolomide in pharmaceutical form. *The Turkish Journal of Pharmaceutical Sciences*.
- KARAMI, F., RANJBAR, S., GHASEMI, Y. & NEGAHDARIPOUR, M. 2019. Analytical methodologies for determination of methotrexate and its metabolites in pharmaceutical, biological and environmental samples. *Journal of Pharmaceutical Analysis*, 9, 373-391.
- KASTAN, M. B. & BARTEK, J. 2004. Cell-cycle checkpoints and cancer. *Nature*, 432, 316-323.
- KATAYAMA, K., MASUYAMA, K., YOSHIOKA, S., HASEGAWA, H., MITSUHASHI, J. & SUGIMOTO, Y. 2007. Flavonoids inhibit breast cancer resistance protein-mediated drug resistance: transporter specificity and structure–activity relationship. *Cancer Chemotherapy and Pharmacology*, 60, 789-797.
- KAUR, G. & DUFOUR, J. M. 2012. Cell lines. *Spermatogenesis*, 2, 1-5.
- KAUR, M. & BADHAN, R. K. 2015. Phytoestrogens Modulate Breast Cancer Resistance Protein Expression and Function at the Blood-Cerebrospinal Fluid Barrier. *J Pharm Pharm Sci*, 18, 132-54.
- KAUR, M. & BADHAN, R. K. 2017. Phytochemical mediated-modulation of the expression and transporter function of breast cancer resistance protein at the blood-brain barrier: An in-vitro study. *Brain Res*, 1654, 9-23.
- KAWAMURA, H., SUGIYAMA, T., DM, W., M, K., S, Y., K, K. & DG, P. 2003. ATP: a vasoactive signal in the pericyte-containing microvasculature of the rat retina. *The Journal of physiology*, 551.
- KIM, M., KIZILBASH, S., JK, L., G, G., KE, P., JN, S. & WF, E. 2018. Barriers to Effective Drug Treatment for Brain Metastases: A Multifactorial Problem in the Delivery of Precision Medicine. *Pharmaceutical research*, 35.
- KIMURA, R. M., WM. 1996. Effects of elevated pCO₂ and/or osmolality on the growth and recombinant tPA production of CHO cells. *Biotechnology and bioengineering*, 52.
- KITAZAWA, T., HOSOYA, K. I., WATANABE, M., TAKASHIMA, T., OHTSUKI, S., TAKANAGA, H., UEDA, M., YANAI, N., OBINATA, M. & TERASAKI, T. 2001. *Pharmaceutical Research*, 18, 16-22.
- KLEINMAN, H., LUCKENBILL-EDDS, L., FW, C. & GC, S. 1987. Use of extracellular matrix components for cell culture. *Analytical biochemistry*, 166.
- KLEINMAN, H. K., KLEBE, R. J. & MARTIN, G. R. 1981. Role of collagenous matrices in the adhesion and growth of cells. *Journal of Cell Biology*, 88, 473-485.
- KNAZEK, R., GULLINO, P., PO, K. & RL, D. 1972. Cell culture on artificial capillaries: an approach to tissue growth in vitro. *Science (New York, N.Y.)*, 178.
- KOBAYASHI, S., TANABE, S., SUGIYAMA, M. & KONISHI, Y. 2008. Transepithelial transport of hesperetin and hesperidin in intestinal Caco-

- 2 cell monolayers. *Biochimica et Biophysica Acta (BBA) - Biomembranes*, 1778, 33-41.
- KOLITZ, J., GEORGE, S., G, M., R, V., BL, P., SL, A., DJ, D., TC, S., W, S., MR, B., V, H., K, M., E, H., JW, V., CD, B. & RA, L. 2010. P-glycoprotein inhibition using valspodar (PSC-833) does not improve outcomes for patients younger than age 60 years with newly diagnosed acute myeloid leukemia: Cancer and Leukemia Group B study 19808. *Blood*, 116.
- KONG, Y., FENG, Z., CHEN, A., QI, Q., HAN, M., WANG, S., ZHANG, Y., ZHANG, X., YANG, N., WANG, J., HUANG, B., ZHANG, Q., XIANG, G., LI, W., ZHANG, D., WANG, J. & LI, X. 2019. The Natural Flavonoid Galangin Elicits Apoptosis, Pyroptosis, and Autophagy in Glioblastoma. *Frontiers in Oncology*, 9.
- KOPUSTINSKIENE, D. M., JAKSTAS, V., SAVICKAS, A. & BERNATONIENE, J. 2020. Flavonoids as Anticancer Agents. *Nutrients*, 12, 457.
- KORFEL, A. & THIEL, E. 2007. Targeted therapy and blood-brain barrier. *Recent results in cancer research. Fortschritte der Krebsforschung. Progres dans les recherches sur le cancer*, 176.
- KRAJKA-KUŹNIAK, V., PALUSZCZAK, J. & BAER-DUBOWSKA, W. 2017. The Nrf2-ARE signaling pathway: An update on its regulation and possible role in cancer prevention and treatment. *Pharmacological reports : PR*, 69.
- KRAKHMAL, N., ZAVYALOVA, M., EV, D., SV, V. & VM, P. 2015. Cancer Invasion: Patterns and Mechanisms. *Acta naturae*, 7.
- KREGER, S., BELL, B., J, B., E, S., J, K., B, W. & SL, V.-H. 2010. Polymerization and matrix physical properties as important design considerations for soluble collagen formulations. *Biopolymers*, 93.
- KRIZANAC-BENGEZ, L., MAYBERG, M. & D, J. 2004. The cerebral vasculature as a therapeutic target for neurological disorders and the role of shear stress in vascular homeostatis and pathophysiology. *Neurological research*, 26.
- KROEMER, G., GALLUZZI, L., VANDENABEELE, P., ABRAMS, J., ALNEMRI, E. S., BAEHRECKE, E. H., BLAGOSKLONNY, M. V., EL-DEIRY, W. S., GOLSTEIN, P., GREEN, D. R., HENGARTNER, M., KNIGHT, R. A., KUMAR, S., LIPTON, S. A., MALORNI, W., NUÑEZ, G., PETER, M. E., TSCHOPP, J., YUAN, J., PIACENTINI, M., ZHIVOTOVSKY, B. & MELINO, G. 2009. Classification of cell death: recommendations of the Nomenclature Committee on Cell Death 2009. *Cell Death & Differentiation*, 16, 3-11.
- KRÖLL, S., EL-GINDI, J., G, T., P, P., S, S., C, H. & HJ, G. 2009. Control of the blood-brain barrier by glucocorticoids and the cells of the neurovascular unit. *Annals of the New York Academy of Sciences*, 1165.
- KUMAGAI, T., MÜLLER, C. I., DESMOND, J. C., IMAI, Y., HEBER, D. & KOEFFLER, H. P. 2007. *Scutellaria baicalensis*, a herbal medicine: Anti-proliferative and apoptotic activity against acute lymphocytic leukemia, lymphoma and myeloma cell lines. *Leukemia Research*, 31, 523-530.
- KUMAR, S. & PANDEY, A. K. 2013. Chemistry and biological activities of flavonoids: an overview. *TheScientificWorldJournal*, 2013, 162750.
- KUNNUMAKKARA, A. B., BORDOLOI, D., PADMAVATHI, G., MONISHA, J., ROY, N. K., PRASAD, S. & AGGARWAL, B. B. 2017. Curcumin, the

- golden nutraceutical: multitargeting for multiple chronic diseases. *British Journal of Pharmacology*, 174, 1325-1348.
- KUNTZ, S., WENZEL, U. & DANIEL, H. 1999. Comparative analysis of the effects of flavonoids on proliferation, cytotoxicity, and apoptosis in human colon cancer cell lines. *Eur J Nutr*, 38, 133-42.
- LAKHANPAL, P. & RAL, D. 2007. *Quercetin: a versatile flavonoid* [Online]. Available: https://www.akspublication.com/paper05_jul-dec2007.htm [Accessed].
- LANDREVILLE, S., AGAPOVA, O. A., KNEASS, Z. T., SALESSE, C. & WILLIAM HARBOUR, J. 2011. ABCB1 identifies a subpopulation of uveal melanoma cells with high metastatic propensity. *Pigment Cell & Melanoma Research*, 24, 430-437.
- LAUER, R., BAUER, R., LINZ, B., PITTNER, F., PESCHEK, G. A., ECKER, G., FRIEDL, P. & NOE, C. R. 2004. Development of an in vitro blood–brain barrier model based on immortalized porcine brain microvascular endothelial cells. *Il Farmaco*, 59, 133-137.
- LAVRIK, I. N. 2005. Caspases: pharmacological manipulation of cell death. *Journal of Clinical Investigation*, 115, 2665-2672.
- LAZEBNIK, Y. 2010. What are the hallmarks of cancer? *Nature reviews. Cancer*, 10.
- LE CLAINCHE, C. & CARLIER, M.-F. J. P. R. 2008. Regulation of actin assembly associated with protrusion and adhesion in cell migration. 88, 489-513.
- LEE, J., SCALA, S., Y, M., B, D., R, R., Z, Z., G, A. & SE, B. 1997. Reduced drug accumulation and multidrug resistance in human breast cancer cells without associated P-glycoprotein or MRP overexpression. *Journal of cellular biochemistry*, 65.
- LEE, Y.-K., HWANG, J.-T., KWON, D. Y., SURH, Y.-J. & PARK, O. J. 2010. Induction of apoptosis by quercetin is mediated through AMPK α 1/ASK1/p38 pathway. *Cancer Letters*, 292, 228-236.
- LEGGAS, M., PANETTA, J., Y, Z., JD, S., B, J., F, B., B, S., S, Z., PJ, H. & CF, S. 2006. Gefitinib modulates the function of multiple ATP-binding cassette transporters in vivo. *Cancer research*, 66.
- LEITNER, I., NEMETH, J., T, F., A, A., P, M., H, L., T, E., O, L. & M, Z. 2011. The third-generation P-glycoprotein inhibitor tariquidar may overcome bacterial multidrug resistance by increasing intracellular drug concentration. *The Journal of antimicrobial chemotherapy*, 66.
- LEMMEN, J., TOZAKIDIS, I. & HJ, G. 2013. Pregnane X receptor upregulates ABC-transporter Abcg2 and Abcb1 at the blood-brain barrier. *Brain research*, 1491.
- LEVY-MISHALI, M., ZOLDAN, J. & S, L. 2009. Effect of scaffold stiffness on myoblast differentiation. *Tissue engineering. Part A*, 15.
- LI, C., ZHANG, L., ZHOU, L., WO, S. K., LIN, G. & ZUO, Z. 2012. Comparison of Intestinal Absorption and Disposition of Structurally Similar Bioactive Flavones in Radix Scutellariae. *The AAPS Journal*, 14, 23-34.
- LI, G., ZHANG, H., LIU, Y., KONG, L., GUO, Q. & JIN, F. 2015. Effect of temozolomide on livin and caspase-3 in U251 glioma stem cells. *Experimental and therapeutic medicine*, 9, 744-750.
- LI, J., GONG, X., JIANG, R., LIN, D., ZHOU, T., A, Z., H, L., X, Z., J, W., G, K. & H, L. 2018a. Fisetin Inhibited Growth and Metastasis of Triple-Negative

- Breast Cancer by Reversing Epithelial-to-Mesenchymal Transition via PTEN/Akt/GSK3 β Signal Pathway. *Frontiers in pharmacology*, 9.
- LI, L., AGARWAL, S. & ELMQUIST, W. F. 2013. Brain Efflux Index To Investigate the Influence of Active Efflux on Brain Distribution of Pemetrexed and Methotrexate. *Drug Metabolism and Disposition*, 41, 659-667.
- LI, Y., POLGAR, O., M, O., L, E., SE, B. & D, X. 2007. Towards understanding the mechanism of action of the multidrug resistance-linked half-ABC transporter ABCG2: a molecular modeling study. *Journal of molecular graphics & modelling*, 25.
- LI, Y., WANG, Z., LI, X., GONG, W., XIE, X., YANG, Y., ZHONG, W. & ZHENG, A. 2017. In Vitro Evaluation of Absorption Characteristics of Peramivir for Oral Delivery. *European Journal of Drug Metabolism and Pharmacokinetics*, 42, 757-765.
- LI, Y., YU, H., HAN, F., WANG, M., LUO, Y. & GUO, X. 2018b. Biochanin A Induces S Phase Arrest and Apoptosis in Lung Cancer Cells. *BioMed Research International*, 2018, 1-12.
- LIANG, G. & ZHANG, Y. 2013. Genetic and epigenetic variations in iPSCs: potential causes and implications for application. *Cell stem cell*, 13.
- LIN, C., TSAI, S.-C., TSENG, M. T., PENG, S.-F., KUO, S.-C., LIN, M.-W., HSU, Y.-M., LEE, M.-R., AMAGAYA, S., HUANG, W.-W., WU, T.-S. & YANG, J.-S. 2013. AKT serine/threonine protein kinase modulates baicalin-triggered autophagy in human bladder cancer T24 cells. *International Journal of Oncology*, 42, 993-1000.
- LIN, C.-W., HOU, W.-C., SHEN, S.-C., JUAN, S.-H., KO, C.-H., WANG, L.-M. & CHEN, Y.-C. 2008. Quercetin inhibition of tumor invasion via suppressing PKC delta/ERK/AP-1-dependent matrix metalloproteinase-9 activation in breast carcinoma cells. *Carcinogenesis*, 29, 1807-1815.
- LIN, F., DE GOOIJER, M., EM, R., LC, B., SM, C., JH, B., T, W., JH, B. & O, V. T. 2014. ABCB1, ABCG2, and PTEN determine the response of glioblastoma to temozolomide and ABT-888 therapy. *Clinical cancer research : an official journal of the American Association for Cancer Research*, 20.
- LINK, A., BALAGUER, F. & GOEL, A. 2010. Cancer chemoprevention by dietary polyphenols: Promising role for epigenetics. *Biochemical Pharmacology*, 80, 1771-1792.
- LIOU, G.-Y. & STORZ, P. 2010. Reactive oxygen species in cancer. *Free Radical Research*, 44, 479-496.
- LIPINSKI, C. A., LOMBARDO, F., DOMINY, B. W. & FEENEY, P. J. 1997. Experimental and computational approaches to estimate solubility and permeability in drug discovery and development settings. *Advanced Drug Delivery Reviews*, 23, 3-25.
- LIPPMANN, E. S., AL-AHMAD, A., AZARIN, S. M., PALECEK, S. P. & SHUSTA, E. V. 2015. A retinoic acid-enhanced, multicellular human blood-brain barrier model derived from stem cell sources. *Scientific Reports*, 4.
- LISKOVA, A., KOKLESOVA, L., SAMEC, M., SMEJKAL, K., SAMUEL, S. M., VARGHESE, E., ABOTALEB, M., BIRINGER, K., KUDELA, E., DANKO, J., SHAKIBAEI, M., KWON, T. K., BÜSSELBERG, D. & KUBATKA, P. 2020. Flavonoids in Cancer Metastasis. *Cancers*, 12, 1498.

- LIU, B., CHEN, Y. & ST CLAIR, D. K. 2008. ROS and p53: a versatile partnership. *Free Radical Biology & Medicine*, 44, 1529-1535.
- LIU, F., GAO, S., YANG, Y., ZHAO, X., FAN, Y., MA, W., YANG, D., YANG, A. & YU, Y. 2017. Curcumin induced autophagy anticancer effects on human lung adenocarcinoma cell line A549. *Oncology Letters*, 14, 2775-2782.
- LIU, Q. R., LIU, J. M., CHEN, Y., XIE, X. Q., XIONG, X. X., QIU, X. Y., PAN, F., LIU, D., YU, S. B. & CHEN, X. Q. 2014. Piperlongumine Inhibits Migration of Glioblastoma Cells via Activation of ROS-Dependent p38 and JNK Signaling Pathways. *Oxidative Medicine and Cellular Longevity*, 2014, 1-12.
- LIU, Z.-H., YANG, C.-X., ZHANG, L., YANG, C.-Y. & XU, X.-Q. 2019. Baicalein, as a Prooxidant, Triggers Mitochondrial Apoptosis in MCF-7 Human Breast Cancer Cells Through Mobilization of Intracellular Copper and Reactive Oxygen Species Generation. *OncoTargets and therapy*, 12, 10749-10761.
- LOCKMAN, P. R., MITTAPALLI, R. K., TASKAR, K. S., RUDRARAJU, V., GRIL, B., BOHN, K. A., ADKINS, C. E., ROBERTS, A., THORSHEIM, H. R., GAASCH, J. A., HUANG, S., PALMIERI, D., STEEG, P. S. & SMITH, Q. R. 2010. Heterogeneous Blood–Tumor Barrier Permeability Determines Drug Efficacy in Experimental Brain Metastases of Breast Cancer. *Clinical Cancer Research*, 16, 5664-5678.
- LODISH, H., BERK, A., ZIPURSKY, S. L., MATSUDAIRA, P., BALTIMORE, D. & DARNELL, J. 2000. *Molecular Cell Biology*, W. H. Freeman.
- LOHMANN, C., HÜWEL, S. & HJ, G. 2002. Predicting blood-brain barrier permeability of drugs: evaluation of different in vitro assays. *Journal of drug targeting*, 10.
- LONSER, R., SARNTINORANONT, M., PF, M. & EH, O. 2015. Convection-enhanced delivery to the central nervous system. *Journal of neurosurgery*, 122.
- LORSCH, J. R., COLLINS, F. S. & LIPPINCOTT-SCHWARTZ, J. 2014. Fixing problems with cell lines. *Science*, 346, 1452-1453.
- LOUIS, D. N., OHGAKI, H., WIESTLER, O. D., CAVENEE, W. K., BURGER, P. C., JOUVET, A., SCHEITHAUER, B. W. & KLEIHUES, P. 2007. The 2007 WHO Classification of Tumours of the Central Nervous System. *Acta Neuropathologica*, 114, 97-109.
- LOUIS, D. N., PERRY, A., REIFENBERGER, G., VON DEIMLING, A., FIGARELLA-BRANGER, D., CAVENEE, W. K., OHGAKI, H., WIESTLER, O. D., KLEIHUES, P. & ELLISON, D. W. 2016. The 2016 World Health Organization Classification of Tumors of the Central Nervous System: a summary. *Acta Neuropathologica*, 131, 803-820.
- LU, J., PAPP, L. V., FANG, J., RODRIGUEZ-NIETO, S., ZHIVOTOVSKY, B. & HOLMGREN, A. 2006. Inhibition of Mammalian Thioredoxin Reductase by Some Flavonoids: Implications for Myricetin and Quercetin Anticancer Activity. *Cancer Research*, 66, 4410-4418.
- LU, P., TAKA, I. K., VM, W. & Z, W. 2011. Extracellular matrix degradation and remodeling in development and disease. *Cold Spring Harbor perspectives in biology*, 3.
- LYE, P., BLOISE, E., NADEEM, L., PENG, C., GIBB, W., ORTIGA-CARVALHO, T. M., LYE, S. J. & MATTHEWS, S. G. 2019. Breast

- Cancer Resistance Protein (BCRP/ABCG2) Inhibits Extra Villous Trophoblast Migration: The Impact of Bacterial and Viral Infection. *Cells*, 8, 1150.
- LYLE, L., LOCKMAN, P., CE, A., AS, M., E, S., E, H., D, P., DJ, L., SM, S., W, K., E, I.-S., R, D., N, N., PK, B., PS, S. & B, G. 2016. Alterations in Pericyte Subpopulations Are Associated with Elevated Blood-Tumor Barrier Permeability in Experimental Brain Metastasis of Breast Cancer. *Clinical cancer research : an official journal of the American Association for Cancer Research*, 22.
- LÓPEZ-BAYGHEN, E. & ORTEGA, A. 2011. Glial glutamate transporters: new actors in brain signaling. *IUBMB life*, 63.
- LÖSCHER, W. & POTSCHKA, H. 2005. Drug resistance in brain diseases and the role of drug efflux transporters. *Nature Reviews Neuroscience*, 6, 591-602.
- M., D., RZHETSKY, A. & ALLIKMETS 2001. The human ATP-binding cassette (ABC) transporter superfamily. *Genome research*, 11.
- M. F. GONÇALVES, B., S. P. CARDOSO, D. & U. FERREIRA, M.-J. 2020. Overcoming Multidrug Resistance: Flavonoid and Terpenoid Nitrogen-Containing Derivatives as ABC Transporter Modulators. *Molecules*, 25, 3364.
- MADSHUS, I. H. 1988. Regulation of intracellular pH in eukaryotic cells. *Biochemical Journal*, 250, 1-8.
- MAHRINGER, A., DELZER, J. & FRICKER, G. 2009. A fluorescence-based in vitro assay for drug interactions with breast cancer resistance protein (BCRP, ABCG2). *European journal of pharmaceuticals and biopharmaceutics : official journal of Arbeitsgemeinschaft fur Pharmazeutische Verfahrenstechnik e.V.*, 72.
- MAHRINGER, A. & FRICKER, G. 2010. BCRP at the blood-brain barrier: Genomic regulation by 17 β -estradiol. *Molecular Pharmaceutics*, 7, 1835-1847.
- MALIEPAARD, M., VAN GASTELEN, M., LA, D. J., D, P., RC, V. W., MC, R.-H., BG, F. & JH, S. 1999. Overexpression of the BCRP/MXR/ABCP gene in a topotecan-selected ovarian tumor cell line. *Cancer research*, 59.
- MALINA, K., COOPER, I. & VI, T. 2009. Closing the gap between the in-vivo and in-vitro blood-brain barrier tightness. *Brain research*, 1284.
- MALUMBRES, M. & BARBACID, M. 2009. Cell cycle, CDKs and cancer: a changing paradigm. *Nature Reviews Cancer*, 9, 153-166.
- MAO, C. M., YU, D. H. & GUI, H. 2017. Effect and mechanism of hesperetin on P-selectin mediated breast cancer MDA-MB-231 metastasis. *Chinese Traditional and Herbal Drugs*, 48, 714-721.
- MAO, Q. & UNADKAT, J. 2005. Role of the breast cancer resistance protein (ABCG2) in drug transport. *The AAPS journal*, 7.
- MAO, Q. & UNADKAT, J. D. J. T. A. J. 2015. Role of the breast cancer resistance protein (BCRP/ABCG2) in drug transport—an update. 17, 65-82.
- MATIAS, D., BALÇA-SILVA, J., DA GRAÇA, G. C., WANJIRU, C. M., MACHARIA, L. W., NASCIMENTO, C. P., ROQUE, N. R., COELHO-AGUIAR, J. M., PEREIRA, C. M., DOS SANTOS, M. F., PESSOA, L. S., LIMA, F. R. S., SCHANAIDER, A., FERRER, V. P. & MOURA-NETO, V. 2018. Microglia/Astrocytes–Glioblastoma Crosstalk: Crucial Molecular

- Mechanisms and Microenvironmental Factors. *Frontiers in Cellular Neuroscience*, 12.
- MATSUZAWA, A. & ICHIJO, H. 2008. Redox control of cell fate by MAP kinase: physiological roles of ASK1-MAP kinase pathway in stress signaling. *Biochimica Et Biophysica Acta*, 1780, 1325-1336.
- MATTHES, F., WÖLTE, P., BÖCKENHOFF, A., S, H., M, S., P, H., J, F., V, G., HJ, G. & U, M. 2011. Transport of arylsulfatase A across the blood-brain barrier in vitro. *The Journal of biological chemistry*, 286.
- MAZZEI, D., GUZZARDI, M., S, G. & A, A. 2010. A low shear stress modular bioreactor for connected cell culture under high flow rates. *Biotechnology and bioengineering*, 106.
- MCCARTHY, N. & EVAN, G. 1998. Methods for detecting and quantifying apoptosis. *Current topics in developmental biology*, 36.
- MCCUBREY, J. A., STEELMAN, L. S., CHAPPELL, W. H., ABRAMS, S. L., WONG, E. W. T., CHANG, F., LEHMANN, B., TERRIAN, D. M., MILELLA, M., TAFURI, A., STIVALA, F., LIBRA, M., BASECKE, J., EVANGELISTI, C., MARTELLI, A. M. & FRANKLIN, R. A. 2007. Roles of the Raf/MEK/ERK pathway in cell growth, malignant transformation and drug resistance. *Biochimica Et Biophysica Acta*, 1773, 1263-1284.
- MEISSNER, K., HEYDRICH, B., JEDLITSCHKY, G., SCHWABEDISSEN, H. M. Z., MOSYAGIN, I., DAZERT, P., ECKEL, L., VOGELGESANG, S., WARZOK, R. W., BÖHM, M., LEHMANN, C., WENDT, M., CASCORBI, I. & KROEMER, H. K. 2006. The ATP-binding Cassette Transporter ABCG2 (BCRP), a Marker for Side Population Stem Cells, Is Expressed in Human Heart. *Journal of Histochemistry & Cytochemistry*, 54, 215-221.
- MEMARIANI, Z., ABBAS, S., HASSAN, S., AHMADI, A. & A, C. 2020. Naringin and naringenin as anticancer agents and adjuvants in cancer combination therapy; efficacy and molecular mechanisms of action, a comprehensive narrative review. *Pharmacological research*.
- MERCHANT, M., KRISHNAN, V. & SAFE, S. 1993. Mechanism of action of alpha-naphthoflavone as an Ah receptor antagonist in MCF-7 human breast cancer cells. *Toxicology and applied pharmacology*, 120.
- MIKITSH, J. L. & CHACKO, A.-M. 2014. Pathways for Small Molecule Delivery to the Central Nervous System across the Blood-Brain Barrier. *Perspectives in Medicinal Chemistry*, 6, PMC.S13384.
- MINOCHA, M., KHURANA, V., QIN, B., PAL, D. & MITRA, A. K. 2012. Co-administration strategy to enhance brain accumulation of vandetanib by modulating P-glycoprotein (P-gp/Abcb1) and breast cancer resistance protein (Bcrp1/Abcg2) mediated efflux with m-TOR inhibitors. *International Journal of Pharmaceutics*, 434, 306-314.
- MIRANDA-AZPIAZU, P., PANAGIOTOU, S., JOSE, G. & SAHA, S. 2018. A novel dynamic multicellular co-culture system for studying individual blood-brain barrier cell types in brain diseases and cytotoxicity testing. *Sci Rep*, 8, 8784.
- MIRANDA-FILHO, A., PIÑEROS, M., SOERJOMATARAM, I., DELTOUR, I. & BRAY, F. 2016. Cancers of the brain and CNS: global patterns and trends in incidence. *Neuro-Oncology*, now166.
- MIURA, Y. H., TOMITA, I., WATANABE, T., HIRAYAMA, T. & FUKUI, S. 1998. Active oxygens generation by flavonoids. *Biol Pharm Bull*, 21, 93-6.

- MIYATA, Y., AKASHI, M. & NISHIDA, E. 1999. Molecular cloning and characterization of a novel member of the MAP kinase superfamily. *Genes to Cells*, 4, 299-309.
- MOHAMMAD, R., BANERJEE, S., Y, L., A, A., O, K. & FH, S. 2006. Cisplatin-induced antitumor activity is potentiated by the soy isoflavone genistein in BxPC-3 pancreatic tumor xenografts. *Cancer*, 106.
- MOHANA, S., GANESAN, M., AGILAN, B., KARTHIKEYAN, R., SRITHAR, G., BEAULAH MARY, R., ANANTHAKRISHNAN, D., VELMURUGAN, D., RAJENDRA PRASAD, N. & AMBUDKAR, S. V. 2016. Screening dietary flavonoids for the reversal of P-glycoprotein-mediated multidrug resistance in cancer. *Molecular BioSystems*, 12, 2458-2470.
- MORI, K., SHIBANUMA, M. & NOSE, K. 2004. Invasive potential induced under long-term oxidative stress in mammary epithelial cells. *Cancer Research*, 64, 7464-7472.
- MORRIS, M. E. & ZHANG, S. 2006. Flavonoid–drug interactions: Effects of flavonoids on ABC transporters. *Life Sciences*, 78, 2116-2130.
- MORROW, C. S., PEKLAK-SCOTT, C., BISHWOKARMA, B., KUTE, T. E., SMITHERMAN, P. K. & TOWNSEND, A. J. 2006. Multidrug Resistance Protein 1 (MRP1, ABCC1) Mediates Resistance to Mitoxantrone via Glutathione-Dependent Drug Efflux. *Molecular Pharmacology*, 69, 1499-1505.
- MOURITSEN, O. & JØRGENSEN, K. 1998. A new look at lipid-membrane structure in relation to drug research. *Pharmaceutical research*, 15.
- MUKHTAR, E., ADHAMI, V., SIDDIQUI, I., VERMA, A. & H, M. 2016. Fisetin Enhances Chemotherapeutic Effect of Cabazitaxel against Human Prostate Cancer Cells. *Molecular cancer therapeutics*, 15.
- MUKHTAR, E., ADHAMI, V. M., SECHI, M. & MUKHTAR, H. 2015. Dietary flavonoid fisetin binds to β -tubulin and disrupts microtubule dynamics in prostate cancer cells. *Cancer Letters*, 367, 173-183.
- MURIITHI, W. M., LW. HEMING, PC. ECHEBARRIA, LJ. 2020. ABC transporters and the hallmarks of cancer: roles in cancer aggressiveness beyond multidrug resistance. *cancer biology and medicine*.
- MUSAFARGANI, S., MISHRA, S., M, G., P, M., G, A., P, P. & B, G. 2020. Blood brain barrier: A tissue engineered microfluidic chip. *Journal of neuroscience methods*, 331.
- NAIK, P. & CUCULLO. L 2012. In vitro blood-brain barrier models: current and perspective technologies. *Journal of pharmaceutical sciences*, 101.
- NAIT CHABANE, M., AL AHMAD, A., J, P., CD, M. & G, U. 2009. Quercetin and naringenin transport across human intestinal Caco-2 cells. *The Journal of pharmacy and pharmacology*, 61.
- NAKAGAWA, S., DELI, M. A., KAWAGUCHI, H., SHIMIZUDANI, T., SHIMONO, T., KITTEL, Á., TANAKA, K. & NIWA, M. 2009. A new blood–brain barrier model using primary rat brain endothelial cells, pericytes and astrocytes. *Neurochemistry International*, 54, 253-263.
- NAKAGAWA, S., DELI, M. A., NAKAO, S., HONDA, M., HAYASHI, K., NAKAOKE, R., KATAOKA, Y. & NIWA, M. 2007. Pericytes from Brain Microvessels Strengthen the Barrier Integrity in Primary Cultures of Rat Brain Endothelial Cells. *Cellular and Molecular Neurobiology*, 27, 687-694.

- NAKANISHI, T. & ROSS, D. D. 2012. Breast cancer resistance protein (BCRP/ABCG2): its role in multidrug resistance and regulation of its gene expression. *Chinese Journal of Cancer*, 31, 73-99.
- NAVANEETHAKRISHNAN, S., ROSALES, J. L. & LEE, K.-Y. 2018. Loss of Cdk5 in breast cancer cells promotes ROS-mediated cell death through dysregulation of the mitochondrial permeability transition pore. *Oncogene*, 37, 1788-1804.
- NAŁĘCZ, K. 2016. Solute Carriers in the Blood–Brain Barrier: Safety in Abundance. *undefined*.
- NCI. 2021. *Cancer Classification | SEER Training* [Online]. Available: <https://training.seer.cancer.gov/disease/categories/classification.html> [Accessed].
- NEAGU, M., CONSTANTIN, C., POPESCU, I. D., ZIPETO, D., TZANAKAKIS, G., NIKITOVIC, D., FENGA, C., STRATAKIS, C. A., SPANDIDOS, D. A. & TSATSAKIS, A. M. 2019. Inflammation and Metabolism in Cancer Cell—Mitochondria Key Player. *Frontiers in Oncology*, 9.
- NEREM, R. 1993. Hemodynamics and the vascular endothelium. *Journal of biomechanical engineering*, 115.
- NEREM, R. M., LEVESQUE, M. J. & CORNHILL, J. F. 1981. Vascular Endothelial Morphology as an Indicator of the Pattern of Blood Flow | *Journal of Biomechanical Engineering* | ASME Digital Collection.
- NEUHAUS, W., LAUER, R., OELZANT, S., UP, F., GF, E. & CR, N. 2006. A novel flow based hollow-fiber blood-brain barrier in vitro model with immortalised cell line PBMEC/C1-2. *Journal of biotechnology*, 125.
- NGUYEN, T. T. T., TRAN, E., NGUYEN, T. H., DO, P. T., HUYNH, T. H. & HUYNH, H. 2004. The role of activated MEK-ERK pathway in quercetin-induced growth inhibition and apoptosis in A549 lung cancer cells. *Carcinogenesis*, 25, 647-659.
- NI, Z., BIKADI, Z., MF, R. & Q, M. 2010. Structure and function of the human breast cancer resistance protein (BCRP/ABCG2). *Current drug metabolism*, 11.
- NIELSEN, I., CHEE, W., L, P., E, O.-C., SE, R., H, F., M, E., D, B., MN, H. & G, W. 2006. Bioavailability is improved by enzymatic modification of the citrus flavonoid hesperidin in humans: a randomized, double-blind, crossover trial. *The Journal of nutrition*, 136.
- NIJLAND, P. G., WITTE, M. E., VAN HET HOF, B., VAN DER POL, S., BAUER, J., LASSMANN, H., VAN DER VALK, P., DE VRIES, H. E. & VAN HORSSSEN, J. 2014. Astroglial PGC-1alpha increases mitochondrial antioxidant capacity and suppresses inflammation: implications for multiple sclerosis. *Acta Neuropathologica Communications*, 2, 170.
- NIJVELDT, R., VAN NOOD, E., DE, V. H., PG, B., K, V. N. & PA, V. L. 2001. Flavonoids: a review of probable mechanisms of action and potential applications. *The American journal of clinical nutrition*, 74.
- NOGUCHI, K., KATAYAMA, K., MITSUHASHI, J. & SUGIMOTO, Y. 2009. Functions of the breast cancer resistance protein (BCRP/ABCG2) in chemotherapy. *Advanced Drug Delivery Reviews*, 61, 26-33.
- ODA, R., SHIRAMIZU, B., M, A.-G., J, K. & V, W. 2018. In Vitro Blood-Brain Barrier Modeling adapted for Peripheral Blood Mononuclear Cell Transmigration from HIV-Positive Patients for Clinical Research on Therapeutic Drug Intervention. *Puerto Rico health sciences journal*, 37.

- OHKA, F., NATSUME, A. & WAKABAYASHI, T. J. N. R. I. 2012. Current trends in targeted therapies for glioblastoma multiforme. 2012.
- OHRSUKI, S., HORI, S. & TERASAKI, T. 2003. Molecular mechanisms of drug influx and efflux transport at the blood-brain barrier.
- OHSHIMA, M., KAMEI, S., FUSHIMI, H., MIMA, S., YAMADA, T. & YAMAMOTO, T. 2019. Prediction of Drug Permeability Using In Vitro Blood–Brain Barrier Models with Human Induced Pluripotent Stem Cell-Derived Brain Microvascular Endothelial Cells. *BioResearch Open Access*, 8, 200-209.
- OHTSUKI, S., IKEDA, C., UCHIDA, Y., SAKAMOTO, Y., MILLER, F., GLACIAL, F., DECLEVES, X., SCHERRMANN, J.-M., COURAUD, P.-O., KUBO, Y., TACHIKAWA, M. & TERASAKI, T. 2013. Quantitative Targeted Absolute Proteomic Analysis of Transporters, Receptors and Junction Proteins for Validation of Human Cerebral Microvascular Endothelial Cell Line hCMEC/D3 as a Human Blood–Brain Barrier Model. *Molecular Pharmaceutics*, 10, 289-296.
- OLESEN, J. & LEONARDI, M. 2003. The burden of brain diseases in Europe. *European journal of neurology*, 10.
- OLIVEIRA-MARQUES, V., MARINHO, H., L, C. & F, A. 2009. Modulation of NF-kappaB-dependent gene expression by H₂O₂: a major role for a simple chemical process in a complex biological response. *Antioxidants & redox signaling*, 11.
- ON, N. H. & MILLER, D. W. J. C. P. D. 2014. Transporter-based delivery of anticancer drugs to the brain: Improving brain penetration by minimizing drug efflux at the blood-brain barrier. 20, 1499-1509.
- OOSTENDORP, R., BUCKLE, T., JH, B., O, V. T. & JH, S. 2009. The effect of P-gp (Mdr1a/1b), BCRP (Bcrp1) and P-gp/BCRP inhibitors on the in vivo absorption, distribution, metabolism and excretion of imatinib. *Investigational new drugs*, 27.
- OZVEGY, C., VÁRADI, A. & B, S. 2002. Characterization of drug transport, ATP hydrolysis, and nucleotide trapping by the human ABCG2 multidrug transporter. Modulation of substrate specificity by a point mutation. *The Journal of biological chemistry*, 277.
- OZVEGY-LACZKA, C., KÖBLÖS, G., B, S. & A, V. 2005. Single amino acid (482) variants of the ABCG2 multidrug transporter: major differences in transport capacity and substrate recognition. *Biochimica et biophysica acta*, 1668.
- PAJOUHESH, H. & LENZ, G. R. 2005. Medicinal chemical properties of successful central nervous system drugs. *NeuroRX*, 2, 541-553.
- PALIT, S., KAR, S., SHARMA, G. & DAS, P. K. 2015. Hesperetin Induces Apoptosis in Breast Carcinoma by Triggering Accumulation of ROS and Activation of ASK1/JNK Pathway. *J Cell Physiol*, 230, 1729-39.
- PAN, C., KUMAR, C., S, B., U, K. & M, M. 2009. Comparative proteomic phenotyping of cell lines and primary cells to assess preservation of cell type-specific functions. *Molecular & cellular proteomics : MCP*, 8.
- PAN, Y., ZHENG, Y. M. & HO, W. S. 2018. Effect of quercetin glucosides from Allium extracts on HepG2, PC-3 and HT-29 cancer cell lines. *Oncology Letters*.
- PANCHE, A. N., DIWAN, A. D. & CHANDRA, S. R. 2016. Flavonoids: an overview. *Journal of Nutritional Science*, 5.

- PAPACONSTANTINO, H. T., XIE, C., ZHANG, W., ANSARI, N. H., HELLMICH, M. R., TOWNSEND, C. M. & KO, T. C. 2001. The role of caspases in methotrexate-induced gastrointestinal toxicity. *Surgery*, 130, 859-865.
- PARDRIDGE, W. 2002. Drug and gene targeting to the brain with molecular trojan horses. *Nature Reviews Drug Discovery*, 1, 131-139.
- PARDRIDGE, W. M. 2005. The blood-brain barrier: Bottleneck in brain drug development. *NeuroRX*, 2, 3-14.
- PARENTEAU-BAREIL, R., GAUVIN, R. & BERTHOD, F. 2010. Collagen-Based Biomaterials for Tissue Engineering Applications. *Materials*, 3, 1863-1887.
- PARLOW, M., WÖLTE, P. & HJ, G. 2009. Regulation of major efflux transporters under inflammatory conditions at the blood-brain barrier in vitro. *Journal of neurochemistry*, 111.
- PARRISH, K., SARKARIA, J. & WF, E. 2015. Improving drug delivery to primary and metastatic brain tumors: strategies to overcome the blood-brain barrier. *Clinical pharmacology and therapeutics*, 97.
- PATABENDIGE, A., SKINNER, R. A., MORGAN, L. & ABBOTT, N. J. 2013. A detailed method for preparation of a functional and flexible blood-brain barrier model using porcine brain endothelial cells. *Brain Res*, 1521, 16-30.
- PATEL, M. & PATEL, B. 2017. Crossing the Blood-Brain Barrier: Recent Advances in Drug Delivery to the Brain. *CNS drugs*, 31.
- PATTISON, R. N., SWAMY, J., MENDENHALL, B., HWANG, C. & FROHLICH, B. T. 2000. Measurement and Control of Dissolved Carbon Dioxide in Mammalian Cell Culture Processes Using an in Situ Fiber Optic Chemical Sensor. *Biotechnology Progress*, 16, 769-774.
- PELICANO, H., CARNEY, D. & HUANG, P. 2004. ROS stress in cancer cells and therapeutic implications. *Drug Resistance Updates: Reviews and Commentaries in Antimicrobial and Anticancer Chemotherapy*, 7, 97-110.
- PENG, H., CHENG, F., HUANG, Y., CHEN, C., TSAI, T. J. J. O. C. B. B. S. & APPLICATIONS 1998. Determination of naringenin and its glucuronide conjugate in rat plasma and brain tissue by high-performance liquid chromatography. 714, 369-374.
- PEPPIATT, C., HOWARTH, C., MOBBS, P. & D, A. 2006. Bidirectional control of CNS capillary diameter by pericytes. *Nature*, 443.
- PEREZ-VIZCAINO, F. & FRAGA, C. 2018. Research trends in flavonoids and health. *Archives of biochemistry and biophysics*, 646.
- PEÑA-SOLÓRZANO, D., STARK, S. A., KÖNIG, B., SIERRA, C. A. & OCHOA-PUENTES, C. 2017. ABCG2/BCRP: Specific and Nonspecific Modulators. 37, 987-1050.
- PICK, A., MÜLLER, H., MAYER, R., HAENISCH, B., PAJEVA, I. K., WEIGT, M., BÖNISCH, H., MÜLLER, C. E. & WIESE, M. 2011. Structure-activity relationships of flavonoids as inhibitors of breast cancer resistance protein (BCRP). *Bioorganic & Medicinal Chemistry*, 19, 2090-2102.
- POLLER, B., GUTMANN, H., KRÄHENBÜHL, S., WEKSLER, B., ROMERO, I., COURAUD, P.-O., TUFFIN, G., DREWE, J. & HUWYLER, J. 2008. The human brain endothelial cell line hCMEC/D3 as a human blood-brain

- barrier model for drug transport studies. *Journal of Neurochemistry*, 107, 1358-1368.
- PONIO, J. B.-D., EL-AYOUBI, F., GLACIAL, F., GANESHAMOORTHY, K., DRIANCOURT, C., GODET, M., PERRIÈRE, N., GUILLEVIC, O., COURAUD, P. O. & UZAN, G. 2014. Instruction of Circulating Endothelial Progenitors In Vitro towards Specialized Blood-Brain Barrier and Arterial Phenotypes. *PLoS ONE*, 9, e84179.
- PONTEN, J. 1975. Neoplastic Human Glia Cells in Culture. 175-206.
- PRAKASH, O., KUMAR, A., KUMAR, P. & AJEET, A. 2013. Anticancer Potential of Plants and Natural Products: A Review. *American Journal of Pharmacological Sciences*, 1, 104-115.
- PROCHÁZKOVÁ, D., BOUŠOVÁ, I. & N, W. 2011. Antioxidant and prooxidant properties of flavonoids. *Fitoterapia*, 82.
- PUECH, C., HODIN, S., FOREST, V., HE, Z., MISMETTI, P., DELAVENNE, X. & PEREK, N. 2018. Assessment of HBEC-5i endothelial cell line cultivated in astrocyte conditioned medium as a human blood-brain barrier model for ABC drug transport studies. *International Journal of Pharmaceutics*, 551, 281-289.
- PULGAR, V. 2019. Transcytosis to Cross the Blood Brain Barrier, New Advancements and Challenges | Neuroscience.
- PULIDO, M., MOLINA, A., G, M., G, M., JG, P. & AI, A. 2006. Interaction of enrofloxacin with breast cancer resistance protein (BCRP/ABCG2): influence of flavonoids and role in milk secretion in sheep. *Journal of veterinary pharmacology and therapeutics*, 29.
- PÖRTNER, R., NAGEL-HEYER, S., GOEPFERT, C., P, A. & NM, M. 2005. Bioreactor design for tissue engineering. *Journal of bioscience and bioengineering*, 100.
- QOSA, H., MILLER, D., P, P. & D, T. 2015. Regulation of ABC efflux transporters at blood-brain barrier in health and neurological disorders. *Brain research*, 1628.
- RABINDRAN, S. R., DD.DOYLE, LA.YANG W & LM, G. 2000. Fumitremorgin C reverses multidrug resistance in cells transfected with the breast cancer resistance protein. *Cancer research*, 60.
- RADAELLI, E., CERUTI, R., V, P., M, R., A, D., V, C., F, C., G, S., E, S., E, P. & R, A. 2009. Immunohistopathological and neuroimaging characterization of murine orthotopic xenograft models of glioblastoma multiforme recapitulating the most salient features of human disease. *Histology and histopathology*, 24.
- RADISKY, D. C., LEVY, D. D., LITTLEPAGE, L. E., LIU, H., NELSON, C. M., FATA, J. E., LEAKE, D., GODDEN, E. L., ALBERTSON, D. G., ANGELA NIETO, M., WERB, Z. & BISSELL, M. J. 2005. Rac1b and reactive oxygen species mediate MMP-3-induced EMT and genomic instability. *Nature*, 436, 123-127.
- RAJAMANICKAM, V., GUNASEKARAN, S., BERNINI, R., PAUL, P., RIYASDEEN, A., AKBARSHA, M. A., MENON, V. & N, N. 2012. Role of hesperetin (a natural flavonoid) and its analogue on apoptosis in HT-29 human colon adenocarcinoma cell line--a comparative study. *Food and Chemical Toxicology*, 50, 660-671.
- RASHID, M. I., FAREED, M. I., RASHID, H., AZIZ, H., EHSAN, N., KHALID, S., GHAFFAR, I., ALI, R., GUL, A. & HAKEEM, K. R. 2019. Flavonoids and

- Their Biological Secrets. *Plant and Human Health, Volume 2*. Springer International Publishing.
- REDMOND, E. C., PAUL A. JAMES, V. SITZMANN 1995. Perfused Transcapillary Smooth Muscle and Endothelial Cell Co-Culture: A Novel in vitro Model. *In Vitro Cellular & Developmental Biology. Animal*, 31, 601-609.
- REDZA-DUTORDOIR, M. & AVERILL-BATES, D. A. 2016. Activation of apoptosis signalling pathways by reactive oxygen species. *Biochimica et Biophysica Acta (BBA) - Molecular Cell Research*, 1863, 2977-2992.
- REHMAN, A. U., DUGIC, E., BENHAM, C., LIONE, L. & MACKENZIE, L. S. 2014. Selective inhibition of NADPH oxidase reverses the over contraction of diabetic rat aorta. *Redox Biology*, 2, 61-64.
- REMPE, R., CRAMER, S., QIAO, R. & HJ, G. 2014. Strategies to overcome the barrier: use of nanoparticles as carriers and modulators of barrier properties. *Cell and tissue research*, 355.
- REN, S., SUO, Q., DU, W., H, P., MM, Y., RH, W. & J, L. 2010. [Quercetin permeability across blood-brain barrier and its effect on the viability of U251 cells]. *Sichuan da xue xue bao. Yi xue ban = Journal of Sichuan University. Medical science edition*, 41.
- REN, W., QIAO, Z., WANG, H., ZHU, L. & ZHANG, L. 2003. Flavonoids: promising anticancer agents. *Medicinal Research Reviews*, 23, 519-534.
- RHEE, S. G. 2006. Cell signaling. H₂O₂, a necessary evil for cell signaling. *Science (New York, N.Y.)*, 312, 1882-1883.
- RICE-EVANS, C. A., MILLER, N. J. & PAGANGA, G. 1996. Structure-antioxidant activity relationships of flavonoids and phenolic acids. *Free Radical Biology and Medicine*, 20, 933-956.
- ROBEY, R., HONJO, Y., A, V. D. L., K, M., JT, R., T, L. & SE, B. 2001a. A functional assay for detection of the mitoxantrone resistance protein, MXR (ABCG2). *Biochimica et biophysica acta*, 1512.
- ROBEY, R., PLUCHINO, K., MD, H., AT, F., SE, B. & MM, G. 2018. Revisiting the role of ABC transporters in multidrug-resistant cancer. *Nature reviews. Cancer*, 18.
- ROBEY, R. W., HONJO, Y., VAN DE LAAR, A., MIYAKE, K., REGIS, J. T., LITMAN, T. & BATES, S. E. 2001b. A functional assay for detection of the mitoxantrone resistance protein, MXR (ABCG2). *Biochimica et Biophysica Acta (BBA) - Biomembranes*, 1512, 171-182.
- ROCK, K., MCARDLE, O., FORDE, P., DUNNE, M., FITZPATRICK, D., O'NEILL, B. & FAUL, C. J. T. B. J. O. R. 2012. A clinical review of treatment outcomes in glioblastoma multiforme—the validation in a non-trial population of the results of a randomised Phase III clinical trial: has a more radical approach improved survival? 85, e729-e733.
- RODRÍGUEZ-GARCÍA, C., SÁNCHEZ-QUESADA, C. & GAFORIO, J. J. 2019. Dietary Flavonoids as Cancer Chemopreventive Agents: An Updated Review of Human Studies. *Antioxidants*, 8, 137.
- ROSS, D., YANG, W., ABRUZZO, L., WS, D., E, S., H, L., M, D., L, G., SP, C. & LA, D. 1999. Atypical multidrug resistance: breast cancer resistance protein messenger RNA expression in mitoxantrone-selected cell lines. *Journal of the National Cancer Institute*, 91.
- ROUNDHILL, E. A., FLETCHER, J. I., HABER, M. & NORRIS, M. D. 2015. Clinical Relevance of Multidrug-Resistance-Proteins (MRPs) for

- Anticancer Drug Resistance and Prognosis. In: EFFERTH, T. (ed.) *Resistance to Targeted ABC Transporters in Cancer*. Cham: Springer International Publishing.
- ROUX, F., DURIEU-TRAUTMANN, O., CHAVEROT, N., CLAIRE, M., P, M., JM, B., AD, S. & PO, C. 1994. Regulation of gamma-glutamyl transpeptidase and alkaline phosphatase activities in immortalized rat brain microvessel endothelial cells. *Journal of cellular physiology*, 159.
- ROWINSKY, E. K., SMITH, L., WANG, Y. M., CHATURVEDI, P., VILLALONA, M., CAMPBELL, E., AYLESWORTH, C., ECKHARDT, S. G., HAMMOND, L., KRAYNAK, M., DREGLER, R., STEPHENSON, J., HARDING, M. W. & VON HOFF, D. D. 1998. Phase I and pharmacokinetic study of paclitaxel in combination with biricodar, a novel agent that reverses multidrug resistance conferred by overexpression of both MDR1 and MRP. *Journal of Clinical Oncology: Official Journal of the American Society of Clinical Oncology*, 16, 2964-2976.
- RUBIN, L., HALL, D., S, P., K, B., C, C., HC, H., M, J., CW, L., K, M. & J, M. 1991. A cell culture model of the blood-brain barrier. *The Journal of cell biology*, 115.
- SABLINA, A. A., BUDANOV, A. V., ILYINSKAYA, G. V., AGAPOVA, L. S., KRAVCHENKO, J. E. & CHUMAKOV, P. M. 2005. The antioxidant function of the p53 tumor suppressor. *Nature medicine*, 11, 1306-1313.
- SAK, K. 2014. Cytotoxicity of dietary flavonoids on different human cancer types. *Pharmacognosy reviews*, 8.
- SALDANHA, S. & TOLLEFSBOL, T. 2011. The Role of Nutraceuticals in Chemoprevention and Chemotherapy and Their Clinical Outcomes. *Journal of Oncology*, 2012.
- SAMBANTHAM, S., RADHA, M., PARAMASIVAM, A., ANANDAN, B., MALATHI, R., CHANDRA, S. R. & JAYARAMAN, G. 2013. Molecular Mechanism Underlying Hesperetin-induced Apoptosis by in silico Analysis and in Prostate Cancer PC-3 Cells. *Asian Pacific Journal of Cancer Prevention*, 14, 4347-4352.
- SAMPER, E., NICHOLLS, D. G. & MELOV, S. 2003. Mitochondrial oxidative stress causes chromosomal instability of mouse embryonic fibroblasts. *Aging Cell*, 2, 277-285.
- SAN-GALLI, F., VRIGNAUD, P., ROBERT, J., COINDRE, JM., VRIGNAUD, ROBERT, J., COINDRE, J. M. & COHADON, F. 1989. Assessment of the experimental model of transplanted C6 glioblastoma in wistar rats. *Journal of Neuro-Oncology*, 7, 299-304.
- SANCHEZ-COVARRUBIAS, L., SLOSKY, L., THOMPSON, B., DAVIS, T. & RONALDSON, P. 2014. Transporters at CNS barrier sites: obstacles or opportunities for drug delivery? *Current pharmaceutical design*, 20.
- SANE, R., WU, S.-P., ZHANG, R. & GALLO, J. M. 2014. The Effect of ABCG2 and ABCC4 on the Pharmacokinetics of Methotrexate in the Brain. *Drug Metabolism and Disposition*, 42, 537-540.
- SANTAGUIDA, S., JANIGRO, D., HOSSAIN, M., E, O., E, R. & L, C. 2006. Side by side comparison between dynamic versus static models of blood-brain barrier in vitro: a permeability study. *Brain research*, 1109.
- SANTELLLO, M., CAL, Ì. C. & BEZZ, I. P. 2012. Gliotransmission and the tripartite synapse. *Advances in experimental medicine and biology*, 970.

- SANTOS, B. L., OLIVEIRA, M. N., COELHO, P. L., PITANGA, B. P., DA SILVA, A. B., ADELITA, T., SILVA, V. D., COSTA MDE, F., EL-BACHÁ, R. S., TARDY, M., CHNEIWEISS, H., JUNIER, M. P., MOURA-NETO, V. & COSTA, S. L. 2015. Flavonoids suppress human glioblastoma cell growth by inhibiting cell metabolism, migration, and by regulating extracellular matrix proteins and metalloproteinases expression. *Chem Biol Interact*, 242, 123-38.
- SANTOS, B. L., SILVA, A. R., PITANGA, B. P. S., SOUSA, C. S., GRANGEIRO, M. S., FRAGOMENI, B. O., COELHO, P. L. C., OLIVEIRA, M. N., MENEZES-FILHO, N. J., COSTA, M. F. D., EL-BACHÁ, R. S., VELOZO, E. S., SAMPAIO, G. P., FREIRE, S. M., TARDY, M. & COSTA, S. L. 2011. Antiproliferative, proapoptotic and morphogenic effects of the flavonoid rutin on human glioblastoma cells. *Food Chemistry*, 127, 404-411.
- SARKARIA, J., HU, L., IF, P., DH, P., DH, B., NN, L., C, G., TC, B., SH, K., JK, L., KR, S., TJ, K., PD, B., NYR, A., E, G., JC, B. & WF, E. 2018. Is the blood-brain barrier really disrupted in all glioblastomas? A critical assessment of existing clinical data. *Neuro-oncology*, 20.
- SBRANA, T. & AHLUWALIA, A. 2012. Engineering Quasi-Vivo in vitro organ models. *Advances in experimental medicine and biology*, 745.
- SCHIEBER, M. & CHANDEL, NAVDEEP S. 2014. ROS Function in Redox Signaling and Oxidative Stress. *Current Biology*, 24, R453-R462.
- SCHLAGETER, K., MOLNAR, P., GD, L. & DR, G. 1999. Microvessel organization and structure in experimental brain tumors: microvessel populations with distinctive structural and functional properties. *Microvascular research*, 58.
- SCHNEIDER, J., GONZALEZ-ROCES, S., POLLÁN, M., LUCAS, R., TEJERINA, A., MARTIN, M. & ALBA, A. 2001. Expression of LRP and MDR1 in locally advanced breast cancer predicts axillary node invasion at the time of rescue mastectomy after induction chemotherapy. *Breast Cancer Research*, 3.
- SCHNITTLER, H.-J. 1998. Structural and functional aspects of intercellular junctions in vascular endothelium. *Basic Research in Cardiology*, 93, s030-s039.
- SCHUHMANN, M. K. & FLURI, F. 2017. Effects of fullerenols on mouse brain microvascular endothelial cells.
- SCHULZE, C., SMALES, C., LL, R. & JM, S. 1997. Lysophosphatidic acid increases tight junction permeability in cultured brain endothelial cells. *Journal of neurochemistry*, 68.
- SCOTTO, K. W. 2003. Transcriptional regulation of ABC drug transporters. *Oncogene*, 22, 7496-7511.
- SEELIG, A. 2007. The role of size and charge for blood-brain barrier permeation of drugs and fatty acids. *Journal of molecular neuroscience : MN*, 33.
- SENBABA OGLU, F., CINGOZ, A., KAYA, E., KAZANCIOGLU, S., LACK, N. A., ACILAN, C. & BAGCI-ONDER, T. 2016. Identification of Mitoxantrone as a TRAIL-sensitizing agent for Glioblastoma Multiforme. *Cancer Biology & Therapy*, 17, 546-557.
- SESINK, A., ARTS, I., DE BOER, V., P, B., JH, S., PC, H. & FG, R. 2005. Breast cancer resistance protein (Bcrp1/Abcg2) limits net intestinal

- uptake of quercetin in rats by facilitating apical efflux of glucuronides. *Molecular pharmacology*, 67.
- SEYFRIED, T. N., FLORES, R. E., POFF, A. M. & D'AGOSTINO, D. P. 2014. Cancer as a metabolic disease: implications for novel therapeutics. *Carcinogenesis*, 35, 515-527.
- SHALINI, S., DORSTYN, L., DAWAR, S. & KUMAR, S. 2015. Old, new and emerging functions of caspases. *Cell Death & Differentiation*, 22, 526-539.
- SHANG, H.-S., CHANG, C.-H., CHOU, Y.-R., YEH, M.-Y., AU, M.-K., LU, H.-F., CHU, Y.-L., CHOU, H.-M., CHOU, H.-C., SHIH, Y.-L. & CHUNG, J.-G. 2016. Curcumin causes DNA damage and affects associated protein expression in HeLa human cervical cancer cells. *Oncology Reports*, 36, 2207-2215.
- SHARMA 2009. Curcumin induces caspase and calpain-dependent apoptosis in HT29 human colon cancer cells. *Molecular Medicine Reports*, 2.
- SHARMA, H., SEN, S. & N, S. 2005. Molecular pathways in the chemosensitization of cisplatin by quercetin in human head and neck cancer. *Cancer biology & therapy*, 4.
- SHARMA, V., JOSEPH, C., GHOSH, S., AGARWAL, A., MISHRA, M. K. & SEN, E. 2007a. Kaempferol induces apoptosis in glioblastoma cells through oxidative stress. *Mol Cancer Ther*, 6, 2544-53.
- SHARMA, V., JOSEPH, C., GHOSH, S., AGARWAL, A., MISHRA, M. K. & SEN, E. 2007b. Kaempferol induces apoptosis in glioblastoma cells through oxidative stress. *Molecular Cancer Therapeutics*, 6, 2544-2553.
- SHEN, C., CHEN, R., Z, Q., X, M., T, H., Y, L., Z, C., C, H., C, H. & J, L. 2015. Intestinal absorption mechanisms of MTBH, a novel hesperetin derivative, in Caco-2 cells, and potential involvement of monocarboxylate transporter 1 and multidrug resistance protein 2. *European journal of pharmaceutical sciences : official journal of the European Federation for Pharmaceutical Sciences*, 78.
- SHEN, K.-H., HUNG, S.-H., YIN, L.-T., HUANG, C.-S., CHAO, C.-H., LIU, C.-L. & SHIH, Y.-W. 2010. Acacetin, a flavonoid, inhibits the invasion and migration of human prostate cancer DU145 cells via inactivation of the p38 MAPK signaling pathway. *Molecular and Cellular Biochemistry*, 333, 279-291.
- SHI, X., LUO, X., CHEN, T., GUO, W., LIANG, C., TANG, S. & MO, J. 2021. Naringenin inhibits migration, invasion, induces apoptosis in human lung cancer cells and arrests tumour progression in vitro. *Journal of Cellular and Molecular Medicine*, 25, 2563-2571.
- SHIEH, D., CHENG, H., YEN, M., LC, C. & CC, L. 2006. Baicalin-induced apoptosis is mediated by Bcl-2-dependent, but not p53-dependent, pathway in human leukemia cell lines. *The American journal of Chinese medicine*, 34.
- SHIELDS, C. L., SIOUFI, K., ALSET, A. E., BOAL, N. S., CASEY, M. G., KNAPP, A. N., SUGARMAN, J. A., SCHOEN, M. A., GORDON, P. S., SAY, E. A. T. & SHIELDS, J. A. 2017. Clinical Features Differentiating Benign From Malignant Conjunctival Tumors in Children. *JAMA Ophthalmology*, 135, 215.

- SHIGETA, J., KATAYAMA, K., MITSUHASHI, J., NOGUCHI, K. & SUGIMOTO, Y. 2010. BCRP/ABCG2 confers anticancer drug resistance without covalent dimerization. *Cancer Science*, 101, 1813-1821.
- SHUKLA, S., ROBEY, R., SE, B. & SV, A. 2009a. Sunitinib (Sutent, SU11248), a small-molecule receptor tyrosine kinase inhibitor, blocks function of the ATP-binding cassette (ABC) transporters P-glycoprotein (ABCB1) and ABCG2. *Drug metabolism and disposition: the biological fate of chemicals*, 37.
- SHUKLA, S., ZAHER, H., HARTZ, A., BAUER, B., WARE, J. A. & AMBUDKAR, S. V. 2009b. Curcumin Inhibits the Activity of ABCG2/BCRP1, a Multidrug Resistance-Linked ABC Drug Transporter in Mice. *Pharmaceutical Research*, 26, 480-487.
- SIEGEL, R. L., MILLER, K. D. & JEMAL, A. 2020. Cancer statistics, 2020. *CA: A Cancer Journal for Clinicians*, 70, 7-30.
- SIEGELIN, M. D., REUSS, D. E., HABEL, A., RAMI, A. & VON DEIMLING, A. 2009. Quercetin promotes degradation of survivin and thereby enhances death-receptor-mediated apoptosis in glioma cells. *Neuro-oncology*, 11, 122-131.
- SINGH, R. D., HARIDAS, N., PATEL, J. B., SHAH, F. D., SHUKLA, S. N., SHAH, P. M. & PATEL, P. S. 2010. Matrix metalloproteinases and their inhibitors: correlation with invasion and metastasis in oral cancer. *Indian journal of clinical biochemistry: IJCB*, 25, 250-259.
- SIVAGAMI, G., VINOTHKUMAR, R., PREETHY, C. P., RIYASDEEN, A., AKBARSHA, M. A., MENON, V. P. & NALINI, N. 2012. Role of hesperetin (a natural flavonoid) and its analogue on apoptosis in HT-29 human colon adenocarcinoma cell line – A comparative study. *Food and Chemical Toxicology*, 50, 660-671.
- SIVANDZADE, F. & CUCULLO, L. 2018. In-vitro blood–brain barrier modeling: A review of modern and fast-advancing technologies. *Journal of Cerebral Blood Flow & Metabolism*, 38, 1667-1681.
- SKINNER, R., GIBSON, R., ROTHWELL, N., PINTEAUX, E. & PENNY, J. 2009. Transport of interleukin-1 across cerebrovascular endothelial cells. *British Journal of Pharmacology*, 156, 1115-1123.
- SOBUE, K., YAMAMOTO, N., K, Y., ME, H., K, Y., N, T., T, T., H, K., Y, M., K, A. & T, K. 1999. Induction of blood-brain barrier properties in immortalized bovine brain endothelial cells by astrocytic factors. *Neuroscience research*, 35.
- SOUZA, P., BIANCHI, S., F, F., L, H., KS, M., RM, G., JB, H., CP, K., CG, S., DP, G., VL, B., A, Z. F. & JCF, M. 2018. Anticancer activity of flavonoids isolated from *Achyrocline satureioides* in gliomas cell lines. *Toxicology in vitro : an international journal published in association with BIBRA*, 51.
- SOWNDHARARAJAN, K., DEEPA, P., KIM, M., PARK, S. J. & KIM, S. 2017. Baicalein as a potent neuroprotective agent: A review. *Biomed Pharmacother*, 95, 1021-1032.
- SRIGUNAPALAN, S., LAM, C., WHEELER, A. R. & SIMMONS, C. A. 2011. A microfluidic membrane device to mimic critical components of the vascular microenvironment. *Biomicrofluidics*, 5, 013409.
- STAEDLER, D., IDRIZI, E., BH, K. & L, J.-J. 2011. Drug combinations with quercetin: doxorubicin plus quercetin in human breast cancer cells. *Cancer chemotherapy and pharmacology*, 68.

- STANNESS, K., WESTRUM, L., FORNACIARI, E., P, M., JA, N., SG, S., T, M. & D, J. 2020. Morphological and functional characterization of an in vitro blood-brain barrier model. *Brain Research*, 771, 329-342.
- STANNESS, K. A., WESTRUM, L. E., FORNACIARI, E., MASCAGNI, P., NELSON, J. A., STENGLEIN, S. G., MYERS, T. & JANIGRO, D. 1997. Morphological and functional characterization of an in vitro blood-brain barrier model. *Brain Research*, 771, 329-342.
- STARKOV, A. A. 2008. The Role of Mitochondria in Reactive Oxygen Species Metabolism and Signaling. *Annals of the New York Academy of Sciences*, 1147, 37-52.
- STEINER, O., COISNE, C., CECHELLI, R., BOSCACCI, R., DEUTSCH, U., ENGELHARDT, B. & LYCK, R. 2010. Differential Roles for Endothelial ICAM-1, ICAM-2, and VCAM-1 in Shear-Resistant T Cell Arrest, Polarization, and Directed Crawling on Blood-Brain Barrier Endothelium. *The Journal of Immunology*, 185, 4846-4855.
- STEWART, C., LEGGAS, M., SCHUETZ, J., JC, P., PJ, C., J, P., N, D., JJ, J., R, G., GS, G., FC, H. & PJ, H. 2004. Gefitinib enhances the antitumor activity and oral bioavailability of irinotecan in mice. *Cancer research*, 64.
- STIEGER, B. & GAO, B. J. C. P. 2015. Drug transporters in the central nervous system. 54, 225-242.
- STUPP, R., HEGI, M. E., GILBERT, M. R. & CHAKRAVARTI, A. 2007. Chemoradiotherapy in malignant glioma: standard of care and future directions. *Journal of Clinical Oncology: Official Journal of the American Society of Clinical Oncology*, 25, 4127-4136.
- SUH, Y., AFAQ, F., JOHNSON, J. & H, M. 2009. A plant flavonoid fisetin induces apoptosis in colon cancer cells by inhibition of COX2 and Wnt/EGFR/NF-kappaB-signaling pathways. *Carcinogenesis*, 30.
- SUMMERS, M., MOORE, J. & JW, M. 2004. Use of verapamil as a potential P-glycoprotein inhibitor in a patient with refractory epilepsy. *The Annals of pharmacotherapy*, 38.
- SUN, X., LIU, X., ZHANG, Y., X, K., B, L. & J, G. 2013. A simple and effective pressure culture system modified from a transwell cell culture system. *Biological research*, 46.
- SUN, Y.-L., PATEL, A., KUMAR, P. & CHEN, Z.-S. 2012. Role of ABC transporters in cancer chemotherapy. *Chinese Journal of Cancer*, 31, 51-57.
- SUZUKI, K. T., KAZUHIRO. AOYAMA, TAKAO. & WATANABE, Y. 2019. Usefulness of novobiocin as a selective inhibitor of intestinal breast cancer resistance protein (Bcrp) in rats. <https://doi.org/10.1080/00498254.2019.1708514>.
- SZATROWSKI, T. P. & NATHAN, C. F. 1991. Production of Large Amounts of Hydrogen Peroxide by Human Tumor Cells. *Cancer Research*, 51, 794-798.
- SZLISZKA, E., CZUBA, Z. P., MERTAS, A., PARADYSZ, A. & KROL, W. 2013. The dietary isoflavone biochanin-A sensitizes prostate cancer cells to TRAIL-induced apoptosis. *Urologic Oncology: Seminars and Original Investigations*, 31, 331-342.
- SÁ-PEREIRA, I., BRITES, D. & BRITO, M. 2012. Neurovascular unit: a focus on pericytes. *Molecular neurobiology*, 45.

- TAKAHATA, T., OOKAWA, K., SUTO, K., TANAKA, M., YANO, H., NAKASHIMA, O., KOJIRO, M., TAMURA, Y., TATEISHI, T., SAKATA, Y. & FUKUDA, S. 2008. Chemosensitivity Determinants of Irinotecan Hydrochloride in Hepatocellular Carcinoma Cell Lines. *Basic & Clinical Pharmacology & Toxicology*, 102, 399-407.
- TAMA, I. I. & A., T. I. 2000. Transporter-mediated permeation of drugs across the blood-brain barrier. *Journal of pharmaceutical sciences*, 89.
- TAN, A. C., ASHLEY, D. M., LÓPEZ, G. Y., MALINZAK, M., FRIEDMAN, H. S. & KHASRAW, M. 2020. Management of glioblastoma: State of the art and future directions. *CA: A Cancer Journal for Clinicians*, 70, 299-312.
- TANG, S., LAGAS, J., NA, L., B, P., MJ, H., H, R., JH, B. & AH, S. 2012. Brain accumulation of sunitinib is restricted by P-glycoprotein (ABCB1) and breast cancer resistance protein (ABCG2) and can be enhanced by oral elacridar and sunitinib coadministration. *International journal of cancer*, 130.
- TANG, Y., SOROUSH, F., SUN, S., LIVERANI, E., LANGSTON, J. C., YANG, Q., KILPATRICK, L. E. & KIANI, M. F. 2018. Protein kinase C-delta inhibition protects blood-brain barrier from sepsis-induced vascular damage. *Journal of Neuroinflammation*, 15.
- TARIN, D. 2011. Cell and tissue interactions in carcinogenesis and metastasis and their clinical significance. *Seminars in cancer biology*, 21.
- TARRAGÓ, T., KICHIK, N., CLAASEN, B., R, P., M, T. & E, G. 2008. Baicalin, a prodrug able to reach the CNS, is a prolyl oligopeptidase inhibitor. *Bioorganic & medicinal chemistry*, 16.
- TAUBERT, D., BREITENBACH, T., A, L., P, C., S, H., R, B., W, K. & R, R. 2003. Reaction rate constants of superoxide scavenging by plant antioxidants. *Free radical biology & medicine*, 35.
- TAYLOR, D., PARSONS, C., H, H., A, J. & K, R. 2011. Parallel screening of FDA-approved antineoplastic drugs for identifying sensitizers of TRAIL-induced apoptosis in cancer cells. *BMC cancer*, 11.
- TEIFEL, M. & FRIEDL, P. 1996. Establishment of the permanent microvascular endothelial cell line PBMEC/C1-2 from porcine brains. *Experimental Cell Research*, 228, 50-57.
- TEJEDOR, J., VELA, A., A, G., A, C., L, D. & JF, F.-G. 2011. A genetic comparison of pig, cow and trout isolates of *Lactococcus garvieae* by PFGE analysis. *Letters in applied microbiology*, 53.
- TENNANT, D. A., DURÁN, R. V., BOULAHBEL, H. & GOTTLIEB, E. 2009. Metabolic transformation in cancer. *Carcinogenesis*, 30, 1269-1280.
- THAKKAR, J. P., DOLECEK, T. A., HORBINSKI, C., OSTROM, Q. T., LIGHTNER, D. D., BARNHOLTZ-SLOAN, J. S., VILLANO, J. L. J. C. E. & BIOMARKERS, P. 2014. Epidemiologic and molecular prognostic review of glioblastoma. 23, 1985-1996.
- THOMSEN, L., BURKHART, A. & T, M. 2015. A Triple Culture Model of the Blood-Brain Barrier Using Porcine Brain Endothelial cells, Astrocytes and Pericytes. *PloS one*, 10.
- TIAN, Y., HAN, X. & TIAN, D.-L. 2012. The biological regulation of ABCE1. *IUBMB Life*, 64, 795-800.
- TILLING, T., KORTE, D., D, H. & HJ, G. 1998. Basement membrane proteins influence brain capillary endothelial barrier function in vitro. *Journal of neurochemistry*, 71.

- TIWARI, A. K., SODANI, K., DAI, C.-L., ASHBY, C. R. & CHEN, Z.-S. 2011. Revisiting the ABCs of multidrug resistance in cancer chemotherapy. *Current Pharmaceutical Biotechnology*, 12, 570-594.
- TOROK, M., HUWYLER, J., H, G., G, F. & J, D. 2003. Modulation of transendothelial permeability and expression of ATP-binding cassette transporters in cultured brain capillary endothelial cells by astrocytic factors and cell-culture conditions. *Experimental brain research*, 153.
- TOYODA, Y., TAKADA, T. & SUZUKI, H. 2019. Inhibitors of Human ABCG2: From Technical Background to Recent Updates With Clinical Implications. *Front Pharmacol*, 10, 208.
- TUNG-HU, T. & MEI-CHUN, L. 2004. Determination of unbound theophylline in rat blood and brain by microdialysis and liquid chromatography. *Journal of chromatography. A*, 1032.
- UCHIDA, Y., OHTSUKI, S., KATSUKURA, Y., C, I., T, S., J, K. & T, T. 2011. Quantitative targeted absolute proteomics of human blood-brain barrier transporters and receptors. *Journal of neurochemistry*, 117.
- UH, U. H. 2018. *Brain Tumors: Introduction* [Online]. Available: <https://www.uhhospitals.org/sitecore/content/UHHospitals/Demo/Home/health-and-wellness/health-and-wellness-library/article/cancer-source-v1/types-of-brain-tumors#UH-CloseMenu> [Accessed].
- URICH, E., LAZIC, S., J, M., I, W. & PO, F. 2012. Transcriptional profiling of human brain endothelial cells reveals key properties crucial for predictive in vitro blood-brain barrier models. *PLoS one*, 7.
- VALDAMERI, G., PEREIRA RANGEL, L., SPATAFORA, C., GUITTON, J., GAUTHIER, C., ARNAUD, O., FERREIRA-PEREIRA, A., FALSON, P., WINNISCHOFER, S. M., ROCHA, M. E., TRINGALI, C. & DI PIETRO, A. 2012. Methoxy stilbenes as potent, specific, untransported, and noncytotoxic inhibitors of breast cancer resistance protein. *ACS Chem Biol*, 7, 322-30.
- VALDAMERI, G., RANGEL, L. P. C. S., GUITTON, J., GAUTHIER, C., ARNAUD, O., FERREIRA-PEREIRA, A., FALSON, P., WINNISCHOFER, S. M. B., ROCHA, M. E. M., TRINGALI, C. & PIETRO, A. D. 2011. Methoxy Stilbenes as Potent, Specific, Untransported, and Noncytotoxic Inhibitors of Breast Cancer Resistance Protein.
- VALKO, M., LEIBFRITZ, D., J, M., MT, C., M, M. & J, T. 2007. Free radicals and antioxidants in normal physiological functions and human disease. *The international journal of biochemistry & cell biology*, 39.
- VAN TELLINGEN, O., YETKIN-ARIK, B., MC, D. G., P, W., T, W. & HE, D. V. 2015. Overcoming the blood-brain tumor barrier for effective glioblastoma treatment. *Drug resistance updates : reviews and commentaries in antimicrobial and anticancer chemotherapy*, 19.
- VAN ZIJL, F., KRUPITZA, G. & W, M. 2011. Initial steps of metastasis: cell invasion and endothelial transmigration. *Mutation research*, 728.
- VAUX, D. & SILKE, J. 2003. Mammalian mitochondrial IAP binding proteins. *Biochemical and biophysical research communications*, 304.
- VOLK, E., FARLEY, K., Y, W., F, L., RW, R. & E, S. 2002. Overexpression of wild-type breast cancer resistance protein mediates methotrexate resistance. *Cancer Research*, 62, 5035-5040.

- VOLPE, D. A. A., PATRICK J., CIAVARELLA, A. B., ASAFU-ADJAYE, E. B., ELLISON, C. D., YU, L. X. & HUSSAIN, A. S. 2008. Classification of Drug Permeability with a Caco-2 Cell Monolayer Assay. *Ceased*.
- VOZZI, I. F. H., JM.BADER, A.AHLUWALIA AD 2008. Connected culture of murine hepatocytes and HUVEC in a multicompartamental bioreactor. *Tissue engineering. Part A*, 15, 1291-1299.
- VOZZI, F., HEINRICH, J.-M., BADER, A. & AHLUWALIA, A. D. 2008. Connected Culture of Murine Hepatocytes and Human Umbilical Vein Endothelial Cells in a Multicompartamental Bioreactor. <https://home.liebertpub.com/tea>.
- VU, K., WEKSLER, B., ROMERO, I., COURAUD, P.-O. & GELLI, A. 2009. Immortalized Human Brain Endothelial Cell Line HCMEC/D3 as a Model of the Blood-Brain Barrier Facilitates In Vitro Studies of Central Nervous System Infection by *Cryptococcus neoformans*. *Eukaryotic Cell*, 8, 1803-1807.
- WADA, M., TOH, S., K, T., T, N., T, U., K, K., I, Y., A, K., S, S., Y, A. & M, K. 1998. Mutations in the canalicular multispecific organic anion transporter (cMOAT) gene, a novel ABC transporter, in patients with hyperbilirubinemia II/Dubin-Johnson syndrome. *Human molecular genetics*, 7.
- WALGREN, R., KARNAKY, K., GE, L. & T, W. 2000. Efflux of dietary flavonoid quercetin 4'-beta-glucoside across human intestinal Caco-2 cell monolayers by apical multidrug resistance-associated protein-2. *The Journal of pharmacology and experimental therapeutics*, 294.
- WALTERS, B. & STEGEMANN, J. 2014. Strategies for directing the structure and function of three-dimensional collagen biomaterials across length scales. *Acta biomaterialia*, 10.
- WALTERS, E., AGCA, Y., V, G. & T, E. 2011. Animal models got you puzzled?: think pig. *Annals of the New York Academy of Sciences*, 1245.
- WAN, D. & OUYANG, H. 2017. Baicalin induces apoptosis in human osteosarcoma cell through ROS-mediated mitochondrial pathway. <https://doi.org/10.1080/14786419.2017.1359173>.
- WANDERS, R., VISSER, W., VAN ROERMUND, C., S, K. & HR, W. 2007. The peroxisomal ABC transporter family. *Pflugers Archiv : European journal of physiology*, 453.
- WANG, C., BAKER, B. M., CHEN, C. S. & SCHWARTZ, M. A. 2013. Endothelial Cell Sensing of Flow Direction. *Arteriosclerosis, Thrombosis, and Vascular Biology*, 33, 2130-2136.
- WANG, D., WANG, C., WANG, L. & CHEN, Y. 2019. A comprehensive review in improving delivery of small-molecule chemotherapeutic agents overcoming the blood-brain/brain tumor barriers for glioblastoma treatment. *Drug Delivery*, 26, 551-565.
- WANG, F., JIAO, P., M, Q., M, F., QP, D. & B, Y. 2010a. Turning tumor-promoting copper into an anti-cancer weapon via high-throughput chemistry. *Current medicinal chemistry*, 17.
- WANG, F., XUE, X., WEI, J., Y, A., J, Y., H, C., J, W., C, D., Z, Q., Z, X. & Y, M. 2010b. hsa-miR-520h downregulates ABCG2 in pancreatic cancer cells to inhibit migration, invasion, and side populations. *British journal of cancer*, 103.

- WANG, H. & NEGISHI, M. 2003. Transcriptional regulation of cytochrome p450 2B genes by nuclear receptors. *Curr Drug Metab*, 4, 515-25.
- WANG, L., LING, Y., CHEN, Y., LI, C.-L., FENG, F., YOU, Q.-D., LU, N. & GUO, Q.-L. 2010c. Flavonoid baicalein suppresses adhesion, migration and invasion of MDA-MB-231 human breast cancer cells. *Cancer Letters*, 297, 42-48.
- WANG, M. 2007. Extending the good diet, good health paradigm: modulation of breast cancer resistance protein (BCRP) by flavonoids. *Toxicological Sciences : an Official Journal of the Society of Toxicology*, 96, 203-205.
- WANG, Q., RAGER, J. D., WEINSTEIN, K., KARDOS, P. S., DOBSON, G. L., LI, J. & HIDALGO, I. J. 2005a. Evaluation of the MDR-MDCK cell line as a permeability screen for the blood–brain barrier. *International Journal of Pharmaceutics*, 288, 349-359.
- WANG, Y., CAO, J. & ZENG, S. 2005b. Involvement of P-glycoprotein in regulating cellular levels of Ginkgo flavonols: quercetin, kaempferol, and isorhamnetin. *The Journal of pharmacy and pharmacology*, 57.
- WANG, Y., MENG, Y., ZHANG, S., WU, H., YANG, D., NIE, C. & HU, Q. 2018. Phenformin and metformin inhibit growth and migration of LN229 glioma cells in vitro and in vivo. *Oncotargets and Therapy*, Volume 11, 6039-6048.
- WANG, Y., YU, H., ZHANG, J., GAO, J., GE, X. & LOU, G. 2015. Hesperidin inhibits HeLa cell proliferation through apoptosis mediated by endoplasmic reticulum stress pathways and cell cycle arrest. *BMC Cancer*, 15.
- WANG, Y. I., ABACI, H. E. & SHULER, M. L. 2017. Microfluidic blood-brain barrier model provides in vivo-like barrier properties for drug permeability screening. *Biotechnology and Bioengineering*, 114, 184-194.
- WATANABE, T., DOHGU, S., TAKATA, F., NISHIOKU, T., NAKASHIMA, A., FUTAGAMI, K., YAMAUCHI, A. & KATAOKA, Y. 2013. Paracellular Barrier and Tight Junction Protein Expression in the Immortalized Brain Endothelial Cell Lines bEND.3, bEND.5 and Mouse Brain Endothelial Cell 4. *Biological and Pharmaceutical Bulletin*, 36, 492-495.
- WEKSLER, B., ROMERO, I. A. & COURAUD, P.-O. 2013. The hCMEC/D3 cell line as a model of the human blood brain barrier. *Fluids and Barriers of the CNS*, 10, 16.
- WEKSLER, B., SUBILEAU, E., N, P., P, C., K, H., M, L., H, T.-L., A, N., S, B., P, T., DK, M., F, R., J, G., IA, R. & PO, C. 2005. Blood-brain barrier-specific properties of a human adult brain endothelial cell line. *FASEB journal : official publication of the Federation of American Societies for Experimental Biology*, 19.
- WELCH, D. R. & HURST, D. R. 2019. Defining the Hallmarks of Metastasis. *Cancer Research*, 79, 3011-3027.
- WELLER, M., WICK, W., ALDAPE, K., M, B., M, B., SM, P., R, N., M, R., PY, W., R, S. & G, R. 2015. Glioma. *Nature reviews. Disease primers*, 1.
- WEN, C., FU, L., HUANG, J., DAI, Y., WANG, B., XU, G., WU, L. & ZHOU, H. 2019. Curcumin reverses doxorubicin resistance via inhibition the efflux function of ABCB4 in doxorubicin-resistant breast cancer cells. *Molecular Medicine Reports*.
- WEN, P. & KESARI, S. 2008. Malignant gliomas in adults. *The New England journal of medicine*, 359.

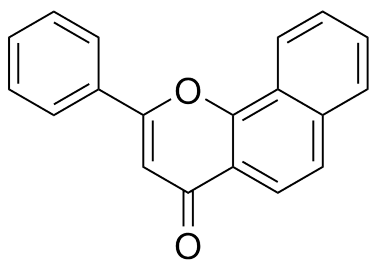
- WIJAYA, J., FUKUDA, Y. & SCHUETZ, J. 2017. Obstacles to Brain Tumor Therapy: Key ABC Transporters. *International Journal of Molecular Sciences*, 18, 2544.
- WIJNHOLDS, J., DELANGE, E., GL, S., DJ, V. D. B., CA, M., M, V. D. V., AH, S., RJ, S., DD, B. & P, B. 2000. Multidrug resistance protein 1 protects the choroid plexus epithelium and contributes to the blood-cerebrospinal fluid barrier. *The Journal of clinical investigation*, 105.
- WILKINSON, J. M. 2017. *Technology Platforms for 3D Cell Culture: A User's Guide*.
- WONG, A. D., YE, M., LEVY, A. F., ROTHSTEIN, J. D., BERGLES, D. E. & SEARSON, P. C. 2013. The blood-brain barrier: an engineering perspective. *Frontiers in Neuroengineering*, 6.
- WONG, D. R., R. DOROVINI-ZIS, K. 2007. Adhesion and migration of polymorphonuclear leukocytes across human brain microvessel endothelial cells are differentially regulated by endothelial cell adhesion molecules and modulate monolayer permeability. *Journal of neuroimmunology*, 184.
- WONG, R. S. 2011. Apoptosis in cancer: from pathogenesis to treatment. *Journal of Experimental & Clinical Cancer Research*, 30, 87.
- WORKMAN, M. J. & SVENDSEN, C. N. 2020. Recent advances in human iPSC-derived models of the blood–brain barrier. *Fluids and Barriers of the CNS*, 17.
- XIAO, Z., PENG, Z., PENG, M., YAN, W., YZ, O. & HL, Z. 2011. Flavonoids health benefits and their molecular mechanism. *Mini reviews in medicinal chemistry*, 11.
- XU, C., LI, C. Y. & KONG, A. N. 2005. Induction of phase I, II and III drug metabolism/transport by xenobiotics. *Arch Pharm Res*, 28, 249-68.
- XU, P., ZHOU, H., LI, Y.-Z., YUAN, Z.-W., LIU, C.-X., LIU, L. & XIE, Y. 2018. Baicalein Enhances the Oral Bioavailability and Hepatoprotective Effects of Silybin Through the Inhibition of Efflux Transporters BCRP and MRP2. *Frontiers in pharmacology*, 9, 1115-1115.
- YAHFOUFI, N., ALSADI, N., JAMBI, M. & MATAR, C. 2018. The Immunomodulatory and Anti-Inflammatory Role of Polyphenols. *Nutrients*, 10, 1618.
- YAMADA, A., ISHIKAWA, T., OTA, I., KIMURA, M., SHIMIZU, D., TANABE, M., CHISHIMA, T., SASAKI, T., ICHIKAWA, Y., MORITA, S., YOSHIURA, K.-I., TAKABE, K. & ENDO, I. 2013. High expression of ATP-binding cassette transporter ABCC11 in breast tumors is associated with aggressive subtypes and low disease-free survival. *Breast Cancer Research and Treatment*, 137, 773-782.
- YANG, S., MEI, S., JIN, H., ZHU, B., TIAN, Y., HUO, J., CUI, X., GUO, A. & ZHAO, Z. 2017. Identification of two immortalized cell lines, ECV304 and bEnd3, for in vitro permeability studies of blood-brain barrier. *PLOS ONE*, 12, e0187017.
- YANG, Y., BAI, L., LI, X., XIONG, J., XU, P., GUO, C. & XUE, M. 2014. Transport of active flavonoids, based on cytotoxicity and lipophilicity: An evaluation using the blood–brain barrier cell and Caco-2 cell models. *Toxicology in Vitro*, 28, 388-396.

- YARLA, N. S. & GANAPATY, S. 2013a. Bioactive Flavonoids as ABC Transporters Inhibitors for Reversion of Multidrug Resistance in Cancer. *Journal of Marine Science: Research & Development*, 4, 1.
- YARLA, S. & GANAPATY, S. 2013b. Bioactive Flavonoids as ABC Transporters Inhibitors for Reversion of Multidrug Resistance in Cancer. *undefined*.
- YEH, S., WANG, W., CH, H. & ML, H. 2005. Pro-oxidative effect of beta-carotene and the interaction with flavonoids on UVA-induced DNA strand breaks in mouse fibroblast C3H10T1/2 cells. *The Journal of nutritional biochemistry*, 16.
- YOH, K., ISHII, G., YOKOSE, T., MINEGISHI, Y., TSUTA, K., GOTO, K., NISHIWAKI, Y., KODAMA, T., SUGA, M. & OCHIAI, A. 2004. Breast Cancer Resistance Protein Impacts Clinical Outcome in Platinum-Based Chemotherapy for Advanced Non-Small Cell Lung Cancer. *Clinical Cancer Research*, 10, 1691-1697.
- YONG, P., ZHAO, F. Z., SHAN, G. C., XIA, Z. Y., YA, D., BIN, J. & WANG, L. Q. 2015. Effects and Mechanism of Baicalin on Apoptosis of Cervical Cancer HeLa Cells In-vitro. 14, 251-261.
- YOSHIKAWA, M., IKEGAMI, Y., SANO, K., H, Y., H, M., S, S. & T, I. 2004. Transport of SN-38 by the wild type of human ABC transporter ABCG2 and its inhibition by quercetin, a natural flavonoid. *Journal of experimental therapeutics & oncology*, 4.
- YOU, G. & MORRIS, M. 2006. Overview of Drug Transporter Families.
- YOU DIM, K. A., DOBBIE, M. S., KUHNLE, G., PROTEGGENTE, A. R., ABBOTT, N. J. & RICE-EVANS, C. J. J. O. N. 2003. Interaction between flavonoids and the blood–brain barrier: in vitro studies. 85, 180-192.
- YOU DIM, K. A., QAISER, M. Z., BEGLEY, D. J., RICE-EVANS, C. A. & ABBOTT, N. J. 2004a. Flavonoid permeability across an in situ model of the blood–brain barrier. *Free Radical Biology and Medicine*, 36, 592-604.
- YOU DIM, K. A., QAISER, M. Z., BEGLEY, D. J., RICE-EVANS, C. A., ABBOTT, N. J. J. F. R. B. & MEDICINE 2004b. Flavonoid permeability across an in situ model of the blood–brain barrier. 36, 592-604.
- YOUN, H., LEE, J., SI, S., K, M., KW, K., YJ, C. & DH, H. 2006. Suppression of MyD88- and TRIF-dependent signaling pathways of Toll-like receptor by (-)-epigallocatechin-3-gallate, a polyphenol component of green tea. *Biochemical pharmacology*, 72.
- YU, A.-R., JEONG, Y. J., HWANG, C. Y., YOON, K.-S., CHOE, W., HA, J., KIM, S. S., PAK, Y. K., YEO, E.-J. & KANG, I. 2019. Alpha-naphthoflavone induces apoptosis through endoplasmic reticulum stress via c-Src-, ROS-, MAPKs-, and arylhydrocarbon receptor-dependent pathways in HT22 hippocampal neuronal cells. *NeuroToxicology*, 71, 39-51.
- YU, Y., PEI, M. & LI, L. 2015. Baicalin induces apoptosis in hepatic cancer cells in vitro and suppresses tumor growth in vivo. *International journal of clinical and experimental medicine*, 8.
- YUAN, J., CHENG, J., LY, J., WD, J., LF, G., JJ, L., XY, X., JS, H., XM, W. & ZX, Z. 2008. Breast cancer resistance protein expression and 5-fluorouracil resistance. *Biomedical and environmental sciences : BES*, 21.
- YUE, B. 2014. Biology of the Extracellular Matrix. *Journal of Glaucoma*, 23, S20-S23.

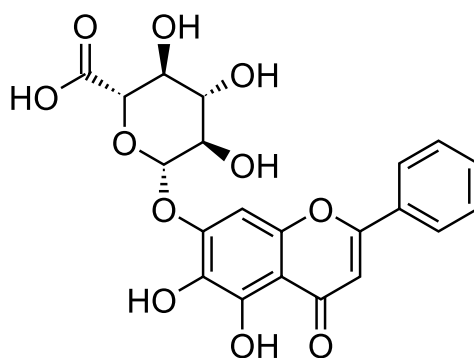
- ZAKKI, A., SHAHBAZ, CUI, Z.-G., SUN, L., FENG, Q.-W., LI, M.-L. & INADERA, H. 2018. Baicalin Augments Hyperthermia-Induced Apoptosis in U937 Cells and Modulates the MAPK Pathway via ROS Generation. *Cellular Physiology and Biochemistry*, 45, 2444-2460.
- ZHANG, B., GU, F., SHE, C., GUO, H., LI, W., NIU, R., FU, L., ZHANG, N. & MA, Y. 2009. Reduction of Akt2 inhibits migration and invasion of glioma cells. *International Journal of Cancer*, 125, 585-595.
- ZHANG, G., WANG, Y., ZHANG, Y., X, W., J, L., K, L., F, W., K, L., Q, L., C, Y., P, Y., Y, H., S, W., P, J., Z, Q., J, L., H, D., L, Z., A, H., S, J., TC, H. & E, W. 2012. Anti-cancer activities of tea epigallocatechin-3-gallate in breast cancer patients under radiotherapy. *Current molecular medicine*, 12.
- ZHANG, J., SONG, J., D, W., J, W. & W, D. 2015a. Hesperetin induces the apoptosis of hepatocellular carcinoma cells via mitochondrial pathway mediated by the increased intracellular reactive oxygen species, ATP and calcium. *Medical oncology (Northwood, London, England)*, 32.
- ZHANG, J., WU, D., VIKASH, SONG, J., WANG, J., YI, J. & DONG, W. 2015b. Hesperetin Induces the Apoptosis of Gastric Cancer Cells via Activating Mitochondrial Pathway by Increasing Reactive Oxygen Species. *Digestive Diseases and Sciences*, 60, 2985-2995.
- ZHANG, S. & MORRIS, M. 2003. Effects of the flavonoids biochanin A, morin, phloretin, and silymarin on P-glycoprotein-mediated transport. *The Journal of pharmacology and experimental therapeutics*, 304.
- ZHANG, S., YANG, X. & MORRIS, M. E. 2004a. Combined Effects of Multiple Flavonoids on Breast Cancer Resistance Protein (ABCG2)-Mediated Transport. *Pharmaceutical Research*, 21, 1263-1273.
- ZHANG, S., YANG, X. & MORRIS, M. E. 2004b. Flavonoids Are Inhibitors of Breast Cancer Resistance Protein (ABCG2)-Mediated Transport. *Molecular Pharmacology*, 65, 1208-1216.
- ZHANG, S., YANG, X. & MORRIS, M. E. 2004c. Flavonoids Are Inhibitors of Breast Cancer Resistance Protein (ABCG2)-Mediated Transport.
- ZHANG, X., ZHANG, N., MENG, X., ZHANG, Y., QIAN, Y. & XIE, Y.-J. 2020. Hesperetin inhibits the proliferation of cerebrally implanted C6 glioma and involves suppression of HIF-1 α /VEGF pathway in rats. *undefined*.
- ZHANG, X. H., ZHANG, N. N., MENG, X. B., ZHANG, Y., QIAN, Y. & XIE, Y. J. 2017. Hesperetin inhibits the proliferation of cerebrally implanted C6 glioma and involves suppression of HIF-1 α /VEGF pathway in rats. 28, 1205-1211.
- ZHAO, H., SUN, P., FAN, T., X, Y., T, Z. & C, S. 2019a. The effect of glutamate-induced excitotoxicity on DNA methylation in astrocytes in a new in vitro neuron-astrocyte-endothelium co-culture system. *Biochemical and biophysical research communications*, 508.
- ZHAO, W., HAN, L., Y, B. & DS, M. 2019b. Lucifer Yellow - A Robust Paracellular Permeability Marker in a Cell Model of the Human Blood-brain Barrier. *Journal of visualized experiments : JoVE*.
- ZHAO, Y., WANG, L., ZHAI, X., CUI, T., WANG, G. & PANG, Q. 2018. The effect of biochanin A on cell growth, apoptosis, and migration in osteosarcoma cells. *Pharmazie*, 73, 335-341.
- ZHOU, S. 2008. Structure, function and regulation of P-glycoprotein and its clinical relevance in drug disposition. *Xenobiotica; the fate of foreign compounds in biological systems*, 38.

- ZHOU, T., ZHANG, A., KUANG, G., GONG, X., JIANG, R., LIN, D., LI, J., LI, H., ZHANG, X., WAN, J. & LI, H. 2017a. Baicalin inhibits the metastasis of highly aggressive breast cancer cells by reversing epithelial-to-mesenchymal transition by targeting β -catenin signaling. *Oncology Reports*.
- ZHOU, Z., SINGH, R. & MM, S. 2017b. Convection-Enhanced Delivery for Diffuse Intrinsic Pontine Glioma Treatment. *Current neuropharmacology*, 15.
- ZHU, J.-J., GERSTNER, E. R., ENGLER, D. A., MRUGALA, M. M., NUGENT, W., NIERENBERG, K., HOCHBERG, F. H., BETENSKY, R. A. & BATCHELOR, T. T. 2009. High-dose methotrexate for elderly patients with primary CNS lymphoma. *Neuro-Oncology*, 11, 211-215.
- ZHU, Y., FANG, J., WANG, H., FEI, M., TANG, T., LIU, K., NIU, W. & ZHOU, Y. 2018a. Baicalin suppresses proliferation, migration, and invasion in human glioblastoma cells via Ca^{2+} -dependent pathway. *Drug Des Devel Ther*, 12, 3247-3261.
- ZHU, Y., FANG, J., WANG, H., FEI, M., TANG, T., LIU, K., NIU, W. & ZHOU, Y. 2018b. Baicalin suppresses proliferation, migration, and invasion in human glioblastoma cells via Ca^{2+} -dependent pathway. *Drug design, development and therapy*, 12, 3247-3261.
- ZIEGLER, U. & GROSCURTH, P. 2004. Morphological features of cell death. *News in physiological sciences : an international journal of physiology produced jointly by the International Union of Physiological Sciences and the American Physiological Society*, 19.
- ZONG, H., VERHAAK, R. G. & CANOLL, P. 2012. The cellular origin for malignant glioma and prospects for clinical advancements. *Expert Review of Molecular Diagnostics*, 12, 383-394.
- ÖZVEGY, C., LITMAN, T., SZAKÁCS, G., NAGY, Z., BATES, S., VÁRADI, A. & SARKADI, B. 2001. Functional Characterization of the Human Multidrug Transporter, ABCG2, Expressed in Insect Cells. *Biochemical and Biophysical Research Communications*, 285, 111-117.

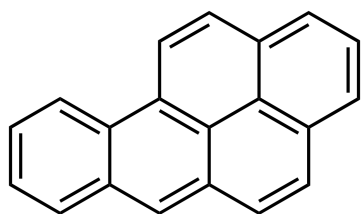
Appendix A: Chemical structures



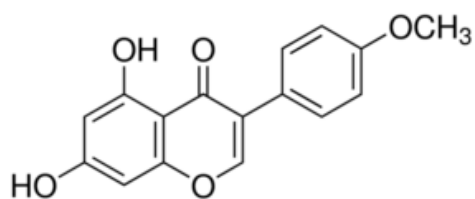
α -Naphthoflavone



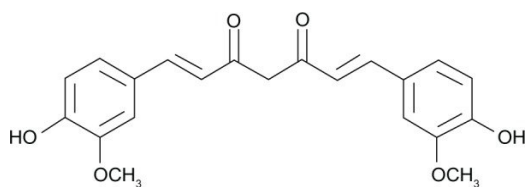
Baicalin



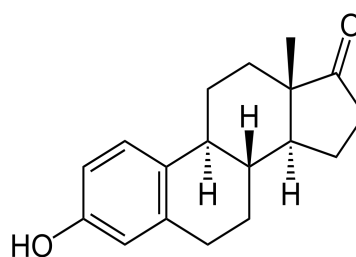
Benzo-a-pyrene



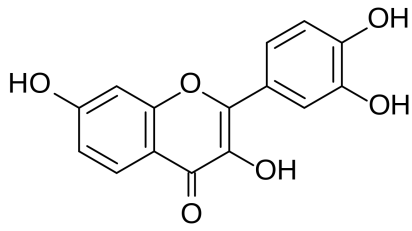
Biochanin-a



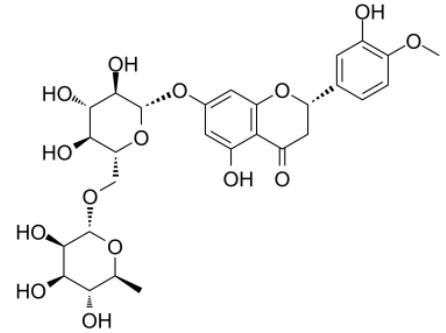
Curcumin



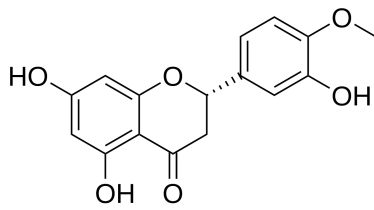
Estrone



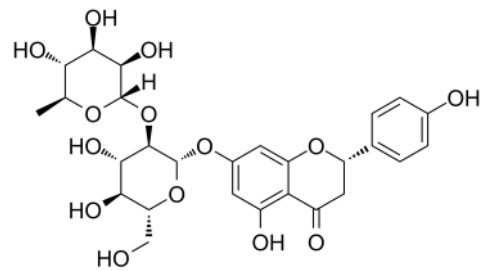
Fisetin



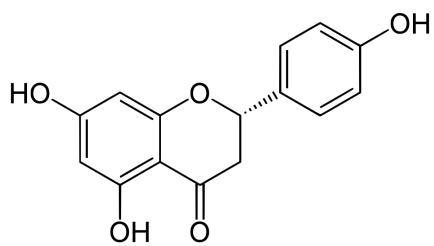
Hesperidin



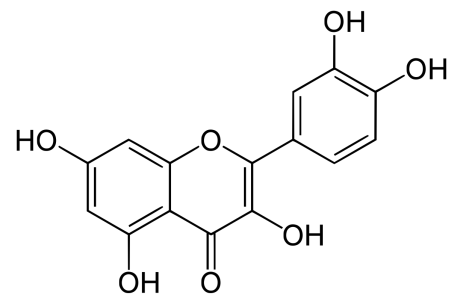
Hesperetin



Naringin



Naringenin



Quercetin

